



UvA-DARE (Digital Academic Repository)

Transcriptional control of cytotoxic lymphocytes

An unexpected journey with Hobit

Vieira Braga, F.A.

Publication date

2017

Document Version

Final published version

License

Other

[Link to publication](#)

Citation for published version (APA):

Vieira Braga, F. A. (2017). *Transcriptional control of cytotoxic lymphocytes: An unexpected journey with Hobit*.

General rights

It is not permitted to download or to forward/distribute the text or part of it without the consent of the author(s) and/or copyright holder(s), other than for strictly personal, individual use, unless the work is under an open content license (like Creative Commons).

Disclaimer/Complaints regulations

If you believe that digital publication of certain material infringes any of your rights or (privacy) interests, please let the Library know, stating your reasons. In case of a legitimate complaint, the Library will make the material inaccessible and/or remove it from the website. Please Ask the Library: <https://uba.uva.nl/en/contact>, or a letter to: Library of the University of Amsterdam, Secretariat, Singel 425, 1012 WP Amsterdam, The Netherlands. You will be contacted as soon as possible.

Transcriptional control of cytotoxic lymphocytes

An unexpected journey with Hobit



FELIPE A. VIEIRA BRAGA

Transcriptional control of cytotoxic lymphocytes: an unexpected journey with Hobit

Felipe Augusto Vieira Braga

Printing was supported by:
Sanquin Blood Supply Foundation, Amsterdam NL

©Felipe A Vieira Braga, 2017

ISBN: 978-94-92683-53-3

Cover: Optima Grafische Communicatie

Cover figure: creative commons license

Lay-out: Felipe A Vieira Braga.

Printed by: Optima Grafische Communicatie

Transcriptional control of cytotoxic lymphocytes: an unexpected journey with Hobit

ACADEMISCH PROEFSCHRIFT

ter verkrijging van de graad van doctor

aan de Universiteit van Amsterdam

op gezag van de Rector Magnificus

prof. dr. ir. K.I.J. Maex

ten overstaan van een door het College voor Promoties ingestelde commissie,

in het openbaar te verdedigen in de Agnietenkapel

op donderdag 08 Juni 2017, te 12:00 uur

door

Felipe Augusto Vieira Braga

geboren te Teresina, Brazilië

Promotiecommissie:

Promotor:	Prof. dr. R.A.W. van Lier	AMC-UvA
Copromotor:	Dr. K.P.J.M van Gisbergen	AMC-UvA
Overige leden:	Dr. D. Amsen	Sanquin Research
	Prof. dr. J. Borst	AMC-UvA
	Prof. dr. E.F. Eldering	AMC-UvA
	Prof. dr. A. Oxenius	ETH Zurich
	Prof. dr. H.R. Waterham	AMC-UvA
	Dr. F.M. Wensveen	University of Rijeka, Croatia

Faculteit der Geneeskunde

“The world is changed. I feel it in the water. I feel it in the earth. I smell it in the air. Much that once was is lost; for none now live who remember it.”

J.R.R Tolkien

Table of content

Chapter 1	Introduction <u>Eur. J. Immunol. 2015; 45:2433–2445.</u>	9
Chapter 2	Blimp-1 homolog Hobit identifies effector-type lymphocytes in humans. <u>Eur. J. Immunol. 2015; 45:2433–2445</u>	31
Chapter 3	The transcription factor Hobit identifies human cytotoxic CD4 T cells <u>Frontiers in Immunology . in press</u>	57
Chapter 4	Hobit regulates metabolism and maintenance of human cytotoxic lymphocytes	77
Chapter 5	Hobit but not blimp-1 maintains cytotoxicity in memory CD8 T cells	99
Chapter 6	Hobit regulates human natural killer cell development and effector function	123
Chapter 7	The Adhesion G Protein-Coupled Receptor GPR56/ADGRG1 Is an Inhibitory Receptor on Human NK Cells <u>Cell Rep. 2016; 15:1757–1770.</u>	139
Chapter 8	General Discussion	173
Appendix	English Summary	184
	Nederlandse Samenvatting	187
	List of co-authors and their contribution to the manuscript	190
	PhD portfolio	192
	List of publications	194
	Curriculum Vitae	195
	Acknowledgments	196

CHAPTER 1

Introduction

European Journal of Immunology 2015; 45:2433–2445

Anti-viral immune response

Upon viral infection the immune system engages lymphocytes such as NK cells, CD4+ and CD8+ T cells to eliminate the virus. CD4+ and CD8+ T cells recognize viral peptides presented by MHC class II (MHC-II) and MHC class I (MHC-I) molecules respectively. CD8+ T-cells specific for the infecting pathogen first undergo massive expansion before they differentiate into cytotoxic cells capable of producing high levels of effector molecules such as IL-2, IFN- γ , TNF- α , perforin and granzyme B [1;2]. Naïve CD4+ T cells also expand and develop an effector (Th1) phenotype capable of secreting copious amounts of IFN- γ , IL-2 and TNF- α to assist CD8+ T-cell and B-cell responses [3]. To avoid T-cell detection and lysis of the infected cells, viruses of the Herpesviridae family including human cytomegalovirus (HCMV) have evolved mechanisms to downregulate MHC-I molecules on infected cells [4;5]. In turn, NK cells can detect downregulation of MHC expression and produce inflammatory cytokines such as IFN- γ , TNF- α , and cytotoxic granules containing effector molecules, such as perforin and the serine protease granzyme B, to eliminate infected cells [6;7].

HCMV is a member of the Herpesviridae family of double-stranded DNA viruses and has co-evolved with humans for millions of years [8]. HCMV has a broad tropism for a wide range of tissues including endothelium, fibroblasts, smooth muscle and hematopoietic cells. HCMV is a prevalent human pathogen, with 40-70% of the western population being seropositive for HCMV [9]. HCMV induces persistent infection, which can be divided into acute and latent phases, and which are respectively characterized by active replication and quiescence of the virus [10]. The majority of HCMV-infected individuals do not develop any symptoms, but immunocompromised individuals, such as transplant recipients and HIV+ patients, are a risk group for HCMV infection and can present with symptoms such as vascular complications [8].

In order to follow T cell responses in humans, we and others have made extensive use of instances of primary HCMV infection of transplant patients, which occurs when an HCMV- recipient receives an organ transplant from an HCMV+ donor. Using this system, the data show that the initial early T-cell response against HCMV peaks on average 7 days after the first detection of circulating CMV-DNA. The T-cell response is initially dominated by CD4+ T-cells that have a T helper 1 type cytokine signature, with high production of the cytokines IFN- γ and TNF- α , but not of the classical T helper 2 cytokine IL-4 [11]. A few days after the initial CD4+ T-cell response, HCMV-specific CD8+ T cells with high cytotoxic potential can be detected in blood. Remarkably, after the early phase of infection, the HCMV-specific CD8+ T cell population does not contract and is maintained with an effector phenotype during the latent phase [12;13]. Furthermore, NK cells are also activated after HCMV infection, and play a role during the early phase, before T cell responses are induced, as well as during latency after the establishment of T cell responses. The depletion of both NK and T cells has been shown to lead to HCMV reactivation, suggesting that both these lymphocyte subsets are essential for suppression of HCMV infection [14-16]. It is important to note that HCMV also activates monocytes and macrophages [17;18], induces antibody responses [19;20], and elicits a characteristic $\gamma\delta$ T-cell response [21-23]. However, we will focus here on HCMV-specific $\alpha\beta$ CD8+ T-cells and compare their responses with those of $\alpha\beta$ CD4+ T cells and NK cells.

CD8+ T cells can be divided into different subpopulations by the use of surface markers important for T cell function, such as the co-stimulatory receptors CD27 and CD28, the chemokine receptor CCR7, and the common leukocyte antigen isoforms CD45RA and CD45RO (recently reviewed in [24]). We and others have previously demonstrated that HCMV infection generates a very specific fingerprint within the CD8+ T cell compartment during latency, with enrichment for a specific subpopulation of CD8+ T cells that are characterized as CD45RA+CD27-CD28-CCR7-cells [12;25;26]. In the rest of this review we will refer to this population as CD45RA+ effector CD8+ T cells. These CD45RA+ effector cells are phenotypically different from other virus-specific cells, such as CD8+ T cells directed against influenza virus (CCR7+CD27+CD28+CD45RA-, referred to as classical memory CD8+ T cells), EBV (CCR7-CD27+CD28+CD45RA-) or HIV (CCR7-CD27+CD28-CD45RA-, referred to as exhausted CD8+ T cells) [2;27-29].

The HCMV-specific CD8+ T cell compartment expands with age and in older HCMV+ individuals these cells can constitute up to 50-70% of all circulating CD8+ T cells [28;30]. The HCMV-specific CD8+ T cells maintain an explicit effector rather than memory phenotype as exemplified by constitutive high expression of granzyme B and perforin, and provide lifelong protection against reoccurrence of HCMV infection [26;31]. A major question that has not been fully answered yet is how HCMV-specific CD8+ T cells can be maintained for a lifetime as effector cells with immediate and efficient capacity to counter viral replication. From a therapeutic standpoint, CD8+ T cells with long-term survival and the potential to immediately respond to challenge are highly useful in adoptive transfer strategies to treat malignancies and infection. Therefore, the maintenance requirements of HCMV-specific CD8+ T cells can be highly interesting from a vaccine perspective.

Maintenance of HCMV-specific CD8+ T cells

In humans, the populations of CD8+ T cells recognizing epitopes of HCMV are much larger than CD8+ T cell populations specific for other viruses such as influenza [32]. The percentage of HCMV-specific CD8+ T-cells progressively increases with age, and elderly HCMV-infected individuals have been shown to have T-cell repertoires that are dominated by a few HCMV-specific CD8+ T clones [30]. The expansion of HCMV-specific memory CD8+ T-cells within the circulation has been termed memory inflation [28;30] (Figure 1). Memory inflation is an interesting aspect of CD8+ T cell differentiation that also occurs after persistent latent infection with parvo and polyoma viruses [33;34], but that does not occur after acute infection such as with influenza and LCMV. After resolution of acute infection with pathogens, the effector CD8+ T cell pool has been shown to contract and a much reduced memory CD8+ T cell population is formed, which is thereafter stably maintained (Figure 1). These memory cells have high expression of the cytokine receptors for IL-7 and IL-15 (IL-7R α and IL-15R β), and are maintained by homeostatic proliferation in response to these cytokines rather than to antigen, as is the case for effector CD8+ T cells [35;36]. One important difference between HCMV-specific CD8+ T cells and other memory populations (such as that specific for influenza) is that the HCMV-specific memory population lacks expression of the receptor for IL-7, and shows only intermediate expression of IL-15R β [37;38]. The data suggest that HCMV-specific cells are not maintained on homeostatic cytokines, in contrast to conventional memory cells,

and rather rely on other, yet-undefined survival factors for their maintenance. The difference between the maintenance mechanisms of HCMV-specific cells and, for instance, influenza-specific cells suggests that these cells are not competing for similar environmental stimuli. Indeed, the expansion of HCMV-specific CD8⁺ T cells does not appear to occur at the expense of memory CD8⁺ T-cell populations specific for other viruses, such as influenza and EBV [39].

The murine cytomegalovirus (MCMV) is a useful model to address questions that cannot be addressed in the HCMV model of primary infection. The overlap between the transcriptomes of murine CD8⁺ T cells after MCMV infection, and those of human CD8⁺ T cells after HCMV infection, suggests that the murine model is largely representative of HCMV infection in humans [40]. MCMV induces persistent infection with similar kinetics to HCMV infection, including early and latency phases [10]. CD8⁺ T cell differentiation after MCMV infection depends on the epitope. The viral proteins M45 and M57 induce classical memory CD8⁺ T cell responses similar to those after infection with influenza [41]. In contrast, the viral proteins M38, m139 and IE3 contain epitopes that have been shown to induce memory inflation. MCMV-specific CD8⁺ T cells directed against these epitopes have a comparable effector phenotype with HCMV-specific CD8⁺ T cells [41]. Snyder et al. [41] have compared inflationary and conventional memory CD8⁺ T cells after MCMV infection, to study the maintenance requirements of these populations. In contrast to conventional memory CD8⁺ T cells, inflationary MCMV-specific cells were shown not to express the IL-7 and IL-15 receptors and are not maintained via these cytokines [41]. Inflationary MCMV specific cells had short half-lives compared with those of memory cells. The inflated CD8⁺ T cell pool in mice appears to be maintained via the recruitment of newly generated inflationary cells from CD8⁺ T cells primed early after infection and from thymus-derived naïve CD8⁺ T cells rather than via homeostatic turnover of the inflationary cells themselves [40;41].

This model of memory maintenance during MCMV infection does not entirely fit with the data on CD8⁺ T cell dynamics after HCMV infection. The HCMV-specific CD8⁺ repertoire in the blood remains remarkably stable for a period of years during primary infection and latency [39;42]. This suggests that CMV-specific CD8⁺ T cells in humans are not constantly recruited from the thymic naïve pool during latency, but that maintenance largely occurs via homeostatic turnover in the periphery. Experiments using deuterium-labelled glucose for direct *in vivo* measurement of T cell turnover in humans have shown that HCMV-specific CD45RA⁺ effector CD8⁺ T cells display a long life span, which contrasts with inflationary MCMV-specific CD8⁺ T cells in mice [30]. The differences between HCMV and MCMV CD8⁺ T cell dynamics may reflect the reduced dependency on thymic output for T-cell maintenance in humans compared to mice. The slow turnover aligns with the observation that HCMV-specific CD8⁺ T cells have very short telomeres. High expression of KLRG1 and CD57 and low expression of CD28 [29;43-47], which are characteristics of terminally differentiated cells also indicate slow turnover of the HCMV-specific CD8⁺ T cell population [44;48]. These adaptations of HCMV-specific CD8⁺ T cells may ensure long-term persistence in the order of decades rather than months, as is sufficient in mice.

Tissue distribution of HCMV-specific CD8+ T cells

Much of our understanding about memory T cells in humans is based on cells isolated from peripheral blood. The tissue distribution of HCMV-specific CD8+ T cells is relatively restricted to this compartment. HCMV-specific cells are present at high levels in the blood, but not within the lymph nodes [39]. In general, CD8+ T cells depend on specific chemokine and adhesion receptors for entry and retention within different tissues. CCR7 and CD62L, for example, are receptors important for cellular entry into lymph nodes [49] [24]. Central memory T cells that circulate through the secondary lymphoid tissues in contrast to effector memory T cells have been shown to have high expression of CCR7 and CD62L [49]. In contrast, circulating HCMV-specific CD8+ T cells are mainly CCR7- and CD62L- [37;50;51], in line with their limited capacity to enter the lymph nodes. Interestingly, the few HCMV-specific CD8+ T cells found within the lymph nodes do express CD62L and CCR7 [39;52]. In addition, lymph node-resident HCMV-specific CD8+ T cells display other characteristics of central memory T cells, including high levels of IL-7R α expression [38;39;42]. This suggests that these cells have different maintenance requirements compared with those of circulating cells. We have made use of next-generation sequencing of the T-cell receptor (TCR) between paired lymph nodes and blood samples to study clonal relationships between cells in lymph nodes and in circulation [39;52]. The TCR usage suggests that HCMV-specific CD8+ T cell clones within blood and lymph node are largely distinct, implying that lymph node-resident T cells do not significantly contribute to the supply of new effector cells within the circulating pool [39;52;53]. Only recently, the availability of post-mortem material from organ donors has allowed a thorough analysis of CD8+ T cell differentiation throughout human tissues within a single individual [53-55]. In these studies classical memory cells were present throughout tissues in contrast to CD45RA+ effector CD8+ T cells, which were present in peripheral blood, bone marrow, spleen and lungs, but largely absent from other tissues such as ileum, jejunum and colon [53-55]. It is possible that the distribution of CD45RA+ CD8+ T cells largely reflects blood-derived cells, as they appear enriched within highly vascularized tissues.

Recently, tissue-resident populations of T cells (Trm) have been defined using expression of CD69 and CD103 [56;57]. These Trm cells localize within epithelium of the skin, lungs and intestine [55;56;58] and have been shown to play an important role in early and local protection against pathogens through the rapid production of IFN- γ [57-60]. CD45RA+ CD8+ T cells have been shown not to express CD69 [55], suggesting that these cells are largely circulating cells and do not contain a tissue-resident population. Supporting these data, HCMV-specific CD8+ T cells within the lungs do not express CD103, while the majority of influenza-specific cells in the lungs express high levels of CD103 [56]. The lack of CD103 expression within the HCMV-specific CD8+ compartment suggests that these cells do not have access to the epithelium, but are present in residual blood of the lung tissue [56].

The low prevalence of HCMV-specific cells within the lymphoid and peripheral compartments and the high prevalence of circulating HCMV-specific cells suggest that these cells might be patrolling the endothelial cells that line the bloodstream. In support of such a role for HCMV-specific CD8+ T cells, endothelial cells of blood vessels constitute one critical site for HCMV replication and latency [61]. Stressed endothelial cells, such as HCMV-infected endothelial cells, have been shown to

upregulate several chemokines such as CXCL10 and fractalkine to attract immune cells [62;63]. HCMV-specific CD8+ T cells express high levels of CXCR3 and CX3CR1 [37], the chemokine receptors that bind CXCL10 and fractalkine respectively. CD45RA+ effector CD8+ T cells have the capacity to migrate towards CXCL10 and fractalkine, suggesting that these cells are involved in the control HCMV infection within the endothelial layer of blood vessels [64]. Therefore, in parallel to tissue-resident T cell populations, we consider it an interesting possibility that HCMV-specific CD8+ T cells have developed as blood-resident T cells, which continually patrol the endothelium.

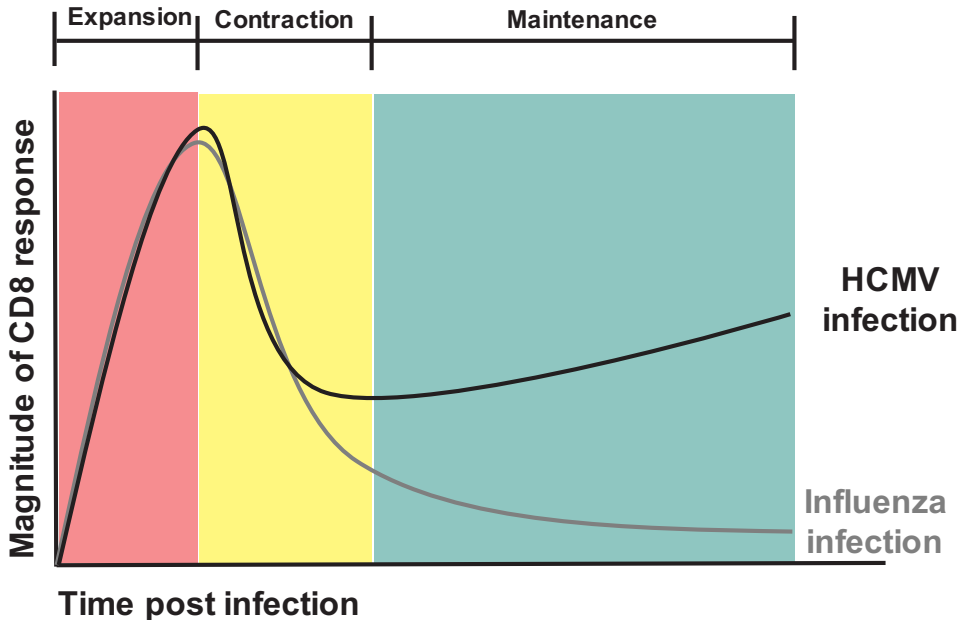


Figure 1. CD8+ T-cell dynamics after HCMV and influenza infection. After resolution of primary infection, HCMV-specific CD8+ T-cell numbers do not decrease to the same extent as those specific for influenza. The initially contracting HCMV memory population later expands over time, whereas the influenza memory population contracts and thereafter is stably maintained at low numbers.

HCMV-specific CD8+ T cells: Cytotoxicity and effector function

Different types of memory cells have developed different strategies to counter re-infection. Memory cells, such as those specific for influenza, stimulated *in vitro* with anti-CD3/CD28 antibodies, show a robust proliferative response and strong production of effector cytokines such as TNF- α and IFN- γ , suggesting that they can quickly expand and differentiate into effector cells upon re-infection *in vivo* [65]. Unlike memory cells, HCMV-specific T cells have a very low proliferative response upon TCR triggering [66], suggesting that these cells are inferior at mounting secondary T cell responses compared to memory cells (Figure 2). Memory T cells support proliferation through autocrine and paracrine production of the T cell growth factor IL-2. HCMV-specific cells do not produce IL-2 themselves [67]. However, the

proliferative capacity of HCMV-specific cells is not completely absent, and these cells have been shown to proliferate in response to TCR stimulation in the presence of cytokines such as IL-2, IL-15 or IL-21 [66].

One of the major functions of HCMV-specific CD8⁺ T cells is the lysis of virus-infected cells through the secretion of perforin and granzyme B. These cytotoxic molecules cooperate to induce apoptosis of target cells through perforin-mediated permeabilization of the cell membrane, and granzyme B-mediated cleavage and activation of pro-apoptotic target proteins, such as caspases and Bid [68]. Memory cells have high transcript levels of granzyme B, but only express granzyme B protein upon activation. In contrast, HCMV-specific CD8⁺ T cells not only have elevated granzyme B transcripts, but also high levels of pre-formed granzyme B molecules stored in intracellular granules [67]. This suggests that these cells can quickly respond and lyse infected target cells in a more efficient manner than other memory populations (Figure 2) [7;26;56;67;69].

HCMV-specific CD8⁺ T cells maintain high levels of IFN- γ and TNF- α mRNA and can produce high levels of these cytokines within hours after stimulation [37]. IFN- γ is a pro-inflammatory cytokine that has direct anti-viral activity and plays a role in the activation and differentiation of immune cells such as B cells, T cells, NK cells and macrophages [70]. HCMV-specific CD8⁺ T cells also produce chemokines that attract immune cells to the site of infection, such as CCL4 and CCL5, which recruit macrophages, NK cells, monocytes as well as activated T cells [71-74]. Thus, HCMV-specific CD8⁺ T cells are polyfunctional cells with strong effector functions, as they are able to co-produce multiple cytokines and chemokines, which induce and sustain immune responses.

During chronic viral infections such as those with hepatitis B and HIV, CD8⁺ T cells have been shown to have a reduced capacity for fighting the viral infection, as they are unable to induce production of cytokines such as IL-2, IFN- γ and TNF- α upon TCR activation [75;76]. These cells are classified as having an exhausted phenotype (Figure 2). Functionally exhausted cells are also identified by the persistent high expression of several inhibitory receptors, such as PD1, CTLA4, LAG3, CD160 and TIM-3, in the chronic phase of infection (Figure 2). HCMV-specific CD8⁺ T cells express low levels of PD1 [37], suggesting that they do not have an exhausted phenotype, which is compatible with the long-term maintenance of polyfunctional effector functions. However, HCMV-specific cells have been shown to express high levels of LAG3 and CD160 [37], suggesting that these fully functional effector cells may be subject to regulation by inhibitory receptors.

Metabolism of CD8 + effector T-cells

During viral infection, CD8⁺ T cells transition from a quiescent catabolic state into a highly active anabolic state to meet the increased metabolic demands of proliferation and effector differentiation [77;78]. The two main pathways for energy production in these cells are oxidative phosphorylation (OXPHOS) and glycolysis. OXPHOS occurs in the mitochondria and generates approximately 31.5 molecules of ATP per molecule of sugar, while glycolysis is an oxygen-independent metabolic route that occurs in the cytosol and, from one sugar molecule, generates only two molecules of ATP (reviewed in [79]). Effector CD8⁺ T cells in particular upregulate the energy-inefficient glycolytic pathway, as this allows for the production of effector cytokines

such as IFN- γ [80;81].

After clearance of the pathogen, memory CD8+ T cells switch back to a quiescent catabolic metabolism [77]. Compared with that of naïve CD8+ T cells, memory CD8+ T cells have higher basal levels of both OXPHOS and glycolysis [82;83]. One of the main factors that sustain the enhanced energy metabolism of memory cells is their greater mitochondrial mass [83]. Consistent with the increased numbers of mitochondria, memory CD8+ T cells also have a higher spare respiratory capacity than naïve CD8+ T cells [83]. The high spare respiratory capacity allows memory cells to sustain mitochondrial ATP production in situations of increased demands, such as upon re-challenge with pathogens [82]. This fits with the higher proliferative capacity of memory cells compared to naïve cells upon antigen encounter [77;78;82;83].

The metabolic control of HCMV specific CD8 T-cells has not been directly addressed so far. In contrast, the study of CD45RA+ effector CD8+ T cells that phenotypically resemble HCMV-specific CD8+ T cells has shown that these cells adopt a metabolic strategy, which differs from that of memory populations [44]. The mitochondrial mass and respiration of CD45RA+ effector CD8+ T cells is lower compared with that of CD45RO+ memory CD8+ T cells [44]. The mitochondria of CD45RA+ CD8+ T cells also show several characteristics of metabolic impairment, as they contain high ROS levels and depolarized membranes [44;79], which indicate suboptimal mitochondrial respiration [79]. The low respiratory capacity of CD45RA+ effector CD8+ T cells is in line with the low proliferative capacity of these cells upon re-stimulation. However, CD45RA+ effector cells have high levels of basal glycolysis, indicating a preferential use of glycolysis over mitochondrial respiration for energy generation [44]. Memory cells maintain the high rate of glycolysis via the upregulation of glucose receptors (GLUT1) and increased glucose uptake. In contrast, CD45RA+ effector CD8+ T cells do not upregulate GLUT1 expression [44], but instead fuel the enhanced glycolytic capacity via autophagy [44]. Glycolysis has been shown to drive IFN- γ production upon TCR activation, suggesting that the elevated glycolysis in CD45RA+ effector cells sustains the high capacity to produce IFN- γ within these cells [44;80;81]. These findings regarding the metabolism of CD45RA+ CD8+ T cells may translate to the metabolic wiring of HCMV-specific CD8+ T cells. We are only beginning to understand how the metabolism of HCMV-specific CD8+ T cells is regulated, but the available data indicates that their metabolic status is an integrated part of the maintenance and effector function of these long-lived effector cells.

HCMV-specific CD4+ T-cell responses

CD4+ T cells are important for antiviral protection against HCMV infection. The development of CD4+ T cell responses is associated with asymptomatic HCMV infection [84]. Antiviral therapy has been shown to rescue CD4+ T cell responses in symptomatic patients, suggesting that CD4+ T cells are essential for an effective anti-HCMV immune response [84]. Moreover, the mouse model of CMV infection provides another indication for the importance of CD4+ T cells: adoptive transfer of MCMV-specific CD4+ T cells - taken during the peak of infection - into recipient mice protects against primary MCMV infection [85].

The phenotype of HCMV-specific CD4+ cells has been extensively characterized at different stages of infection [11;86;87]. During the peak of HCMV infection, HCMV-specific CD4+ T cells are CD45RA/CD45RO double positive, and express CD27,

CD28, CD38 and CD40L [11;86;88]. During latency, the HCMV-specific CD4+ T cell compartment is enriched for CD27/CD28 double negative cells [11;85-87].

The memory inflation observed in the CD4+ T cell compartment is not to the same extent as in the CD8+ T-cell compartment. During latency, CD27-CD28- cells can make up 5 to 10% of total CD4+ T cells, which is relatively high, when compared with other memory populations, but still 5- to 10-fold lower than HCMV-specific cells in the CD8+ T cell compartment [86].

The maintenance requirements of HCMV-specific CD4+ T cells appear to be similar to that of HCMV-specific CD8+ T cells. CD27-CD28- CD4+ cells also lack expression of IL-7R α [88], suggesting that maintenance occurs independently of homeostatic IL-7. HCMV-specific CD27-CD28- CD4+ T cells have features of terminally differentiated cells, such as CD57 and KLRG1 expression, short telomeres and reduced proliferative capacity upon re-activation [88]. These phenotypic characteristics suggest that, similar to CD8+ T cells, HCMV-specific CD4+ T cells are a terminally differentiated population [88;89].

The distribution pattern of CD27-CD28- CD4+ resembles that of CD8+ T cells, as these cells accumulate in blood, lungs and bone marrow, but not in lymph nodes, jejunum, ileum or colon [3]. The TCR β repertoire of HCMV-specific CD4+ T cells during latency is very restricted and has very little overlap with the clones detected during the acute phase of primary infection [90]. This suggests that the majority of the clones found in the circulation have expanded after the initial antiviral response, but currently it is unclear where these clones originate from [3;54;88;90].

Classical Th1 CD4+ T cells are characterized by the capacity to produce IL-2, IFN- γ and TNF- α . HCMV-specific CD4+ T cells, both during the peak of infection and in latency, have been shown to produce the classical Th1 cytokines IL-2, IFN- γ and TNF- α [11]. Besides these effector cytokines, this population uniquely expresses granzyme B and perforin [88], which, as discussed earlier, are classically associated with NK cells and effector CD8+ T cells. The expression of granzyme B and perforin enables HCMV-specific CD4+ T cells, similar to CD45RA+ effector CD8+ T cells, to mediate lysis of HCMV-infected cells [91;92]. It is important to note that HCMV-infected cells can induce impairment of HCMV-specific effector CD4+ T cell responses [93]. A subpopulation of HCMV-specific CD4+ T cells has been shown to express Foxp3 and to perform functions similar to regulatory T cells, such as the production of IL-10 [94].

HCMV-specific NK-cell responses

Natural killer cells play a major role in controlling CMV infection, during both the early and latent phases of infection [10;14;95]. After primary HCMV infection, a specific NK-cell population characterized by NKG2C $^{\text{bright}}$ expression has been shown to expand over time [96;97]. These NKG2C $^{\text{bright}}$ NK cells are phenotypically distinct from NKG2C $^{-}$ and NKG2C $^{\text{dim}}$ NK cells, as in contrast to these populations, NKG2C $^{\text{bright}}$ NK cells express high levels of CD57, CD158b (KIR2DL3) and LIR-1 and low levels of NKp30, NKp46, CD161 and NKG2A [98-102].

NKG2C is a member of the NKG2 family of C-type lectin-like receptors and forms heterodimers with CD94 that enable interactions with HLA-E molecules [98-101;103]. HCMV infection down-regulates the expression of several HLA class I molecules but increases HLA-E expression [104]. The specific expansion of NKG2C $^{\text{bright}}$ cells may

enable these cells to control HCMV infection through recognition of HLA-E molecules [105]. However, so far, there is no direct evidence for a role of NKG2C/CD94 and HLA-E in the control of HCMV infection [105].

NKG2C^{bright} NK cells are considered to form a population of HCMV-specific memory NK cells. NKG2C^{bright} NK cells have characteristics typical of memory cells as they express a restricted clonal KIR repertoire [106], and display restricted pathogen specificity. In contrast to HCMV, infection with other viruses such as EBV and HSV does not induce the expansion of NKG2C^{bright} NK cells [107]. Most importantly, NKG2C^{bright} cells are long-lived cells which have been shown to steadily increase in number after primary infection [98-101]. The expansion of NKG2C^{bright} NK cells after HCMV infection is paralleled by the specific expansion of Ly49H⁺ NK cells after MCMV infection in mice. These LY49H⁺ cells have memory properties in common with NKG2C^{bright} NK cells after HCMV infection, such as a clonal-like expansion after infection and the establishment of long-lived populations [99;101;106]. Ly49H⁺ NK cells also display a more robust secondary response against re-infection with MCMV, which is a typical property of memory cells [98-101]. In mice, expansion of the Ly49H⁺ NK-cell population relies on the recognition of the viral protein, m157 on infected cells. So far, it is not clear whether HCMV-specific NKG2C^{bright} cells also recognize a specific viral protein [108].

The maintenance requirements of NKG2C^{bright} NK cells are not entirely clear. NKG2C^{bright} NK cells have been shown to accumulate after hematopoietic stem cell transplantation of HCMV⁺ donors into HCMV⁻ recipients, suggesting that primary HCMV infection drives the generation of NKG2C^{bright} NK cells [101]. NKG2C^{bright} NK cells have also been shown to accumulate, although less dramatically, after hematopoietic stem cell transplantation of HCMV⁺ donors into HCMV⁺ recipients [100;101]. These findings imply that the constitutive presence of viral ligands is essential for the maintenance of NKG2C^{bright} NK cells. However, increased numbers of NKG2C^{bright} NK cells have been detected during the acute phase of Chikungunya virus [109], HIV [110] and hantavirus [111] infection in HCMV⁺ patients, but not in HCMV⁻ patients. This indicates that HCMV triggers the generation of NKG2C^{bright} NK cells, but that the expansion and maintenance of NKG2C^{bright} NK cells can take place in response to unrelated viral infections.

NK cells produce a plethora of effector molecules such as granzyme B, granzyme K, IFN- γ and TNF- α . Compared to NKG2C⁻ NK cells, NKG2C^{bright} NK cells have higher constitutive expression of granzyme B and lower levels of granzyme K. NKG2C^{bright} NK cells are highly polyfunctional and upon activation these cells produce increased amounts of IFN- γ and TNF- α , and degranulate more rapidly than NKG2C⁻ cells, as suggested by CD107a upregulation [99]. Specific epigenetic remodelling of the IFN- γ locus may underlie the enhanced IFN- γ production in NKG2C^{bright} NK cells [112]. Taken together, the maintenance and effector differentiation of NKG2C^{bright} NK cells after HCMV infection displays striking similarities with the characteristics of HCMV-specific CD8⁺ and CD4⁺ T cells.

Common transcriptional regulation of lymphocytes during HCMV infection

HCMV infection induces the formation of long-lived populations of NKG2C⁺ NK cells and effector CD4⁺ and CD8⁺ T cells, all of which share many characteristics in maintenance, distribution, effector function and metabolism (Table 1). The reasons behind the induction of similar effector lymphocytes within the different lineages are not entirely clear. HCMV has acquired extensive mechanisms of immune evasion, which include the downregulation of MHC class I molecules on infected cells [113]. As neither NKG2C⁺ NK cells nor effector CD4⁺ T cells require MHC class I molecules to eliminate target cells, these effector lymphocytes may have evolved to support effector CD8⁺ T cells in suppression of HCMV infection. The overlap in effector phenotype between HCMV-specific CD4⁺ and CD8⁺ T cells and HCMV-induced NK-cell populations suggests similar aspects in the differentiation pathways of these lymphocytes. Transcription factors regulate distinct steps of effector differentiation by repressing or inducing the expression of target genes. For understandable reasons, the transcriptional regulation of human lymphocytes has received much less attention than that of murine lymphocytes. Currently, it is unclear which transcription factors drive the differentiation of long-lived effector T cells and NK cells that arise after infection with CMV.

We have performed longitudinal micro-array analysis on HCMV-specific CD8⁺ T cells after HCMV infection to monitor the transcriptomes of these virus-reactive T cells at distinct stages of infection. We observed that transcription factors that were upregulated during the effector phase of acute infection with LCMV or influenza in mice, such as T-bet, Eomes and Blimp-1, were also upregulated in HCMV-specific CD8⁺ T cells during primary infection [37]. In mice, T-bet and Blimp-1 have been shown to induce terminal differentiation of short-lived effectors at the expense of the generation of memory precursors upon acute infection with LCMV or influenza [114-116]. In contrast, Eomes is expressed in CD8⁺ memory T-cell precursors and contributes to memory formation [117]. T-bet and Eomes also have been shown to co-regulate effector functions such as IFN- γ production and granzyme B expression in CD8⁺ T cells [118;119]. Similarly, Blimp-1 regulates granzyme B expression and cytotoxicity in CD8⁺ T cells [115;116]. Interestingly, the expression of T-bet, Eomes and Blimp-1 in HCMV-specific CD8⁺ T cells was shown to be maintained into the latency phase, suggesting that these transcription factors are important for the maintenance of effector functions [37]. The recent development of antibodies that detect T-bet and Eomes for flow cytometry analysis have enabled detailed expression analysis of these T-box factors at the protein level in subsets of CD8⁺ T cells. Human CD45RA⁺ effector CD8⁺ T cells displayed high expression of T-bet and Eomes compared to memory CD8⁺ T-cell populations in peripheral blood [120]. The high level of T-bet and Eomes expression was confirmed in HCMV-specific CD8⁺ T cells during viral latency, and was distinct from that in other virus-specific populations [121]. For example, exhausted HIV-1-specific CD8⁺ T cells display high Eomes and intermediate T-bet expression, whereas influenza-specific CD8⁺ T cells have low levels of both T-bet and Eomes [121;122]. The expression levels of T-bet and Eomes are relevant, as a high Eomes-to-T-bet ratio in CD8⁺ T cells during chronic LCMV infection has been shown to drive functional exhaustion [123]. In contrast, the elevated expression levels of T-bet compared to Eomes in HCMV-specific CD8⁺ T cells from lung transplant patients undergoing primary HCMV infection correlated

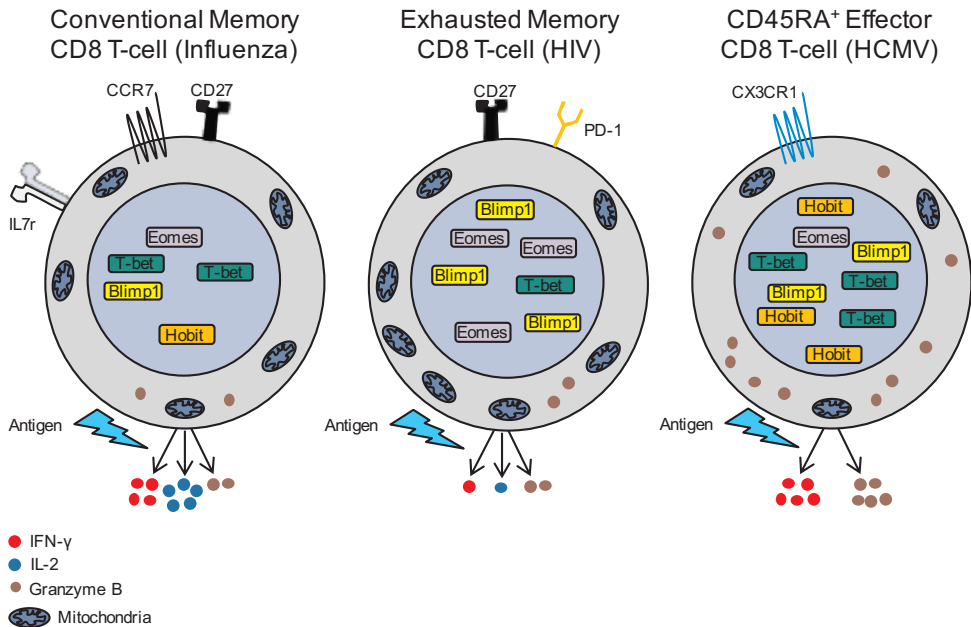


Figure 2. Acute influenza infection, latent HCMV infection and chronic HIV infection induce distinct CD8+ T cell responses. Conventional influenza memory CD8+ T cells are maintained by interleukin 7 and can respond to pathogen re-encounter by secreting IL-2 and IFN- γ , thereby supporting T-cell proliferation and pro-inflammatory immune responses. Expression of the chemokine receptor CCR7 ensures that a large fraction of these cells is located within the lymph nodes. In contrast, exhausted memory CD8+ T cells during chronic HIV infection constitutively express the inhibitory receptor PD1 and lose the ability to produce large amounts of IL-2 and IFN- γ . CD45RA⁺ effector CD8+ T cells present during latent HCMV infection express specific chemokine receptors such as CX3CR1 that attract the cells to inflamed blood vessels. These cells can produce copious amounts of IFN- γ and granzyme B, but not IL-2. The differences in expression levels of Hobit, Blimp1, T-bet and Eomes between the CD8+ T-cell subsets suggests that regulation by these transcription factors underlies the differences in CD8+ T-cell differentiation and effector function.

with stronger effector function and enhanced viral control [124]. Thus, high co-expression of T-bet, Eomes and Blimp-1 in CD45RA⁺ effector CD8+ T cells appears to reflect the capacity of these cells to maintain explicit effector functions such as IFN- γ and granzyme B production.

Preliminary findings indicate that the transcriptional regulation of CD45RA⁺ effector CD8+ T cells is conserved in effector CD4+ T cells and NKG2C⁺ NK cells. Specifically, the expression of T-bet and Eomes has been shown to be higher in CD27-CD28⁻ effector CD4+ T cells than in other CD4+ T-cell populations [120]. Currently, the expression of Blimp-1 in CD27-CD28⁻ effector CD4+ T cells is unclear and the functional relevance of all of these transcription factors has not been analysed in effector CD4+ T cells. Epigenetic remodelling of Eomes, T-bet and Blimp-1 loci in NKG2C⁺ NK cells of HCMV⁺ donors suggests that expression of these transcription factors correlates with active IFN- γ transcription in NKG2C⁺ NK cells [112]. Blimp-1 plays an active role in NKG2C⁺ NK cells, as it induces terminal differentiation of these cells after MCMV infection by antagonizing ZBTB32 [125]. The total NK-cell

Table 1. Phenotypic comparison between the HCMV-specific populations in the CD4⁺, CD8⁺ and NK cell compartment with CD8⁺ T cells after influenza and HIV infection.

Virus specificity	Influenza	HIV	HCMV		
	Conventional Memory CD8 ⁺ T-cell	Exhausted Memory CD8 ⁺ T-cell	CD8 ⁺ T-cell	CD4 ⁺ T-cell	NK cell
Phenotype	CD45RO ⁺ CD27 ⁺ CD28 ⁺ CCR7 ⁺	CD45RO ⁺ CD27 ⁺ CD28 ⁻ PD1 ⁺	CD45RA ⁺ CD27 ⁻ CD28 ⁻ CX3CR1 ⁺ KLRG1 ⁺ CD57 ⁺	CD27 ⁻ CD28 ⁻ KLRG1 ⁺ CD57 ⁺	NKG2C ⁺ KLRG1 ⁺ CD57 ⁺
Differentiation	Early	Intermediate	Terminal	Terminal	Terminal
Memory Inflation	Not present	Not present	High	Intermediate	High
Proliferation upon re-activation	High	Low	Low	Low	Not known
Telomeres	Normal	Short	Short	Short	Not known
Life span	Intermediate	Not known	Long	Not known	Not known
Tissue distribution	Lymph nodes / Blood / Spleen / Lungs / Bone marrow / Gut	Lymph nodes / Blood / Spleen	Blood / Spleen / Lungs / Bone marrow	Blood / Spleen / Lungs / Bone marrow	Blood (no data available on other tissues)
Cytotoxicity	Intermediate	Intermediate	High	High	High
Metabolism	High respiration High glycolysis	High respiration Unknown glycolysis	Low respiration High glycolysis	Not known	Not known
Transcription Factors	T-bet ^{low} Eomes ^{low} Blimp1 ^{int} Hobit ^{low}	T-bet ^{low} Eomes ^{high} Blimp1 ^{high} Hobit ^{low}	T-bet ^{high} Eomes ^{low} Blimp1 ^{int} Hobit ^{high}	T-bet ^{high} Eomes ^{low} Blimp1 ^{int} Hobit ^{high}	T-bet ^{high} Eomes ^{low} Blimp1 ^{int} Hobit ^{high}

Table 1. Phenotypic comparison between the HCMV-specific populations in the CD4⁺, CD8⁺ and NK cell compartment with CD8⁺ T cells after influenza and HIV infection.

population expresses high levels of T-bet, Blimp-1 and Eomes, suggesting that these factors do not mediate unique transcriptional regulation in NKG2C⁺ NK cells. In mice, T-bet and Eomes have been shown to maintain IL-15-responsive lymphocytes, including almost the entire population of NK cells, by regulating the expression of IL-15Rb [118;119]. Blimp-1 regulates the terminal differentiation of NK cells in mice, including the acquisition of granzyme B expression [126]. Blimp-1 is also broadly

expressed in human NK cells, although Blimp-1 has no clear effect on granzyme B regulation [127]. Thus, CD27-CD28- effector CD4+ T cells and NK cells, including NKG2C+ NK cells, appear to share expression of transcription factors involved in effector differentiation with CD45RA+ effector CD8+ T cells.

One of the most prominently upregulated transcription factors during differentiation of HCMV-specific CD8+ T cells is zinc finger protein (ZNF)683 [37]. ZNF683, also known as Hobit (Homologue of Blimp-1 in T cells), has high homology with Blimp-1, in particular in the functional zinc finger domains [128]. In mice, Hobit expression has been shown to be confined to tissue resident CD8 T cells, tissue resident NK cells and NKT cells. Murine Hobit cooperates with Blimp-1 to regulate the generation and/or maintenance of these populations. Similar to Blimp-1 in effector CD8 T cells [128], Hobit in NKT cells also regulates effector functions, such as the production of granzyme B and IFN- γ [128,129]. In the following chapters of this thesis, the role of Hobit in the human immune system, including its expression pattern, expression regulation and functional roles has been explored.

Scope of the thesis

The general aim of this thesis is to study the role of the transcription factor Hobit in the human immune system. In chapter 2, we characterized Hobit expression in the human immune system. Our findings showed that Hobit is specifically expressed in effector-type CD8+ T cells and NK cells and that Hobit regulated essential effector functions, including the production of IFN- γ . In Chapter 3, we describe the expression pattern of Hobit in CD4 T cells. We found that Hobit was confined to effector-type cells within the CD4 T cell lineage, suggesting overlapping transcriptional regulation of effector CD4 and CD8 T cells. In Chapter 4, we have characterized the metabolism of CD45RA+ effector CD8 T cells (EMRA cells). We show that Hobit acts as a metabolic suppressor in effector lymphocytes to regulate cell survival during mitogenic stimulation and cytokine deprivation. In Chapter 5, we have investigated the expression regulation of Hobit and Blimp-1 in mice and men. We reveal the impact of the expression regulation of these transcription factors on their collaborative roles in regulating granzyme B expression and the cytotoxic potential of effector and memory lymphocytes. Chapters 6 and 7 are devoted to the role of Hobit in human NK cell development and effector function. In Chapter 6 we describe the expression pattern of Hobit in NK cells from adult and neonatal tissues as well as the dynamics of Hobit expression during NK cell development. Finally, in Chapter 7, we describe that Hobit is involved in the regulation of GPR56, an adhesion G protein-coupled receptor, which inhibits the natural cytotoxicity of human NK cells. In conclusion, we demonstrate in this thesis that Hobit expression in humans is restricted to lymphocytes with cytotoxic potential, and that Hobit regulates aspects of the maintenance and effector function of these cytotoxic lymphocytes.

References

1. Wherry, E.J. and Ahmed, R., Memory CD8 T-cell differentiation during viral infection. *J.Virol.* 2004. 78: 5535-5545.
2. van Lier, R.A., ten Berge, I.J., and Gamadia, L.E., Human CD8(+) T-cell differentiation in response to viruses. *Nat.Rev.Immunol.* 2003. 3: 931-939.
3. Farber, D.L., Yudanin, N.A., and Restifo, N.P., Human memory T cells: generation, compartmentalization and homeostasis. *Nat.Rev.Immunol.* 2014. 14: 24-35.
4. Petersen, J.L., Morris, C.R., and Solheim, J.C., Virus evasion of MHC class I molecule presentation. *J.Immunol.* 2003. 171: 4473-4478.
5. Ploegh, H.L., Viral strategies of immune evasion. *Science* 1998. 280: 248-253.
6. Huard, B. and Fruh, K., A role for MHC class I down-regulation in NK cell lysis of herpes virus-infected cells. *Eur.J.Immunol.* 2000. 30: 509-515.
7. Thiery, J., Keefe, D., Boulant, S., Boucrot, E., Walch, M., Martinvalet, D., Goping, I.S.et al., Perforin pores in the endosomal membrane trigger the release of endocytosed granzyme B into the cytosol of target cells. *Nat.Immunol.* 2011. 12: 770-777.
8. Sinclair, J. and Sissons, P., Latency and reactivation of human cytomegalovirus. *J.Gen.Virol.* 2006. 87: 1763-1779.
9. Ludwig, A. and Hengel, H., Epidemiological impact and disease burden of congenital cytomegalovirus infection in Europe. *Euro.Surveill* 2009. 14: 26-32.
10. Babic, M., Krmpotic, A., and Jonjic, S., All is fair in virus-host interactions: NK cells and cytomegalovirus. *Trends Mol.Med.* 2011. 17: 677-685.
11. Rentenaar, R.J., Gamadia, L.E., van, D.N., van Diepen, F.N., Boom, R., Weel, J.F., Wertheim-van Dillen, P.M.et al., Development of virus-specific CD4(+) T cells during primary cytomegalovirus infection. *J.Clin.Invest* 2000. 105: 541-548.
12. Kuijpers, T.W., Vossen, M.T., Gent, M.R., Davin, J.C., Roos, M.T., Wertheim-van Dillen, P.M., Weel, J.F.et al., Frequencies of circulating cytolytic, CD45RA+CD27-, CD8+ T lymphocytes depend on infection with CMV. *J.Immunol.* 2003. 170: 4342-4348.
13. Mackus, W.J., Frakking, F.N., Grummels, A., Gamadia, L.E., de Bree, G.J., Hamann, D., van Lier, R.A.et al., Expansion of CMV-specific CD8+CD45RA+CD27- T cells in B-cell chronic lymphocytic leukemia. *Blood* 2003. 102: 1057-1063.
14. Kuijpers, T.W., Baars, P.A., Dantin, C., van den Burg, M., van Lier, R.A., and Roosnek, E., Human NK cells can control CMV infection in the absence of T cells. *Blood* 2008. 112: 914-915.
15. Enblad, G., Hagberg, H., Erlanson, M., Lundin, J., MacDonald, A.P., Repp, R., Schetelig, J.et al., A pilot study of alemtuzumab (anti-CD52 monoclonal antibody) therapy for patients with relapsed or chemotherapy-refractory peripheral T-cell lymphomas. *Blood* 2004. 103: 2920-2924.
16. Lundin, J., Kimby, E., Bjorkholm, M., Broliden, P.A., Celsing, F., Hjalmar, V., Mollgard, L.et al., Phase II trial of subcutaneous anti-CD52 monoclonal antibody alemtuzumab (Campath-1H) as first-line treatment for patients with B-cell chronic lymphocytic leukemia (B-CLL). *Blood* 2002. 100: 768-773.
17. Chan, G., Bivins-Smith, E.R., Smith, M.S., Smith, P.M., and Yurochko, A.D., Transcriptome analysis reveals human cytomegalovirus reprograms monocyte differentiation toward an M1 macrophage. *J.Immunol.* 2008. 181: 698-711.
18. Smith, M.S., Bentz, G.L., Alexander, J.S., and Yurochko, A.D., Human cytomegalovirus induces monocyte differentiation and migration as a strategy for dissemination and persistence. *J.Virol.* 2004. 78: 4444-4453.
19. Klein, M., Schoppel, K., Amvrossiadis, N., and Mach, M., Strain-specific neutralization of human cytomegalovirus isolates by human sera. *J.Virol.* 1999. 73: 878-886.
20. Schoppel, K., Schmidt, C., Einsele, H., Hebart, H., and Mach, M., Kinetics of the antibody response against human cytomegalovirus-specific proteins in allogeneic bone marrow transplant recipients. *J.Infect.Dis.* 1998. 178: 1233-1243.
21. Khairallah, C., Netzer, S., Villacreses, A., Juzan, M., Rousseau, B., Dulanto, S., Giese, A.et al., gammadelta T cells confer protection against murine cytomegalovirus (MCMV). *PLoS.Pathog.* 2015. 11: e1004702.

22. Couzi, L., Pitard, V., Moreau, J.F., Merville, P., and Dechanet-Merville, J., Direct and Indirect Effects of Cytomegalovirus-Induced γ T Cells after Kidney Transplantation. *Front Immunol.* 2015. 6: 3.
23. Sell, S., Dietz, M., Schneider, A., Holtappels, R., Mach, M., and Winkler, T.H., Control of murine cytomegalovirus infection by γ T cells. *PLoS.Pathog.* 2015. 11: e1004481.
24. Mahnke, Y.D., Brodie, T.M., Sallusto, F., Roederer, M., and Lugli, E., The who's who of T-cell differentiation: human memory T-cell subsets. *Eur.J.Immunol.* 2013. 43: 2797-2809.
25. ten Berge, I.J., Gamadia, L.E., Remmerswaal, E.B., Surachno, S., Weel, J.F., Toebes, M., Schumacher, T.N.et al., Differentiation of CMV-specific CD8(POS) T lymphocytes in primary CMV infection after renal transplantation. *Transplant.Proc.* 2001. 33: 3630.
26. Gamadia, L.E., Rentenaar, R.J., Baars, P.A., Remmerswaal, E.B., Surachno, S., Weel, J.F., Toebes, M.et al., Differentiation of cytomegalovirus-specific CD8(+) T cells in healthy and immunosuppressed virus carriers. *Blood* 2001. 98: 754-761.
27. Jackson, S.E., Mason, G.M., Okecha, G., Sissons, J.G., and Wills, M.R., Diverse specificities, phenotypes, and antiviral activities of cytomegalovirus-specific CD8+ T cells. *J.Virol.* 2014. 88: 10894-10908.
28. van de Berg, P.J., van, S.A., ten Berge, I.J., and van Lier, R.A., A fingerprint left by cytomegalovirus infection in the human T cell compartment. *J.Clin.Virol.* 2008. 41: 213-217.
29. Weekes, M.P., Carmichael, A.J., Wills, M.R., Mynard, K., and Sissons, J.G., Human CD28-CD8+ T cells contain greatly expanded functional virus-specific memory CTL clones. *J.Immunol.* 1999. 162: 7569-7577.
30. Wallace, D.L., Masters, J.E., De Lara, C.M., Henson, S.M., Worth, A., Zhang, Y., Kumar, S.R.et al., Human cytomegalovirus-specific CD8(+) T-cell expansions contain long-lived cells that retain functional capacity in both young and elderly subjects. *Immunology* 2011. 132: 27-38.
31. Rentenaar, R.J., Gamadia, L.E., van der Hoek, N., van Diepen, F.N., Wertheim-van Dillen, P.M., Weel, J.F., Surachno, S.et al., CD8(POS) lymphocyte dynamics in primary CMV infection. *Transplant.Proc.* 2001. 33: 1867-1869.
32. van Leeuwen, E.M., Koning, J.J., Remmerswaal, E.B., van, B.D., van Lier, R.A., and ten Berge, I.J., Differential usage of cellular niches by cytomegalovirus versus EBV- and influenza virus-specific CD8+ T cells. *J.Immunol.* 2006. 177: 4998-5005.
33. Simmons, R., Sharp, C., Sims, S., Kloverpris, H., Goulder, P., Simmonds, P., Bowness, P.et al., High frequency, sustained T cell responses to PARV4 suggest viral persistence in vivo. *J.Infect.Dis.* 2011. 203: 1378-1387.
34. Swanson, P.A., Hofstetter, A.R., Wilson, J.J., and Lukacher, A.E., Cutting edge: shift in antigen dependence by an antiviral MHC class Ib-restricted CD8 T cell response during persistent viral infection. *J.Immunol.* 2009. 182: 5198-5202.
35. Kaech, S.M., Tan, J.T., Wherry, E.J., Konieczny, B.T., Surh, C.D., and Ahmed, R., Selective expression of the interleukin 7 receptor identifies effector CD8 T cells that give rise to long-lived memory cells. *Nat.Immunol.* 2003. 4: 1191-1198.
36. Antia, R., Bergstrom, C.T., Pilyugin, S.S., Kaech, S.M., and Ahmed, R., Models of CD8+ responses: 1. What is the antigen-independent proliferation program. *J.Theor.Biol.* 2003. 221: 585-598.
37. Hertoghs, K.M., Moerland, P.D., van, S.A., Remmerswaal, E.B., Yong, S.L., van de Berg, P.J., van Ham, S.M.et al., Molecular profiling of cytomegalovirus-induced human CD8+ T cell differentiation. *J.Clin.Invest* 2010. 120: 4077-4090.
38. van Leeuwen, E.M., de Bree, G.J., Remmerswaal, E.B., Yong, S.L., Tesselaar, K., ten Berge, I.J., and van Lier, R.A., IL-7 receptor alpha chain expression distinguishes functional subsets of virus-specific human CD8+ T cells. *Blood* 2005. 106: 2091-2098.
39. Remmerswaal, E.B., Havenith, S.H., Idu, M.M., van Leeuwen, E.M., van Donselaar, K.A., Ten, B.A., Bom-Baylon, N.et al., Human virus-specific effector-type T cells accumulate in blood but not in lymph nodes. *Blood* 2012. 119: 1702-1712.
40. Quinn, M., Turula, H., Tandon, M., Deslouches, B., Moghbeli, T., and Snyder, C.M., Memory T cells specific for murine cytomegalovirus re-emerge after multiple challenges and recapitulate immunity in various adoptive transfer scenarios. *J.Immunol.* 2015. 194: 1726-1736.
41. Snyder, C.M., Cho, K.S., Bonnett, E.L., van, D.S., Shellam, G.R., and Hill, A.B., Memory inflation during chronic viral infection is maintained by continuous production of short-lived, functional T cells. *Immunity.* 2008. 29: 650-659.
42. Klarenbeek, P.L., Remmerswaal, E.B., ten Berge, I.J., Doorenspleet, M.E., van Schaik,

- B.D., Esveldt, R.E., Koch, S.D. et al., Deep sequencing of antiviral T-cell responses to HCMV and EBV in humans reveals a stable repertoire that is maintained for many years. *PLoS.Pathog.* 2012. 8: e1002889.
43. van de Berg, P.J., Griffiths, S.J., Yong, S.L., Macaulay, R., Bemelman, F.J., Jackson, S., Henson, S.M. et al., Cytomegalovirus infection reduces telomere length of the circulating T cell pool. *J.Immunol.* 2010. 184: 3417-3423.
 44. Henson, S.M., Lanna, A., Riddell, N.E., Franzese, O., Macaulay, R., Griffiths, S.J., Puleston, D.J. et al., p38 signaling inhibits mTORC1-independent autophagy in senescent human CD8(+) T cells. *J.Clin.Invest* 2014. 124: 4004-4016.
 45. Hamann, D., Kostense, S., Wolthers, K.C., Otto, S.A., Baars, P.A., Miedema, F., and van Lier, R.A., Evidence that human CD8+CD45RA+CD27- cells are induced by antigen and evolve through extensive rounds of division. *Int.Immunol.* 1999. 11: 1027-1033.
 46. Hathcock, K.S., Kaech, S.M., Ahmed, R., and Hodes, R.J., Induction of telomerase activity and maintenance of telomere length in virus-specific effector and memory CD8+ T cells. *J.Immunol.* 2003. 170: 147-152.
 47. Weekes, M.P., Wills, M.R., Mynard, K., Hicks, R., Sissons, J.G., and Carmichael, A.J., Large clonal expansions of human virus-specific memory cytotoxic T lymphocytes within the CD57+ CD28- CD8+ T-cell population. *Immunology* 1999. 98: 443-449.
 48. Henson, S.M., Franzese, O., Macaulay, R., Libri, V., Azevedo, R.I., Kiani-Alikhan, S., Plunkett, F.J. et al., KLRG1 signaling induces defective Akt (ser473) phosphorylation and proliferative dysfunction of highly differentiated CD8+ T cells. *Blood* 2009. 113: 6619-6628.
 49. Sallusto, F., Lenig, D., Forster, R., Lipp, M., and Lanzavecchia, A., Two subsets of memory T lymphocytes with distinct homing potentials and effector functions. *Nature* 1999. 401: 708-712.
 50. van Leeuwen, E.M., van Buul, J.D., Remmerswaal, E.B., Hordijk, P.L., ten Berge, I.J., and van Lier, R.A., Functional re-expression of CCR7 on CMV-specific CD8+ T cells upon antigenic stimulation. *Int.Immunol.* 2005. 17: 713-719.
 51. Faint, J.M., Annels, N.E., Curnow, S.J., Shields, P., Pilling, D., Hislop, A.D., Wu, L. et al., Memory T cells constitute a subset of the human CD8+CD45RA+ pool with distinct phenotypic and migratory characteristics. *J.Immunol.* 2001. 167: 212-220.
 52. Remmerswaal, E.B., Klarenbeek, P.L., Alves, N.L., Doorenspleet, M.E., van Schaik, B.D., Esveldt, R.E., Idu, M.M. et al., Clonal Evolution of CD8+ T Cell Responses against Latent Viruses: Relationship among Phenotype, Localization, and Function. *J.Virol.* 2015. 89: 568-580.
 53. Letsch, A., Knoedler, M., Na, I.K., Kern, F., Asemissen, A.M., Keilholz, U., Loesch, M. et al., CMV-specific central memory T cells reside in bone marrow. *Eur.J.Immunol.* 2007. 37: 3063-3068.
 54. Sathaliyawala, T., Kubota, M., Yudanin, N., Turner, D., Camp, P., Thome, J.J., Bickham, K.L. et al., Distribution and compartmentalization of human circulating and tissue-resident memory T cell subsets. *Immunity*. 2013. 38: 187-197.
 55. Thome, J.J., Yudanin, N., Ohmura, Y., Kubota, M., Grinshpun, B., Sathaliyawala, T., Kato, T. et al., Spatial map of human T cell compartmentalization and maintenance over decades of life. *Cell* 2014. 159: 814-828.
 56. Piet, B., de Bree, G.J., Smids-Dierdorp, B.S., van der Loos, C.M., Remmerswaal, E.B., von der Thusen, J.H., van Haarst, J.M. et al., CD8(+) T cells with an intraepithelial phenotype upregulate cytotoxic function upon influenza infection in human lung. *J.Clin.Invest* 2011. 121: 2254-2263.
 57. Mackay, L.K., Stock, A.T., Ma, J.Z., Jones, C.M., Kent, S.J., Mueller, S.N., Heath, W.R. et al., Long-lived epithelial immunity by tissue-resident memory T (TRM) cells in the absence of persisting local antigen presentation. *Proc.Natl.Acad.Sci.U.S.A* 2012. 109: 7037-7042.
 58. Jiang, X., Clark, R.A., Liu, L., Wagers, A.J., Fuhlbrigge, R.C., and Kupper, T.S., Skin infection generates non-migratory memory CD8+ T(RM) cells providing global skin immunity. *Nature* 2012. 483: 227-231.
 59. Klonowski, K.D., Williams, K.J., Marzo, A.L., Blair, D.A., Lingenheld, E.G., and Lefrancois, L., Dynamics of blood-borne CD8 memory T cell migration in vivo. *Immunity*. 2004. 20: 551-562.
 60. Teijaro, J.R., Turner, D., Pham, Q., Wherry, E.J., Lefrancois, L., and Farber, D.L., Cutting edge: Tissue-retentive lung memory CD4 T cells mediate optimal protection to respiratory virus infection. *J.Immunol.* 2011. 187: 5510-5514.
 61. Fish, K.N., Soderberg-Naucler, C., Mills, L.K., Stenglein, S., and Nelson, J.A., Human cytomegalovirus persistently infects aortic endothelial cells. *J.Virol.* 1998. 72: 5661-5668.
 62. van de Berg, P.J., Yong, S.L., Remmerswaal, E.B., van Lier, R.A., and ten Berge, I.J., Cytomegalovirus-induced effector T cells cause endothelial cell damage. *Clin.Vaccine Immunol.* 2012. 19:

772-779.

63. Imaizumi, T, Yoshida, H., and Satoh, K., Regulation of CX3CL1/fractalkine expression in endothelial cells. *J.Atheroscler.Thromb.* 2004. 11: 15-21.
64. Bolovan-Fritts, C.A., Trout, R.N., and Spector, S.A., Human cytomegalovirus-specific CD4+T-cell cytokine response induces fractalkine in endothelial cells. *J.Virol.* 2004. 78: 13173-13181.
65. Schluns, K.S. and Lefrancois, L., Cytokine control of memory T-cell development and survival. *Nat.Rev.Immunol.* 2003. 3: 269-279.
66. van Leeuwen, E.M., Gamadia, L.E., Baars, P.A., Remmerswaal, E.B., ten Berge, I.J., and van Lier, R.A., Proliferation requirements of cytomegalovirus-specific, effector-type human CD8+ T cells. *J.Immunol.* 2002. 169: 5838-5843.
67. Hamann, D., Baars, P.A., Rep, M.H., Hooibrink, B., Kerkhof-Garde, S.R., Klein, M.R., and van Lier, R.A., Phenotypic and functional separation of memory and effector human CD8+ T cells. *J.Exp.Med.* 1997. 186: 1407-1418.
68. Afonina, I.S., Cullen, S.P., and Martin, S.J., Cytotoxic and non-cytotoxic roles of the CTL/NK protease granzyme B. *Immunol.Rev.* 2010. 235: 105-116.
69. van Leeuwen, E.M., Remmerswaal, E.B., Vossen, M.T., Rowshani, A.T., Wertheim-van Dillen, P.M., van Lier, R.A., and ten Berge, I.J., Emergence of a CD4+CD28- Granzyme B+, Cytomegalovirus-Specific T Cell Subset after Recovery of Primary Cytomegalovirus Infection. *J.Immunol.* 2004. 173: 1834-1841.
70. Billiau, A. and Matthys, P., Interferon-gamma: a historical perspective. *Cytokine Growth Factor Rev.* 2009. 20: 97-113.
71. Raport, C.J., Gosling, J., Schweickart, V.L., Gray, P.W., and Charo, I.F., Molecular cloning and functional characterization of a novel human CC chemokine receptor (CCR5) for RANTES, MIP-1beta, and MIP-1alpha. *J.Biol.Chem.* 1996. 271: 17161-17166.
72. Cocchi, F., DeVico, A.L., Garzino-Demo, A., Arya, S.K., Gallo, R.C., and Lusso, P., Identification of RANTES, MIP-1 alpha, and MIP-1 beta as the major HIV-suppressive factors produced by CD8+ T cells. *Science* 1995. 270: 1811-1815.
73. Slimani, H., Charnaux, N., Mbemba, E., Saffar, L., Vassy, R., Vita, C., and Gattegno, L., Interaction of RANTES with syndecan-1 and syndecan-4 expressed by human primary macrophages. *Biochim.Biophys.Acta* 2003. 1617: 80-88.
74. Atemezem, A., Mbemba, E., Vassy, R., Slimani, H., Saffar, L., and Gattegno, L., Human alpha1-acid glycoprotein binds to CCR5 expressed on the plasma membrane of human primary macrophages. *Biochem.J.* 2001. 356: 121-128.
75. Petrovas, C., Chaon, B., Ambrozak, D.R., Price, D.A., Melenhorst, J.J., Hill, B.J., Geldmacher, C.et al., Differential association of programmed death-1 and CD57 with ex vivo survival of CD8+ T cells in HIV infection. *J.Immunol.* 2009. 183: 1120-1132.
76. Wherry, E.J., Ha, S.J., Kaech, S.M., Haining, W.N., Sarkar, S., Kalia, V., Subramaniam, S.et al., Molecular signature of CD8+ T cell exhaustion during chronic viral infection. *Immunity.* 2007. 27: 670-684.
77. van der Windt, G.J. and Pearce, E.L., Metabolic switching and fuel choice during T-cell differentiation and memory development. *Immunol.Rev.* 2012. 249: 27-42.
78. Pearce, E.L., Metabolism in T cell activation and differentiation. *Curr.Opin.Immunol.* 2010. 22: 314-320.
79. Weinberg, S.E., Sena, L.A., and Chandel, N.S., Mitochondria in the Regulation of Innate and Adaptive Immunity. *Immunity.* 2015. 42: 406-417.
80. Chang, C.H., Curtis, J.D., Maggi, L.B., Jr., Faubert, B., Villarino, A.V., O'Sullivan, D., Huang, S.C.et al., Posttranscriptional control of T cell effector function by aerobic glycolysis. *Cell* 2013. 153: 1239-1251.
81. Gubser, P.M., Bantug, G.R., Razik, L., Fischer, M., Dimeloe, S., Hoenger, G., Durovic, B.et al., Rapid effector function of memory CD8+ T cells requires an immediate-early glycolytic switch. *Nat.Immunol.* 2013. 14: 1064-1072.
82. van der Windt, G.J., Everts, B., Chang, C.H., Curtis, J.D., Freitas, T.C., Amiel, E., Pearce, E.J.et al., Mitochondrial respiratory capacity is a critical regulator of CD8+ T cell memory development. *Immunity.* 2012. 36: 68-78.
83. van der Windt, G.J., O'Sullivan, D., Everts, B., Huang, S.C., Buck, M.D., Curtis, J.D., Chang, C.H.et al., CD8 memory T cells have a bioenergetic advantage that underlies their rapid recall ability. *Proc.Natl.Acad.Sci.U.S.A* 2013. 110: 14336-14341.
84. Gamadia, L.E., Remmerswaal, E.B., Weel, J.F., Bemelman, F., van Lier, R.A., and ten Berge, I.J., Primary immune responses to human CMV: a critical role for IFN-gamma-producing CD4+ T

cells in protection against CMV disease. *Blood* 2003. 101: 2686-2692.

85. Jeitziner, S.M., Walton, S.M., Torti, N., and Oxenius, A., Adoptive transfer of cytomegalovirus-specific effector CD4+ T cells provides antiviral protection from murine CMV infection. *Eur.J.Immunol.* 2013. 43: 2886-2895.

86. Gamadia, L.E., Rentenaar, R.J., van Lier, R.A., and ten Berge, I.J., Properties of CD4(+) T cells in human cytomegalovirus infection. *Hum.Immunol.* 2004. 65: 486-492.

87. Rentenaar, R.J., Gamadia, L.E., van der Hoek, N., van Diepen, F.N., Boom, R., Weel, J.F., van Lier, R.A.et al., CD4(+) T-cell dynamics in primary cytomegalovirus infection. *Transplant.Proc.* 2001. 33: 2313-2314.

88. Libri, V., Azevedo, R.I., Jackson, S.E., Di, M.D., Lachmann, R., Fuhrmann, S., Vukmanovic-Stejic, M.et al., Cytomegalovirus infection induces the accumulation of short-lived, multifunctional CD4+CD45RA+CD27+ T cells: the potential involvement of interleukin-7 in this process. *Immunology* 2011. 132: 326-339.

89. Di, M.D., Azevedo, R.I., Henson, S.M., Libri, V., Riddell, N.E., Macaulay, R., Kipling, D.et al., Reversible senescence in human CD4+CD45RA+. *J.Immunol.* 2011. 187: 2093-2100.

90. Herndler-Brandstetter, D., Landgraf, K., Jenewein, B., Tzankov, A., Brunauer, R., Brunner, S., Parson, W.et al., Human bone marrow hosts polyfunctional memory CD4+ and CD8+ T cells with close contact to IL-15-producing cells. *J.Immunol.* 2011. 186: 6965-6971.

91. Hegde, N.R., Dunn, C., Lewinsohn, D.M., Jarvis, M.A., Nelson, J.A., and Johnson, D.C., Endogenous human cytomegalovirus gB is presented efficiently by MHC class II molecules to CD4+ CTL. *J.Exp.Med.* 2005. 202: 1109-1119.

92. van Leeuwen, E.M., Remmerswaal, E.B., Heemskerk, M.H., ten Berge, I.J., and van Lier, R.A., Strong selection of virus-specific cytotoxic CD4+ T-cell clones during primary human cytomegalovirus infection. *Blood* 2006. 108: 3121-3127.

93. Mason, G.M., Poole, E., Sissons, J.G., Wills, M.R., and Sinclair, J.H., Human cytomegalovirus latency alters the cellular secretome, inducing cluster of differentiation (CD)4+ T-cell migration and suppression of effector function. *Proc.Natl.Acad.Sci.U.S.A* 2012. 109: 14538-14543.

94. Mason, G.M., Jackson, S., Okecha, G., Poole, E., Sissons, J.G., Sinclair, J., and Wills, M.R., Human cytomegalovirus latency-associated proteins elicit immune-suppressive IL-10 producing CD4(+) T cells. *PLoS.Pathog.* 2013. 9: e1003635.

95. Quinnan, G.V. and Manischewitz, J.E., The role of natural killer cells and antibody-dependent cell-mediated cytotoxicity during murine cytomegalovirus infection. *J.Exp.Med.* 1979. 150: 1549-1554.

96. Guma, M., Angulo, A., Vilches, C., Gomez-Lozano, N., Malats, N., and Lopez-Botet, M., Imprint of human cytomegalovirus infection on the NK cell receptor repertoire. *Blood* 2004. 104: 3664-3671.

97. Lopez-Verges, S., Milush, J.M., Schwartz, B.S., Pando, M.J., Jarjoura, J., York, V.A., Houchins, J.P.et al., Expansion of a unique CD57(+)/NKG2Chi natural killer cell subset during acute human cytomegalovirus infection. *Proc.Natl.Acad.Sci.U.S.A* 2011. 108: 14725-14732.

98. Wu, Z., Sinzger, C., Frascaroli, G., Reichel, J., Bayer, C., Wang, L., Schirmbeck, R.et al., Human cytomegalovirus-induced NKG2C(hi) CD57(hi) natural killer cells are effectors dependent on humoral antiviral immunity. *J.Virol.* 2013. 87: 7717-7725.

99. Beziat, V., Dalgard, O., Asselah, T., Halfon, P., Bedossa, P., Boudifa, A., Hervier, B.et al., CMV drives clonal expansion of NKG2C+ NK cells expressing self-specific KIRs in chronic hepatitis patients. *Eur.J.Immunol.* 2012. 42: 447-457.

100. Foley, B., Cooley, S., Verneris, M.R., Pitt, M., Curtsinger, J., Luo, X., Lopez-Verges, S.et al., Cytomegalovirus reactivation after allogeneic transplantation promotes a lasting increase in educated NKG2C+ natural killer cells with potent function. *Blood* 2012. 119: 2665-2674.

101. Foley, B., Cooley, S., Verneris, M.R., Curtsinger, J., Luo, X., Waller, E.K., Anasetti, C.et al., Human cytomegalovirus (CMV)-induced memory-like NKG2C(+) NK cells are transplantable and expand in vivo in response to recipient CMV antigen. *J.Immunol.* 2012. 189: 5082-5088.

102. Muntasell, A., Lopez-Montanes, M., Vera, A., Heredia, G., Romo, N., Penafiel, J., Moraru, M.et al., NKG2C zygosity influences CD94/NKG2C receptor function and the NK-cell compartment redistribution in response to human cytomegalovirus. *Eur.J.Immunol.* 2013. 43: 3268-3278.

103. Lanier, L.L., NK cell recognition. *Annu.Rev.Immunol.* 2005. 23: 225-274.

104. Tomasec, P., Braud, V.M., Rickards, C., Powell, M.B., McSharry, B.P., Gadola, S., Cerundolo, V.et al., Surface expression of HLA-E, an inhibitor of natural killer cells, enhanced by human cytomegalovirus gpUL40. *Science* 2000. 287: 1031.

105. Muntasell, A., Vilches, C., Angulo, A., and Lopez-Botet, M., Adaptive reconfiguration

of the human NK-cell compartment in response to cytomegalovirus: a different perspective of the host-pathogen interaction. *Eur.J.Immunol.* 2013. 43: 1133-1141.

106. Beziat, V., Liu, L.L., Malmberg, J.A., Ivarsson, M.A., Sohlberg, E., Bjorklund, A.T., Retiere, C.et al., NK cell responses to cytomegalovirus infection lead to stable imprints in the human KIR repertoire and involve activating KIRs. *Blood* 2013. 121: 2678-2688.

107. Guma, M., Budt, M., Saez, A., Brckalo, T., Hengel, H., Angulo, A., and Lopez-Botet, M., Expansion of CD94/NKG2C+ NK cells in response to human cytomegalovirus-infected fibroblasts. *Blood* 2006. 107: 3624-3631.

108. Sun, J.C., Beilke, J.N., and Lanier, L.L., Adaptive immune features of natural killer cells. *Nature* 2009. 457: 557-561.

109. Petitdemange, C., Becquart, P., Wauquier, N., Beziat, V., Debre, P., Leroy, E.M., and Vieillard, V., Unconventional repertoire profile is imprinted during acute chikungunya infection for natural killer cells polarization toward cytotoxicity. *PLoS.Pathog.* 2011. 7: e1002268.

110. Guma, M., Cabrera, C., Erkizia, I., Bofill, M., Clotet, B., Ruiz, L., and Lopez-Botet, M., Human cytomegalovirus infection is associated with increased proportions of NK cells that express the CD94/NKG2C receptor in aviremic HIV-1-positive patients. *J.Infect.Dis.* 2006. 194: 38-41.

111. Bjorkstrom, N.K., Lindgren, T., Stoltz, M., Fauriat, C., Braun, M., Evander, M., Michaelsson, J.et al., Rapid expansion and long-term persistence of elevated NK cell numbers in humans infected with hantavirus. *J.Exp.Med.* 2011. 208: 13-21.

112. Luetke-Eversloh, M., Hammer, Q., Durek, P., Nordstrom, K., Gasparoni, G., Pink, M., Hamann, A.et al., Human cytomegalovirus drives epigenetic imprinting of the IFNG locus in NKG2Chi natural killer cells. *PLoS.Pathog.* 2014. 10: e1004441.

113. Karre, K., Ljunggren, H.G., Piontek, G., and Kiessling, R., Selective rejection of H-2-deficient lymphoma variants suggests alternative immune defence strategy. *Nature* 1986. 319: 675-678.

114. Joshi, N.S., Cui, W., Chande, A., Lee, H.K., Urso, D.R., Hagman, J., Gapin, L.et al., Inflammation directs memory precursor and short-lived effector CD8(+) T cell fates via the graded expression of T-bet transcription factor. *Immunity.* 2007. 27: 281-295.

115. Rutishauser, R.L., Martins, G.A., Kalachikov, S., Chande, A., Parish, I.A., Meffre, E., Jacob, J.et al., Transcriptional repressor Blimp-1 promotes CD8(+) T cell terminal differentiation and represses the acquisition of central memory T cell properties. *Immunity.* 2009. 31: 296-308.

116. Kallies, A., Xin, A., Belz, G.T., and Nutt, S.L., Blimp-1 transcription factor is required for the differentiation of effector CD8(+) T cells and memory responses. *Immunity.* 2009. 31: 283-295.

117. Banerjee, A., Gordon, S.M., Intlekofer, A.M., Paley, M.A., Mooney, E.C., Lindsten, T., Wherry, E.J.et al., Cutting edge: The transcription factor eomesodermin enables CD8+ T cells to compete for the memory cell niche. *J.Immunol.* 2010. 185: 4988-4992.

118. Pearce, E.L., Mullen, A.C., Martins, G.A., Krawczyk, C.M., Hutchins, A.S., Zediak, V.P., Banica, M.et al., Control of effector CD8+ T cell function by the transcription factor Eomesodermin. *Science* 2003. 302: 1041-1043.

119. Intlekofer, A.M., Takemoto, N., Wherry, E.J., Longworth, S.A., Northrup, J.T., Palanivel, V.R., Mullen, A.C.et al., Effector and memory CD8+ T cell fate coupled by T-bet and eomesodermin. *Nat. Immunol.* 2005. 6: 1236-1244.

120. Knox, J.J., Cosma, G.L., Betts, M.R., and McLane, L.M., Characterization of T-bet and eomes in peripheral human immune cells. *Front Immunol.* 2014. 5: 217.

121. van Aalderen, M.C., Remmerswaal, E.B., Verstegen, N.J., Hombrink, P., Ten, B.A., Pircher, H., Kootstra, N.A.et al., Infection history determines the differentiation state of human CD8+ T cells. *J.Virol.* 2015. 89: 5110-5123.

122. Buggert, M., Tauriainen, J., Yamamoto, T., Frederiksen, J., Ivarsson, M.A., Michaelsson, J., Lund, O.et al., T-bet and Eomes are differentially linked to the exhausted phenotype of CD8+ T cells in HIV infection. *PLoS.Pathog.* 2014. 10: e1004251.

123. Paley, M.A., Kroy, D.C., Odorizzi, P.M., Johnnidis, J.B., Dolfi, D.V., Barnett, B.E., Bikoff, E.K.et al., Progenitor and terminal subsets of CD8+ T cells cooperate to contain chronic viral infection. *Science* 2012. 338: 1220-1225.

124. Popescu, I., Pipeling, M.R., Shah, P.D., Orens, J.B., and McDyer, J.F., T-bet:Eomes balance, effector function, and proliferation of cytomegalovirus-specific CD8+ T cells during primary infection differentiates the capacity for durable immune control. *J.Immunol.* 2014. 193: 5709-5722.

125. Beaulieu, A.M., Zawislak, C.L., Nakayama, T., and Sun, J.C., The transcription factor Zbtb32 controls the proliferative burst of virus-specific natural killer cells responding to infection. *Nat. Immunol.* 2014. 15: 546-553.

126. Kallies, A., Carotta, S., Huntington, N.D., Bernard, N.J., Tarlinton, D.M., Smyth, M.J.,

and Nutt, S.L., A role for Blimp1 in the transcriptional network controlling natural killer cell maturation. *Blood* 2011. 117: 1869-1879.

127. Smith, M.A., Maurin, M., Cho, H.I., Becknell, B., Freud, A.G., Yu, J., Wei, S. et al., PRDM1/Blimp-1 controls effector cytokine production in human NK cells. *J.Immunol.* 2010. 185: 6058-6067.

128. van Gisbergen, K.P., Kragten, N.A., Hertoghs, K.M., Wensveen, F.M., Jonjic, S., Hamann, J., Nolte, M.A. et al., Mouse Hobit is a homolog of the transcriptional repressor Blimp-1 that regulates NKT cell effector differentiation. *Nat.Immunol.* 2012. 13: 864-871.

129. Mackay LK, Minnich M, Kragten NAM, Liao Y, Nota B, Seillet C, Zaid A, et al. Hobit and Blimp1 instruct a universal transcriptional program of tissue residency in lymphocytes. *Science.* 2016; 352:459–463.

The Blimp-1 homologue Hobit identifies effector-type lymphocytes in humans

European Journal of Immunology 2015; 45:2945–2958

Felipe A. Vieira Braga^{1,6}, Kirsten M.L. Hertoghs^{2,6}, Natasja A.M. Kragten^{1,2}, Gina M. Doody⁵, Nicholas A. Barnes⁵, Ester B.M. Remmerswaal^{2,3}, Cheng-Chih Hsiao², Perry D. Moerland⁴, Diana Wouters¹, Ingrid A.M. Derks², Amber van Stijn^{2,3}, Marc Demkes², Jörg Hamann², Eric Eldering², Martijn A. Nolte^{1,2}, Reuben M. Tooze⁵, Ineke J.M. ten Berge³, Klaas P.J.M. van Gisbergen^{1,2,7}, and René A.W. van Lier^{1,2,7}

¹ Department of Hematopoiesis, Sanquin Research and Landsteiner Laboratory
AMC/UvA, Plesmanlaan 125, 1066 CX, Amsterdam, The Netherlands

Departments of ² Experimental Immunology, ³ Internal Medicine; Renal Transplant Unit, and ⁴ Biostatistics and Bioinformatics, AMC, Meibergdreef 9, 1105 AZ, Amsterdam, The Netherlands

⁵ Section of Experimental Haematology, Leeds Institute of Cancer and Pathology, University of Leeds, Leeds LS9 7TF, UK

⁶ Contributed equally for 1st authorship

⁷ Contributed equally for senior authorship

Abstract

Human cytomegalovirus (CMV) induces the formation of effector CD8⁺ T cells that are maintained for decades during the latent stage of infection. Effector CD8⁺ T cells appear quiescent, but maintain constitutive cytolytic capacity and can immediately produce inflammatory cytokines such as IFN- γ after stimulation. It is unclear how effector CD8⁺ T cells can be constitutively maintained in a terminal stage of effector differentiation in the absence of overt viral replication. We have recently described the zinc finger protein Homologue of Blimp-1 in T cells (Hobit) in murine NKT cells. Here, we show that human Hobit was uniformly expressed in effector-type CD8⁺ T cells, but not in naive or in most memory CD8⁺ T cells. Human CMV-specific but not influenza-specific CD8⁺ T cells expressed high levels of Hobit. Consistent with the high homology between the DNA-binding Zinc Finger domains of Hobit and Blimp-1, Hobit displayed transcriptional activity at Blimp-1 target sites. Expression of Hobit strongly correlated with T-bet and IFN- γ expression within the CD8⁺ T cell population. Furthermore, Hobit was both necessary and sufficient for the production of IFN- γ . These data implicate Hobit as a novel transcriptional regulator in quiescent human effector-type CD8⁺ T cells that regulates their immediate effector functions.

Introduction

The CD8⁺ T cell compartment responds to viral infection through the massive expansion of virus-specific clones from the naïve repertoire. These cells differentiate into cycling effector cells that can efficiently clear viral infection through upregulation of effector molecules such as interferon (IFN)- γ , granzyme B, and perforin. An important aspect of CD8⁺ T cell differentiation is the generation of memory CD8⁺ T cells that remain present after viral clearance and that provide enhanced protection against re-infection. Naïve cells can form both effector and memory cells, as evidenced by the transfer of single naïve T cells and molecular bar-coding that have established the pluripotent nature of naïve T cells [1;2]. At early time points during primary infection, memory precursor effector cells (MPECs) that have the potential to generate memory cells separate from short-lived effector cells (SLECs) that lack this capacity [3;4]. MPECs are defined as CD127+KLRG1⁻ cells, whereas SLECs are characterized as CD127-KLRG1⁺ cells. Although only a fraction of MPECs will form bona fide memory cells, the characterization of CD8⁺ T cells as MPECs or SLECs has been instrumental in unraveling the roles of transcription factors in effector and memory differentiation of CD8⁺ T cells. The differentiation of CD8⁺ T cells into MPECs and SLECs is under the control of a network of transcription factors that are specifically upregulated in either MPECs or SLECs. T-bet [5], Blimp-1 [6;7] and Id2 [8] are enriched in SLECs and are essential for SLEC formation, whereas Id3 [8;9], STAT3 [10], Tcf1 [11] and Eomes [12] are upregulated in MPECs and are required for MPEC differentiation. These transcription factors act as a rheostat that balances the ratio of SLECs and MPECs during primary infection to efficiently combat infection without compromising the formation of memory cells.

During chronic infection, CD8⁺ T cells can persist as effector-type cells [13;14]. Effector CD8⁺ T cells in productive infection with chronic viruses such as with HIV-1 in humans and LCMV Docile or Clone 13 in mice display an exhausted phenotype and have limited capacity to produce cytokines such as IFN- γ , TNF- γ and IL-2 [15]. Transcription factors that are expressed in SLECs such as Blimp-1 and T-bet are also important for the generation of effector T cells during productive chronic infection [16;17]. Eomes is highly expressed in chronic effector CD8⁺ T cells in contrast to SLECs and is important in the regulation of the exhaustive phenotype [16]. During chronic latent infection, such as with murine cytomegalovirus (mCMV) in mice, virus-specific CD8⁺ T cells are also constitutively maintained, but T cell exhaustion does not occur [13]. The mCMV-specific effector CD8⁺ T cells remain fully functional and can respond immediately with the production of cytokines [13]. In humans, tetramers have been used to characterize human CMV (hCMV) specific CD8⁺ T cells [18-20]. These CD8⁺ T cells typically express CD45RA but lack CD27 and phenotypically resemble long-lived and fully functional effector CD8⁺ T cells found in mice after mCMV infection [13;18-20]. Human CD45RA⁺CD27⁻ effector CD8⁺ T cells maintain high levels of granzyme B protein and produce high levels of IFN- γ immediately upon stimulation [21]. Similar to memory cells these effector-type cells survive in the absence of detectable levels of virus, but in contrast to memory cells they lack expression of CD122 and CD127 and are not maintained on homeostatic cytokines such as IL-7 and IL-15 [22]. The presence of low amounts of antigen during latent infection imposes conditions on the maintenance of effector

CD8+ T cells that are distinct from those during productive infection, suggesting the requirement for unique transcriptional regulation.

Previously, we have performed microarray analysis on hCMV-specific CD8+ T cells to establish transcription factors that are upregulated during the differentiation of long-lived effector cells in humans [22]. The analysis revealed that transcription factors that are upregulated in murine SLECs such as T-bet and Blimp-1 are also upregulated in human long-lived effector CD8+ T cells. Moreover, Eomes was also upregulated in human long-lived effector cells. However, as all of these transcription factors are strongly upregulated during primary and chronic infection in the presence of high antigen loads, they cannot solely account for the unique behavior of long-lived effector cells during antigen scarcity. Interestingly, our microarray screening revealed that Homologue of Blimp-1 in T cells (Hobit; alias for ZNF683) was specifically upregulated in long-lived effector CD8+ T cells [22]. Hobit is closely related to the transcriptional repressor Blimp-1 that regulates the terminal differentiation of B cells into plasma cells and CD8+ T cells into cytotoxic effectors [23]. Recently, we have described that Hobit is expressed in NKT cells, and required to maintain NKT cells in a quiescent state of terminal effector differentiation in mice [24]. Hobit also regulates immediate effector functions of NKT cells, such as the production of IFN- γ and granzyme B [24]. Therefore, we hypothesized that in humans, Hobit would act to regulate effector-type CD8+ T cells. Here, we describe the expression profile, expression regulation and function of human Hobit. We found that Hobit was specifically expressed in effector-type lymphocytes within the CD8+ T cell, NK and NKT cell lineages. We show that Hobit acts as a transcriptional repressor at Blimp-1 target sites and regulates effector functions.

Results

Human Hobit is specifically expressed in effector-type lymphocytes

Previously, we have identified Hobit as a transcription factor that is specifically up-regulated late during effector differentiation in a microarray study of hCMV-specific CD8+ T cells [22]. To confirm and extend our microarray data, we used qPCR to analyze the expression of Hobit in a panel of leukocyte subsets. As expected, Hobit was expressed in total CD8+ T cells, but expression was not confined to CD8+ T cells, as shown by the abundant expression of Hobit in NK cells (Fig. 1A). Hobit was not expressed or only at low levels in total CD4+ T cells, regulatory T cells and DCs (Fig. 1A). Using CD27 and CD45RA to separate CD8+ T cells into naive (CD27+CD45RA+), effector (CD27-CD45RA+) and memory cells (CD27+CD45RA-), we found that Hobit was expressed at much higher levels in effector cells than in naive and memory cells (Fig. 1B). Within the NK cell lineage, the expression of Hobit was enriched in the CD56dim population compared with the CD56bright population (Fig. 1C). CD56dim NK cells are terminally differentiated cytotoxic cells with low proliferative capacity. In contrast, CD56bright NK cells have a high proliferative capacity and low cytotoxic potential [25]. Thus, Hobit is specifically found in lymphocytes with immediate effector function.

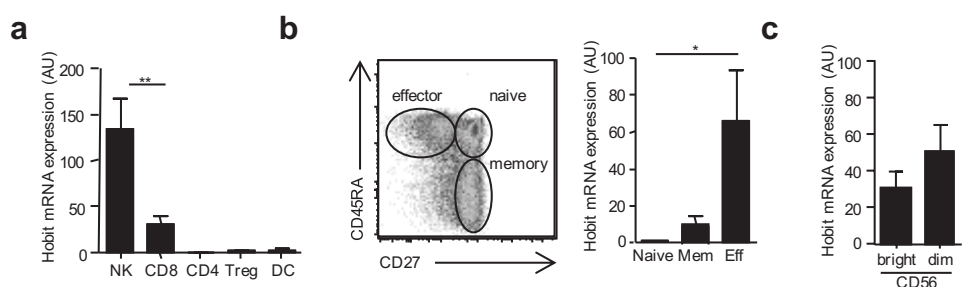


Figure 1. Hobit mRNA expression is confined to effector CD8+ T cells and NK cells. (A) The expression of Hobit was analyzed at the mRNA level using qPCR in the indicated subsets of leukocytes. (B) (Left panel) Dotplot depicts the sorting strategy for naive, memory and effector subsets of CD8+ T cells that were identified by CD27 and CD45RA expression as indicated. (Right panel) Subsets of naive, memory (mem) and effector (eff) CD8+ T cells were isolated and analyzed for Hobit expression using qPCR. (C) Hobit expression was analyzed in CD56bright and CD56dim subsets of NK cells. (A-C) Data are shown as mean \pm SEM (n=3 (A and B) or 5 (C)) and are representative of two independent experiments. * $p < 0.05$; ** $p < 0.01$; Anova with post-hoc Bonferroni test.

Protein expression of Hobit identifies effector-type lymphocytes

We generated a monoclonal antibody (Sanquin-Hobit/1) against a truncated form of Hobit to enable analysis of Hobit protein expression by flow cytometry (Fig. 2A). The Hobit specificity of this antibody was verified using NK92 cells that have endogenous Hobit expression and NK92-Hobit knockdown (KD) cells, in which Hobit mRNA expression was reduced using Hobit-targeting shRNA (Fig. 2B). Staining with the antibody was reduced in NK92-Hobit KD cells compared with mock transduced NK92 cells confirming its specificity for Hobit (Fig. 2, C and D). We used this newly developed anti-Hobit antibody to analyze effector differentiation of CD8+ T cells in human

peripheral blood (Fig. 3, A and B). We found that Hobit is uniformly expressed in effector CD8⁺ T cells and in a subset of effector memory CD8⁺ T cells, but not in naïve and central memory CD8⁺ T cells (Fig. 3, A and B). Hobit expression in circulating EM cells was bimodal, suggesting heterogeneity within this population (Fig. 3A). We observed that KLRG1⁺ in contrast to KLRG1⁻ EM CD8⁺ T cells displayed substantial expression of Hobit (Fig. 3, C and D). KLRG1 is a receptor associated with terminal differentiation of effector lymphocytes [26]. Therefore, the correlation between Hobit and KLRG1 expression within EM CD8⁺ T cells suggests that Hobit expression is associated with terminal differentiation of CD8⁺ T cells. We analyzed the CD8⁺ T cell compartment in tonsils to determine Hobit expression within secondary lymphoid tissues. As effector CD8⁺ T cells are nearly absent from tonsils [27], CD8⁺ T cells were separated into naïve and memory cells and analyzed for Hobit expression. We observed that Hobit expression was low on naïve and memory CD8⁺ T cells within tonsils (Fig. 3, E and F), which is in line with the absence of CD8⁺ T cells with explicit effector functions from the secondary lymphoid tissues. Staining for Hobit on virus-specific populations of CD8⁺ T cells that were identified using tetramers, showed strong expression in hCMV-specific CD8⁺ T cells (hCMV-IPS and hCMV-NLV), intermediate expression in lytic EBV-specific CD8⁺ T cells (EBV-EPL), but no or low expression in non-lytic EBV specific (EBV-HPV) and Flu-specific CD8⁺ T cells (Flu-GIL, Fig. 3G and Table S1). These results substantiate the expression profile of Hobit in CD8⁺ T cell subsets identified by CD27 and CD45RA phenotype, as hCMV-specific CD8⁺ T cells are largely maintained as quiescent effector cells and non-lytic EBV specific and flu-specific CD8⁺ T cells as memory cells [18;19;28]. The intermediate expression levels of Hobit in lytic EBV-specific CD8⁺ T cells are consistent with the more pronounced effector or effector memory phenotype of these cells compared with non-lytic EBV specific CD8⁺ T cells [18;19;28]. Similar to effector CD8⁺ T cells, CD56dim NK cells in peripheral blood uniformly expressed Hobit (Fig. 4, A, C and D). In line with Hobit mRNA expression (Fig. 1, A and C), CD56dim NK cells expressed more Hobit protein than CD56bright NK cells (Fig. 4, A and D). Consistent with the lack of Hobit expression in tonsillar CD8⁺ T cells, CD56dim and CD56bright NK cells within tonsils did not express Hobit (Fig. 4, B, C and D). In addition to NK cells, we observed Hobit expression in a considerable fraction of the NKT cell population (Fig. 4, E and F). We did not detect substantial expression of Hobit in B cells, CD4⁺ T cells including regulatory T cells, subsets of dendritic cells, monocytes and neutrophils (Fig. 4G). Thus, similar to Hobit mRNA expression, Hobit protein expression is confined to effector-type lymphocytes within the CD8⁺ T cell, NK cell, and NKT cell lineage.

Transcriptional variants of Hobit display distinct activity at Blimp-1 target sites

Human Hobit is a putative zinc finger-containing transcription factor of 504 amino acids that contains 4 C2H2-type zinc fingers and shares approximately 58% overall identity with mouse Hobit [24]. The gene encoding human Hobit (ZNF683) contains 6 exons and is located on chromosome 1p36.11 (Fig. 5A). The genomic context, which is conserved with the mouse gene [24], suggests that ZNF683 and the adjacent gene AIM1L arose through duplication from the region spanning PRDM1

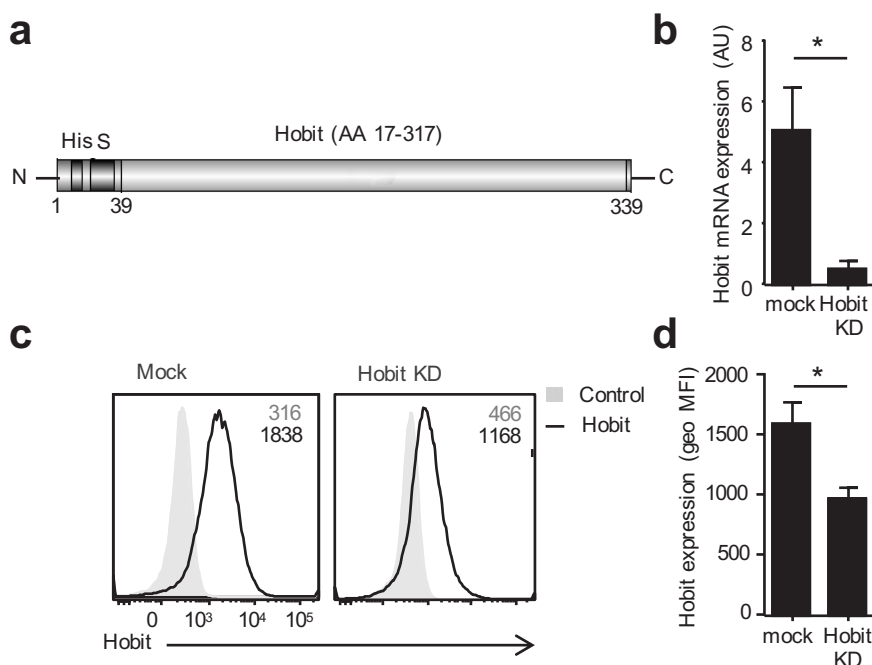


Figure 2. Clone Sanquin-Hobit/1 specifically recognizes Hobit in NK92 cells. (A) Schematic representation of the truncated Hobit protein that was used for immunization to generate anti-Hobit antibodies. (B) Hobit mRNA expression was determined in NK92 cells that were transduced with a mock or Hobit KD construct by qPCR. (C-D) Sanquin-Hobit/1 specificity was determined using intracellular flow cytometry in NK92 cells that were transduced with a mock or Hobit KD construct. (C) Histogram overlay depicts the expression of Hobit. Numbers in upper right corner show geometric mean fluorescence intensity (geo MFI) of Hobit expression. (D) The geo MFI of Hobit expression in mock and Hobit KD NK92 cells was determined. (B and D) Data are shown as mean \pm SEM ($n=5$) and are pooled data of five independent experiments. * $p < 0.05$; Two-tailed paired t-test.

(encoding Blimp-1) and AIM1 (Fig. 5B). Human Hobit shares considerable homology with Blimp-1 within the zinc finger region (78% identity and 91% similarity with the 4 most N-terminal zinc fingers of Blimp-1), but lacks the SET domain that characterizes Blimp-1 and the other members of the PRDM family (Fig. 5A). Thus, Hobit resembles the Blimp-1 isoform, which initiates from an intragenic promoter and encodes a protein lacking the SET domain. Sequencing of individual clones after molecular cloning of Hobit from PBMCs resulted in the identification of 3 different transcripts of the ZNF683 gene. These transcripts encode 3 different proteins that we designated as Hobit Large (L), Hobit Extra Large (XL) and Hobit Small (S, Fig. 5A). Compared with Hobit L, Hobit XL contains 20 additional amino acids between zinc finger 2 and 3 that are encoded by an alternative exon in between exons 5 and 6 of Hobit L. Therefore, the zinc finger domains of Hobit L, but not those of Hobit XL, are spatially aligned in the same manner as the first 4 zinc finger domains of Blimp-1 (Fig. 5A). The Hobit S transcript contains a deletion of 20 base pairs compared with Hobit L, which arises from alternative splicing of exon 4 onto exon 5. This deletion

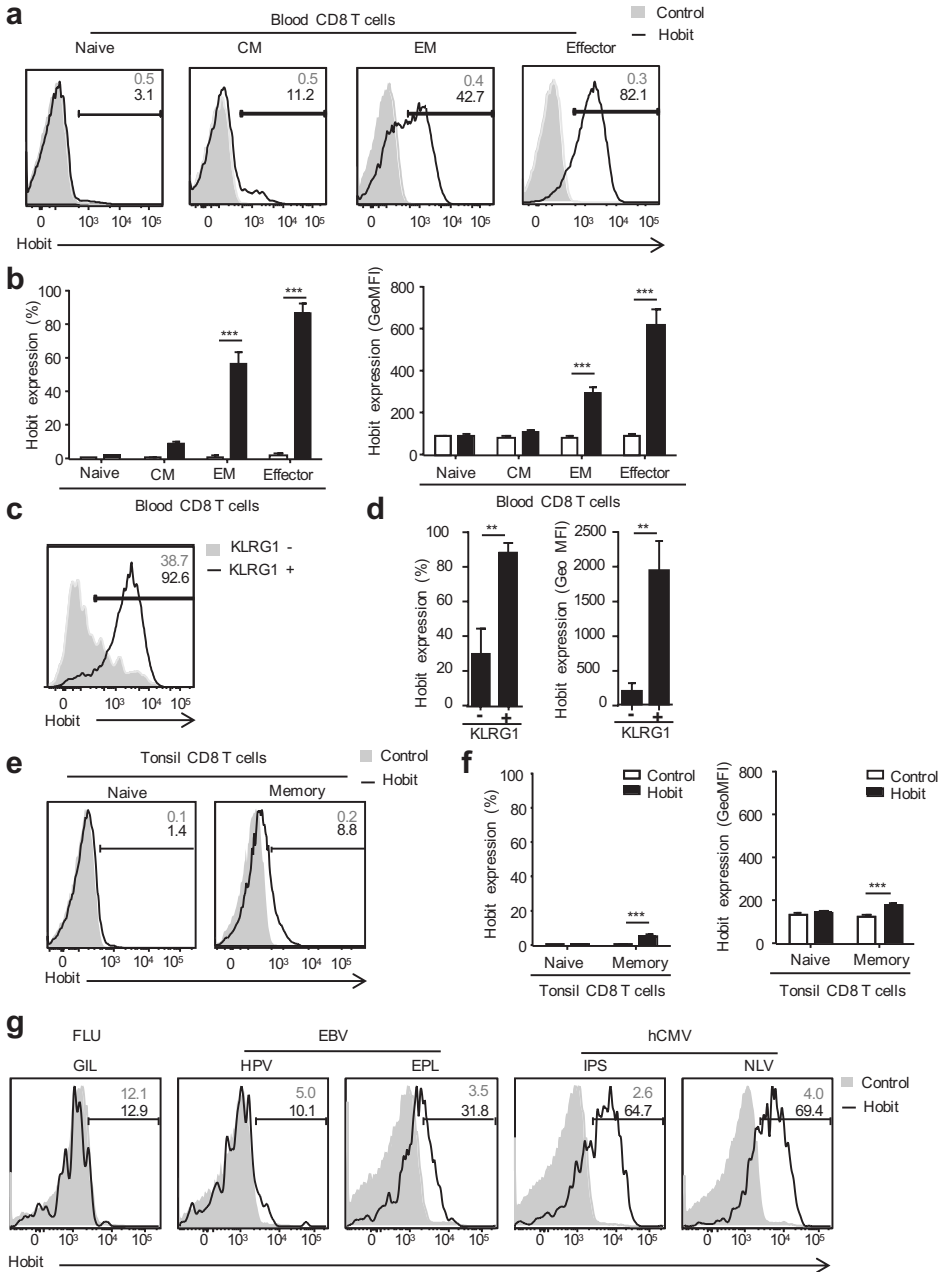


Figure 3. Hobit protein is expressed under steady state conditions in cytotoxic CD8+ T-cells.

(A-F) Hobit protein expression was assessed in the indicated CD8+ T cell subsets that were identified using staining for CD27, CD45RA and CCR7 to separate naïve (CD27+CD45RA+CCR7+), total memory (CD27+CD45RA-), central memory (CM; CD27+CD45RA-CCR7+), effector memory (EM; CD27+CD45RA-CCR7-), effector cells (CD27-CD45RA+CCR7-). (A) Histogram overlays depict the expression of Hobit in blood CD8+ T-cells. Numbers in upper right corner show percentage of Hobit+ CD8+ T-cells. (B) Bar graphs display the percentage of Hobit+ cells and the geometric mean fluorescence intensity (geo MFI) of Hobit expression in blood CD8+ T cell subsets. (C) Histogram overlays depict the expression of Hobit

in KLRG1- and KLRG1+ EM CD8+ T-cells. (D) Bar graphs display the percentage of Hobit positive cells and the geo MFI of Hobit expression in KLRG1- and KLRG1+ EM CD8+ T cells. (E) Histogram overlays depict the expression of Hobit in the indicated subsets of tonsillar CD8+ T cells. (F) Bar graphs display percentage of Hobit+ cells and Hobit geo MFI in tonsil CD8+ T cells. (G) Hobit histogram overlays of the indicated subsets of virus-specific CD8+ T cells that were identified by tetramer binding and staining for CD8. (A, C and E) Data shown are representative of six donors (unpaired samples) or (G) three donors. (B, D and F) Data are shown as mean \pm SEM (n=6 (B and F) or 4 (D), from a pool of two independent experiments experiments. ** p<0.01; *** p<0.001; Anova with post-hoc Bonferroni test.

introduces a frameshift and results in a premature stop codon that truncates Hobit S within the first zinc finger domain (Fig. 5A). The abundance of the Hobit isoforms was determined in subsets of NK cells and CD8+ T cells using a PCR that distinguishes between the 3 transcripts, as verified using transfectants that over-expressed either Hobit XL, L or S (Fig. 5, C and D). The analysis showed that Hobit L was present at higher levels than Hobit XL in EM and effector CD8+ T cells as well as in CD56dim and CD56bright NK cells. The levels of Hobit S were below detection limit. Thus, Hobit L, which displayed the highest similarity with Blimp-1, is the most prominently expressed isoform of Hobit.

Blimp-1 has been reported to primarily function as a transcriptional repressor using target sites that overlap with those of IRF1 and IRF2 [29;30]. As the zinc finger domains confer DNA-binding specificity of Blimp-1 and this region is most highly conserved with Hobit, we analyzed whether Hobit was able to recognize known target sites of Blimp-1. Previously, binding sites of Blimp-1 have been demonstrated within the promoter regions of TAPASIN, BTN3A3 and SP110 [31;32]. Therefore, we generated the Hobit isoforms with an HA-tag to enable supershift. We found that Hobit XL and L, similar to Blimp-1, bound to target sequences present in the promoters of TAPASIN, BTN3A3 and SP110 using EMSA (Fig. 6A). The defect in DNA binding of Hobit S showed that the zinc finger region of Hobit was essential (Fig. 6A). Reciprocally, a construct containing only the zinc finger domains of Hobit showed that the minimal region sufficient for DNA binding activity was located within the zinc finger region (Fig. 6A). Using a luciferase reporter assay, we established that Hobit L similar to Blimp-1 acted as a transcriptional repressor at these sites (Fig. 6B). Furthermore, the zinc finger domains of Hobit were both essential and sufficient for Hobit to suppress expression of the luciferase reporter. Interestingly, although Hobit XL was able to bind to the same target sequences as Hobit L, the Hobit XL isoform lacked transcriptional repressor activity (Fig. 6, A and B). This underlines the importance of the spacing of the zinc fingers in the functional activity of Hobit and suggests that Hobit XL can act as a negative regulator of Hobit L. Thus, the dominant Hobit L isoform functions as a transcriptional repressor that uses similar target sites as Blimp-1, indicating that Hobit and Blimp-1 are transcription factors with overlapping roles.

Hobit is expressed in IFN- γ producing CD8+ T cells and regulates IFN- γ production. Quiescent effector CD8+ T cells in latent hCMV infection have constitutive expression of IFN- γ mRNA that enables them to immediately produce IFN- γ upon antigenic triggering [22]. To identify transcription factors in these cells that displayed a synchronous expression profile with IFN- γ , we compared microarray data [22] from hCMV-specific cells at peak, 1 year post-infection and during latency with naive CD8+

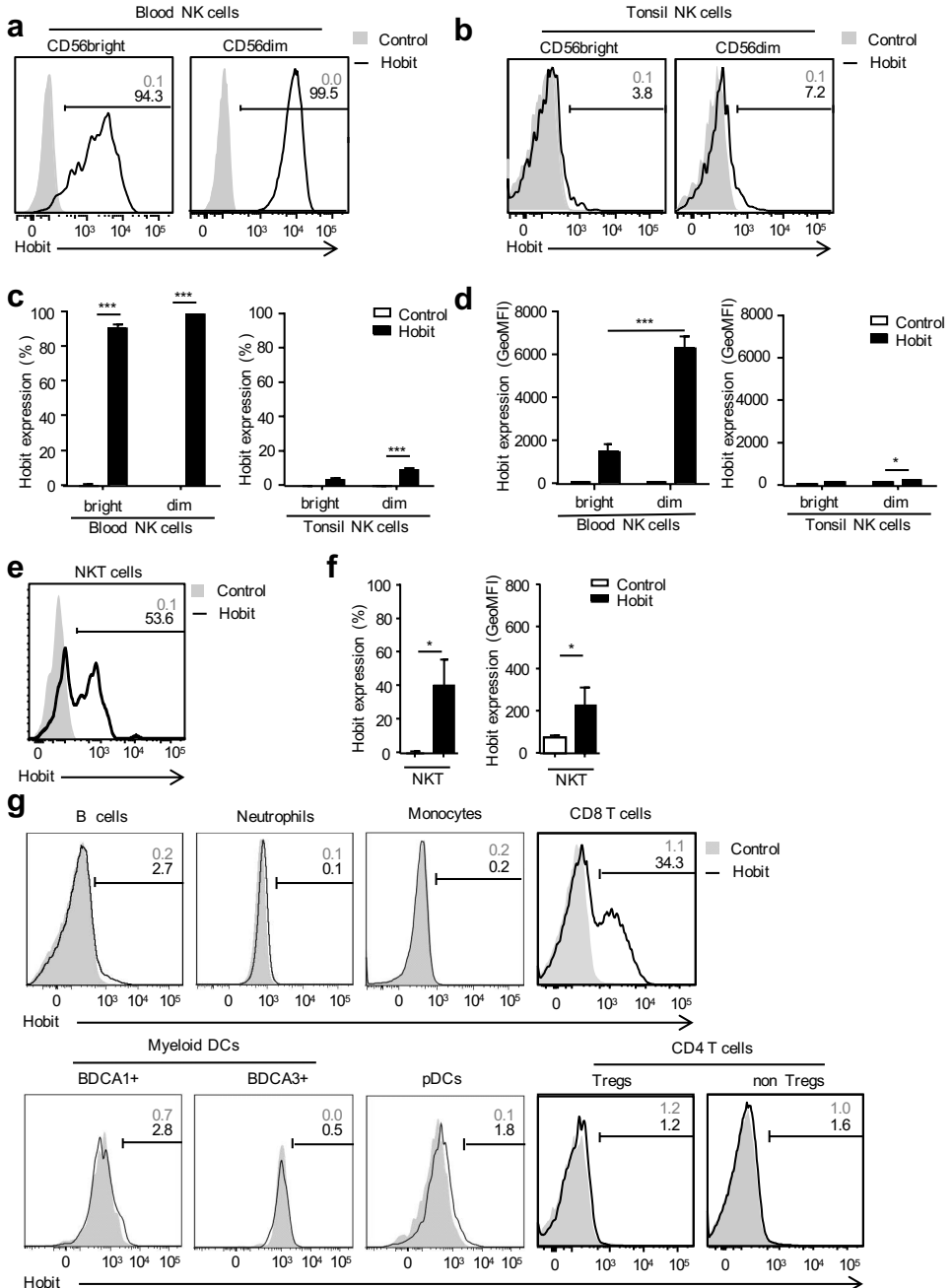


Figure 4. Hobit protein is expressed under steady state conditions in cytotoxic NK and NKT cells. (A and B) Histogram overlays depict the expression of Hobit in (A) blood and (B) tonsil NK cells. Numbers in upper right corner show percentage of Hobit⁺ cells. (C and D) Bar graphs display (C) percentage of Hobit⁺ cells or (D) the geometric mean fluorescence intensity (geo MFI) of Hobit expression in NK cells. (E) Histogram overlays depict the expression of Hobit in NKT cells. (F) Bar graphs display percentage of Hobit⁺ cells or geo MFI of Hobit expression in NKT cells. (G) Histograms depict the expression of Hobit in the indicated subsets of leukocytes from peripheral blood. Neutrophils were obtained from

the polymorphonuclear fraction and the other subsets from the mononuclear fraction after Ficoll gradient centrifugation. B cells were identified as CD3-CD19+CD20+ cells, neutrophils as CD16+ cells, monocytes as CD3-CD14+ cells, myeloid dendritic cells (DCs) as CD3-CD14-CD19-CD56-HLADR+ cells and then subdivided in the indicated fractions based on BDCA1, BDCA3 expression, plasmacytoid DCs (pDCs) as CD3-CD14-CD19-CD56-HLADR+BDCA4+ cells, regulatory T cells (Tregs) as CD3+CD4+Foxp3+ cells, non Tregs as CD3+CD4+Foxp3- cells and CD8+ T cells as CD3+CD8+ cells. Numbers in upper right corner represent percentage of Hobit+ cells. (A, B, E and G) Data shown are representative of six donors (A and B) or four donors (E) or two donors (G). (C, D and F) Data are shown as mean \pm SEM (n=6 (C and D) or 4 (F)) and are pooled data of two (C and D) or one (F) independent experiment. * p<0.05; *** p<0.001; Anova with post-hoc Bonferroni test (C and D); Two-tailed paired t-test (F).

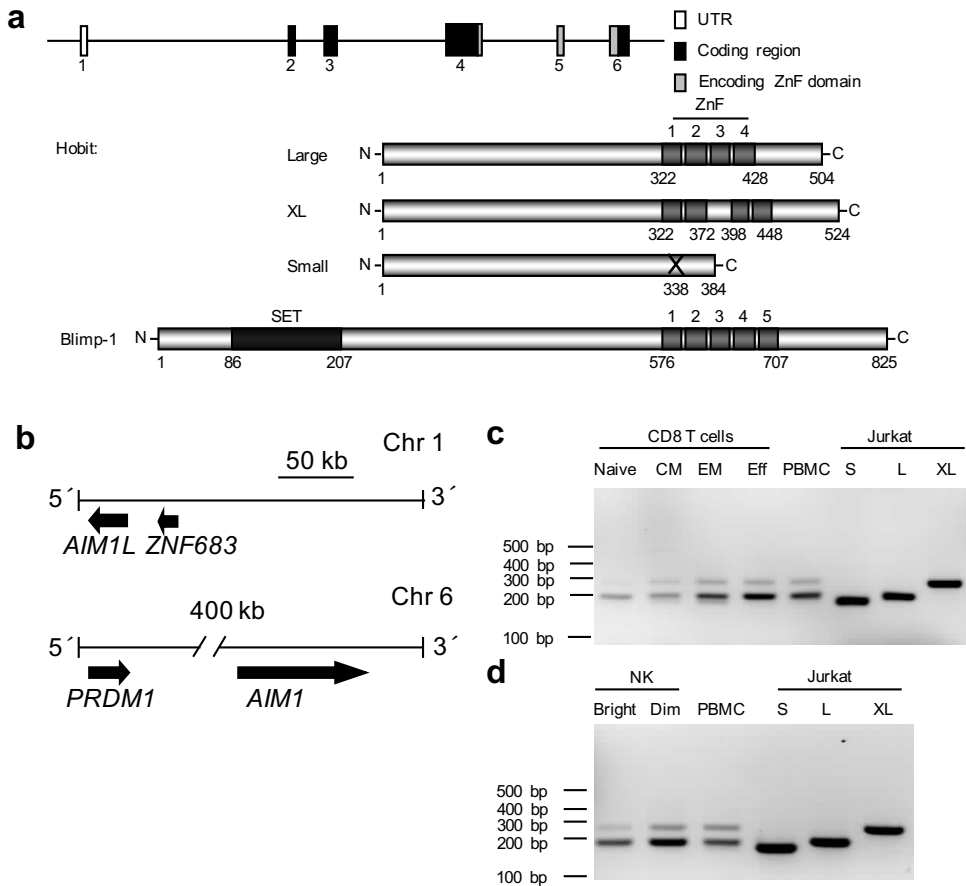


Figure 5. Alternative splicing results in expression of 3 different Hobit isoforms. (A) Schematic models of the genomic structure of ZNF683 (encoding Hobit, top) and the protein structures of Hobit Large, XL and Small and Blimp-1 (bottom). (B) The orientation of ZNF683 and AIM1L on chromosome 1 and PRDM1 (encoding Blimp-1) and AIM1 on chromosome 6 is depicted. (C,D) The relative expression of Hobit isoforms was analyzed using a PCR that distinguishes between the isoforms in (C) CD8+ T cell subsets and in (D) NK cell subsets. Jurkat cells transduced with Hobit XL, Large (L) or Small (S) were used as controls. Data shown are representative of two independent experiments.

T cells, using nearest neighbor analysis with IFN- γ as a starting point. We found 31 genes that clustered together with IFN- γ , as similar to IFN- γ , they were highly expressed during all stages of hCMV infection, but not in naive CD8 $^{+}$ T cells (Fig. 7A). As expected, T-bet, which is essential to induce IFN- γ expression, associated with IFN- γ in hCMV-specific CD8 $^{+}$ T cells (Fig. 7A). Strikingly, the expression pattern of Hobit and Blimp-1 more closely resembled the expression profile of IFN- γ than that of T-bet (Fig. 7A), suggesting that Hobit and Blimp-1 may be involved in the regulation of IFN- γ expression in hCMV-specific effector CD8 $^{+}$ T cells. We did not find other transcription factors that had an expression profile that matched that of IFN- γ (Fig. 7A). IFN- γ protein expression requires activation, making it impossible to directly analyze for co-expression of Hobit and IFN- γ protein in CD8 $^{+}$ T cells under resting conditions. Supporting the nearest neighbor analysis, Hobit and T-bet were stringently co-expressed in CD8 $^{+}$ T cells using flow cytometry (Fig. 7B). Moreover, Hobit also strictly correlated with T-bet expression in virus-specific CD8 $^{+}$ T cells, as Flu-specific, EBV-specific and CMV-specific CD8 $^{+}$ T cells displayed low, intermediate and high expression of Hobit and T-bet, respectively (Fig. 7C and Table S1). This suggests that Hobit, similar to T-bet, may be involved in the regulation of IFN- γ expression.

The strong correlation of Hobit expression with T-bet and IFN- γ expression prompted us to study the role of Hobit in IFN- γ production. Therefore, NK92 cells were transduced with shRNAs that induced specific knockdown of Hobit expression (Fig. 2, B-D). Mock transduced NK92 cells upregulated expression of IFN- γ mRNA and protein to a higher extent than NK92-Hobit KD cells after stimulation with PMA and ionomycin (Fig. 7, D and E). This shows that Hobit is involved in the regulation of IFN- γ production. To examine whether Hobit was sufficient to induce IFN- γ expression, Jurkat cells that do not express endogenous Hobit were transduced with Hobit L, Hobit XL, or Hobit S or with an empty vector as a control (Fig. 7F). After brief stimulation with PMA and ionomycin, Jurkat cells expressing Hobit L, in contrast to control, or Hobit XL or Hobit S expressing Jurkat cells, produced IFN- γ , as measured by ELISA (Fig. 7F). Thus, Hobit L is the functionally active isoform of Hobit that is both necessary and sufficient to induce production of IFN- γ .

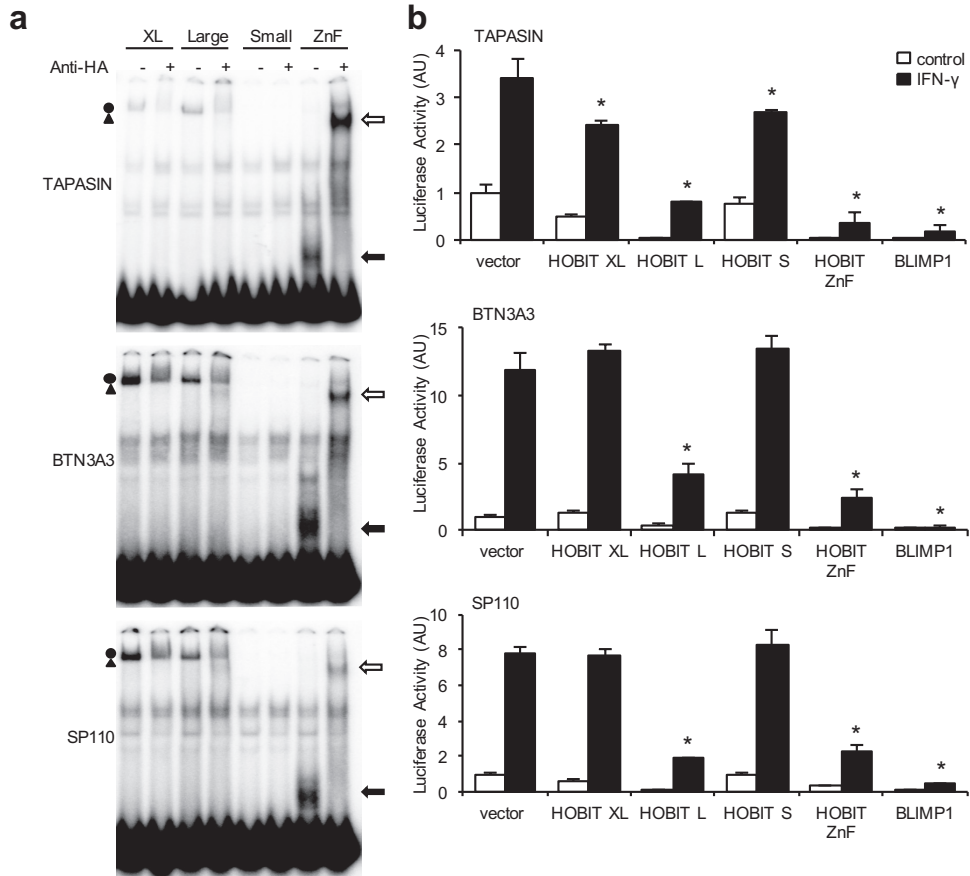


Figure 6. The Hobit isoforms display distinct binding and transcriptional activity at Blimp-1 target sequences. (A) EMSA evaluation of Hobit variants is shown on previously identified Blimp-1 binding sites in the promoter sequences of TAPASIN (top panel), BTN3A3 (center panel), and SP110 (bottom panel). Comparable amounts of in vitro translated proteins representing the Extra Large (XL), Large, Small or Zinc Finger region only (ZnF) forms of Hobit were assessed in the absence or presence of an antibody to the HA epitope tag. The position of Hobit XL (closed circle, non-supershifted), Large (closed triangle, non-supershifted), and ZnF (closed arrow, non-supershifted and open arrow, supershifted) proteins are indicated. Supershifted Hobit XL and Large are not visible. (B) The repressive capacity of Hobit and Blimp-1 was analyzed at promoter sequences of TAPASIN (top panel), BTN3A3 (center panel), and SP110 (bottom panel) in HeLa cells transduced with luciferase reporter constructs containing these promoter sequences and the indicated overexpression constructs of Hobit and Blimp-1. Luciferase activity was assessed in the absence or presence of 200 IU/ml IFN- γ . The data are displayed as arbitrary units (AU) with unstimulated cells co-transfected with the empty overexpression vector set at 1. (A and B) Data are representative of two independent experiments using separate plasmid preparations. (B) Data are shown as mean \pm SD (n=3, technical replicates). * $p < 0.05$; Anova with post-hoc Bonferroni test.

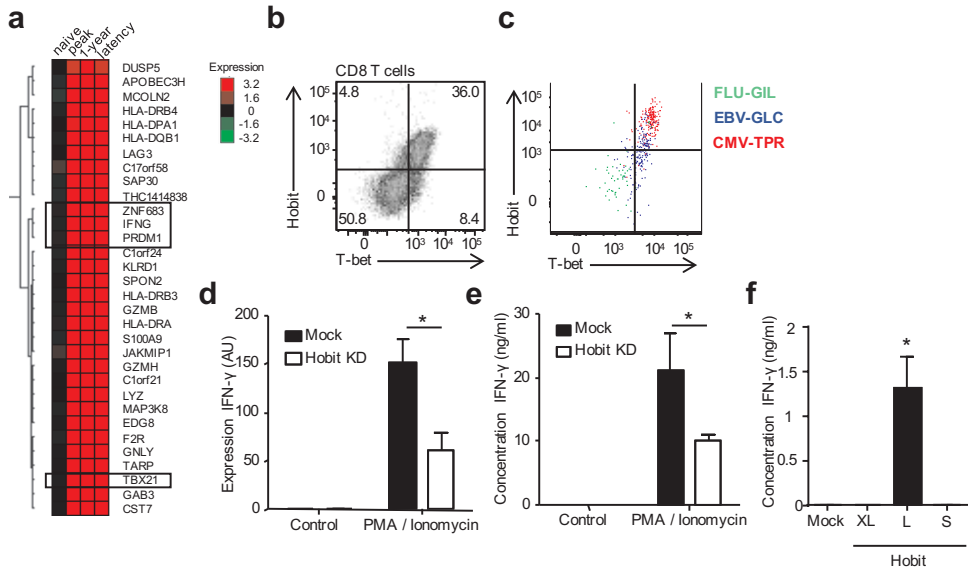


Figure 7. Hobit strongly correlates with IFN- γ production in CD8+ T cells and induces IFN- γ expression. (A) The genes that co-cluster with IFN- γ are depicted, using nearest neighbor analysis with IFN- γ as a starting point on microarray data of naive and hCMV-specific CD8+ T cells at peak of infection, 1-year post-infection and during latency. Shown are the mean changes in transcript levels with respect to naive CD8+ T cells. (B) Dotplot depicts CD8+ T-cells that were analyzed for intracellular co-expression of T-bet and Hobit. Numbers represent percentage of cells within quadrant. (C) Dot plot depicts expression of T-bet and Hobit in flu-specific (green), EBV-specific (blue) and CMV-specific (red) CD8+ T cell populations. (D-F) IFN- γ production was analyzed by (D) qPCR and (E) ELISA in NK92 cells that were transduced with mock or Hobit KD constructs and cultured in the absence or presence of PMA and ionomycin. (F) IFN- γ production was examined using ELISA in Jurkat cells that were transduced with empty vector, Hobit XL, Hobit Large or Hobit Small and briefly cultured in the presence of PMA and ionomycin. (B and C) Data are representative of six donors from three independent experiments (B) or of two donors from one experiment (C). (D, E and F) Data are shown as mean \pm SEM ($n=6$ (D and E) or 3 (F)) and are pooled of three independent experiments. * $p < 0.05$; Two-tailed t-test (D and E); Anova with post-hoc Bonferroni test (F).

Discussion

The differentiation of CD8⁺ T cells into effector and memory cells is controlled through a well-established network of transcription factors. Here, we have described that human CD8⁺ T cells in a resting effector state specifically expressed the Blimp-1 homologue Hobit both at the mRNA and protein level. Consistent with the specific expression in effector-type CD8⁺ T cells, Hobit was present at higher levels in hCMV- than in EBV- and Flu-specific CD8⁺ T cells. Hobit was able to function as a transcriptional repressor that recognized the same target sites as Blimp-1, suggesting overlapping roles for the homologous transcription factors. We found that Hobit regulated the induction of IFN- γ production.

Hobit shares high homology with Blimp-1, in particular within the Zinc finger region. In line with the structural similarity, we have shown that Hobit recognized known target sites of Blimp-1 including those within the TAPASIN, BTN3A3 and SP110 promoters [31]. The Zinc fingers of Blimp-1 show extensive evolutionary conservation and conserved target site recognition between evolutionary distant species [32]. The data presented here demonstrate that the conservation of the Zinc finger domains between Hobit and Blimp-1 is reflected in the capacity to recognize similar binding sites. This suggests that both transcription factors may have largely overlapping site recognition *in vivo*. The 2 most N-terminal zinc finger domains of Blimp-1 are crucial for Blimp-1 to bind its target sequences [33]. Similarly, we found that the Zinc finger domains of Hobit were both required and sufficient to recognize Blimp-1 target sites. Hobit lacks the PR-domain that is typical for Blimp-1 and the other members of the PRDM family [34]. The PR-domain which is similar to the SET domain, confers endogenous methyltransferase activity, but appeared dispensable for Blimp-1 to induce histone modifications [33]. Indeed, a functional isoform of Blimp-1, Blimp-1 α , lacking the PR-domain is observed in human myeloma plasma cells as well as NK cells [35-37]. Rather than directly inducing histone methylation, Blimp-1 has been described to recruit the G9a methyltransferase through the 2 most N-terminal Zinc finger domains [38]. In addition, Blimp-1 recruits the histone deacetylase HDAC2 and Groucho proteins through these Zinc finger domains and a proline rich region directly upstream [39;40]. The high homology between Hobit and Blimp-1 within the Zinc finger domains suggests that the ability to recruit these histone-modifying proteins may be conserved between the transcription factors. Consistent with this notion, we observed that Hobit similar to Blimp-1 acted as a transcriptional repressor. Of the three splice variants of Hobit that we detected, Hobit XL and L in contrast to Hobit S were commonly expressed in human NK cells and CD8⁺ T cells. Although Hobit XL and L both bound to known Blimp-1 target sites, only Hobit L displayed transcriptional repressor activity, suggesting that Hobit XL may function as a dominant negative Hobit isoform that suppresses the function of Hobit L. Also Hobit S may function as a dominant negative isoform, but its limited expression, suggests that it only has a modest role in human lymphocytes under homeostatic conditions. Thus, Hobit, in particular Hobit L, and Blimp-1 may regulate similar transcriptional programs in effector-type CD8⁺ T cells and NK cells.

At a functional level the limited available evidence suggests that Hobit and Blimp-1 regulate similar programs, as both have been reported to control the expression of granzyme B and IFN- γ [6;7;17;24;37;41]. We have shown previously that Hobit

induces granzyme B and represses IFN- γ in murine NKT cells [24] and Blimp-1 has been shown to regulate granzyme B and IFN- γ in a similar manner in murine CD8+ T cells and NK cells [6;7;17;37;41]. A role for human Hobit in the regulation of granzyme B is suggestive, as expression of Hobit is confined to cytotoxic populations of CD8+ T cells and NK cells. However, we did not find evidence for the regulation of granzyme B expression by human Hobit (unpublished observations). We found a strong association between Hobit and IFN- γ and the IFN- γ regulating transcription factor T-bet. In NK92 cells, Hobit was required for the regulation of IFN- γ expression and using Jurkat cells we found that Hobit was sufficient to induce IFN- γ expression. Strikingly, Hobit appears to positively regulate IFN- γ whereas it acts as a transcriptional repressor on known motifs of Blimp-1. Although it is possible that Hobit-driven regulation at the IFN- γ locus is indirect, Hobit similar to Blimp-1 may positively induce expression in a direct manner. Blimp-1 has been shown to directly act on the IL-10 locus, which results in enhanced expression of IL-10 [42]. Interestingly, human Hobit positively regulated IFN- γ expression, whereas murine Hobit and Blimp-1 negatively regulated IFN- γ expression [24;37;43]. The reason for these differential effects of Hobit are unclear, but they may be related to differences in cellular context as Hobit is expressed in different cell types in mouse and man. Overall, Hobit is involved in the regulation of immediate effector functions that include the regulation of IFN- γ expression.

The transcriptional regulation of the differentiation and maintenance of hCMV-specific CD8+ T cells is complex. We have previously shown that transcription factors that are essential for the formation of effector cells such as T-bet, Eomes and Blimp-1 are also expressed in hCMV specific CD8+ T cells during latency and at late time points after primary infection [22]. The expression of these transcription factors suggests that the explicit effector phenotype of hCMV-specific CD8+ T cells can be explained through common transcriptional regulation pathways with early effector cells. The capacity of hCMV specific CD8+ T cells to persist late after primary infection suggests that they require a combination of transcription factors that is not found in short-lived effectors for long-term maintenance. Our findings in hCMV-specific CD8+ T cells suggest a role for Hobit in the transcriptional regulation of these long-lived effector-type cells. The role of Hobit is not confined to hCMV-specific cells and long-lived effector-type CD8+ T cells, as we have also found expression of Hobit in the KLRG1+ subset of EM CD8+ T cells. Long-lived effector cells uniformly express KLRG1 [26], suggesting that Hobit expression is upregulated in terminally differentiated CD8+ T cells that are defined by KLRG1 expression. The expression of Hobit within KLRG1+ EM CD8+ T cells is in line with the capacity of these memory cells to rapidly produce cytokines and to exert direct cytotoxic potential similar to effector cells.

The *in vivo* study of Hobit in CD8+ T cell differentiation is complicated as, in contrast to human Hobit, murine Hobit is specifically expressed in NKT cells, but not or at low levels in naïve, memory and effector subsets of CD8+ T cells [24]. Interestingly, murine NKT cells are maintained after development in the thymus as resting cells in an effector or effector memory stage. Similar to long-lived effector CD8+ T cells, NKT cells are able to generate cytokine responses within hours after stimulation and a thymic subset of mature NKT cells displays constitutive granzyme B expression [44]. Hobit not only regulates the expression of granzyme B and IFN- γ in NKT cells,

but also is essential for the maintenance of the mature thymic NKT cell subset [24]. Despite the disparity in expression between human and murine Hobit, this suggests that similar to murine Hobit in NKT cells, human Hobit in CD8+ T cells may regulate the maintenance of long-lived effector cells and their capacity to generate immediate effector responses.

The specific expression of the transcription factor Hobit in long-lived effector cells with immediate effector function such as hCMV-specific CD8+ T cells suggests that these cells undergo a unique and late differentiation process that separates them from other effector and memory cells. Long-term maintenance and the immediate capacity to produce effector molecules are a useful, but uncommon, combination of features of CD8+ T cells in adoptive transfer settings of vaccination. Therefore, our findings on the role of Hobit in the differentiation process of CD8+ T cells may form an important first step in the development of vaccine strategies that employ long-lived effector CD8+ T cells.

Materials and Methods

Structural analysis.

Genomic and amino acid sequences of Hobit and Blimp-1 were derived from the Ensembl project of genome databases. Structural domains in Hobit and Blimp-1 were assigned with the SMART simple modular architecture research tool.

Reagents.

The following antibodies were used: anti-CD3 (BD Biosciences), anti-CD4 (BD Biosciences), anti-CD8 (BD Biosciences and BioLegend), anti-CD16 (Sanquin Reagents), anti-CD19 (eBioscience), anti-CD25 (BD Biosciences), anti-CD27 (Sanquin Reagents), anti-CD45RA (BD Biosciences), anti-CD56 (BD Biosciences), anti-CCR7 (BD Biosciences), anti-granzyme B (Invitrogen), anti-TCR V β 11 (Immunotech), anti-TCR V α 24J18 (eBioscience), anti-IFN- γ (BD Biosciences), and anti-T-bet (BioLegend). Anti-HA antibodies were purchased from Abcam and Roche. The following tetramers to identify virus-specific CD8⁺ T cells were used: hCMV-NLV, hCMV-TPR and hCMV-IPS for hCMV, EBV-EPL, EBV-HPL and EBV-GLC for EBV, and Flu-GIL for influenza. Details of these tetramers are provided in Table S1.

Plasmids.

The Hobit isoforms XL, L and S were cloned from cDNA of PBMCs into LZRS pBM-IRES-EGFP retroviral vectors as a XhoI and EcoRI fragment to generate HA-tagged proteins. A bi-cistronic expression vector pIRES2-EGFP (Clontech) encoding full-length (FL) Blimp1 has been described previously [45]. Sequences encoding Hobit isoforms were excised from the LZRS pBM-IRES EGFP vectors and cloned into both pBluescript (Stratagene) and pIRES2 EGFP (Clontech) between EcoR1/XhoI and EcoRI/SalI sites, respectively.

Lentiviral pKLO.1 plasmids containing shRNA that target Hobit (TRCN0000162720; CAGAAGAGCTTCACTCAACTT) or that do not target Hobit as a control (MISSION Non-Target shRNA Control SHC002: CCGCAACAAGATGAAGAGCACCAACTC) were obtained from Sigma (MISSION shRNA Lentiviral Transduction Particles).

Cell culture.

NK92 cells were maintained in RPMI 1640 (Gibco) containing 10% heat inactivated FCS (ICN Biomedicals), IL-2 (50 U/ml; Biotest), streptomycin (100 ng/ml; Life Technologies), and penicillin (10 U/ml; Yamanouchi, Pharma). NK92 cells were transduced using lentiviruses containing pKLO.1 plasmids with control or Hobit KD shRNA. Transduced NK92 cells were selected on puromycin (Sigma-Aldrich) containing medium. Jurkat cells were grown in Iscove's modified Dulbecco's medium (IMDM; Gibco) containing 10% FCS, streptomycin (100 ng/ml), penicillin (10 U/ml) and 0.0004% β -mercapto-ethanol (Merck). Jurkat cells were transduced using retroviruses containing LZRS pBM-IRES-EGFP with Hobit XL, Large or Small on retronectin (Takara Shuzo) coated plates. Transduced Jurkat cells were sorted to over 95% purity flow cytometry based sorting using GFP expression as a selection marker.

Human PBMCs were obtained from fresh heparinized blood or buffy coats of healthy donors using Ficoll-Paque Plus (GE Healthcare) gradient centrifugation. Total, naive, effector and memory CD8⁺ T cells were isolated using magnetic sorting with CD8

microbeads (Miltenyi Biotec) and then flow-cytometric sorting for CD27 and CD45RA on a FACS Aria (BD Biosciences) to obtain CD27+CD45RA+ naive, CD27-CD45RA+ effector and CD27+CD45RA- memory cells. NK cells were isolated using flow-cytometric sorting for CD3, CD56 and CD16 to obtain the CD3-CD16+CD56dim and CD3-CD16-CD56bright NK cell subsets or total CD3-CD56+ NK cells.

For activation cells were cultured with PMA (2 ng/ml; Sigma-Aldrich) and ionomycin (1 µg/ml; Sigma-Aldrich) for 4 hours.

PCR and quantitative PCR.

To detect Hobit XL, L and S splice variants a PCR was performed using the following forward: 5'-TTGGGAGCTCTCCAATCTC-3' and reverse: 5'-GCAGGTGGGTCTTGAGGT-TA-3' primers. The amplification products of Hobit XL (260 bps), Hobit L (200 bps) and Hobit S (180 bps) were separated on agarose gel.

RNA was isolated using the Invisorb RNA isolation kit (Invitex) or Trizol reagent (Invitrogen). Then, cDNA was synthesized using RevertAID H Minus Reverse Transcriptase (Thermo Scientific) and random primers (Invitrogen) or poly dT oligos (Invitrogen). Quantitative PCR was performed on a Lightcycler (Roche) or a StepOnePlus RT PCR system (Applied Biosystems) using Fast SYBR Green Master Mix (Applied Biosystems) and the following primers sets: Hobit (forward: 5'-CATATGTGG-CAAGAGCTTTGG-3', reverse: 5'-AGAGTTCACTCAACTTGCC-3'), Blimp-1 (forward: 5'-CAACAACCTTTGGCCTCTTCC-3', reverse: 5'-GCATTCATGTGGCTTTTCTC-3'), IFN-γ (forward: 5'-TTCAGCTCTGCATCGTTTTG-3', reverse: 5'-TCTTTTGGATGCTCTGGT-CA-3'), and 18S (forward: 5'-GGACAACAAGCTCCGTGAAGA-3', reverse: 5'-CAGAA-GTGACGCAGCCCTCTA-3'). Values are represented relative to that of 18S and calibrated relative to naive CD8+ T cells unless indicated otherwise.

Generation of anti-Hobit antibodies.

To generate antibodies against Hobit, the non-Zinc finger part of Hobit was cloned from PBMC cDNA into vector p-ET-30a between KpnI and EcoRI restriction sites (Fig. 2A). Truncated and His tagged Hobit protein was purified using Ni²⁺ columns and imidazole elution. Balb/c mice were immunized 3 times with isolated Hobit protein (25 µg/ml) in montanide adjuvants. Splenocytes were isolated and fused to immortalized SP2/0 myeloma cells using polyethylene glycol 4000 (Merck). Monoclonal hybridomas that produced anti-Hobit antibodies were selected using a flow cytometry-based screening method, in which PBMCs of hCMV+ donors were labeled with hybridoma supernatants and goat anti-mouse Ig (Dako) in the secondary step. We detected one monoclonal antibody (Sanquin-Hobit/1) that specifically stained Hobit, as verified using staining of NK92 cells that were transduced with mock or Hobit KD shRNA constructs (Fig. 2, C and D).

Flow cytometry.

Cells were labeled with fluorochrome-conjugated or biotinylated antibodies in PBS 0.5% BSA for 30 min at 4°C. In case of biotinylated antibodies, fluorochrome-conjugated streptavidin was added in a second step. For intracellular and nuclear staining, cells were fixed and permeabilized using fixation and permeabilization buffers of BD Biosciences and eBioscience, respectively. Expression was analyzed on FACSCanto II, BD LSRFortessa or BD LSR II flow cytometers (BD Biosciences).

EMSA.

To generate Hobit proteins representative of the different isoforms or the zinc finger region alone, *in vitro* transcription-translation reactions were performed using mMESSAGE mMACHINE and Retic Lysate IVT kits (Ambion). Protein expression was verified by Western blot. The double-stranded probes used for EMSA contained the following sequences: TAPASIN: (5'-TTTGGAGGAAAGTCAAAGTCAAAGGAGGAAG-3'), BTN3A3: (5'-TGAAATGAAAAGTCAAAGTACATTGAATTGT-3'), SP110: (5'-AGAAAA-GAAAAGTCAAAGTTTTTCGGAGTTTG-3'). DNA probes end-labeled with T4 polynucleotide kinase were incubated with *in vitro* translation products, adjusted for expression levels, in the presence of poly(I:C) (Amersham) for 30 min at room temperature. Supershift was performed by the addition of rabbit anti-HA antibodies prior to mixing with radioactive probe.

Luciferase Assays.

HeLa cells were seeded to reach 80% confluency on the day of transfection and then co-transfected with GeneJuice (Novagen) reagent according to the manufacturer's instructions with the indicated luciferase reporter constructs and overexpression vectors of Hobit and Blimp-1. The firefly luciferase reporter constructs containing sequences from the promoters for human TAPASIN, BTN3A3 and SP110 have been described previously [31;32]. A control Renilla luciferase vector was used for normalization. Luciferase activity was assessed 6 h after treatment with medium alone or medium containing 200 IU/ml IFN- γ . Experiments were conducted using the Promega dual luciferase assay system and analyzed on a Berthold Lumat LB Luminometer.

Microarray analysis.

Microarray data was obtained from naïve CD8+ T cells and hCMV specific CD8+ T cells at peak of infection, 1 year after infection, and during latency, as described [22]. Expander software was used to perform nearest neighbor analysis on the microarray data. IFN- γ was taken as a starting point and a neighbor joining tree was constructed based on the expression pattern of the genes in the indicated subsets of CD8+ T cells.

ELISA.

Production of IFN- γ was measured in the supernatants of cell cultures using PeliPair human IFN- γ reagent set (Sanquin Reagents) according to the manufacturer's protocol.

Statistics.

Values are expressed as mean \pm SD or SEM as indicated. Differences between two groups were assessed by Student's t test. Differences between more than two groups were assessed using one-way ANOVA followed by a Bonferroni post-hoc test. A p-value of less than 0.05 was considered statistically significant (* = $p < 0.05$; ** = $p < 0.01$; *** = $p < 0.001$).

Study Approval.

All donors gave written informed consent prior to inclusion in the study and the study was approved by the Amsterdam Medical Center institutional medical ethics

committee.

Acknowledgements

The authors thank Erik Mul, Tomasz Poplonski and Berend Hooibrink for expert cell sorting and Mieke Brouwer for expert help with the hybridoma culture and screening.

KPJMvG was supported by Vidi grant 917.13.338 from The Netherlands Organization of Scientific Research; KMLH, MD and RAWvL were supported by Vici grant 918.46.606 from The Netherlands Organization of Scientific Research; AvS was supported by grant C03.2034 from the Dutch Kidney Foundation.

Conflict of interest

The authors declare no financial or commercial conflict of interest

References:

1. Stemberger, C., Huster, K.M., and Busch, D.H., Defining correlates of T cell protection against infection. *Discov.Med.* 2006. 6: 148-152.
2. Gerlach, C., van Heijst, J.W., Swart, E., Sie, D., Armstrong, N., Kerkhoven, R.M., Zehn, D., Bevan, M.J., Schepers, K., and Schumacher, T.N., One naive T cell, multiple fates in CD8+ T cell differentiation. *J.Exp.Med.* 2010. 207: 1235-1246.
3. Kaech, S.M., Tan, J.T., Wherry, E.J., Konieczny, B.T., Surh, C.D., and Ahmed, R., Selective expression of the interleukin 7 receptor identifies effector CD8 T cells that give rise to long-lived memory cells. *Nat.Immunol.* 2003. 4: 1191-1198.
4. Huster, K.M., Busch, V., Schiemann, M., Linkemann, K., Kerksiek, K.M., Wagner, H., and Busch, D.H., Selective expression of IL-7 receptor on memory T cells identifies early CD40L-dependent generation of distinct CD8+ memory T cell subsets. *Proc.Natl.Acad.Sci.U.S.A* 2004. 101: 5610-5615.
5. Joshi, N.S., Cui, W., Chandele, A., Lee, H.K., Urso, D.R., Hagman, J., Gapin, L., and Kaech, S.M., Inflammation directs memory precursor and short-lived effector CD8(+) T cell fates via the graded expression of T-bet transcription factor. *Immunity.* 2007. 27: 281-295.
6. Kallies, A., Xin, A., Belz, G.T., and Nutt, S.L., Blimp-1 transcription factor is required for the differentiation of effector CD8(+) T cells and memory responses. *Immunity.* 2009. 31: 283-295.
7. Rutishauser, R.L., Martins, G.A., Kalachikov, S., Chandele, A., Parish, I.A., Meffre, E., Jacob, J., Calame, K., and Kaech, S.M., Transcriptional repressor Blimp-1 promotes CD8(+) T cell terminal differentiation and represses the acquisition of central memory T cell properties. *Immunity.* 2009. 31: 296-308.
8. Yang, C.Y., Best, J.A., Knell, J., Yang, E., Sheridan, A.D., Jesionek, A.K., Li, H.S., Rivera, R.R., Lind, K.C., D'Cruz, L.M., Watowich, S.S., Murre, C., and Goldrath, A.W., The transcriptional regulators Id2 and Id3 control the formation of distinct memory CD8+ T cell subsets. *Nat.Immunol.* 2011. 12: 1221-1229.
9. Ji, Y., Pos, Z., Rao, M., Klebanoff, C.A., Yu, Z., Sukumar, M., Reger, R.N., Palmer, D.C., Borman, Z.A., Muranski, P., Wang, E., Schrumpp, D.S., Marincola, F.M., Restifo, N.P., and Gattinoni, L., Repression of the DNA-binding inhibitor Id3 by Blimp-1 limits the formation of memory CD8+ T cells. *Nat. Immunol.* 2011. 12: 1230-1237.
10. Cui, W., Liu, Y., Weinstein, J.S., Craft, J., and Kaech, S.M., An interleukin-21-interleukin-10-STAT3 pathway is critical for functional maturation of memory CD8+ T cells. *Immunity.* 2011. 35: 792-805.
11. Zhou, X., Yu, S., Zhao, D.M., Harty, J.T., Badovinac, V.P., and Xue, H.H., Differentiation and persistence of memory CD8(+) T cells depend on T cell factor 1. *Immunity.* 2010. 33: 229-240.
12. Banerjee, A., Gordon, S.M., Intlekofer, A.M., Paley, M.A., Mooney, E.C., Lindsten, T., Wherry, E.J., and Reiner, S.L., Cutting edge: The transcription factor eomesodermin enables CD8+ T cells to compete for the memory cell niche. *J.Immunol.* 2010. 185: 4988-4992.
13. Snyder, C.M., Cho, K.S., Bonnett, E.L., van, D.S., Shellam, G.R., and Hill, A.B., Memory inflation during chronic viral infection is maintained by continuous production of short-lived, functional T cells. *Immunity.* 2008. 29: 650-659.
14. Wherry, E.J., Barber, D.L., Kaech, S.M., Blattman, J.N., and Ahmed, R., Antigen-independent memory CD8 T cells do not develop during chronic viral infection. *Proc.Natl.Acad.Sci.U.S.A* 2004. 101: 16004-16009.
15. Wherry, E.J., Ha, S.J., Kaech, S.M., Haining, W.N., Sarkar, S., Kalia, V., Subramaniam, S., Blattman, J.N., Barber, D.L., and Ahmed, R., Molecular signature of CD8+ T cell exhaustion during chronic viral infection. *Immunity.* 2007. 27: 670-684.
16. Paley, M.A., Kroy, D.C., Odorizzi, P.M., Johnnidis, J.B., Dolfi, D.V., Barnett, B.E., Bikoff, E.K., Robertson, E.J., Lauer, G.M., Reiner, S.L., and Wherry, E.J., Progenitor and terminal subsets of CD8+ T cells cooperate to contain chronic viral infection. *Science* 2012. 338: 1220-1225.
17. Shin, H., Blackburn, S.D., Intlekofer, A.M., Kao, C., Angelosanto, J.M., Reiner, S.L., and Wherry, E.J., A role for the transcriptional repressor Blimp-1 in CD8(+) T cell exhaustion during chronic viral infection. *Immunity.* 2009. 31: 309-320.
18. Appay, V., Dunbar, P.R., Callan, M., Klenerman, P., Gillespie, G.M., Papagno, L., Ogg, G.S., King, A., Lechner, F., Spina, C.A., Little, S., Havlir, D.V., Richman, D.D., Gruener, N., Pape, G., Waters, A., Easterbrook, P., Salio, M., Cerundolo, V., McMichael, A.J., and Rowland-Jones, S.L., Memory CD8+ T cells vary in differentiation phenotype in different persistent virus infections. *Nat.Med.* 2002. 8: 379-385.

19. van Lier, R.A., ten Berge, I.J., and Gamadia, L.E., Human CD8(+) T-cell differentiation in response to viruses. *Nat.Rev.Immunol.* 2003. 3: 931-939.
20. Newell, E.W., Sigal, N., Bendall, S.C., Nolan, G.P., and Davis, M.M., Cytometry by time-of-flight shows combinatorial cytokine expression and virus-specific cell niches within a continuum of CD8+ T cell phenotypes. *Immunity.* 2012. 36: 142-152.
21. Hamann, D., Baars, P.A., Rep, M.H., Hooibrink, B., Kerkhof-Garde, S.R., Klein, M.R., and van Lier, R.A., Phenotypic and functional separation of memory and effector human CD8+ T cells. *J.Exp.Med.* 1997. 186: 1407-1418.
22. Hertoghs, K.M., Moerland, P.D., van, S.A., Remmerswaal, E.B., Yong, S.L., van de Berg, P.J., van Ham, S.M., Baas, F., ten Berge, I.J., and van Lier, R.A., Molecular profiling of cytomegalovirus-induced human CD8+ T cell differentiation. *J.Clin.Invest.* 2010. 120: 4077-4090.
23. Nutt, S.L., Fairfax, K.A., and Kallies, A., BLIMP1 guides the fate of effector B and T cells. *Nat.Rev.Immunol.* 2007. 7: 923-927.
24. van Gisbergen, K.P., Kragten, N.A., Hertoghs, K.M., Wensveen, F.M., Jonjic, S., Hamann, J., Nolte, M.A., and van Lier, R.A., Mouse Hobit is a homolog of the transcriptional repressor Blimp-1 that regulates NKT cell effector differentiation. *Nat.Immunol.* 2012. 13: 864-871.
25. Freud, A.G. and Caligiuri, M.A., Human natural killer cell development. *Immunol.Rev.* 2006. 214: 56-72.
26. Henson, S.M., Franzese, O., Macaulay, R., Libri, V., Azevedo, R.I., Kiani-Alikhan, S., Plunkett, F.J., Masters, J.E., Jackson, S., Griffiths, S.J., Pircher, H.P., Soares, M.V., and Akbar, A.N., KLRG1 signaling induces defective Akt (ser473) phosphorylation and proliferative dysfunction of highly differentiated CD8+ T cells. *Blood* 2009. 113: 6619-6628.
27. Remmerswaal, E.B., Havenith, S.H., Idu, M.M., van Leeuwen, E.M., van Donselaar, K.A., Ten, B.A., Bom-Baylon, N., Bemelman, F.J., van Lier, R.A., and ten Berge, I.J., Human virus-specific effector-type T cells accumulate in blood but not in lymph nodes. *Blood* 2012. 119: 1702-1712.
28. Hislop, A.D., Gudgeon, N.H., Callan, M.F., Fazou, C., Hasegawa, H., Salmon, M., and Rickinson, A.B., EBV-specific CD8+ T cell memory: relationships between epitope specificity, cell phenotype, and immediate effector function. *J.Immunol.* 2001. 167: 2019-2029.
29. Kuo, T.C. and Calame, K.L., B lymphocyte-induced maturation protein (Blimp)-1, IFN regulatory factor (IRF)-1, and IRF-2 can bind to the same regulatory sites. *J.Immunol.* 2004. 173: 5556-5563.
30. Keller, A.D. and Maniatis, T., Identification and characterization of a novel repressor of beta-interferon gene expression. *Genes Dev.* 1991. 5: 868-879.
31. Doody, G.M., Care, M.A., Burgoyne, N.J., Bradford, J.R., Bota, M., Bonifer, C., Westhead, D.R., and Tooze, R.M., An extended set of PRDM1/BLIMP1 target genes links binding motif type to dynamic repression. *Nucleic Acids Res.* 2010. 38: 5336-5350.
32. Doody, G.M., Stephenson, S., McManamy, C., and Tooze, R.M., PRDM1/BLIMP-1 modulates IFN-gamma-dependent control of the MHC class I antigen-processing and peptide-loading pathway. *J.Immunol.* 2007. 179: 7614-7623.
33. Keller, A.D. and Maniatis, T., Only two of the five zinc fingers of the eukaryotic transcriptional repressor PRDI-BF1 are required for sequence-specific DNA binding. *Mol.Cell Biol.* 1992. 12: 1940-1949.
34. Hohenauer, T. and Moore, A.W., The Prdm family: expanding roles in stem cells and development. *Development.* 2012. 139: 2267-2282.
35. Gyory, I., Fejer, G., Ghosh, N., Seto, E., and Wright, K.L., Identification of a functionally impaired positive regulatory domain I binding factor 1 transcription repressor in myeloma cell lines. *J.Immunol.* 2003. 170: 3125-3133.
36. Ocana, E., Gonzalez-Garcia, I., Gutierrez, N.C., Mora-Lopez, F., Brieva, J.A., and Campos-Caro, A., The expression of PRDI-BF1 beta isoform in multiple myeloma plasma cells. *Haematologica* 2006. 91: 1579-1580.
37. Smith, M.A., Maurin, M., Cho, H.I., Becknell, B., Freud, A.G., Yu, J., Wei, S., Djeu, J., Celis, E., Caligiuri, M.A., and Wright, K.L., PRDM1/Blimp-1 controls effector cytokine production in human NK cells. *J.Immunol.* 2010. 185: 6058-6067.
38. Gyory, I., Wu, J., Fejer, G., Seto, E., and Wright, K.L., PRDI-BF1 recruits the histone H3 methyltransferase G9a in transcriptional silencing. *Nat.Immunol.* 2004. 5: 299-308.
39. Ren, B., Chee, K.J., Kim, T.H., and Maniatis, T., PRDI-BF1/Blimp-1 repression is mediated by corepressors of the Groucho family of proteins. *Genes Dev.* 1999. 13: 125-137.
40. Yu, J., Angelin-Duclos, C., Greenwood, J., Liao, J., and Calame, K., Transcriptional repression by blimp-1 (PRDI-BF1) involves recruitment of histone deacetylase. *Mol.Cell Biol.* 2000. 20:

2592-2603.

41. Kallies, A., Carotta, S., Huntington, N.D., Bernard, N.J., Tarlinton, D.M., Smyth, M.J., and Nutt, S.L., A role for Blimp1 in the transcriptional network controlling natural killer cell maturation. *Blood*. 2011. 117: 1869-1879.

42. Cretney, E., Xin, A., Shi, W., Minnich, M., Masson, F., Miasari, M., Belz, G.T., Smyth, G.K., Busslinger, M., Nutt, S.L., and Kallies, A., The transcription factors Blimp-1 and IRF4 jointly control the differentiation and function of effector regulatory T cells. *Nat.Immunol*. 2011. 12: 304-311.

43. Cimmino, L., Martins, G.A., Liao, J., Magnusdottir, E., Grunig, G., Perez, R.K., and Calame, K.L., Blimp-1 attenuates Th1 differentiation by repression of ifng, tbx21, and bcl6 gene expression. *J.Immunol*. 2008. 181: 2338-2347.

44. Godfrey, D.I., Stankovic, S., and Baxter, A.G., Raising the NKT cell family. *Nat.Immunol*. 2010. 11: 197-206.

45. Doody, G.M., Stephenson, S., and Tooze, R.M., BLIMP-1 is a target of cellular stress and downstream of the unfolded protein response. *Eur.J.Immunol*. 2006. 36: 1572-1582.

The transcription factor *Hobit* identifies human cytotoxic CD4+ T cells

Front. Immunol., 24 March 2017, in press

Anna E. Oja^{#1}, **Felipe A. Vieira Braga**^{#1}, Ester B. M. Remmerswaal^{2,3}, Natasja A. M. Kragten¹, Kirsten M.L. Hertoghs², Jianmin Zuo⁴, Paul Moss⁴, René A.W. van Lier¹, Klaas P. J. M. van Gisbergen^{1,2##*}, Pleun Hombrink^{1##*}

¹Department of Hematopoiesis, Sanquin Research and Landsteiner Laboratory, Amsterdam, The Netherlands.

²Department of Experimental Immunology, Academic Medical Center, Amsterdam, The Netherlands.

³Renal Transplant Unit, Division of Internal Medicine, Academic Medical Centre, The Netherlands

⁴University of Birmingham, College of Medical and Dental Sciences, Institute of Immunology and Immunotherapy, Edgbaston, Birmingham, United Kingdom.

[#]These authors contributed equally for first authorship

^{##}These authors contributed equally for senior authorship

Abstract

The T cell lineage is commonly divided into CD4 expressing helper T cells that polarize immune responses through cytokine secretion and CD8 expressing cytotoxic T cells that eliminate infected target cells by virtue of the release of cytotoxic molecules. Recently, a population of CD4⁺ T cells that conforms to the phenotype of cytotoxic CD8⁺ T cells has received increased recognition. These cytotoxic CD4⁺ T cells display constitutive expression of granzyme B and perforin at the protein level and mediate HLA class II-dependent killing of target cells. In humans, this cytotoxic profile is found within the human cytomegalovirus (hCMV)-specific, but not within the influenza- or Epstein Barr virus (EBV)-specific CD4⁺ T cell populations, suggesting that, in particular, hCMV infection induces the formation of cytotoxic CD4⁺ T cells. We have previously described that the transcription factor Homologue of Blimp-1 in T cells (Hobit) is specifically upregulated in CD45RA⁺ effector CD8⁺ T cells that arise after hCMV infection. Here, we describe the expression pattern of Hobit in human CD4⁺ T cells. We found Hobit expression in cytotoxic CD4⁺ T cells and accumulation of Hobit⁺ CD4⁺ T cells after primary hCMV infection. The Hobit⁺ CD4⁺ T cells displayed highly overlapping characteristics with Hobit⁺ CD8⁺ T cells, including the expression of cytotoxic molecules, T-bet and CX3CR1. Interestingly, $\gamma\delta$ ⁺ T cells that arise after CMV infection also upregulate Hobit expression and display a similar effector phenotype as cytotoxic CD4⁺ and CD8⁺ T cells. These findings suggest a shared differentiation pathway in CD4⁺, CD8⁺ and $\gamma\delta$ ⁺ T cells that may involve Hobit-driven acquisition of long-lived cytotoxic effector function.

Introduction

After activation, CD4+ T cells differentiate into various subsets that can be distinguished based on their unique cytokine milieu and transcription factor profile. To date numerous T helper (TH) subsets have been described, including TH1, TH2, TH17 and T follicular helper CD4+ T cells (1–3). Classically, CD4+ T cells are referred to as cells that exert their helper functions to support other immune cells in their activation and maintenance. For example, CD4+ T cells assist B cells in inducing antibody class switching and establishing germinal centers through the secretion of cytokines (4). On the other hand, the capacity to lyse infected target cells, referred to as cytotoxicity, has been attributed to CD8+ T cells. However, recently, interest in the cytotoxic capacity of CD4+ T cells has been revived. In mice and humans, it has been shown that cytotoxic CD4+ T cells play protective roles in Cytomegalovirus (CMV) infections (5, 6). While the population of cytotoxic CD4+ T cells is less abundant than that of cytotoxic CD8+ T cells, cytotoxic CD4+ T cells are as capable as their CD8 equivalents in the killing of target cells (7–9).

Early during infection, human CMV (hCMV) specific CD4+ T cells were demonstrated to produce IFN γ and exhibit a TH1 phenotype. During the course of infection, these TH1-type CD4+ T cells acquire a cytotoxic profile, lose CD27 and CD28 and obtain granzyme B (10). Furthermore, these cells gain the ability to lyse infected target cells in an HLA class II dependent manner (7). The cytotoxic CD4+ T cells retained the capacity to produce IFN γ and also co-produced a multitude of other cytokines, including TNF α . Only recently, HLA Class II tetramers have become available that allow for the identification and phenotyping of antigen-specific CD4+ T cells directly *ex vivo* (11). Using HLA class II tetramers, hCMV-specific CD4+ T cells have been described to conform to the effector-like phenotype with high cytotoxic potential. Similar to their cytotoxic CD8+ counterparts, the hCMV-specific CD4+ T cells contain lytic granules loaded with granzyme B and perforin that mediate lysis of infected target cells. Cytotoxic hCMV-specific CD4+ T cells also express CX3CR1, which may direct migration to inflamed endothelium, a major site of hCMV infection (12, 13).

Previously, we have shown that the transcription factor Homolog of Blimp-1 in T cells (Hobit) is upregulated in CD45RA+ effector-type CD8+ T cells as well as in hCMV-specific CD8+ T cells that display the phenotype of CD45RA+ effector-type CD8+ T cells. We have also demonstrated that Hobit is involved in the transcriptional regulation of effector functions, including the production of IFN γ and granzyme B (14, 15). As the characteristics of cytotoxic CD8+ and CD4+ T cells strongly overlap, we hypothesized that these cells share a transcriptional program. In search of relevant transcriptional regulators of cytotoxicity in CD4+ T cells, we set out to investigate the involvement of Hobit in the regulation of cytotoxic CD4+ T cells.

Results

Hobit is expressed in CD4+CD28- effector-type T cells

Using microarray analysis, we have previously identified Hobit, encoded by ZNF683, as one of the most distinctly expressed transcription factors in CD45RA+ effector CD8+ T cells (16). To investigate the expression pattern of Hobit in CD4+ T cell differentiation, we isolated CD4+ T cells from the peripheral blood of healthy donors. Effector CD4+ T cell differentiation is characterized by the stepwise loss of CD27 and CD28 (10, 12), and therefore, we sorted CD4+ T cells into three populations based on the expression of the costimulatory molecules CD28 and CD27. Naïve cells co-express CD27 and CD28, intermediately differentiated cells downregulate CD27 but not CD28, and terminally differentiated cytotoxic CD4+ T cells are characterized by the lack of these two molecules (10, 17, 18). We used qPCR to analyze the expression of Hobit mRNA. Hobit expression was high in cytotoxic CD4+CD28-CD27- T cells, but nearly absent in CD4+CD28+CD27+ and CD4+CD28+CD27- T cells (Figure 1a). As Hobit has high homology with Blimp-1, which has been shown to regulate effector T cell differentiation in mice (19), we also assessed the expression of Blimp-1 in the three CD4+ T cell populations. In contrast to Hobit, Blimp-1 was equally upregulated in intermediately and terminally differentiated CD4+ T cells subsets compared to CD4+CD27+CD28+ T cells (Figure 1b). Reflecting the mRNA analysis, Hobit protein expression was found in terminally differentiated, but not in other CD4+ T cells (Figure 1c). Cytotoxic CD4+ T cells are described to express either CD45RA or CD45RO (10, 12, 13). Hobit was uniformly expressed by CD4+ effector T cells (CD45RA +CD27-) and by a fraction of effector memory CD4+ T cells (CD45RA-CD27-) (Figure 1d).

Hobit+ CD4+ effector-type cells display a cytotoxic profile

In order to further characterize the cytotoxic potential of Hobit+ CD4+ T cells, we addressed the expression of proteins that are required for the killing of target cells. We found that both perforin and granzyme A and B are highly co-expressed with Hobit, with approximately 75% of Hobit+ CD4+ T cells expressing perforin, granzyme A and / or B (Figure 2a,b,c). In contrast, the cytotoxic molecule granzyme K did not associate with Hobit (Figure 2d). This result is supported by previous reports showing that granzyme K, in contrast to Hobit, is not abundantly expressed in effector CD8+ T cells (20). To further investigate the characteristics of Hobit+ T cells, we assessed the association of this transcription factor with key properties of cytotoxic T cells. CX3CR1 has been shown to mark cytotoxic CD4+ and CD8+ T cells and direct them towards fractalkine on activated endothelium (21, 22). It was also recently reported that hCMV-specific CD4+ T cells express CX3CR1 (12). We demonstrate that the majority of Hobit+ CD4+ and CD8+ T cells express CX3CR1 (Figure 2e). Of interest is that vice versa nearly all of the CX3CR1+ CD4+ and CD8+ T cells express Hobit (data not shown).

Previously, CD4+ effector T cell differentiation was shown to be associated with the loss of the chemokine receptor CCR7 (7, 10), which mediates the migration of immune

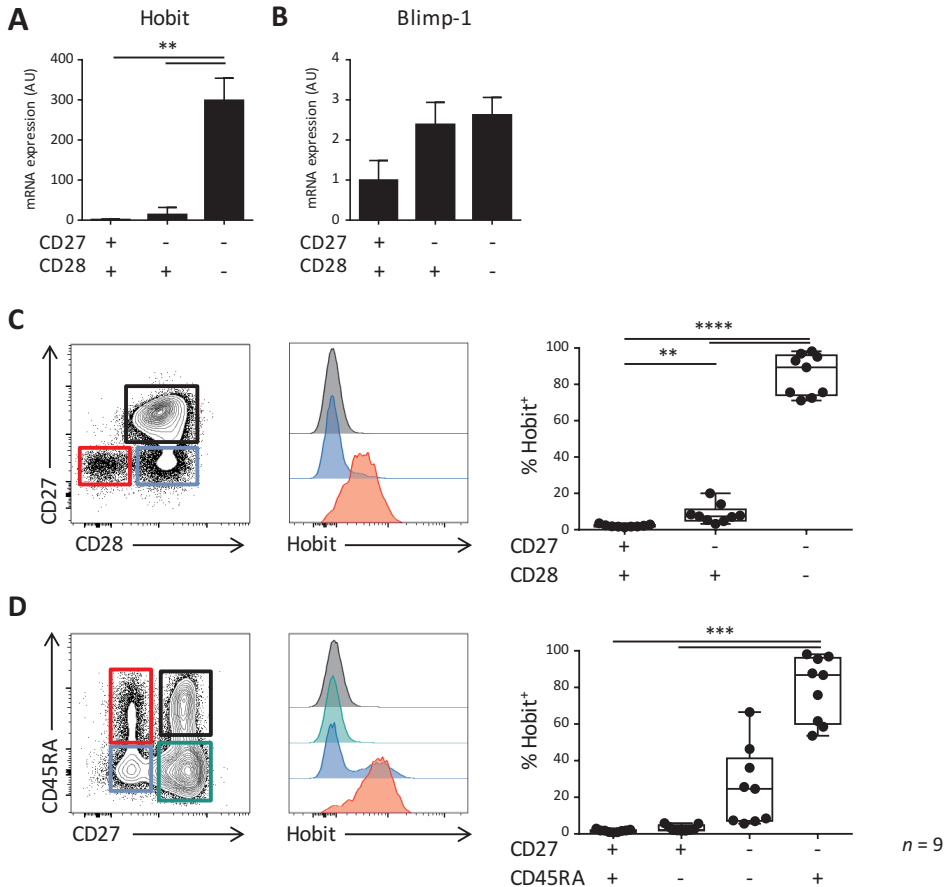


Figure 1: Hobit is expressed in CD4+CD28-CD27- effector-type T cells.

Total CD4+ T cells can be divided in three fractions based on the expression of CD28 and CD27. (a) Healthy donor peripheral blood derived CD4+ T cells were sorted based on the expression of CD28 and CD27 and RNA was isolated. Hobit and Blimp-1 mRNA was measured by qPCR. Values are depicted relative to 18S and calibrated using naïve CD4+ T cells. (b,c) Hobit protein expression was identified in different CD4+ T cell subsets based on (b) the expression of CD27 and CD28 or (c) based on the expression of CD45RA and CD27. Representative contour plots are depicted on the left. Stacked histograms (maximum set to 100%) for the colour indicated subsets are depicted in the center panels. On the right the quantification of the percentage of Hobit+ cells in the different populations is displayed. n = 9. ** p < 0.01, *** p < 0.001, **** p < 0.0001; 1-way ANOVA with Holm-Sidak's multiple comparisons test.

cells to secondary lymphoid organs. As Hobit directly suppresses CCR7 expression of lymphocytes in mice (14), we analyzed the expression of this chemokine receptor by human Hobit+ T cells. In contrast to the Hobit- fraction, the Hobit+ CD4+ and CD8+ T cells lacked CCR7 expression (Figure 2f). These data suggest that Hobit+ T cells do not respond to CCR7-dependent signals that instruct homing to lymphoid organs, in line with the observation that cytotoxic CD4+ and CD8+ T cells are absent from this compartment (20).

KLRG1 and CD127 are frequently used to differentiate between memory (precursor) cells (KLRG1-CD127+) and effector cells (KLRG1+CD127-) (23). In line with effector

differentiation, we found that the majority of the Hobit⁺ CD4⁺ T cells and CD8⁺ T cells expressed KLRG1 (Figure 2g). Strikingly, the majority of the Hobit⁺CD4⁺ T cells also expressed CD127, while this molecule was absent on Hobit⁺CD8⁺ T cells (Figure 2h). The mean fluorescence intensity of CD127 was lower in Hobit⁺CD4⁺ T cells than in Hobit⁻CD4⁺ T cells (Suppl Figure 1). These findings suggest that Hobit⁺CD4⁺ T cells downregulate CD127 similar to effector CD8⁺ T cells, but that the downregulation is incomplete. Homeostatic IL-7 signaling for the maintenance of T cells is mediated by CD127, encoding the IL-7Ra chain (24) indicating that Hobit⁺CD4⁺ T cells may rely on homeostatic IL-7 signaling for their maintenance. It has been previously demonstrated that the transcription factors T-bet and Eomes are essential for the formation and maintenance of CD8⁺ effector T cells. Hobit expression strongly overlaps with that of T-bet in CD8⁺ effector T cells (25). Similarly, we observed a high degree of overlap between Hobit and T-bet expression in CD4⁺ T cells, with up to 98% of Hobit⁺ cells expressing T-bet (Figure 2i). Strict co-expression was not observed between Hobit and Eomes. CD4⁺ T cells that expressed Eomes were Hobit⁺ (data not shown), but not all Hobit⁺ CD4⁺ T cells expressed Eomes (Figure 2j). In the case of CD8⁺ T cells, there is substantial co-expression of Hobit and Eomes, however, Hobit⁻ CD8⁺ T cells that express Eomes also exist. Together these data demonstrate that Hobit expression identifies CD4⁺ T cells with a cytotoxic profile, suggesting that Hobit is a key mediator of CD4⁺ effector T cell differentiation. The phenotype of Hobit⁺ CD4⁺ T cells parallels that of Hobit⁺ CD8⁺ T cells, suggesting a common transcriptional program of cytotoxicity between the two lineages.

hCMV-specific CD4⁺ T cells express Hobit

As hCMV induces the differentiation of cytotoxic CD4⁺ T cells, we analyzed expression of Hobit in hCMV-specific CD4⁺ T cells of hCMV-seropositive donors using class II tetramers specific for various hCMV epitopes. The frequencies of hCMV-specific CD4⁺ T cells varied between 0.1 and 4.6% of total T cells in the three different individuals (Figure 3a). The hCMV-specific CD4⁺ T cells recognizing the analyzed epitopes all expressed Hobit to a substantial degree (Figure 3b), similar to hCMV-specific CD8⁺ T cells, as we have previously shown (25). Thus, the hCMV-driven differentiation of cytotoxic CD4⁺ T cells includes the upregulation of Hobit expression.

Hobit⁺ CD4⁺ T cells increase over time during primary hCMV infection in vivo.

To investigate Hobit expression after primary hCMV infection, we analyzed CD4⁺ T cells in samples derived from three hCMV seronegative recipients that received hCMV positive kidney transplants 35 weeks previously. As hCMV infection is known to also induce the expansion of CD8⁺ and $\gamma\delta$ ⁺ effector T cells (26, 27), we analyzed these T cell lineages in parallel to CD4⁺ T cells. In one patient (pt 153), Hobit expression within CD4⁺ T cells and the abundance of Hobit⁺ CD4⁺ T cells, remained low compared to the massive expansion of Hobit⁺ $\gamma\delta$ ⁺ and CD8⁺ T cells (Figure 4a, b). Although the CD4⁺ response was low, it still passed the threshold of 0.5% cytotoxic CD28⁻CD4⁺ T cells previously shown to be the minimal indication of

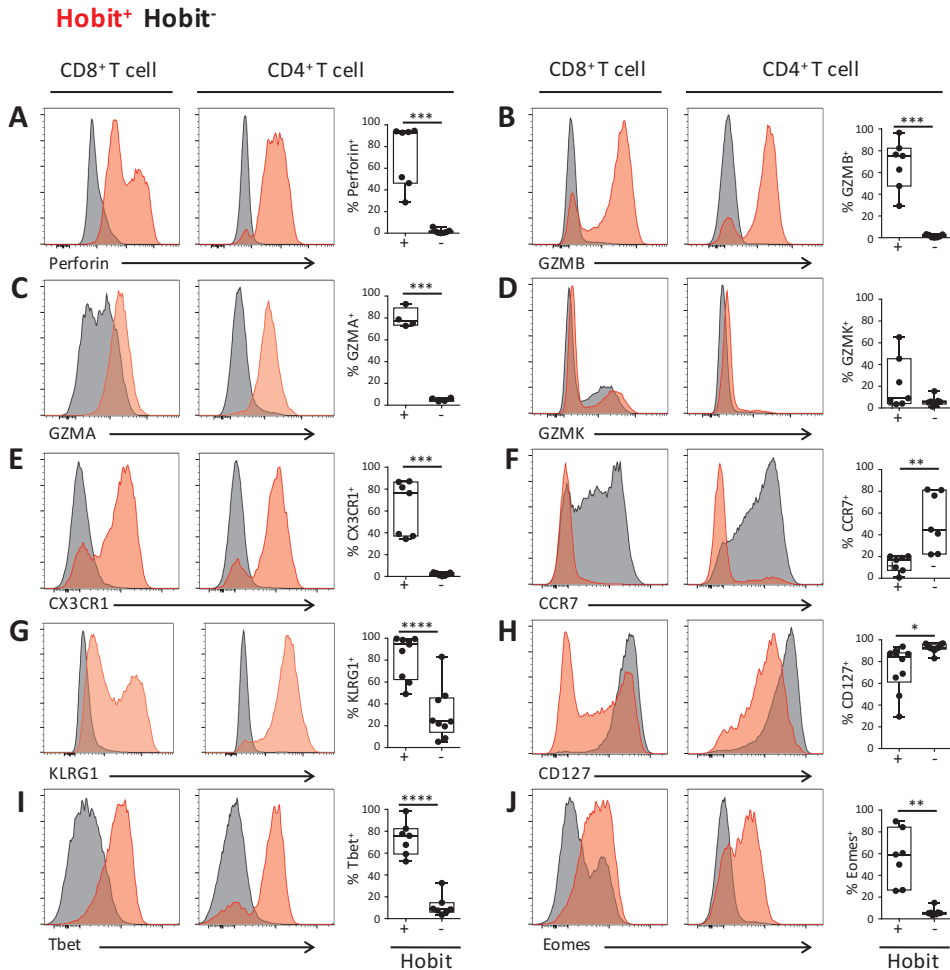


Figure 2: Hobit+ CD4+ effector-type cells display a cytotoxic profile

(a-j) Representative histograms (maximum set to 100%) and quantification of the expression of perforin (a), granzyme B (b), granzyme A (c), granzyme K (d), CX3CR1 (e), CCR7 (f), KLRG1 (g), CD127 (h), Tbet (i), and Eomes (j) by Hobit+ (in red) and Hobit- (in black) CD8+ (left column) and CD4+ T cells (right column). Box and whiskers plots show the percentage of Hobit+ and Hobit- non-naïve CD4+ T cells expressing the different molecules. n = 4-10. * p < 0.05, ** p < 0.01, *** p < 0.001, **** p < 0.0001; paired T test.

hCMV infection (10). In contrast, the other two patients (pt 156 and 333) showed a substantial expansion of Hobit+ cells within the CD4+ T cell compartment as well as the CD8+ and $\gamma\delta$ + T cell compartments (Figure 4a,b). We analyzed the kinetics of the expansion of the three T cell lineages further (Figure 4c,d,e,f,g; Suppl Figure 2). The accumulation of Hobit+ CD4+ T cells only started after clearance of viral infection between weeks 11 and 13 (Figure 4c,f). After about 15 weeks, the Hobit expressing CD4+ T cell population stabilized at around 40% of CD4+ T cells and 10% of total lymphocytes (Figure 4f and g). These findings closely correspond with the kinetics of the emergence of a CD4+CD28- population after hCMV infection (10). Furthermore, the kinetics of the CD4+ effector response appeared similar to that of

the effector CD8+ T cell and $\gamma\delta$ + T cell response, except that the overall magnitude was lower for the response of the CD4+ and $\gamma\delta$ + T cells than for that of the CD8+ T cells (Figure 4c,d,e,f,g).

Hobit identifies CD4+ effector-type T cells during primary hCMV infection *in vivo*.

Surface expression of CD45RA and CD27 defines naïve (CD45RA+CD27+), memory (CD45RA-) and effector (CD45RA+CD27-) T cells. As expected during the latency stage of infection (week 28 and onwards) the majority of Hobit+ CD4+ T cells expressed an effector phenotype (Figure 5a). In contrast, pre-transplant and at early time points post-transplant, Hobit+ CD4+ T cells are mainly characterized by a memory phenotype. The Hobit+CD4+ T cells first downregulate CD27 at around week 11, followed by the upregulation of CD45RA at around week 15, thereby completing the acquisition of the effector phenotype. Similar downregulation of CD27 preceding

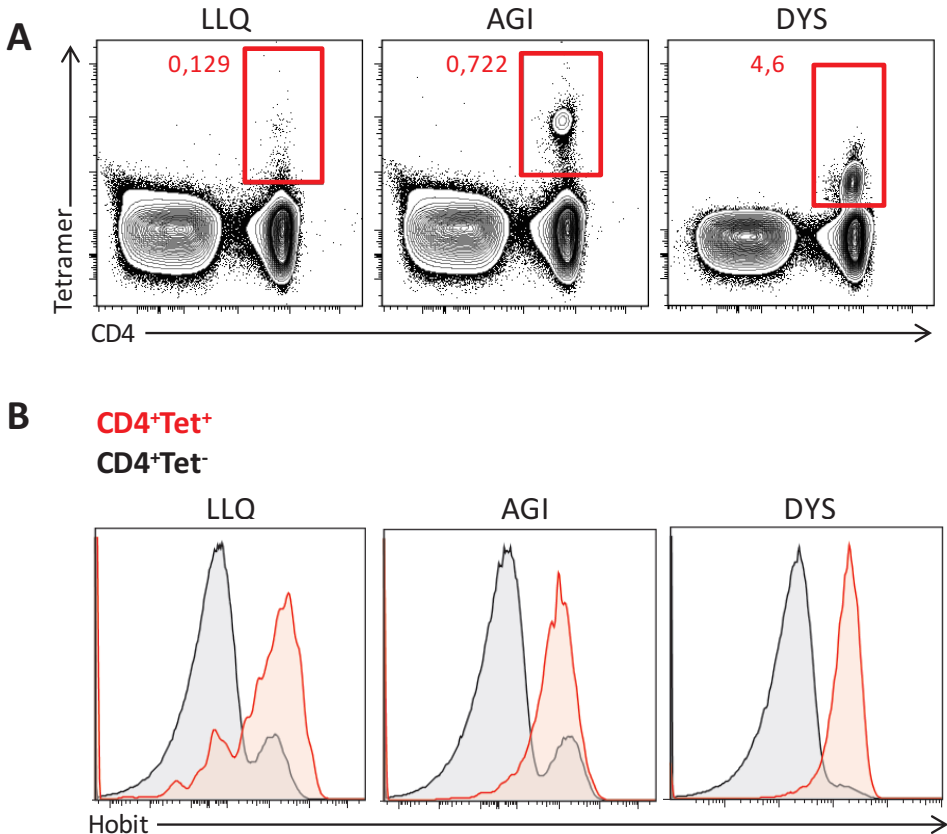


Figure 3: hCMV-specific CD4+ T cells express Hobit.

The expression of Hobit was analyzed in hCMV-specific CD4+ T cells using class II tetramers. (a) Populations of hCMV-specific CD4+ T cells were identified in three donors using three different tetramers, indicated by the first three letters of the peptide sequence (LLQ, AGI, DYS). The contour plots show total PBMCs with CD4 on the x-axis and tetramer on the y-axis. (b) The histograms show the expression of Hobit on CD4+ tetramer+ T cells (red) and CD4+ tetramer- T cells (black) of three donors.

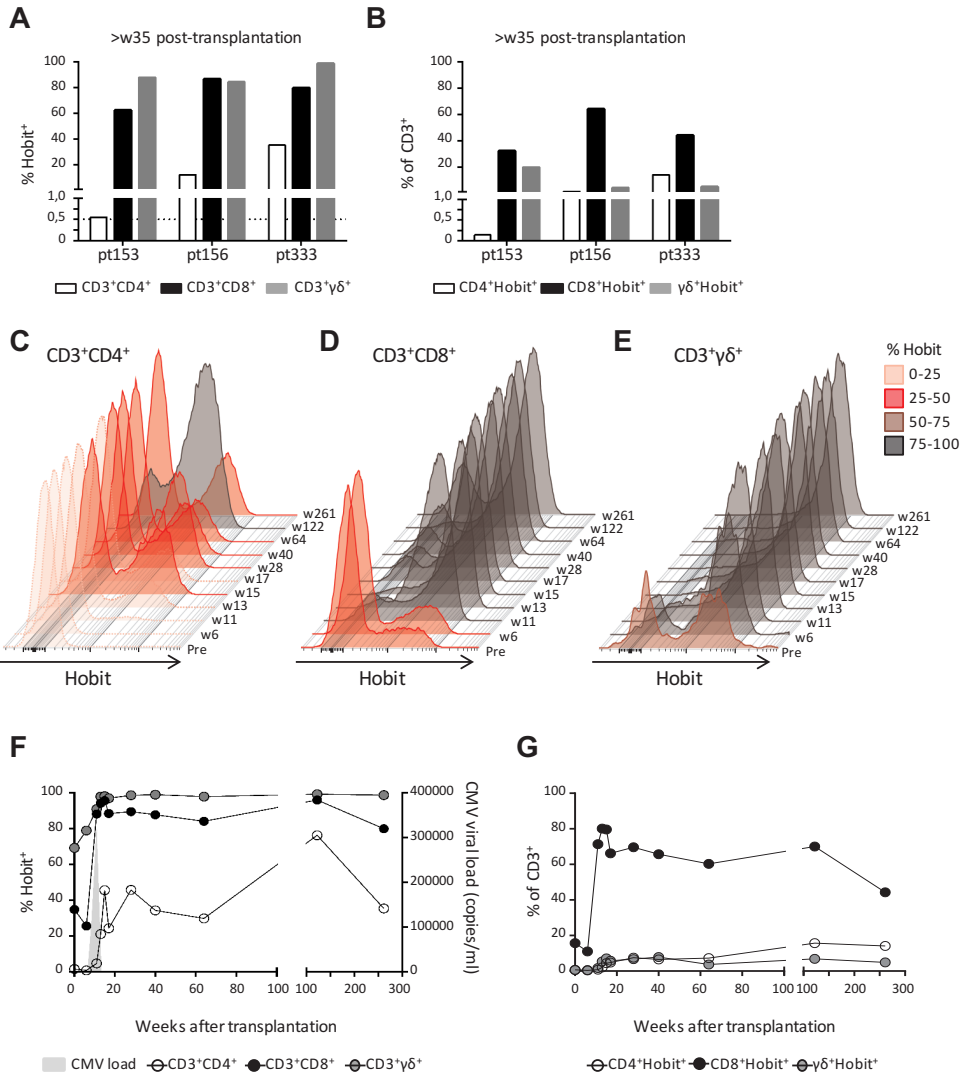


Figure 4: Hobit⁺ CD4⁺ T cell increase over time during primary hCMV infection in vivo.

The induction of Hobit expression in CD4⁺, CD8⁺ and γδ⁺ effector type T cells was followed over the course of primary hCMV infection. (a) Frequency of Hobit⁺ cells of CD4⁺, CD8⁺ and γδ⁺ T cells within the population and (b) the abundance of Hobit⁺CD4⁺, Hobit⁺CD8⁺ and Hobit⁺γδ⁺ in the total CD3⁺ T cells in three hCMV seronegative recipients (pt153, pt156 and pt333) was analyzed at more than 35 weeks after kidney transplantation from a hCMV seropositive donor. The dotted line in (a) indicates the percentage of cytotoxic CD4⁺ T cells minimally induced by hCMV infection (c-e) The overlaid histograms (maximum set to 100%), demonstrate the kinetics of Hobit expression in total (c) CD4⁺, (d) CD8⁺ and (e) γδ⁺ T cells over the course of primary hCMV infection in pt333. On the right the sampling time points are indicated in weeks (w) post-transplantation. The color code indicates the percentage of Hobit⁺ cells according to the depicted key. (f) The line graph shows the induction of Hobit expression (left y-axis) in CD4⁺ (white), CD8⁺ (black), and γδ⁺ (grey) T cells after kidney transplantation in pt333. The x-axis shows the weeks post-transplantation. Viral loads (determined by qPCR and in light grey) is plotted on the right y-axis as copies of hCMV per ml of blood. (g) The abundance of the Hobit⁺CD4⁺, Hobit⁺CD8⁺ and Hobit⁺γδ⁺ in the total CD3⁺ T cells is shown over the course of the hCMV infection for pt333.

the upregulation of CD45RA was found for Hobit+ CD8+ and Hobit+ $\gamma\delta$ + T cells, albeit with faster kinetics (Figure 5b,c). Importantly, the phenotypic composition of the Hobit- CD4+, CD8+ and $\gamma\delta$ + T cell population stably represented naïve T cells throughout the sampling period (Suppl Figure 3), suggesting that the events in T cell differentiation during the course of hCMV infection are restricted to the Hobit+ cells. Taken together, these data suggest that Hobit expression precedes the development of terminally differentiated effector T cells, which supports an instructive role of the transcription factor in the acquisition of the effector profile.

Transcriptional programming of cytotoxic CD4+ T cells

The parallels between cytotoxic CD4+ and CD8+ T cells prompted us to compare the transcriptional profiles of these cells. Therefore, we made a comparison of the microarray data on hCMV-specific CD4+ T cells (12) with microarray data on CD8+ T cells during a primary hCMV response (16). We found substantial overlap between the transcriptional profiles of the effector CD4+ and CD8+ T cells (Figure 6a). The CD4+ microarray did not include the probe set for ZNF683 (Hobit), which excluded Hobit from the comparison. Genes encoding perforin, granzyme B, CX3CR1, Tbet, CD27 and CCR7 (highlighted in red) were similarly regulated in cytotoxic CD4+ and CD8+ T cells (Figure 6a), in contrast to genes encoding the IL-7R and CD28 (also highlighted in red). These findings largely substantiate our results as the products of these genes except for the IL-7R associated with Hobit in both CD4+ and CD8+ T cells (Figure 1 and 2).

Within the shared up- and downregulated genes we also identified known targets of Hobit that include GZMB, CCR7 and TCF7 (14, 15). To confirm the microarray data, we sorted CD28-CD27-, CD28+CD27-, and CD28+CD27+ CD4+ T cells and performed qPCRs for these Hobit targets (Figure 6b). We found that GZMB was exclusively expressed in the CD28-CD27- subset, while mRNA expression of CCR7 and TCF7 was low in this subset, intermediate in the CD28+CD27- subset and high in the CD28+CD27+ subset. These findings are in line with a role for Hobit in the regulation of the transcriptional program of cytotoxic CD4+ T cells.

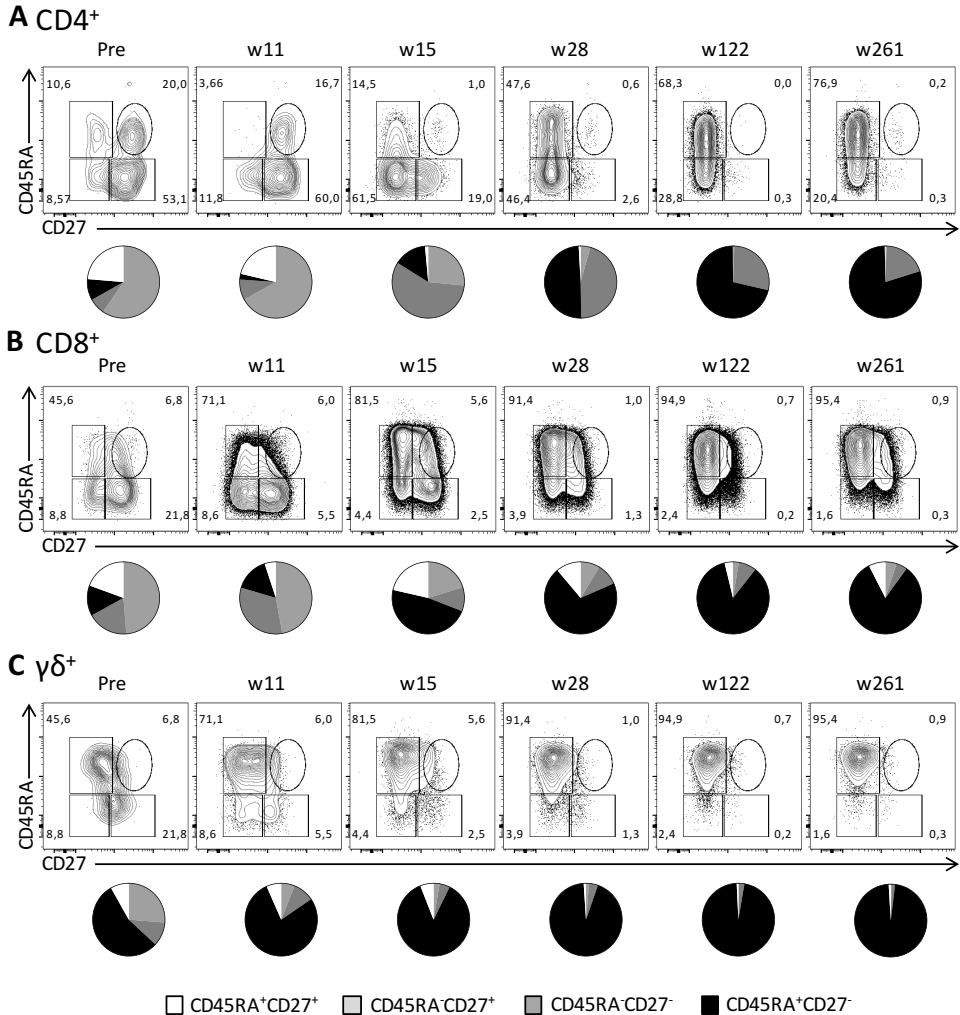


Figure 5: Hobit identifies expanded CD4⁺ effector-type T cells during primary hCMV infection in vivo.

The distribution of CD45RA/CD27 expression by Hobit⁺ (a) CD4⁺, (b) CD8⁺ and (c) γδ⁺ T cells was characterized over the course of hCMV infection for pt333. Top panels show contour plots of CD45RA/CD27 of Hobit⁺ T cells for the indicated time points after transplantation. Lower panels show pie charts representing the distribution of CD45RA/CD27 expression by Hobit⁺ T cells of the three lineages.

Figure 6: Transcriptional profile of cytotoxic CD4⁺ T cells.

3

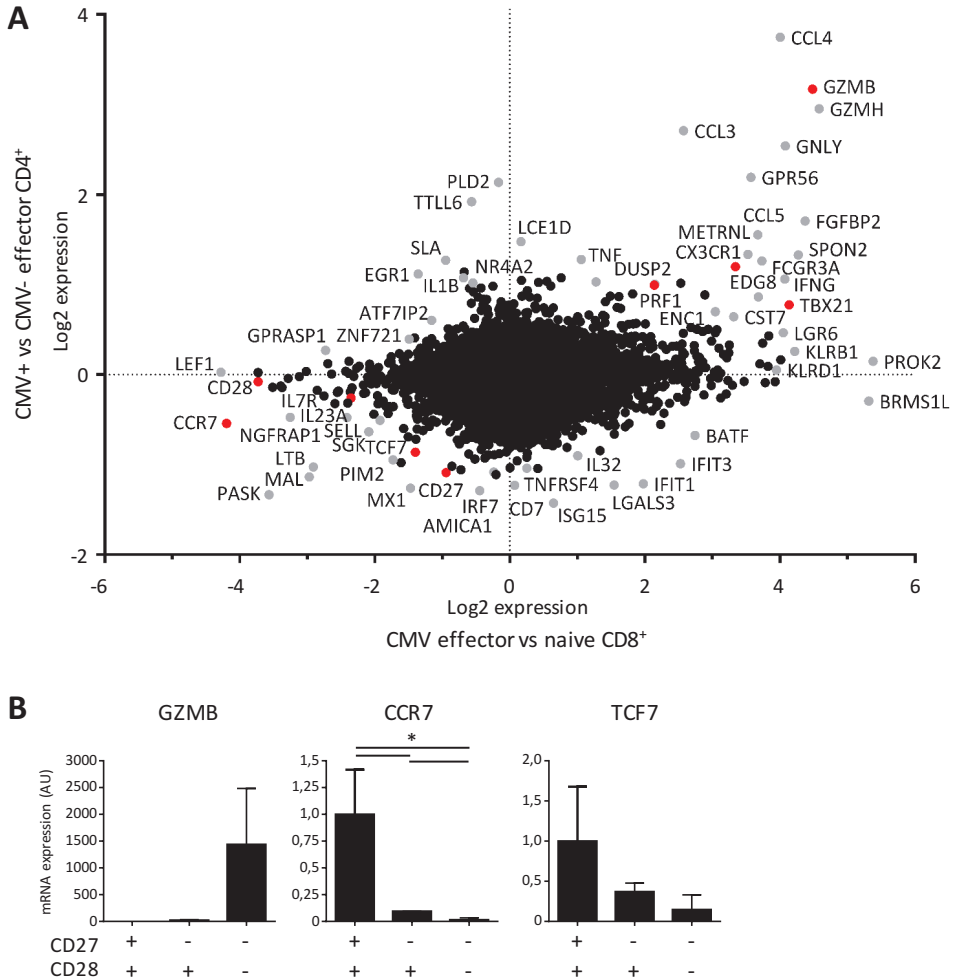
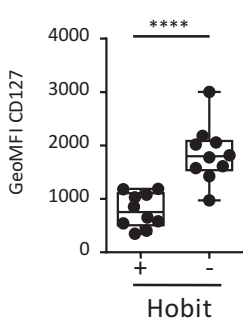


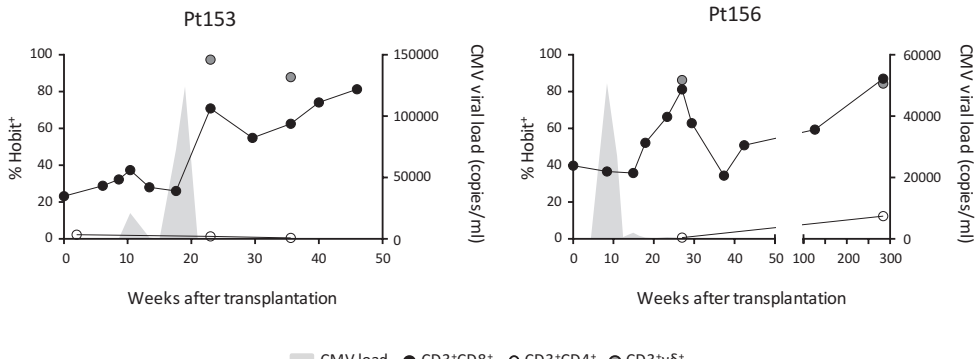
Figure 6: Transcriptional profile of cytotoxic CD4+ T cells.

The transcriptional profile of cytotoxic CD4+ T cells was determined by comparing the signature of hCMV-specific CD4+ T cells to effector CD8+ T cells during a primary hCMV infection. (a) The dot plot shows the genes that are up- and downregulated by hCMV-specific CD4+ T cells compared to CMV- effector CD4+ T cells on the y-axis and the genes that are up- and downregulated by effector CD8+ T cells in a primary hCMV infection compared to naive CD8+ T cells on the x-axis. The changes shown are on a log2 scale on both axes. The differentially regulated genes in either comparison are depicted in grey except for the genes described at protein level in Hobit+CD4+ T cells in Figures 1 and 2, which are shown in red. (b) The specific target genes of Hobit that were differentially expressed, GZMB, CCR7 and TCF7, were confirmed by qPCR in sorted CD4+ T cell subsets (CD28+CD27+, CD28+CD27-, CD28-CD27-). The values are depicted as relative to 18S and calibrated to naive CD4+ T cells. For the qPCR data n = 4. * p < 0.05; 1-way ANOVA with Holm-Sidak's multiple comparisons test.



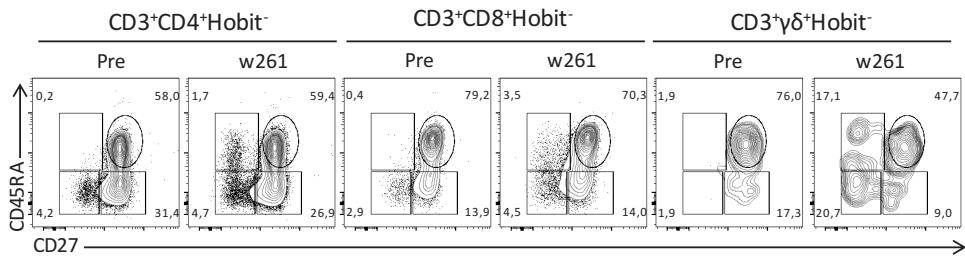
Supplementary Figure 1: Geometric mean fluorescence intensity of CD127 by Hobit+ and Hobit- CD4+ T cells

The geometric mean fluorescence intensity of CD127+ cells was quantified for the Hobit+ and Hobit- non-naïve CD4+ T cells. n = 10. **** p < 0.0001; paired T test.



Supplementary Figure 2: Expansion of Hobit+ T cells over time after primary hCMV infection.

The line graphs show the time course analysis of Hobit expression in CD4+, CD8+, and γδ+ T cells after kidney transplantation in pt153 and pt156. Left y-axis depicts the percentage of Hobit+ cells within the CD4+ (white), CD8+ (black), and γδ+ (grey) T cell populations. The CD4+ and γδ+ T cells were analyzed at three and two time points, respectively. The CD8+ expansion was measured more frequently. Viral loads (determined by qPCR) (light grey) are depicted on the right y-axis as copies of hCMV per ml of blood.



Supplementary Figure 3: Phenotype of Hobit- T cells before and after primary hCMV infection.

Distribution of CD45RA/CD27 expression, shown with contour plots, by Hobit- CD4+, CD8+ and γδ+ T cells was characterized prior to transplantation and 261 weeks post transplantation of hCMV infection for pt333.



Discussion

Transcription factors initiate differentiation processes by instructing lineage-specific gene programs. Therefore, they are interesting candidates in the identification of cell subsets through their expression profiles that are strongly associated with unique cell populations. In this report, we have identified the transcription factor Hobit as a marker of cytotoxic CD4⁺ T cells in humans. Hobit is expressed by all cytotoxic CD4⁺ T cells, but absent from other CD4⁺ T cell populations in peripheral blood including regulatory T cells, as described previously (25). Expression of Hobit in CD4⁺ T cells on its own was sufficient to adequately identify cytotoxic CD4⁺ T cells, suggesting that the transcription factor is a useful alternative for the identification of these cells. The advantage of Hobit over the classical definition of cytotoxic CD4⁺ T cells using CD27 and CD28 is that in contrast to these co-stimulatory molecules, Hobit acts as a positive marker, which improves the accuracy of the typing of these cytotoxic CD4⁺ T cells. Furthermore, as Hobit expression precedes development of effector-type CD4⁺ T cells, Hobit may allow for earlier recognition of the expanding cytotoxic CD4⁺ T cell population.

Hobit is also expressed outside of the CD4⁺ T cell lineage in CD45RA⁺ effector CD8⁺ T cells and CD56dim NK cells (25). Interestingly, here we showed that the spectrum of Hobit⁺ lymphocytes also includes effector $\gamma\delta$ ⁺ T cells. Similar to Hobit⁺ CD4⁺ T cells, these Hobit⁺ populations within the CD8⁺ T cell, $\gamma\delta$ ⁺ T cell and NK cell lineages are cytotoxic lymphocytes that maintain constitutive protein expression of granzyme B and perforin. The overlap in the expression profiles between the cytotoxic populations of lymphocytes extends beyond the expression of cytotoxic molecules and includes the downregulation of CD27, CD28 and CCR7 and the upregulation of CX3CR1 and T-bet. The similarity in phenotypes suggests that these cytotoxic lymphocytes are under the control of overlapping transcriptional programs. Currently, direct evidence for a role of Hobit in the transcriptional regulation of cytotoxicity in human lymphocytes is not available. Given that we have previously shown that Hobit is essential for the upregulation of granzyme B expression in NKT cells in mice (15), it is conceivable that Hobit also instructs the cytotoxic program of human lymphocytes. In support of an instructive role of Hobit in cytotoxic CD4⁺ T cells, we found that granzyme B and other target genes of Hobit, including CCR7 and TCF7, were up- or down-regulated at the transcript level in these cells. The co-expression of T-bet and Hobit, and to a lesser extent Eomes, suggests that these transcription factors may concordantly contribute to the transcriptional regulation of the cytotoxic program in human cytotoxic lymphocytes.

CD4⁺ T cells with a cytotoxic phenotype arise after primary infection with hCMV in humans (7, 10, 28). Peptide restimulation, proliferation, and tetramer studies have also identified hCMV-specific cells within the population of cytotoxic CD4⁺ T cells (7, 10, 12). It has been suggested that cytotoxic CD4⁺ T cells have arisen to provide an additional layer of HLA class II-dependent protection in response to the immune evasive strategies of the hCMV virus that are targeted at CD8⁺ T cell and NK cell-driven immunity (7). We describe that the CD4⁺ T cells that accumulate after primary hCMV infection in transplant patients express Hobit, suggesting that upregulation of Hobit is an integral part of the cytotoxic CD4⁺ T cell response against hCMV. Furthermore, our class II tetramer studies directly showed that hCMV-specific

CD4+ T cells nearly uniformly express Hobit. At this time, it remains unclear which signals drive the expression of Hobit in cytotoxic CD4+ T cells after hCMV infection. Previously, we have described that T-bet and IL-15 induce Hobit expression in murine CD8+ T cells (14). Consistent with these findings, T-bet and Hobit are strongly co-expressed in human CD4+ T cells and, as described previously, in human CD8+ T cells (25). Antigenic stimulation downregulates expression of Hobit in NKT cells (15). Interestingly, the Hobit+CD4+ T cell response demonstrated relative similar kinetics as the CD8+ and $\gamma\delta$ + T cell responses after resolution of primary hCMV infection, suggesting that antigenic stimulation also antagonizes Hobit expression in human T cells. Thus, it is plausible that after viral clearance T-bet mediates the upregulation of Hobit expression in CD4+ T cells.

Similar to CD45RA+ effector CD8+ T cells, cytotoxic CD4+ T cells are long-lived and highly effective in the elimination of infected target cells (7). The combination of these useful properties suggests that cytotoxic CD4+ T cells may be of potential interest in adoptive transfer strategies for the treatment of patients. However, many hurdles need to be overcome before cytotoxic CD4+ T cells can be used in cellular therapy. CD4+ T cells appear fragile after isolation, do not robustly expand after TCR stimulation and may be difficult to maintain on homeostatic cytokines such as IL-7 due to low expression of CD127. Therefore, a better understanding of the role of Hobit in the differentiation pathway of these cells may be instrumental to improve protocols for the formation and expansion of cytotoxic CD4+ T cells.

Materials and methods

Subjects

PBMCs were isolated from buffy coats of healthy donors supplied by Sanquin Blood Supply Foundation. The CMV status of the healthy donors is unknown. We also received samples longitudinally from two kidney transplant patients (patient 153 and 156), who were seronegative for EBV and hCMV prior to the transplant. We also received samples from one patient kidney transplant patient (patient 333) who was EBV seropositive but hCMV seronegative prior to the transplant. Two of the patients (patient 153 and 333) developed a primary hCMV infection while the other (patient 156) developed a primary EBV and hCMV infection after receiving a kidney from an EBV+ and hCMV+ donor. The patients received immunosuppressive treatment, including prednisolone, cyclosporine A and mycophenolate mofetil. Patient 333 received prednisolone, cyclosporine Am, myfortix and basiliximab.

Ethics Statement

Written informed consent was given by all of the patients. The Amsterdam Medical Center Medical Ethical Committee approved the study according to the Declaration of Helsinki.

Isolation of mononuclear cells from peripheral blood

PBMCs were isolated from heparinized peripheral blood samples with standard density gradient centrifugation method and cryopreserved until further analysis.

Flow cytometric cell sorting

For the analysis of Hobit, Blimp1, GZMB, CCR7 and TCF7 mRNA, CD3+CD4+CD28+CD27+, CD3+CD4+CD28+CD27- and CD3+CD4+CD28-CD27- T cells were isolated using flow cytometric sorting for CD3, CD4, CD28 and CD27 using FACS Aria (BD).

Quantitative PCR

RNA was isolated from the sorted samples using Invisorb RNA isolation kit (Invitex) or Trizol reagent (Invitrogen). cDNA was synthesized using RevertAID H Minus Reverse Transcriptase (Thermo Scientific) and random primers (Invitrogen) or poly dT oligos (Invitrogen). qPCR analysis was performed using Power SYBR Green (Applied Biosystem) with StepOnePlus Real-Time PCR system (Applied Biosystem). The following primers were used: Hobit (forward: 5'-CATATGTGGCAAGAGCTTTGG-3'; reverse: 5'-AGAGCTTCACTCAACTTGCC-3'), Blimp-1 (forward: 5'-CAACAACCTTTGGCCTCTTCC-3'; reverse: 5'-GCATTCATGTGG CTTTTCTC-3'), GZMB (forward: 5'-TGCGAATCTGACTTACGCCAT-3'; reverse: 5'-GGAGGCATGCCATTGTTTCG-3'), CCR7 (forward: 5'-CAGCCTTCCTGTGTGGTTTT-3'; reverse: 5'-AAATGACAAGGAGAGCCACC-3') and TCF7 (forward: 5'-AGAGAGAGAGTTGGGGGACA-3'; reverse: 5'-TCTGCTCATGCAT-TACCCAC-3'), and 18S (forward: 5'-GGACAACAAGCTCCGTGAAGA-3'; reverse: 5'-CAGAAGTGACGCAGCCCTCTA-3'). Values are depicted as relative to 18S and calibrated to naïve CD4+ T cells.

Flow cytometry analysis

PBMC were labelled with different combinations of the following antibodies: CD4 BUV737 (BD, clone SK3), CD8 BV786 (BD, clone RPA-T8), CD8 BUV805 (BD, clone SK1), CD3 V500 (BD, clone UCHT1), CD3 eVolve605 (eBioscience clone OKT3), CD27 APC-eFluor780 (eBioscience, clone), CD27 BV510 (Biolegend, clone O323), CD45RA BV650 (BD, clone HI100), CD45RA Qdot655 (Invitrogen, clone MEM-56), CD28 PE-Cy7 (BD, clone 28.2), CX3CR1 APC (eBioscience, clone 2A9-1), CCR7 BV421 (Biolegend, clone G043H7), CD127 BV421 (Biolegend, clone A019D5). Near-IR fixable dye (Invitrogen) was used to exclude dead cells from the analysis. For intracellular staining the following antibodies were used: Hobit IgM (BD, clone Sanquin-Hobit/1), Eomes eFluor660 (eBioscience, clone WD1928), Tbet BV421 (Biolegend, clone 4B10), Granzyme B AF700 (BD, clone GB11), Perforin FITC (eBioscience, clone dG9), Perforin PE (eBioscience, clone B-D48), Granzyme K PE (Immunotools, clone 24C3), Granzyme K FITC (Immunotools, clone 24C3). To stain for Hobit IgM, a secondary anti-IgM labelled with PE or FITC was used. The cells were labelled according to manufacturer's instructions. For the intracellular staining the cells were fixed and permeabilized using the Foxp3/Transcription Factor Staining kit (eBioscience). The samples were measured in PBS 0.5% FCS with a LSR Fortessa (BD). The analysis was done using FlowJo Version 10 software.

Class II tetramer analysis

The class II tetramers used in this study and the staining protocol were previously described by Pachnio et al (12). Briefly, three tetramers were used against three different hCMV epitopes; gB-derived epitope DYSNTHSTRYV (HLA-DRB1*07:01) and pp65-derived epitopes AGILARNNLVPMVATV (HLA-DRB3*02:02) and LLQTGIHVRVSPSL (HLA-DQB1*06:02).

Statistics

To determine the significance of our results we used the paired T test or one-way ANOVA and Holm-Sidak's multiple comparisons test using GraphPad Prism 6. A p-value of less than 0.05 was considered statistically significant (* = $p < 0.05$; ** = $p < 0.01$, *** = $p < 0.001$, **** = $p < 0.0001$).

Conflict of Interest

The authors declare no financial or commercial conflict of interest.

Author Contributions

AO, RL, KG and PH designed the project and experiments. AO, FVB, ER, NK, KH, JZ performed the experiments. All authors contributed to the interpretation and discussion of the data. AO, KG and PH wrote the manuscript. All authors read and approved the manuscript.

Funding

KG was supported by Vidi grant 917.13.338 from The Netherlands Organization of Scientific Research. This study was funded by the Dutch Kidney Foundation (14OKG05, Kolff Physician Researcher Grant and CP09.04, Consortium Grant "ALLOVIR").

Acknowledgments

We would like to thank Prof. Dr. Ineke ten Berge for providing us with the PBMC samples from the primary hCMV patients. We are also very grateful to the patients who participated in this study.

References

1. Boyce JA et al. Mechanisms of allergic diseases Mechanisms underlying helper T-cell plasticity: Implications for immune-mediated disease. *J. Allergy Clin. Immunol.* 2013;131:1276–1287.
2. Nakayamada S, Takahashi H, Kanno Y, O JJ. Helper T cell diversity and plasticity. *Curr. Opin. Immunol.* 2012;24:297–302.
3. Crotty S. Follicular Helper CD4 T Cells (T_H) [Internet]. *Annu. Rev. Immunol.* 2011;29(1):621–663.
4. Swain SL, McKinstry KK, Strutt TM. Expanding roles for CD4+ T cells in immunity to viruses [Internet]. *Nat. Rev. Immunol.* 2012;12(2):136–148.
5. Verma S et al. Cytomegalovirus-specific CD4 T cells are cytolytic and mediate vaccine protection [Internet]. *J. Virol.* 2015;90(2):JVI.02123-15.
6. Wilkinson TM et al. Preexisting influenza-specific CD4+ T cells correlate with disease protection against influenza challenge in humans [Internet]. *Nat. Med.* 2012;18(2):274–280.
7. Leeuwen EMM Van, Remmerswaal EBM, Heemskerk MHM, Berge IJM, Lier R a W Van. Strong selection of virus-specific cytotoxic CD4² T-cell clones during primary human cytomegalovirus infection. *Infection* 2006;108(9):3121–3127.
8. Brown DM, Lee S, Garcia-Hernandez M de la L, Swain SL. Multifunctional CD4 cells expressing gamma interferon and perforin mediate protection against lethal influenza virus infection. [Internet]. *J. Virol.* 2012;86(12):6792–803.
9. Hua L et al. Cytokine-dependent induction of CD4+ T cells with cytotoxic potential during influenza virus infection. [Internet]. *J. Virol.* 2013;87(21):11884–93.
10. van Leeuwen EMM et al. Emergence of a CD4+CD28- granzyme B+, cytomegalovirus-specific T cell subset after recovery of primary cytomegalovirus infection.. *J. Immunol.* 2004;173(3):1834–1841.
11. Su LF, Kidd BA, Han A, Kotzin JJ, Davis MM. Virus-Specific CD4+ Memory-Phenotype T Cells Are Abundant in Unexposed Adults [Internet]. *Immunity* 2013;38(2):373–383.
12. Pachnio A et al. Cytomegalovirus Infection Leads to Development of High Frequencies of Cytotoxic Virus-Specific CD4+ T Cells Targeted to Vascular Endothelium [Internet]. *PLOS Pathog.* 2016;12(9):e1005832.
13. D W et al. Dengue virus infection elicits highly polarized CX3CR1+ cytotoxic CD4+ T cells associated with protective immunity [Internet]. *Proc. Natl. Acad. Sci. U. S. A.* 2015;112(31):E4256–E4263.
14. Mackay LK et al. Hobit and Blimp1 instruct a universal transcriptional program of tissue residency in lymphocytes. *Science (80-.).* 2016;352(6284).
15. van Gisbergen KPJM et al. Mouse Hobit is a homolog of the transcriptional repressor Blimp-1 that regulates NKT cell effector differentiation [Internet]. *Nat. Immunol.* 2012;13(9):864–871.
16. Hertoghs KML et al. Molecular profiling of cytomegalovirus-induced human CD8+ T cell differentiation [Internet]. *J. Clin. Invest.* 2010;120(11):4077–4090.
17. Appay V et al. Characterization of CD4(+) CTLs ex vivo. [Internet]. *J. Immunol.* 2002;168(11):5954–8.
18. van de Berg PJ, van Leeuwen EM, ten Berge IJ, van Lier R. Cytotoxic human CD4+ T cells. *Curr. Opin. Immunol.* 2008;20(3):339–343.
19. Kallies A, Xin A, Belz GT, Nutt SL. Blimp-1 Transcription Factor Is Required for the Differentiation of Effector CD8+ T Cells and Memory Responses. *Immunity* 2009;31(2):283–295.
20. van Aalderen MC et al. Infection history determines the differentiation state of human CD8+ T cells. [Internet]. *J. Virol.* 2015;89(9):5110–23.
21. Nishimura M et al. Dual functions of fractalkine/CX3C ligand 1 in trafficking of perforin+/granzyme B+ cytotoxic effector lymphocytes that are defined by CX3CR1 expression.. *J. Immunol.* 2002;168(12):6173–6180.
22. Kim K et al. In vivo structure / function and expression analysis of the CX 3 C chemokine fractalkine. *Blood* 2011;118(22):156–167.
23. Kaech SM et al. Selective expression of the interleukin 7 receptor identifies effector CD8 T cells that give rise to long-lived memory cells. [Internet]. *Nat. Immunol.* 2003;4(12):1191–8.
24. Surh CD, Sprent J. Homeostasis of Naive and Memory T Cells. *Immunity* 2008;29(6):848–862.
25. Vieira Braga FA et al. Blimp-1 homolog Hobit identifies effector-type lymphocytes in humans. *Eur. J. Immunol.* 2015;45(10):2945–2958.
26. Pitard V et al. Long-term expansion of effector/memory Va2gd T cells is a specific blood signature of CMV infection doi:10.1182/blood-2008-01-136713
27. Klenerman P, Oxenius A. T cell responses to cytomegalovirus. [Internet]. *Nat. Rev. Immunol.* 2016;16(6):367–77.
28. Gamadia LE et al. Primary immune responses to human CMV : a critical role for IFN- γ - producing CD4+T cells in protection against CMV disease. *Infection* 2003;101(7):2686–2692.

Hobit regulates metabolism and maintenance of human cytotoxic lymphocytes

Felipe A Vieira Braga¹, Anna.T. Hoekstra², Wikky Tigchelaar³, Natasja A.M. Kragten¹, Nicole N van der Wel³, Rene van Lier¹, Celia R. Berkers² and Klaas P.J.M. van Gisbergen¹

1 Department of Hematopoiesis, Sanquin Research and Landsteiner Laboratory AMC/ UvA, Plesmanlaan 125, 1066 CX, Amsterdam, The Netherlands

2 Biomolecular Mass Spectrometry and Proteomics, Bijvoet Center for Biomolecular Research, Padualaan 8, 3584 CH Utrecht, The Netherlands.

3 van Leeuwenhoek Center for Advanced Microscopy, Amsterdam Medical Centre, Meibergdreef 9, 1105 AZ Amsterdam-Zuidoost.

Abstract

Human cytomegalovirus infection generates a long lived population of CD45RA+ effector CD8 T cells (EMRA cells) characterized by a quiescent phenotype, strong IFN- γ production and high protein expression of cytotoxic molecules. The long term maintenance of these cells is poorly understood. In particular, it is unclear how these cells maintain a strong effector like phenotype in the absence of detectable antigenic stimuli. Metabolic regulation has been shown to play an essential role in T cell memory formation and maintenance and reactivation. Memory CD8 T cells have increased mitochondrial capacity and upon antigen contact can quickly increase both their respiratory capacity and glycolytic activity. Here, we show that in contrast to conventional memory CD8 T cells, EMRA cells have a suppressed metabolic state, with low mitochondrial numbers and activity and low basal glycolysis. We also describe that Hobit (ZNF683), a transcription factor previously shown to induce IFN- γ production, works as a metabolic suppressor in effector lymphocytes. Hobit suppresses both glycolysis and mitochondrial respiration and it plays an essential role in lymphocytes survival. These findings suggest that Hobit contributes to different aspects of the effector phenotype of EMRA cells including IFN- γ production, cytotoxicity and the low metabolic status.

Introduction

CD8 T cells are an important effector arm of the adaptive immune response involved in the killing of virally infected cells [1]. Viral infections such as influenza (FLU) [2], Epstein-Bar virus (EBV) [3] and human cytomegalovirus (HCMV) [4] generate an effector CD8 T cell response that participates in clearance of the infection. A subpopulation of effector CD8 T cells contributes to the formation of memory cells [5]. Different types of memory cells have been defined such as central memory (CM), effector memory (EM) [6] and tissue-resident memory (Trm) cells [7]. The dominant memory population depends on the type of pathogen [8]. CM and EM dominate memory T cell populations in peripheral blood after FLU or EBV infection, respectively [9]. In contrast, HCMV memory cells are predominantly maintained as CD45RA+ cells that lack expression of the co-stimulatory receptors CD27 and CD28 (EMRA CD8 T cells) [10],[11]. EMRA CD8 T cells express high mRNA levels of TNF- α , IFN- γ , perforin, and granzymes A, B, and H [10],[11]. Additionally, EMRA cells have cytolytic granules with pre-formed granzyme and perforin protein [10],[11]. The high expression of cytotoxic molecules by EMRA cells is reflected in their strong capacity to kill target cells [10],[12]. EMRA CD8 T cells have poor proliferative capacity [10] [12], but are much more efficient in the early production of IFN- γ and TNF- α upon restimulation compared to CM and EM cells *in vitro* [12]. Deuterated glucose studies in humans have established that, *in vivo*, EMRA cells have reduced turnover and increased life span in comparison to CM and EM cells [13]. Thus, EMRA CD8 T cells appear to be quiescent and long-lived effector cells with high cytolytic potential and the ability to rapidly produce pro-inflammatory cytokines [12] [9].

T cell maintenance and effector functions are dependent on the adequate supply of energy and the synthesis of new molecules [14]. The glycolytic pathway uses glucose to generate pyruvate to fuel the tricarboxylic acid (TCA cycle). The TCA cycle generates nicotinamide adenine dinucleotide (NADH) that acts as an electron donor for oxidative phosphorylation (OXPHOS) in mitochondria. During OXPHOS oxygen is consumed for the efficient production of ATP [14][15]. Naïve CD8 T cells are catabolic cells that maintain their energy demands largely via OXPHOS [14],[16],[17]. Upon antigen encounter, naïve T cells expand and upregulate the expression of effector molecules to differentiate into effector cells [5]. During effector differentiation, T cells are reprogrammed from a catabolic state to an anabolic state to meet the increased biosynthetic demands. This anabolic shift is mainly sustained by an increase in glycolysis [18]. The high rate of glycolysis in effector cells is a key regulator of cytokine production in particular of IFN- γ , rather than proliferation [19]–[21]. After antigen clearance, memory cells develop that revert to catabolic metabolism. Memory CD8 T cells have high mitochondrial content and their basal energy consumption is fuelled mainly via fatty acid oxidation in the mitochondria [22] [23]. The expanded mitochondrial capacity of memory cells is essential for enhanced proliferation during recall responses [22]–[26]. Moreover, memory cells retain the capacity to switch from a catabolic to an anabolic state upon antigen re-encounter [19],[21].

The metabolic requirements for the maintenance of human EMRA CD8 T cell are unknown. A recent report from Henson et al. [27] addressed how the metabolism of EMRA cells is regulated during recall responses. In contrast to conventional memory cells, *in vitro* activated EMRA CD8 T cells have defective mitochondrial function

[27]. Despite their reduced mitochondrial fitness, EMRA CD8 T cells have the ability to engage glycolysis after activation to fuel the production of cytokines [27]. The dysfunctional mitochondrial capacity of activated EMRA CD8 T cells suggests that these cells might have unique metabolic requirements for their maintenance *in vivo*. In the present report we have performed extensive analysis of the activity and metabolite levels of both glycolysis and oxidative phosphorylation in EMRA CD8 T cells. In contrast to CM and EM cells, EMRA CD8 T cells have low basal glycolytic flux, high glycolytic reserve and low TCA cycle activity. Additionally, we found that the transcription factor Hobit suppresses metabolic activity in these cytotoxic lymphocytes.

Results

Quiescent EMRA CD8 T cells have low basal glycolysis, but high glycolytic reserve.

Upon antigen encounter, quiescent memory CD8 T cells initiate a recall response of effector cells. The strong proliferative burst to generate effector cells requires an increase in global metabolism. The newly formed effector cells meet these demands by changing from a catabolic state into a highly anabolic state through engaging glycolysis [18]. We were interested in the metabolism of long-lived effector-type EMRA CD8 T cells. To investigate the glycolytic activity of EMRA CD8 T cells, we measured their acidification rate. EMRA CD8 T cells displayed basal glycolysis comparable to that of naïve CD8 T cells (Fig. 1, A and B), but lower than that of CM and EM CD8 T cells (Fig. 1, A and B). These findings indicate that EMRA cells are non-glycolytic in contrast to primary effectors. Interestingly, EMRA CD8 T cells had a glycolytic reserve comparable to that of CM and EM cells (Fig. 1C), suggesting that EMRA CD8 T cells have the potential to strongly increase glycolytic activity upon re-stimulation similar to CM and EM cells (Fig. 1, A-C) [10]. To understand how the glycolytic potential of EMRA cells is regulated, we analyzed the metabolite profile of CD8 T cell populations *ex vivo* (Fig. 1D). Despite their low basal glycolysis (Fig. 1B), EMRA CD8 T cells had high levels of several metabolites from the glycolytic pathway, such as fructose-6-phosphate, dihydroxyacetone phosphate and pyruvate compared to naïve and memory cells (Fig. 1D). The high level of glycolytic intermediates in EMRA CD8 T cells led us to investigate their glucose uptake using the fluorescent glucose analogue 2-NDBG [28]. EMRA CD8 T cells do not maintain the higher metabolite levels through enhanced glucose uptake, as they displayed equivalent glucose uptake compared to memory CD8 T cells (Fig. 1E). Therefore, the unique glycolytic profile of EMRA CD8 T cells is not maintained by differential glucose uptake. In conclusion, EMRA CD8 T cells display low basal glycolysis but are able to accumulate high levels of glycolytic intermediates that may contribute to the high potential to up-regulate glycolysis upon activation.

EMRA CD8 T cells have reduced mitochondrial capacity

Memory cells not only elevate glycolysis during effector differentiation, but also upregulate their TCA cycle activity in the mitochondria [23],[24],[26],[29],[30]. In contrast, EMRA CD8 T-cells are incapable of efficiently engaging mitochondrial metabolism upon antigen encounter [27]. We analyzed the TCA cycle activity of quiescent CD8 T cells by measuring their oxygen consumption. We did not detect differences in the basal oxygen consumption between naïve, CM, EM and EMRA CD8 T cells during steady state (Fig. 2 A and B). However, EMRA cells had a reduced spare respiratory capacity (SRC) compared to memory populations (Fig. 2C), in line with their reduced potential to proliferate upon stimulation. We performed metabolomics of quiescent CD8 T cell populations to examine whether metabolite levels of the TCA cycle support our findings on oxygen consumption. In line with their basal oxygen consumption, EMRA CD8 T cells contained equivalent amounts of most of the

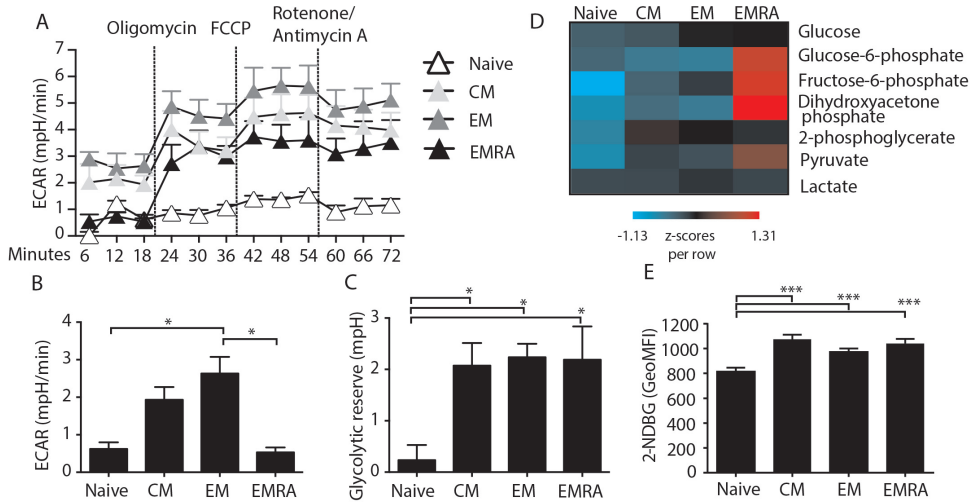
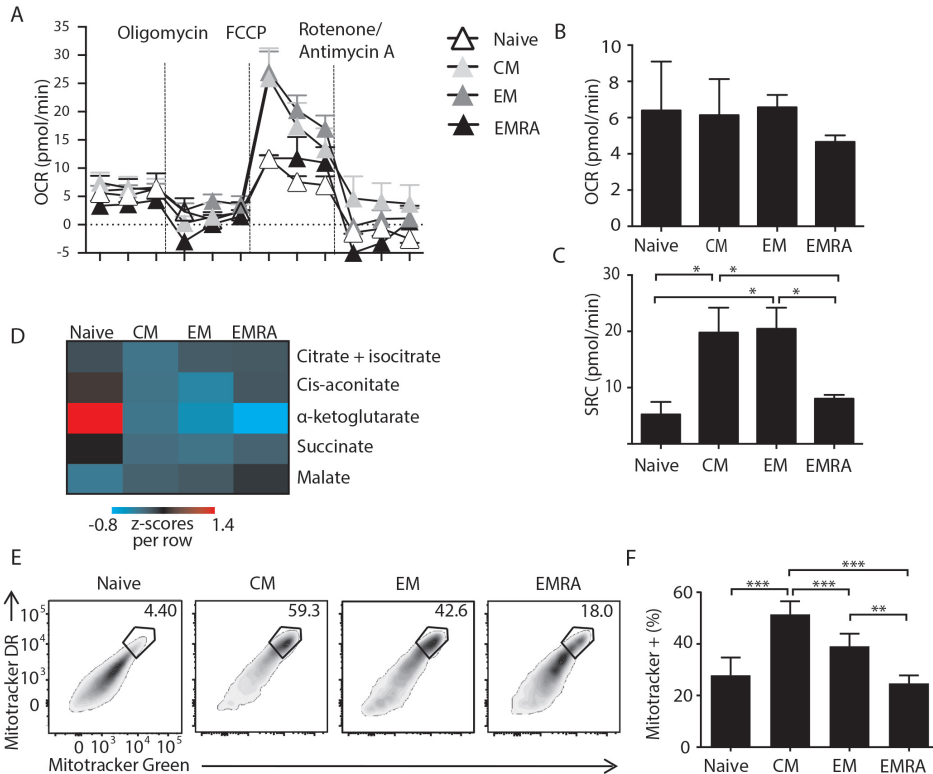


Figure 1. Quiescent EMRA CD8 T cells have low basal glycolysis, but high glycolytic reserve. The glycolytic activity of human CD8 T cell subsets was analyzed ex vivo using the Seahorse FX Analyzer. (a) Graph indicates extracellular acidification rate (ECAR) of naïve, central memory (CM), effector memory (EM) and CD45RA⁺ effector cells (EMRA) after consecutive addition of oligomycin, carbonylcy-anide p-trifluoromethoxyphenylhydrazide (FCCP) and rotenone plus antimycin A. (b) Graph displays the basal ECAR measured before injection of oligomycin. (c) The glycolytic reserve is displayed as the difference between maximal ECAR (after FCCP treatment) and ECAR under basal conditions. (d) Metabolite analysis was performed using LC-MS of ex vivo isolated naïve, CM, EM and EMRA CD8 T cells. Heatmap displays the relative levels of the indicated nutrients of the glycolysis pathway in the CD8 T cell subsets. (e) The uptake of 2-NDBG was measured in naïve, CM, EM and EMRA cells using flow cytometry. Data in (a), (b) and (c) depicts one out of five representative donors from four different experiments, with at least three technical replicates per cell subset, data in (d) represents three different donors from two separate experiments and data in (e) represents the compiled data of six different donors from two separate experiments. * $p < 0.05$, *** $p < 0.001$ in ANOVA multiple comparison test. Graphs are displayed as mean + SEM.

TCA cycle metabolites compared to CM and EM CD8 T cells (Fig. 2D). Remarkably, naïve CD8 T cells had higher levels of most of the examined TCA metabolites compared to the antigen-experienced cells (Fig. 2D). In particular, α -ketoglutarate and succinate were highly present in naïve cells, while malate strongly accumulated in EMRA CD8 T cells (Fig. 2D). To analyze whether mitochondrial capacity underlied the reduced maximum in oxygen consumption, we stained CD8 T cells with the probes Mitotracker Green and Mitotracker Deep Red that visualize the mass and activity of mitochondria, respectively [31]. The mitochondrial mass and activity of quiescent EMRA CD8 T cells were equivalent to those of naïve cells (Fig. 2, E and F), but reduced compared to those of CM and EM CD8 T cells (Fig. 2, E and F). In summary, our results show that in contrast to CM and EM populations, quiescent EMRA CD8 T cells have low mitochondrial levels and low SRC, suggesting that they are unable to increase their TCA cycle activity to the same extent as other memory cells during recall responses.

Hobit positive CD8 T cells have low mitochondrial activity

We have recently found that the transcription factor Hobit (ZNF683) is expressed by



quiescent EMRA CD8 T cells, but not by naïve or by the majority of memory CD8 T cells [32][5],[9]. Hobit regulates direct effector functions such as IFN- γ and granzyme B production, suggesting that Hobit plays a major role in effector functions of EMRA CD8 T cells [33] [32]. Co-staining of Hobit and Mitotracker Deep Red in naïve, memory and EMRA CD8 T cells showed that Hobit expression is preferentially found in CD8 T cells with reduced mitochondrial activity, such as EMRA CD8 T cells and a fraction of memory CD8 T cells (Fig. 3A, B). This difference is particularly prominent within the memory population, in which Hobit+ cells have a lower mitotracker

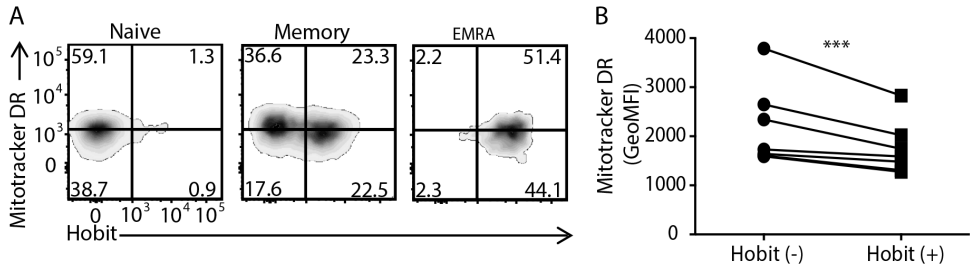


Figure 3. Hobit+ CD8 T cells have low mitochondrial activity.

The mitochondrial activity of Hobit+ CD8 T cells was analyzed using flow cytometry. (a) Density plots display mitochondrial activity using the fixable dye mitotracker deep red (DR) and Hobit expression in naïve, memory and CD45RA+ effector cells (EMRA) CD8 T cells. (b) Graph displays the geometrical mean fluorescence intensity (GeoMFI) of the fixable mitochondrial dye mitotracker DR in Hobit- and Hobit+ memory CD8 T cells. Data points of individual donors are connected. Data in (a) depicts one out of seven representative donors from two independent experiments and data in (b) depicts seven donors from two independent experiments. *** $p < 0.001$ in ANOVA multiple comparison test.

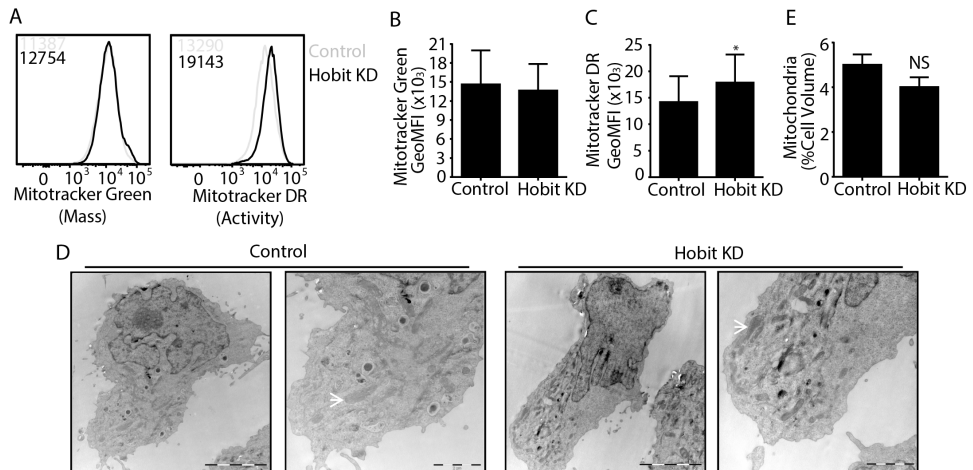


Figure 4. Hobit suppresses mitochondrial respiration.

The mitochondrial activity and mass of control and Hobit knockdown (KD) NK92 cells was analyzed using flow cytometry and transmission electron microscopy. (a) Graph displays flow cytometric analysis of control and Hobit knockdown NK92 cells stained with the probes Mitotracker Green to measure mitochondrial mass and Mitotracker Deep Red (DR) to measure mitochondrial activity. Grey line represents control cells and black line represents Hobit KD cells. (b,c) Graph displays geometrical mean fluorescence intensity (GeoMFI) of control and Hobit KD NK92 cells stained for (b) Mitotracker Green and (c) Mitotracker DR. (d) Representative images of control (left panels) and Hobit KD NK92 cells (right panels) that were taken by transmission electron microscopy are shown. Bar represents 5 μm (first and third panel) or 2 μm (second and fourth panel). White arrows indicate mitochondria. (e) Quantification of transmission electron microscopy images of control and Hobit KD NK92 cells. Mitochondrial area was calculated as the area occupied by mitochondria divided by the total area of the cytoplasm. Data in (a) depicts 1 out of 5 representative experiments, Data in (b, c) depict pooled data of 5 different experiments, data in (d) depicts one representative picture of at least 20 acquired per group, and data in (e) represents quantification of 12 cells per group. *** $p < 0.001$ in ANOVA multiple comparison test. Graphs are displayed as mean + SEM.

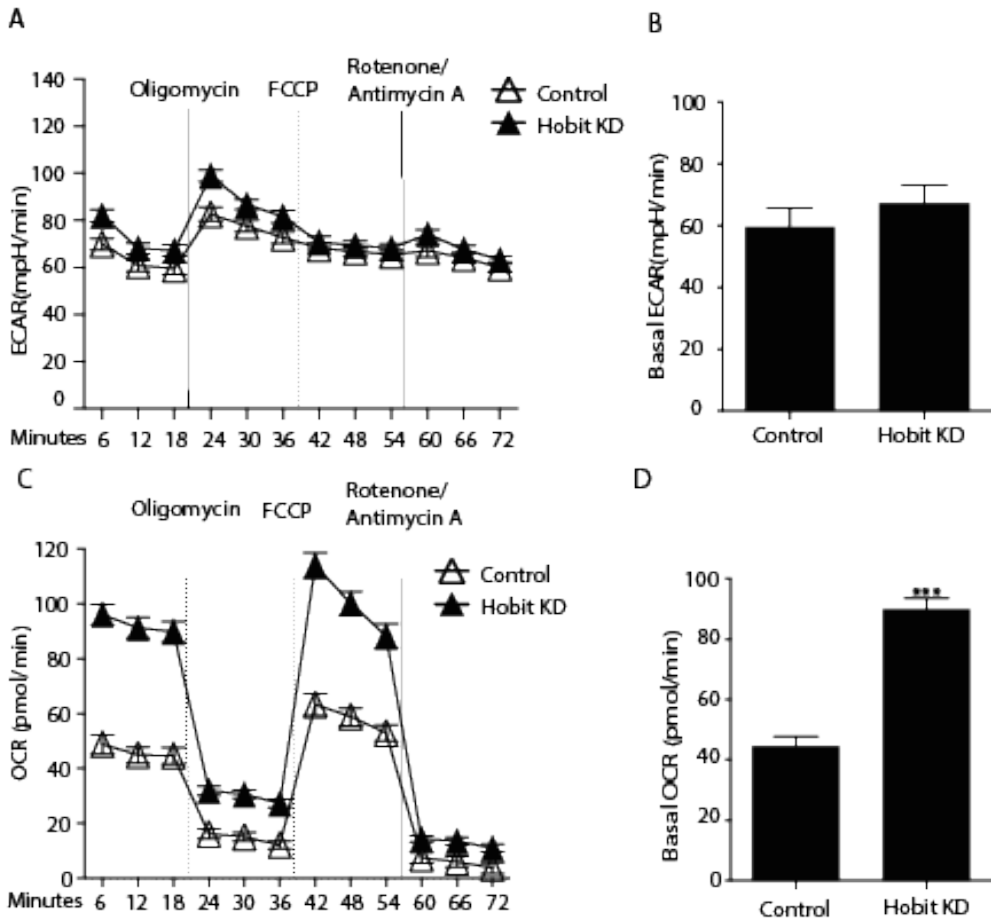


Figure 5. Hobit knockdown increases metabolic activity of effector lymphocytes. The glycolytic activity and oxygen consumption of NK92 cells transduced with control and Hobit knockdown (KD) constructs were analyzed using the Seahorse FX Analyzer. (a) The extracellular acidification rate (ECAR) of control and Hobit KD NK92 cells was measured under the indicated conditions. (b) Graph displays the basal ECAR of control and Hobit KD NK92 cells measured under steady state conditions (c) The oxygen consumption rate (OCR) of control and Hobit KD NK92 cells was followed in real time under steady state conditions and after serial addition of oligomycin, FCCP and rotenone plus antimycin A. (d) Graph displays the basal OCR measured before injection of oligomycin. Data in (a-d) depicts one out of three representative experiments with six technical replicates per experiment. *** $p < 0.001$ in ANOVA multiple comparison test. Graphs are displayed as mean + SEM.

staining compared to Hobit- cells (Fig. 3B). These data suggest that Hobit might be involved in suppression of the metabolism of human quiescent CD8 T cells.

Hobit suppresses mitochondrial activity

To investigate whether Hobit impacts mitochondrial activity, we used the NK92 cell line. NK92 cells express high levels of Hobit mRNA and protein [32]. We stained control and Hobit-knockdown (KD) NK92 cells with the mitochondrial probes Mitotracker Green and Mitotracker Deep Red [31]. Hobit knockdown led to an increase in mitochondrial activity, but not in mitochondrial mass (Fig. 4A, B and C), suggesting that

Hobit suppresses mitochondrial function without affecting the number of mitochondria. Indeed, quantification of mitochondria using electron microscopy showed that control and Hobit-KD NK92 cells contained equal numbers of mitochondria per cell (Fig. 4D and E). Gross morphological and structural features of the mitochondria were not altered upon Hobit KD (Fig. 4D). Thus, Hobit can suppress the mitochondrial activity of cytotoxic lymphocytes without changing their mitochondrial numbers and mass.

Hobit is a global metabolic suppressor in lymphocytes

To expand our analysis on the role of Hobit in metabolism, we performed direct measures of oxygen and glucose consumption in control and Hobit-KD NK92 cells.

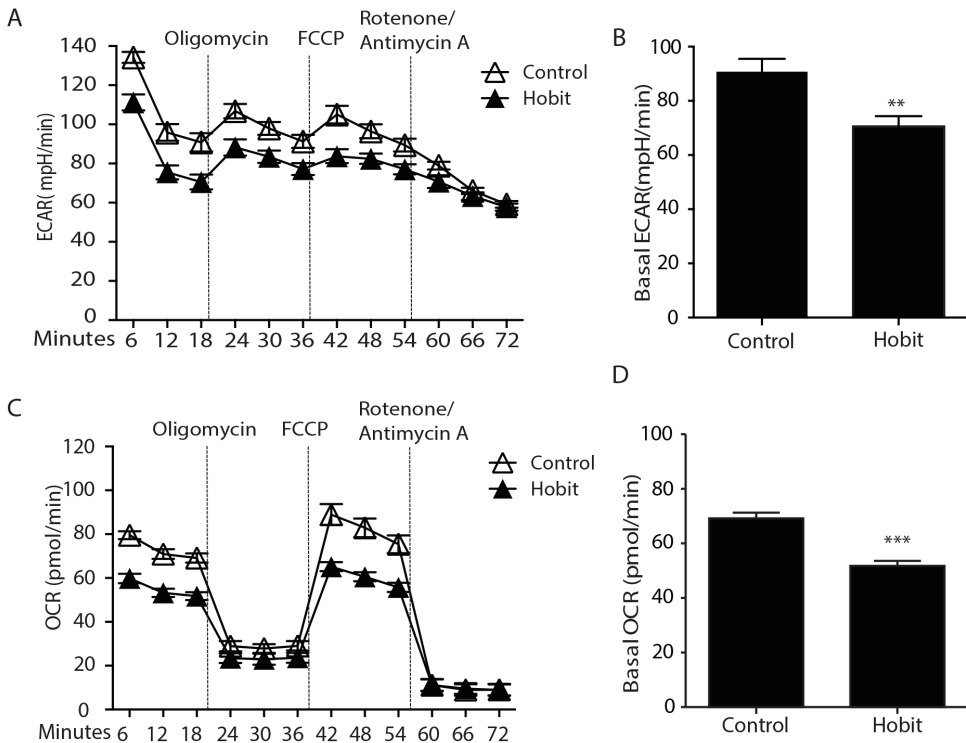


Figure 6. Hobit expression is sufficient for metabolic suppression in T cells. The glycolytic activity and oxygen consumption of mock and Hobit transduced Jurkat cells were analyzed using the Seahorse FX Analyzer. (a) Graph indicates the extracellular acidification rate (ECAR) of control and Hobit transduced Jurkat cells in real time under steady state and after sequential addition of oligomycin, carbonyl cyanide p-trifluoromethoxyphenylhydrazone (FCCP) and rotenone plus antimycin A. (b) Graph displays the basal glycolytic flux of control and Hobit transduced Jurkat cells under steady state conditions. (c) The oxygen consumption rate (OCR) of control and Hobit transduced Jurkat cells was analyzed in real time after sequential addition of oligomycin, FCCP and rotenone plus antimycin A. (d) Graph displays the basal oxygen consumption of control and Hobit transduced Jurkat cells measured under basal conditions. Data in (a-d) depicts one out of four representative experiments with six technical replicates per experiment. *** $p < 0.001$ in ANOVA multiple comparison test. Graphs are displayed as mean + SEM.

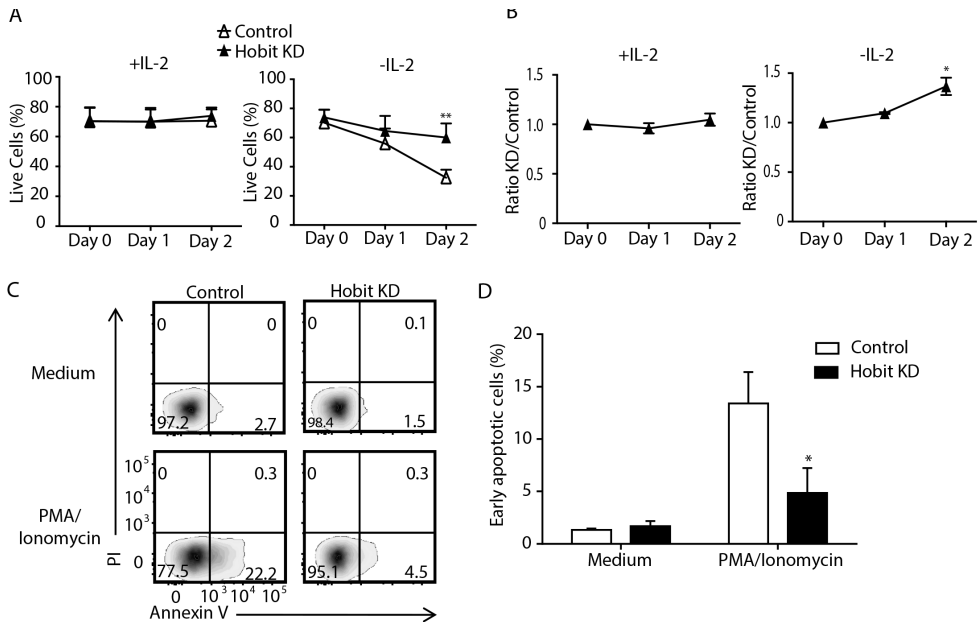


Figure 7. Hobit regulates cell survival during cytokine deprivation and mitogenic activation. Cell survival of control and Hobit knockdown (KD) NK92 cells was analyzed upon IL-2 deprivation or PMA/Ionomycin activation. (a) Control and Hobit knockdown NK92 cells were cultured in the presence or absence of IL-2 (50 IU/ml) for two days. Live cells were determined using the Near IR fixable viability dye and displayed as percentage of total events. (b) Control and Hobit KD NK92 cells, which were identified using CTV or CFSE labeling respectively, were mixed in a 1:1 ratio and cultured in the presence or absence of IL-2 (50 IU/ml) for two days. The ratio of Hobit KD and mock transduced NK92 cells was determined over time. Data was normalized for day zero. (c) Control and Hobit KD NK92 cells were stimulated with or without PMA plus Ionomycin for 4 hr. and analyzed for apoptosis using the membrane impermeable DNA binding dye Propidium Iodide (PI) and the phosphatidyl serine binding lectin Annexin V. (d) Graph displays the percentage of early apoptotic cells (Annexin V+, PI-) of control and Hobit KD NK92 cells after stimulation with PMA plus Ionomycin. Data in (a, b) depicts pooled results from four different experiments. Data in (c) displays one out of three representative experiments and data in (d) depicts pooled data from three different experiments. * $p < 0.05$, ** $p < 0.01$ in Student's t-test (a, d) or ANOVA multiple comparison test (b). Graphs are displayed as mean + SEM.

We did not observe differences in the maximal or in the basal glycolytic flux of NK92 cells upon Hobit knockdown (Fig. 5A and B). The high glycolytic activity of NK92 cells [32] may not provide sufficient window for Hobit to further increase glycolysis in these cells. In contrast, we detected a substantial increase in the respiration of Hobit KD NK92 cells compared to mock transduced NK92 cells (Figs. 5C and D), suggesting that Hobit was essential to suppress oxidative phosphorylation. To address whether Hobit was also sufficient to modulate the metabolism of lymphocytes, we analyzed its impact by over-expressing full length Hobit [32] in Hobit- Jurkat cells [32]. Jurkat cells are highly glycolytic and highly proliferative T cells that do not express endogenous Hobit [34]. Ectopic Hobit expression suppressed the glycolytic activity of Jurkat cells, as evidenced by a reduction in the acidification rate under steady state conditions (Fig. 6A and B). Despite the high rate of glycolysis, Jurkat cells also consumed copious amounts of oxygen (Fig. 6C). The introduction of Hobit was able to suppress mitochondrial respiration in Jurkat cells (Fig. 6C and D). The

capacity to suppress both glycolysis and respiration in Jurkat cells indicated that Hobit globally suppressed the metabolic activity of Jurkat cells. These data confirm a role for Hobit in suppressing oxygen consumption in human lymphocytes and suggest that Hobit also impairs glycolysis. Thus, Hobit may instruct general suppression of metabolism in lymphocytes.

Hobit regulates cell survival during cytokine deprivation and mitogenic activation

NK92 cells are dependent on IL-2 during culture and do not survive for more than 3 days in the absence of IL-2 [35]. We made use of the strict IL-2 dependency of NK92 cells to investigate the impact of Hobit on survival upon cytokine deprivation [36]. Two days after IL-2 withdrawal, Hobit KD cells showed improved survival in comparison to control cells (Fig. 7A). Hobit did not increase the survival of NK92 cells in the presence of IL-2 (Fig 7A). Co-culture of control and Hobit KD cells indicated that Hobit KD cells expanded equally under optimal conditions (+IL-2) (Fig. 7B, left panel). However, upon cytokine withdrawal, Hobit-KD NK92 cells showed improved expansion compared to control NK92 cells (Fig. 7B, right panel). To test whether Hobit would also play a role during mitogenic challenge, we briefly activated NK92 cells with PMA plus Ionomycin. Upon stimulation with PMA/Ionomycin, NK92 cells became apoptotic, as detected by Annexin V staining in the absence of PI staining (Fig. 7C, bottom left panel). We observed that Hobit KD cells were resistant to PMA/Ionomycin induced apoptosis (Fig. 7C and D). Thus, Hobit makes lymphocytes sensitive to cell death under stressful conditions such as nutrient deprivation and cellular activation.

Discussion

Here, we have analyzed the basal metabolic state of EMRA CD8 T cells. The maintenance requirements of terminally differentiated long lived EMRA CD8 T cells differed substantially from those of classical CM and EM cells. EMRA cells appear to have low glycolytic activity compared to CM and EM cells. The accumulation of metabolite intermediates of the glycolysis pathway in EMRA cells suggests that these cells retain the capacity to rapidly upregulate their glycolytic capacity similar to CM and EM cells. EMRA CD8 T cells display low spare respiratory capacity in contrast to CM and EM cells, suggesting that they lack the ability to strongly upregulate oxphos upon stimulation. We show that the transcription factor Hobit is involved in the suppression of both glycolysis and mitochondrial respiration. The metabolic regulation may sensitize these lymphocytes to cell death upon cytokine deprivation or mitogenic stimulation. Our analysis of the metabolism of EMRA cells shows that these long-lived effector cells display the metabolic phenotype of quiescent cells, as they have low mitochondrial and glycolytic activity [37],[38]. Mitochondria are important in the regulation of apoptosis through the release of cytochrome c that activates the caspase pathway to ultimately induce cell death. An increased mitochondrial mass in CD8 T cells has been associated with a higher rate of spontaneous apoptosis [39]. Therefore, the reduced mitochondrial content of EMRA CD8 T cells may constitute an adaptation to avoid spontaneous apoptosis and thereby extend their lifespan. The metabolic characteristics of EMRA cells contrast with those of primary effector cells that display high glycolytic activity despite the abundance of oxygen. This difference between primary effector cells and EMRA cells reflects their environment. Primary effector cells arise during infection in the presence of both antigen and an inflammatory milieu [40]. In contrast, EMRA CD8 T cells are maintained in healthy individuals during quiescence in the absence of detectable levels of antigen and inflammatory signals. The glycolytic potential of primary effectors and EMRA CD8 T cells may underlie their functional characteristics. Primary effector CD8 T cells are highly proliferative, terminally differentiated cells that express high levels of effector molecules such as perforin, granzymes, IFN- γ and TNF- α [41]. Similarly, EMRA cells express high levels of cytotoxic molecules at the protein level such as granzymes and perforin. In contrast, cytokines such as IFN- γ and TNF- α are maintained at the mRNA level in EMRA cells and require restimulation for production. Previously, it has been shown that glycolysis drives IFN- γ protein expression via posttranscriptional regulation of IFN- γ mRNA translation [19]. Therefore, the suppression of glycolysis in EMRA cells may prevent these cells to engage energetically demanding effector functions such as the production of IFN- γ . The persistence of cytotoxic potential in EMRA [11][10] cells suggests that granzymes and perforin in contrast to cytokines are maintained long-term at low energetic costs in the absence of high glycolytic activity. Upon re-activation, memory CD8 T cells rapidly upregulate IFN- γ production [21],[42]. Antigen stimulation in CM and EM cells results in the sequential activation of the serine-threonine kinase Akt and its downstream target mTOR activation to increase the glycolytic flux and support the production of IFN- γ [20]. Despite defective Akt phosphorylation [43], EMRA CD8 T cells are capable of producing large amounts of IFN- γ at early timepoints after activation [10]. The defective Akt machinery in EMRA cells suggests that they employ an alternative pathway to fuel glycolysis and to produce IFN- γ . We observed

that EMRA CD8 T cells have substantial spare glycolytic capacity and accumulate glycolytic intermediate metabolites such as glucose-6-phosphate, fructose-6-phosphate and pyruvate. Thus, our data suggest that EMRA cells may have developed a unique strategy to fuel glycolysis and IFN- γ production through the establishment of an adequate source of glycolytic intermediates.

We observed that EMRA cells contain low numbers of mitochondria and reduced SRC compared to CM and EM cells. Mitochondrial mass and SRC contribute to the efficiency of recall responses [22]. The high mitochondrial mass that relates to high SRC allows memory cells to establish strong proliferative responses [22] and to up-regulate effector functions during re-activation [44]. In line with the low mitochondrial mass and SRC, EMRA cells have limited ability to expand after activation [45]. The mitogen-activated protein kinase (MAPK) p38 signaling pathway is constitutively active in EMRA CD8 T cells [46]. Blockage of p38 after TCR activation increases the mitochondrial mass and partially restores the proliferative impairment of EMRA CD8 T cells but it does not impair their cytokine response [46] [27]. Thus, the low mitochondrial content might be central for the inhibition of proliferative responses of EMRA cells without compromising their effector function.

Here, we report that Hobit acts as a metabolic suppressor, repressing both glycolysis and mitochondrial respiration. Hobit is a zinc-finger transcription factor that shares extensive homology with the transcription factor Blimp-1, especially within the zinc finger region [32]. Hobit and Blimp-1 have highly similar DNA binding motifs and share a large number of targets such as *S1pr1*, *Tcf7* and *Ccr7* [32],[47]. In line with the strong overlap in target genes, Hobit and Blimp-1 co-regulate the formation or maintenance of NKT cells and tissue resident memory T cells (TRM) [47]. In contrast to Hobit, Blimp-1 is expressed in plasma cells and regulates plasma cell development and function [48] [49]. Upon activation, B cells down-regulate their mitochondrial numbers and activity in a Blimp-1 dependent manner, as evidenced using Blimp-1 deficient B cells that maintain a high mitochondrial activity compared to WT B cells after stimulation [50]. It has been shown that Blimp-1 regulates a large set of genes including nutrient transporters and other genes involved in metabolism during plasma cell differentiation [48]. It remains to be investigated how Hobit regulates metabolism, but the functional overlap with Blimp-1 may suggest that Hobit regulates metabolism in EMRA cells in a similar manner as Blimp-1 in plasma cells.

We describe that Hobit plays a key role in sensitizing lymphocytes to cell death during cytokine deprivation and mitogenic stimulation. Similar to Hobit, Blimp-1 has been shown to induce cell death upon cytokine deprivation [51]. However, despite the large number of shared transcriptional targets between Hobit and Blimp-1, it is not clear whether both transcription factors regulate cell death via the same mechanism. Metabolism can play a role in the regulation of cell death. When cells fail to meet their bioenergetic demands, cell death is triggered via apoptosis [53]. However, the exact molecular mechanisms linking metabolism and apoptosis are not fully understood [53]. Glucose deprivation promotes apoptosis in activated T cells [54], while high mitochondrial activity can increase the levels of reactive oxygen species and initiate T-cell apoptosis [55]. Our observation that Hobit sensitizes lymphocytes to cell death upon nutrient deprivation and mitogenic stimulation suggests a connection with the Hobit-driven suppression of metabolism. Thus, we identify Hobit as a key regulator of effector lymphocyte maintenance, as it controls both metabolism

and survival of these cells.

EMRA cells are long-lived cells that display immediate effector function, suggesting that these cells may have therapeutic potential. Several other groups have proposed metabolic regulation of T cells as a new immunotherapeutic tool in the treatment of cancer and autoimmunity [59],[60]. Our characterization of the role of Hobit in metabolism may offer new insights for the use of the Hobit+ EMRA cells in immunotherapy.

Material and Methods

Antibodies.

The following antibodies were used: anti-CD3 (BD Biosciences), anti-CD8 (BD Biosciences and BioLegend), anti-CD16 (Sanquin Reagents), anti-CD27 (Sanquin Reagents), anti-CD45RA (BD Biosciences), anti-CD56 (BD Biosciences), anti-CCR7 (BD Biosciences), anti-FLAG (Life technologies) and anti-Hobit (Sanquin-Hobit/1), anti-mouse IgM (BD, clone DS-1)

Flow cytometry

Antibody labelling: cells were labeled with fluorochrome-conjugated or biotinylated antibodies in PBS 0.5% BSA for 30 min at RT. In case of biotinylated antibodies, fluorochrome-conjugated streptavidin was added in a second step. For intracellular and nuclear staining, cells were fixed and permeabilized using fixation and permeabilization buffers of BD Biosciences and eBioscience, respectively. Expression was analyzed on FACSCanto II, BD LSRFortessa or BD LSR II flow cytometers (BD Biosciences). Hobit staining: cells were fixed for 30 min at RT using the Foxp3 staining kit (eBioscience), washed, and then labeled with anti-Hobit antibodies for 30 min at 4°C. The primary antibodies were washed away, and Hobit expression was visualized using secondary antibodies conjugated with a fluorescent label after another incubation for 30 min at 4°C.

Mitochondria staining: isolated PBMCs were adjusted to a concentration of 1×10^6 cells/100 μ l of culture medium. The mitochondrial probes Mitotracker Green (Cell Signaling) or Mitotracker Deep Red (Cell Signaling) were added to the cells in a final concentration of 100nM (Mitotracker Green) or 2 nM (Mitotracker Deep Red). After 30 min incubation at 37°C, cells were washed and analyzed using the flow cytometer. Glucose uptake: isolated PBMCs were incubated with 30 μ M of 2-NDBG (Thermo Fisher) in medium for two hours at 37°C. Cells were washed twice, and analyzed using flow cytometry.

Plasmids.

Lentiviral pKLO.1 plasmids containing shRNA that target Hobit (TRCN0000162720; CAGAAGAGCTTCACTCAACTT) or that do not target Hobit as a control (MISSION Non-Target shRNA Control SHC002: CCGGCAACAAGATGAAGAGCACCAACTC) were obtained from Sigma (MISSION shRNA Lentiviral Transduction Particles).

Cell culture.

NK92 cells were maintained in RPMI 1640 (Gibco) containing 10% heat inactivated FCS (ICN Biomedicals), IL-2 (50 U/ml; Biotest), streptomycin (100 ng/ml; Life Technologies), and penicillin (10 U/ml; Yamanouchi, Pharma). NK92 cells were transduced using lentiviruses containing pKLO.1 plasmids with control or Hobit KD shRNA. Transduced NK92 cells were selected on puromycin (Sigma-Aldrich) containing medium. Jurkat cells were grown in Iscove's modified Dulbecco's medium (IMDM; Gibco) containing 10% FCS, streptomycin (100 ng/ml), penicillin (10 U/ml) and 0.0004% β -mercapto-ethanol (Merck). Jurkat cells were transduced using lentiviruses containing FUV-1 mCherry with human Hobit or control (empty vector). After 2 days, mCherry positive cells were sorted and expanded further. Transfected Jurkat cells

were cultured with doxycycline (2 µg/ml) for two days before the experiments to induce Hobit expression.

Human PBMCs were obtained from fresh heparinized blood or buffy coats of healthy donors using Ficoll-Paque Plus (GE Healthcare) gradient centrifugation. Total, naive, effector and memory CD8 T cells were isolated using magnetic sorting with CD8 microbeads (Miltenyi Biotec) and flow-cytometric sorting for CD27 and CD45RA on a FACS Aria (BD Biosciences) to obtain CD27+CD45RA+ naive, CD27-CD45RA+ EMRA, CD27+CD45RA-CCR7- EM cells and CD27+CD45RA-CCR7+ CM cells.

For activation cells were cultured with PMA (2 ng/ml; Sigma-Aldrich) and ionomycin (1 µg/ml; Sigma-Aldrich) for 4 hours.

Oxygen consumption rate and extracellular acidification rate measurement.

Primary CD8 T cells were sorted then rested on ice three hours prior to seahorse measurement. Seahorse plates were coated with 100 µl of 0.01% poly-L-Lysine (Sigma) for 10 min at RT. Then, cells (0.25×10^6) were seeded into multiple individual wells in 40 µl of seahorse medium. Plates were spun down for 5 min at 360 G. Extra seahorse medium was added to a total of 180 µl/well. Oxygen consumption rates (OCR) and extracellular acidification rates (ECAR) were measured using the XF-96 Extracellular Flux Analyzer (Seahorse Bioscience). Seahorse medium: non-buffered DMEM medium containing 25 mM glucose, 2 mM L-glutamine, and 1 mM sodium pyruvate. Reading of OCR and ECAR were taken every 7 min. Under steady state and after serial injection of 15 µM oligomycin; 10 µM FCCP; and 25 µM rotenone plus 12.5 µM antimycin A.

Electron Microscopy

NK92 cells were cultured in RPMI 10% FCS plus IL-2. Fixation was performed by adding an equal volume of 4% paraformaldehyde, and 0.4% glutaraldehyde in PIPES/HEPES/EGTA/magnesium buffer to the warm culture medium. Fixed cells were collected, pelleted, embedded, and processed for cryosectioning with a Leica FC. Samples were trimmed using a diamond Cryotrim 90 knife at -100°C (Diatome, Biel, Switzerland), and ultrathin sections of 50 nm were cut at -120°C by using an ultramicrotome cryo knife. Images were analysed by defining the total cell area, nuclei and mitochondria. Cytoplasm area was defined as total cell surface area minus nuclei area. Mitochondrial surface area was defined by dividing the total mitochondrial surface area by the cytoplasm area and displayed as percentage.

Analysis of Metabolites by LC-MS

CD8 T cell subpopulations were sorted by flow cytometry using chilled tubes. Cells were spun down, washed twice with chilled PBS. Metabolites were extracted using methanol/acetonitrile/dH₂O (2:2:1). Samples were vortexed and incubated on ice 30 minutes then centrifuged at 16000g for 15min at 4°C and supernatants collected. LC-MS analysis was performed on an Exactive mass spectrometer (Thermo Scientific) coupled to a Dionex Ultimate 3000 autosampler and pump (Thermo Scientific). The MS operated in polarity-switching mode with spray voltages of 4.5 kV and -3.5 kV. Metabolites were separated using a Sequant ZIC-pHILIC column (2.1 x 150 mm, 5

μm , guard column 2.1 x 20 mm, 5 μm ; Merck) using a linear gradient of acetonitrile and eluent A (20 mM $(\text{NH}_4)_2\text{CO}_3$, 0.1% NH_4OH in ULC/MS grade water (Biosolve)). Flow rate was set at 150 $\mu\text{l}/\text{min}$. Metabolites were identified and quantified using LCquan software (Thermo Scientific) on the basis of exact mass within 5 ppm and further validated by concordance with retention times of standards. Peak intensities were normalized based on TIC.

Statistics.

Values are expressed as mean \pm SD or SEM as indicated. Differences between two groups were calculated by student's t test. Differences between more groups were calculated using 1 way Anova followed by Bonferroni's test for multiple comparisons. A p-value of less than 0.05 was considered significantly different.

Acknowledgements

We would like to thank Dr. Gerritje J. W. van der Windt for the useful discussions and Dr. Riekelt H. Houtkooper for the support in the Seahorse FX assays.

References

1. Wherry EJ, Ahmed R. Memory CD8 T-cell differentiation during viral infection. *J. Virol.* 2004; 78:5535–5545.
2. Hillaire MLB, van Trierum SE, Bodewes R, van Baalen CA, van Binnendijk RS, Koopmans MP, Fouchier RAM, et al. Characterization of the human CD8+ T cell response following infection with 2009 pandemic influenza H1N1 virus. *J. Virol.* 2011; 85:12057–12061.
3. Steven NM, Leese AM, Annels NE, Lee SP, Rickinson AB. Epitope focusing in the primary cytotoxic T cell response to Epstein-Barr virus and its relationship to T cell memory. *J. Exp. Med.* 1996; 184:1801–1813.
4. Gamadia LE, Rentenaar RJ, Baars PA, Remmerswaal EB, Surachno S, Weel JF, Toebes M, et al. Differentiation of cytomegalovirus-specific CD8(+) T cells in healthy and immunosuppressed virus carriers. *Blood.* 2001; 98:754–761.
5. Cui W, Kaech SM. Generation of effector CD8+ T cells and their conversion to memory T cells. *Immunol. Rev.* 2010; 236:151–166.
6. Sallusto F, Lenig D, Förster R, Lipp M, Lanzavecchia A. Two subsets of memory T lymphocytes with distinct homing potentials and effector functions. *Nature.* 1999; 401:708–712.
7. Gebhardt T, Thomas G, Wakim LM, Liv E, Reading PC, Heath WR, Carbone FR. Memory T cells in non-lymphoid tissue that provide enhanced local immunity during infection with herpes simplex virus. *Nat. Immunol.* 2009; 10:524–530.
8. van Lier RAW, ten Berge IJM, Gamadia LE. Human CD8 T-cell differentiation in response to viruses. *Nat. Rev. Immunol.* 2003; 3:931–939.
9. Vieira Braga FA, Hertoghs KML, van Lier RAW, van Gisbergen KPJM. Molecular characterization of HC-MV-specific immune responses: Parallels between CD8(+) T cells, CD4(+) T cells, and NK cells. *Eur. J. Immunol.* 2015; 45:2433–2445.
10. Hamann D, Baars PA, Rep MH, Hooibrink B, Kerkhof-Garde SR, Klein MR, van Lier RA. Phenotypic and functional separation of memory and effector human CD8+ T cells. *J. Exp. Med.* 1997; 186:1407–1418.
11. Hertoghs KML, Moerland PD, van Stijn A, Remmerswaal EBM, Yong SL, van de Berg PJEJ, van Ham SM, et al. Molecular profiling of cytomegalovirus-induced human CD8+ T cell differentiation. *J. Clin. Invest.* 2010; 120:4077–4088.
12. van Leeuwen EM, Gamadia LE, Baars PA, Remmerswaal EB, ten Berge IJ, van Lier RA. Proliferation requirements of cytomegalovirus-specific, effector-type human CD8+ T cells. *J. Immunol.* 2002; 169:5838–5843.
13. Wallace DL, Masters JE, de Lara CM, Henson SM, Andrew W, Yan Z, Kumar SR, et al. Human cytomegalovirus-specific CD8 T-cell expansions contain long-lived cells that retain functional capacity in both young and elderly subjects. *Immunology.* 2010; 132:27–38.
14. Pearce EL, Pearce EJ. Metabolic pathways in immune cell activation and quiescence. *Immunity.* 2013; 38:633–643.
15. Fox CJ, Hammerman PS, Thompson CB. Fuel feeds function: energy metabolism and the T-cell response. *Nat. Rev. Immunol.* 2005; 5:844–852.
16. Frauwirth KA, Thompson CB. Regulation of T lymphocyte metabolism. *J. Immunol.* 2004; 172:4661–4665.
17. Grossman Z, Zvi G, Booki M, Martin M-S, Paul WE. Opinion: Concomitant regulation of T-cell activation and homeostasis. *Nat. Rev. Immunol.* 2004; 4:387–395.
18. Windt GJW, Pearce EL. Metabolic switching and fuel choice during T-cell differentiation and memory development. *Immunol. Rev.* 2012; 249:27–42.
19. Chang C-H, Curtis JD, Maggi LB Jr, Faubert B, Villarino AV, O'Sullivan D, Huang SC-C, et al. Posttranscriptional control of T cell effector function by aerobic glycolysis. *Cell.* 2013; 153:1239–1251.
20. Gubser PM, Bantug GR, Razik L, Fischer M, Dimeloe S, Hoenger G, Durovic B, et al. Rapid effector function of memory CD8+ T cells requires an immediate-early glycolytic switch. *Nat. Immunol.* 2013; 14:1064–1072.
21. Cham CM, Driessens G, O'Keefe JP, Gajewski TF. Glucose deprivation inhibits multiple key gene expression events and effector functions in CD8+ T cells. *Eur. J. Immunol.* 2008; 38:2438–2450.
22. van der Windt GJW, O'Sullivan D, Everts B, Huang SC-C, Buck MD, Curtis JD, Chang C-H, et al. CD8 memory T cells have a bioenergetic advantage that underlies their rapid recall ability. *Proc. Natl. Acad. Sci. U. S. A.* 2013; 110:14336–14341.
23. O'Sullivan D, David O, van der Windt GJW, Huang SC-C, Curtis JD, Chih-Hao C, Buck MD, et al. Memory CD8 T Cells Use Cell-Intrinsic Lipolysis to Support the Metabolic Programming Necessary for Development. *Immunity.* 2014; 41:75–88.
24. van der Windt GJW, van der Windt GJW, Bart E, Chih-Hao C, Curtis JD, Freitas TC, Eyal A, et al. Mi-

- tochondrial Respiratory Capacity Is a Critical Regulator of CD8 T Cell Memory Development. *Immunity*. 2012; 36:68–78.
25. Sukumar M, Madhusudhanan S, Jie L, Yun J, Murugan S, Crompton JG, Zhiya Y, et al. Inhibiting glycolytic metabolism enhances CD8 T cell memory and antitumor function. *J. Clin. Invest.* 2013; 123:4479–4488.
26. Weinberg SE, Sena LA, Chandel NS. Mitochondria in the regulation of innate and adaptive immunity. *Immunity*. 2015; 42:406–417.
27. Henson SM, Lanna A, Riddell NE, Franzese O, Macaulay R, Griffiths SJ, Puleston DJ, et al. p38 signaling inhibits mTORC1-independent autophagy in senescent human CD8+ T cells. *J. Clin. Invest.* 2014; 124:4004–4016.
28. Yoshioka K, Takahashi H, Homma T, Saito M, Oh KB, Nemoto Y, Matsuoka H. A novel fluorescent derivative of glucose applicable to the assessment of glucose uptake activity of *Escherichia coli*. *Biochim. Biophys. Acta*. 1996; 1289:5–9.
29. Pearce EL, Walsh MC, Cejas PJ, Harms GM, Shen H, Wang L-S, Jones RG, et al. Enhancing CD8 T-cell memory by modulating fatty acid metabolism. *Nature*. 2009; 460:103–107.
30. MacIver NJ, Michalek RD, Rathmell JC. Metabolic regulation of T lymphocytes. *Annu. Rev. Immunol.* 2013; 31:259–283.
31. Poot M, Zhang YZ, Krämer JA, Wells KS, Jones LJ, Hanzel DK, Lugade AG, et al. Analysis of mitochondrial morphology and function with novel fixable fluorescent stains. *J. Histochem. Cytochem.* 1996; 44:1363–1372.
32. Vieira Braga FA, Hertoghs KML, Kragten NAM, Doody GM, Barnes NA, Remmerswaal EBM, Hsiao C-C, et al. Blimp-1 homolog Hobit identifies effector-type lymphocytes in humans. *Eur. J. Immunol.* 2015; 45:2945–2958.
33. van Gisbergen KPJM, Kragten NAM, Hertoghs KML, Wensveen FM, Jonjic S, Hamann J, Nolte MA, et al. Mouse Hobit is a homolog of the transcriptional repressor Blimp-1 that regulates NKT cell effector differentiation. *Nat. Immunol.* 2012; 13:864–871.
34. Kinet S, Swainson L, Lavanya M, Mongellaz C, Montel-Hagen A, Craveiro M, Manel N, et al. Isolated receptor binding domains of HTLV-1 and HTLV-2 envelopes bind Glut-1 on activated CD4+ and CD8+ T cells. *Retrovirology*. 2007; 4:31.
35. Gong JH, Maki G, Klingemann HG. Characterization of a human cell line (NK-92) with phenotypical and functional characteristics of activated natural killer cells. *Leukemia*. 1994; 8:652–658.
36. Oliveira JB. Evaluation of IL-2-Withdrawal-Induced Apoptosis in Human T Lymphocytes. In: *Methods in Molecular Biology*; 2013:25–31.
37. Valcourt JR, Lemons JMS, Haley EM, Kojima M, Demuren OO, Collier HA. Staying alive: metabolic adaptations to quiescence. *Cell Cycle*. 2012; 11:1680–1696.
38. Lum JJ, Bauer DE, Kong M, Harris MH, Li C, Lindsten T, Thompson CB. Growth factor regulation of autophagy and cell survival in the absence of apoptosis. *Cell*. 2005; 120:237–248.
39. Petrovas C, Mueller YM, Dimitriou ID, Altork SR, Banerjee A, Sklar P, Mounzer KC, et al. Increased mitochondrial mass characterizes the survival defect of HIV-specific CD8(+) T cells. *Blood*. 2007; 109:2505–2513.
40. Flynn KJ, Belz GT, Altman JD, Ahmed R, Woodland DL, Doherty PC. Virus-specific CD8+ T cells in primary and secondary influenza pneumonia. *Immunity*. 1998; 8:683–691.
41. Joshi NS, Kaech SM. Effector CD8 T cell development: a balancing act between memory cell potential and terminal differentiation. *J. Immunol.* 2008; 180:1309–1315.
42. Cham CM, Gajewski TF. Glucose availability regulates IFN-gamma production and p70S6 kinase activation in CD8+ effector T cells. *J. Immunol.* 2005; 174:4670–4677.
43. Henson SM, Franzese O, Macaulay R, Libri V, Azevedo RI, Kiani-Alikhan S, Plunkett FJ, et al. KLRG1 signaling induces defective Akt (ser473) phosphorylation and proliferative dysfunction of highly differentiated CD8+ T cells. *Blood*. 2009; 113:6619–6628.
44. Sena LA, Li S, Jairaman A, Prakriya M, Ezponda T, Hildeman DA, Wang C-R, et al. Mitochondria are required for antigen-specific T cell activation through reactive oxygen species signaling. *Immunity*. 2013; 38:225–236.
45. Azuma M, Phillips JH, Lanier LL. CD28- T lymphocytes. Antigenic and functional properties. *J. Immunol.* 1993; 150:1147–1159.
46. Henson SM, Macaulay R, Riddell NE, Nunn CJ, Akbar AN. Blockade of PD-1 or p38 MAP kinase signaling enhances senescent human CD8(+) T-cell proliferation by distinct pathways. *Eur. J. Immunol.* 2015; 45:1441–1451.
47. Mackay LK, Minnich M, Kragten NAM, Liao Y, Nota B, Seillet C, Zaid A, et al. Hobit and Blimp1 instruct a universal transcriptional program of tissue residency in lymphocytes. *Science*. 2016; 352:459–463.

48. Tellier J, Shi W, Minnich M, Liao Y, Crawford S, Smyth GK, Kallies A, et al. Blimp-1 controls plasma cell function through the regulation of immunoglobulin secretion and the unfolded protein response. *Nat. Immunol.* 2016; 17:323–330.
49. Rutishauser RL, Martins GA, Kalachikov S, Chandele A, Parish IA, Meffre E, Jacob J, et al. Transcriptional repressor Blimp-1 promotes CD8(+) T cell terminal differentiation and represses the acquisition of central memory T cell properties. *Immunity.* 2009; 31:296–308.
50. Jang K-J, Mano H, Aoki K, Hayashi T, Muto A, Nambu Y, Takahashi K, et al. Mitochondrial function provides instructive signals for activation-induced B-cell fates. *Nat. Commun.* 2015; 6:6750.
51. Küçük C, Iqbal J, Hu X, Gaulard P, De Leval L, Srivastava G, Au WY, et al. PRDM1 is a tumor suppressor gene in natural killer cell malignancies. *Proc. Natl. Acad. Sci. U. S. A.* 2011; 108:20119–20124.
52. Karube K, Nakagawa M, Tsuzuki S, Takeuchi I, Honma K, Nakashima Y, Shimizu N, et al. Identification of FOXO3 and PRDM1 as tumor-suppressor gene candidates in NK-cell neoplasms by genomic and functional analyses. *Blood.* 2011; 118:3195–3204.
53. Altman BJ, Rathmell JC. Metabolic stress in autophagy and cell death pathways. *Cold Spring Harb. Perspect. Biol.* 2012; 4:a008763.
54. Alves NL, Derks IAM, Berk E, Spijker R, van Lier RAW, Eldering E. The Noxa/Mcl-1 axis regulates susceptibility to apoptosis under glucose limitation in dividing T cells. *Immunity.* 2006; 24:703–716.
55. Hildeman DA, Mitchell T, Kappler J, Marrack P. T cell apoptosis and reactive oxygen species. *J. Clin. Invest.* 2003; 111:575–581.
56. Degenhardt K, Mathew R, Beaudoin B, Bray K, Anderson D, Chen G, Mukherjee C, et al. Autophagy promotes tumor cell survival and restricts necrosis, inflammation, and tumorigenesis. *Cancer Cell.* 2006; 10:51–64.
57. Tsuda Y, Parkins CJ, Caposio P, Feldmann F, Botto S, Ball S, Messaoudi I, et al. A cytomegalovirus-based vaccine provides long-lasting protection against lethal Ebola virus challenge after a single dose. *Vaccine.* 2015; 33:2261–2266.
58. Marzi A, Murphy AA, Feldmann F, Parkins CJ, Haddock E, Hanley PW, Emery MJ, et al. Cytomegalovirus-based vaccine expressing Ebola virus glycoprotein protects nonhuman primates from Ebola virus infection. *Sci. Rep.* 2016; 6:21674.
59. O'Sullivan D, Pearce EL. Targeting T cell metabolism for therapy. *Trends Immunol.* 2015; 36:71–80.
60. Wahl DR, Byersdorfer CA, Ferrara JLM, Opipari AW Jr, Glick GD. Distinct metabolic programs in activated T cells: opportunities for selective immunomodulation. *Immunol. Rev.* 2012; 249:104–115.

Hobit but not Blimp-1 maintains cytotoxicity in memory CD8 T cells

Natasja A.M. Kragten¹, **Felipe A. Vieira Braga**^{1*}, Felix M. Behr^{1,2*}, Regina Stark¹, Ester B.M. Remmerswaal², Anna E. Oja¹, Pleun Hombrink¹, Rene A.W. van Lier¹, and Klaas P.J.M. van Gisbergen^{1,2}

¹Dept of Hematopoiesis, Sanquin Research and Landsteiner Laboratory AMC/UvA, Amsterdam, Netherlands;

²Dept of Experimental Immunology, Academic Medical Center, Amsterdam, Netherlands

* Shared second authorship

Abstract:

Human cytomegalovirus (HCMV)-specific CD8 T cells are maintained in a unique differentiation stage that resembles that of effector cells after primary infection. In contrast to primary effector cells, HCMV-specific cells are non-cycling and maintained long-term in the absence of overt virus replication. HCMV-specific effector cells can directly mount cytotoxic responses through the constitutive production of granzyme B and perforin similar to primary effector cells. The recently identified resident memory T cells (Trm) have also been found to maintain granzyme B expression at the protein level. The transcriptional regulation of cytotoxicity in these quiescent lymphocytes remains unclear. We here show that Blimp-1, an important transcriptional regulator of cytotoxicity in primary effector cells, was not expressed at the protein level in quiescent effector and memory CD8 T cells. Here, we demonstrate that Hobit (ZNF683) a transcription factor related to Blimp-1 maintains granzyme B expression and immediate cytotoxic potential in in quiescent effector CD8 T cells and in Trm. These findings indicate that Hobit and Blimp-1 are important during different stages of CD8 T cell differentiation with an early role for Blimp-1 in controlling effector functions during primary infection and a late role for Hobit during quiescence.

Introduction:

CD8 T cells provide an important line of immune defense in viral infection through their ability to eliminate infected cells in an antigen-specific manner. Naive CD8 T cells that recognize viral antigens are triggered to proliferate and differentiate into effector cells within the lymph nodes. The effector cells migrate to the site of infection, where they up-regulate the expression of pro-inflammatory cytokines including IFN- γ and TNF- α and cytotoxic molecules that assist in clearance of infected cells. Effector CD8 T cells engage two major pathways to induce killing of target cells that are mediated through surface-expressed death receptors such as the FasL/Fas and Trail/Trail-R ligand/receptor pairs and through secretory granules containing perforin and granzymes [1;2]. Recognition of antigen in the context of MHC class I molecules triggers CD8 T cells to establish an immunological synapse with target cells that enables the directional release of cytotoxic granules and results in killing of infected, but not of uninfected cells. Granule-dependent cytotoxicity is driven by the pore-forming protein, perforin, which enables the release of proteolytic granzymes into the cytoplasm of target cells. Granzymes consist of a family of serine proteases, of which granzyme A and B have most clearly been associated with the induction of cytotoxicity [3]. Granzyme B induces pro-apoptotic pathways through the cleavage of BID into active truncated BID in humans and pro-caspases into active caspases in mice to establish target cell death [4]. Other granzymes engage alternative pathways of cell death or directly impair components of the viral replication machinery [5]. In mice, the importance of granule-mediated cytotoxicity has been shown by targeted disruption of perforin, which impairs viral clearance after infection with lymphocytic choriomeningitis virus (LCMV) and increases the incidence of carcinogen-induced and spontaneous cancers [6;7]. The effects of deficiency in granzyme A or B are similar, but less dramatic than those of perforin ablation, suggesting substantial redundancy between members of the granzyme family [8].

After resolution of the infection, the effector population contracts into long-lived memory populations to enable more powerful responses upon secondary challenge. Central memory (T_{cm}), effector memory (T_{em}) and CD45RA⁺ effector memory cells (T_{emra}) have been identified as separate long-lived CD8 T cell subsets that are maintained during quiescence in human peripheral blood [9;10]. The peripheral tissues including the epithelial layers of skin, lungs and intestine harbor tissue-resident memory CD8 T cells (T_{rm}) that form distinct populations from the circulating memory cells [11]. Memory subsets of T_{cm}, T_{em} and T_{rm} have been found to develop at late time-points after infection from a subset of effector cells in *in vivo* models using herpes simplex virus (HSV), influenza virus, and lymphocytic choriomeningitis virus (LCMV) infection [12-14]. The ontogeny of T_{emra} cells is less clear, as these cells do not arise in mouse infection models. In contrast to effector cells, memory cells are maintained long-term in the absence of antigenic and inflammatory stimuli, which places constraints on the continuous production of effector molecules. Granzyme B-driven cytotoxicity is strongly down-regulated in memory cells compared to effector cells [15]. T_{cm} and the majority of T_{em} do not express granzyme B or perforin at the protein level, although epigenetic remodeling of the granzyme B locus suggests that it is more easily accessible in these circulating memory cells compared to naive cells

[16;17]. Indeed, Tcm and Tem maintain elevated expression of granzyme B mRNA compared to naive cells, but require up-regulation of granzyme B protein to establish cytotoxic responses [15]. In contrast, Temra have been shown to express granzyme B and perforin at the protein level [9] and can execute antigen-specific cytotoxicity (ref Gamadia). Similarly, Trm that develop in the small intestine and brain after acute infection with LCMV have been reported to express granzyme B during quiescence [18;19]. Thus, a substantial fraction of the long-lived CD8 T cell populations has the potential to immediately engage granzyme B-driven cytotoxicity.

For the improvement of CD8 T cell therapies, it is highly relevant to understand how the immediate cytotoxic potential is maintained into the memory phase. However, at present, the regulation of granzyme B-driven cytotoxicity in Temra and Trm populations is unclear. Previously, we have demonstrated that Hobit is a transcriptional regulator that drives the expression of granzyme B in NKT cells [20]. Interestingly, the expression of Hobit perfectly aligns with long-lived cytotoxic populations, as Hobit is specifically upregulated in Trm and Temra cells within the CD8 T cell lineage [21;22]. Hobit is highly homologous to the transcription factor Blimp-1, which has previously been shown to induce terminal differentiation in the B and T cell lineages [23]. Effector CD8 T cell differentiation is under the control of a set of transcription factors that collaboratively regulate the separation of the short-lived effector and memory precursor lineages. Blimp-1 essentially contributes together with T-bet, Id2 and Notch to the development of short-lived effector cells at the expense of memory precursors [24-28]. Blimp-1 is also involved in the acquisition of the full repertoire of effector functions, as it induces the production of granzyme B in CD8 T cells during the peak of the primary response [26;27]. Therefore, here, we have addressed the role of Hobit and Blimp-1 in the instruction of cytotoxicity during CD8 T cell effector and memory differentiation. Strikingly, we found that Hobit is exclusively important for the maintenance of granzyme B expression during the memory phase.

Results

Blimp-1 protein is not maintained in the absence of antigenic stimulation

Blimp-1 is induced in naive CD8 T cells during effector differentiation and expression is maintained into the memory phase, as evidenced using Blimp-1 reporter mice [26;27]. To study Blimp-1 expression during human CD8 T cell differentiation, we setup an *in vitro* culture protocol (Fig. 1A). Human memory and quiescent effector CD8 T cells expressed Blimp-1 mRNA in contrast to naive CD8 T cells (Fig. 1B), as previously reported [29]. Despite the abundant presence of Blimp-1 mRNA, we observed that Blimp-1 protein expression was nearly absent in memory CD8 T cells (Fig. 1C). Although activation using anti-CD3/28 antibodies in combination with IL-2 did not further increase expression of Blimp-1 mRNA in memory CD8 T cells (Fig. 1B), Blimp-1 protein was strongly induced in these cells (Fig. 1C). These findings suggest that Blimp-1 activity is regulated at the protein level and requires antigenic stimulation in a pro-inflammatory environment. To study the maintenance of Blimp-1 expression after activation, we initially stimulated naive human CD8 T cells using anti-CD3/28 and IL-2, before resting them in the presence of the homeostatic cytokine IL-15 (Fig. 1A). Naive CD8 T cells upregulated Blimp-1 mRNA and protein after stimulation (Fig. 1, B and C). After resting of the cells, Blimp-1 mRNA expression was largely maintained (Fig. 1D), but Blimp-1 protein expression was rapidly lost to near completion (Fig. 1E). The longitudinal analysis indicated that Blimp-1 persists at the mRNA level, but not at the protein level after removal of antigenic stimuli, suggesting that Blimp-1 activity is confined to the effector phase.

Antigenic stimulation down-regulates Hobit expression

To establish whether the Blimp-1 homologue Hobit is also regulated after antigenic stimulation, naive CD8 T cells were stimulated with anti-CD3/28 and IL-2 for 3 days and Hobit expression was analyzed. Antigenic activation of naive CD8 T cells did not induce Hobit expression at the mRNA or protein level (Fig. 2, A-C), suggesting that Hobit in contrast to Blimp-1 is not induced during effector differentiation of CD8 T cells after primary infection. We have previously shown that Hobit is expressed at the mRNA and protein level in long-lived effector cells and a subset of memory cells during quiescence [30]. To establish the regulation of Hobit expression in effector CD8 T cells, we stimulated the cells *in vitro* with anti-CD3/28 and IL-2. In contrast to Blimp-1, Hobit was strongly down-regulated in effector CD8 T cells after 3 days of stimulation with anti-CD3/28 and IL-2 (Fig. 2, A-C). To examine whether the down-regulation of Hobit was a direct effect of T cell activation, we briefly cultured effector CD8 T cells in the presence of PMA and ionomycin. Hobit mRNA was strongly down-regulated in effector CD8 T cells as early as 4 hours after activation with PMA and ionomycin (Fig. 2D). Hobit protein was also down-regulated in effector CD8 T cells after 4 hrs of PMA and ionomycin stimulation, but the down-regulation was not complete at this early time-point (Fig. 2, E and F). To determine whether the expression regulation of human Hobit was similar *in vivo*, we followed HCMV- and EBV-specific CD8 T cells over time after primary HCMV and EBV infection in kidney transplant recipients. HCMV-specific CD8 T cells (HCMV-TPR) and EBV-specific CD8

T cells (EBV-EPL) were divided into proliferating and non-proliferating cells using the proliferation-associated marker Ki67 and analyzed for Hobit expression (Fig. 2G). Ki67^{high} CD8 T cells had reduced expression of Hobit compared to Ki67^{low} CD8 T cells (Fig. 2G), underlining that recent antigen encounter suppresses Hobit expression *in vivo*. Similar results were obtained in a longitudinal study of a second kidney transplant patient (unpublished observations).

Hobit is expressed in granzyme B producing CD8 T cells under resting conditions

Long-lived effector CD8 T cells have direct capacity to lyse infected target cells,

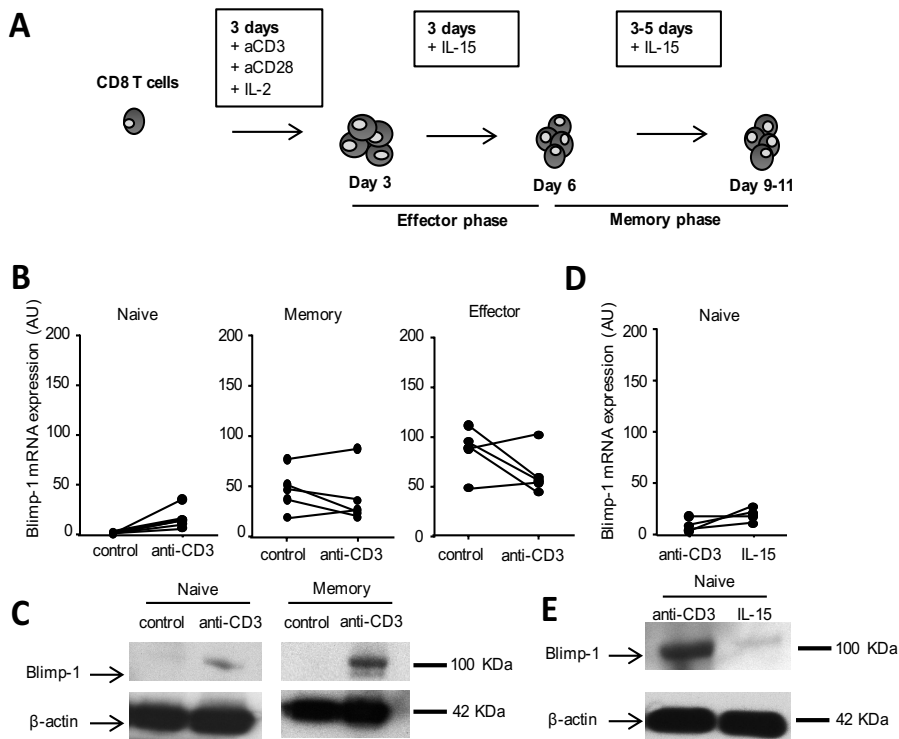


Figure 1: Blimp-1 expression is not maintained at the protein level in human memory CD8 T cells. (A) Schematic representation displays the culture protocol of CD8 T cells. (B,C) CD8 T cells were sorted based on expression of CD27 and CD45RA into naive (CD27+CD45RA+), memory (CD27+CD45RA-) and effector populations (CD27-CD45RA+). Isolated CD8 T cells were not activated (control) or activated with anti-CD3/CD28 antibodies and IL-2 for 3 days. (B) Blimp-1 mRNA expression was analyzed in naive (left panel), memory (center panel) and effector CD8 T cells (right panel) under the indicated conditions. (C) Blimp-1 protein expression (top lane) was analyzed by Westernblot in naive (left panel), memory (center panel) and effector CD8 T cells (right panel) under the indicated conditions. β -actin was used as a loading control (bottom lane). (D,E) Naive CD8 T cells (CD27+CD45RA+) were activated and then rested in IL-15 for 7 days. (D) Blimp-1 mRNA was analyzed using qPCR and (E) Blimp-1 protein was analyzed using Westernblot at the indicated time-points after stimulation. Data displayed in (B) represents five donors from two independent experiments. Data in (C, D and E) display one representative experiment out of at least two independent experiments. The representative experiment in (D) contained four donors. * $p < 0.05$ (two-tailed t-test).

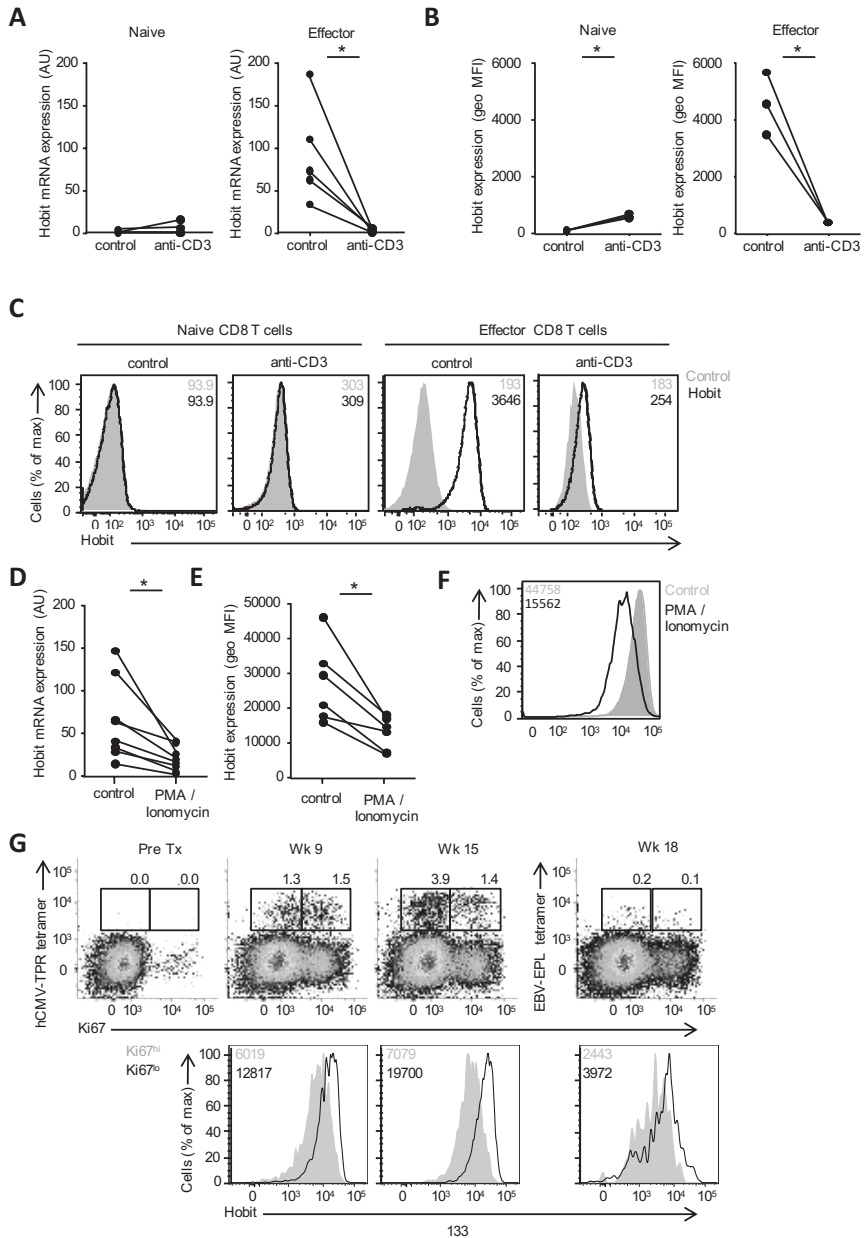


Figure 2. Activation induces downregulation of Hobit expression at the transcriptional level in human CD8 T cells. (A-C) Naive (CD27+CD45RA+) and effector CD8 T cells (CD27-CD45RA+) were isolated using cell sorting and not stimulated (control) or stimulated with anti-CD3/CD28 antibodies and IL-2 for 3 days. The expression of Hobit was determined using (A) qPCR and (B) flow cytometry in naive (left panels) and effector CD8 T cells (right panels) under the indicated conditions. (C) Histograms display binding of secondary antibodies (control; filled grey) and expression of Hobit (black line) in naive and effector CD8 T cells under the indicated conditions. Numbers in upper right corner display geometric mean fluorescence intensity (geo MFI) of Hobit expression. (D-F) Isolated effector CD8 T cells were left unstimulated (control) or were briefly stimulated with PMA and ionomycin. The expression of Hobit was determined using (D) qPCR and (E) flow cytometry. (F) Histogram displays Hobit expression of effector

CD8 T cells under the indicated conditions. Numbers in upper left corner display geo MFI of Hobit expression. (G) The expression of Hobit was determined in the Ki67^{low} and high fractions of hCMV (TPR) and EBV (EPL) specific CD8 T cells at the indicated time points after transplantation of a hCMV+ and EBV+ kidney into an hCMV- and EBV- recipient. Dotplots display tetramer binding and Ki67 expression in CD8 T cells at the indicated weeks (Wk) after transplantation (Tx). Numbers on top of gates represent percentage of cells. Histograms depict Hobit expression in Ki67^{low} and Ki67^{high} tetramer+ CD8 T cells. Numbers in upper left corner represent geometric mean fluorescence intensity (geo MFI) of Hobit expression. Data in (A) displays five donors from two independent experiments. Data in (B) displays one representative experiment with three donors out of at least three independent experiments. Data in (C) shows one representative donor from the data displayed in (B). Data in (D and E) displays at least six donors from three separate experiments. Data in (F) shows one representative donor from the data displayed in (E). Data in (G) displays one representative patient out of two. * $p < 0.05$ (two-tailed t-test).

as they express high levels of granzyme B and perforin protein under steady state conditions [31]. Interestingly, granzyme B clustered together with Hobit and Blimp-1 in microarray analysis of subsets of memory and effector CD8 T cells, suggesting a causal relation of these transcription factors in the regulation of cytotoxicity [29;30]. To address these findings at the protein level, we co-stained CD8 T cells from human peripheral blood for Hobit and granzyme B. Underlining the transcriptional profiling, a strong association between Hobit and granzyme B was found at the protein level. The majority of Hobit+ CD8 T cells co-expressed granzyme B and vice versa the majority of granzyme B+ CD8 T cells co-expressed Hobit (Fig. 3, A and B). CD8 T cells that expressed both Hobit and granzyme B, also contained high amounts of perforin (Fig. 3, C and D), suggesting that they have the machinery for immediate cytotoxicity. Interestingly, Hobit+ CD8 T cells that did not express granzyme B contained low amounts of perforin (Fig. 3, C and D). These cells expressed high amounts of granzyme K instead of granzyme B (Fig. 3, C and D), suggesting that Hobit identifies separate cytotoxic populations that express either granzyme B or K. As predicted, despite the strong overlap between Hobit and granzyme B expression under steady state conditions, naive CD8 T cells expressed granzyme B in the absence of Hobit expression after *in vitro* activation (Fig. 3E). In contrast, Blimp-1 protein was not co-expressed with granzyme B in peripheral blood CD8 T cells under resting conditions, but was induced in granzyme B+ cells after TCR stimulation (Fig. 3F). Thus, Hobit was specifically expressed in CD8 T cells with cytotoxic potential under resting conditions in contrast to Blimp-1 that was upregulated in cytotoxic CD8 T cells after activation.

Resident memory maintains expression of cytotoxic molecules and cytotoxicity

In contrast to human CD8 T cells in peripheral blood, circulating populations of murine memory CD8 T cells do not maintain granzyme B expression at the protein level [15]. The expression regulation of granzyme B and other cytotoxic molecules in Trm populations within the peripheral tissues at late time-points after infection has not been examined in detail. Comparison of memory populations after LCMV infection using RNA sequencing showed that cytotoxicity-associated molecules including granzyme B and C, FasL and Trail were strongly upregulated in gut and liver Trm compared to circulating memory populations (Fig. 4A). To further study the

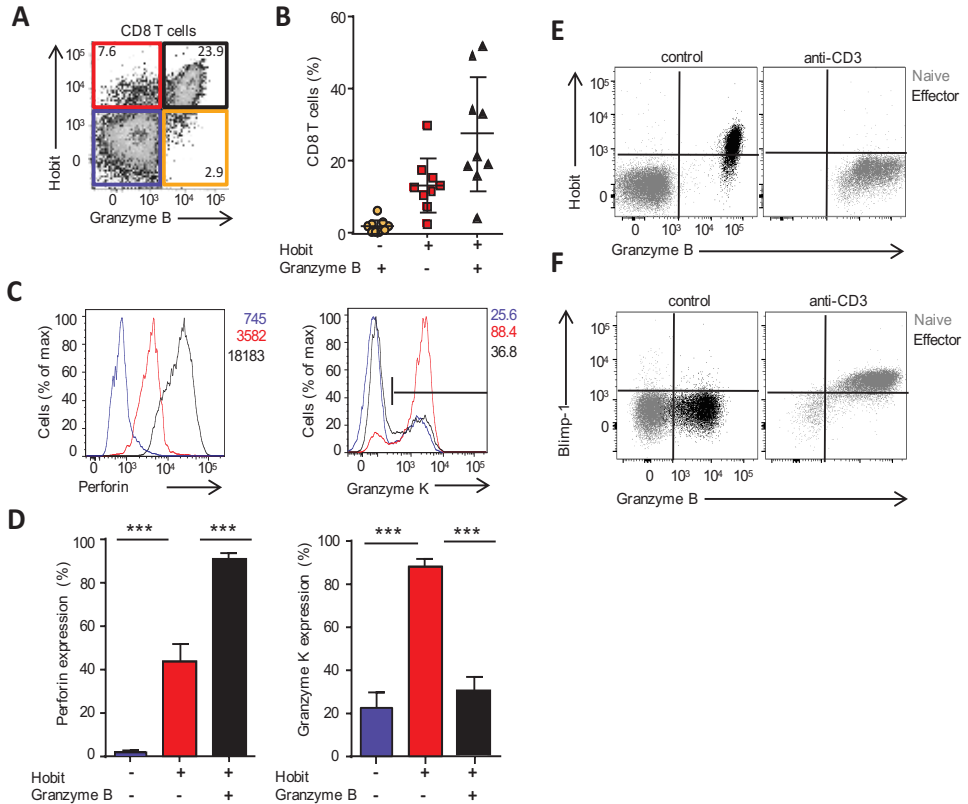


Figure 3: Hobit is co-expressed in human CD8 T cells with granzyme B. (A,B) The co-expression of Hobit and granzyme B was analyzed in CD8 T cells of human peripheral blood. (A) Dot plot depicts Hobit and granzyme B expression in CD8 T cells of a representative donor. Numbers represent percentage of cells within quadrant. (B) The percentage of CD8 T cells expressing only Hobit, only granzyme B or both Hobit and granzyme B was quantified. (C) Histograms and (D) bar graphs depict the expression of perforin (left panels) and granzyme K (right panels) of Hobit-granzyme B⁻ (blue), Hobit+granzyme B⁻ (red) and Hobit+granzyme B⁺ (black) CD8 T cells. (E,F) The expression of (E) Hobit and granzyme B and (F) Blimp-1 and granzyme B was determined in isolated naive (grey dots) and effector CD8 T cells (black dots) under steady state (control) and after activation for 3 days with anti-CD3/CD28 antibodies and IL-2. Data in (A and C) show a representative example from data in (B and D), respectively. Data in (B) displays the pooled results of nine donors from two experiments and data in (D) displays data of 4 donors from one representative experiment out of two. Data in (E and F) are representative of five donors from two independent experiments. *** p < 0.001 (1-way ANOVA).

expression regulation of these cytotoxicity-associated molecules during primary CD8 T cell responses, virus-specific CD8 T cells were followed over time after acute LCMV infection. The expression of granzyme B protein was induced in effector CD8 T cells at day 8 post infection (p.i.) in spleen, liver and gut (Fig. 4, B-D). Expression of granzyme B protein was maintained within LCMV-specific Trm from liver and gut, but not within LCMV-specific Tem from spleen and liver (Fig. 4, B-D). Similar to granzyme B, FasL protein was enriched on liver Trm compared to Tem (Fig. 4E). In contrast, protein expression of Trail was not detectable on these memory populations in comparison to resident NK cells (Fig. 4F). Granzyme B and FasL mediate important pathways that enable cytotoxic T cells to eliminate target cells [1;2], suggesting that Trm

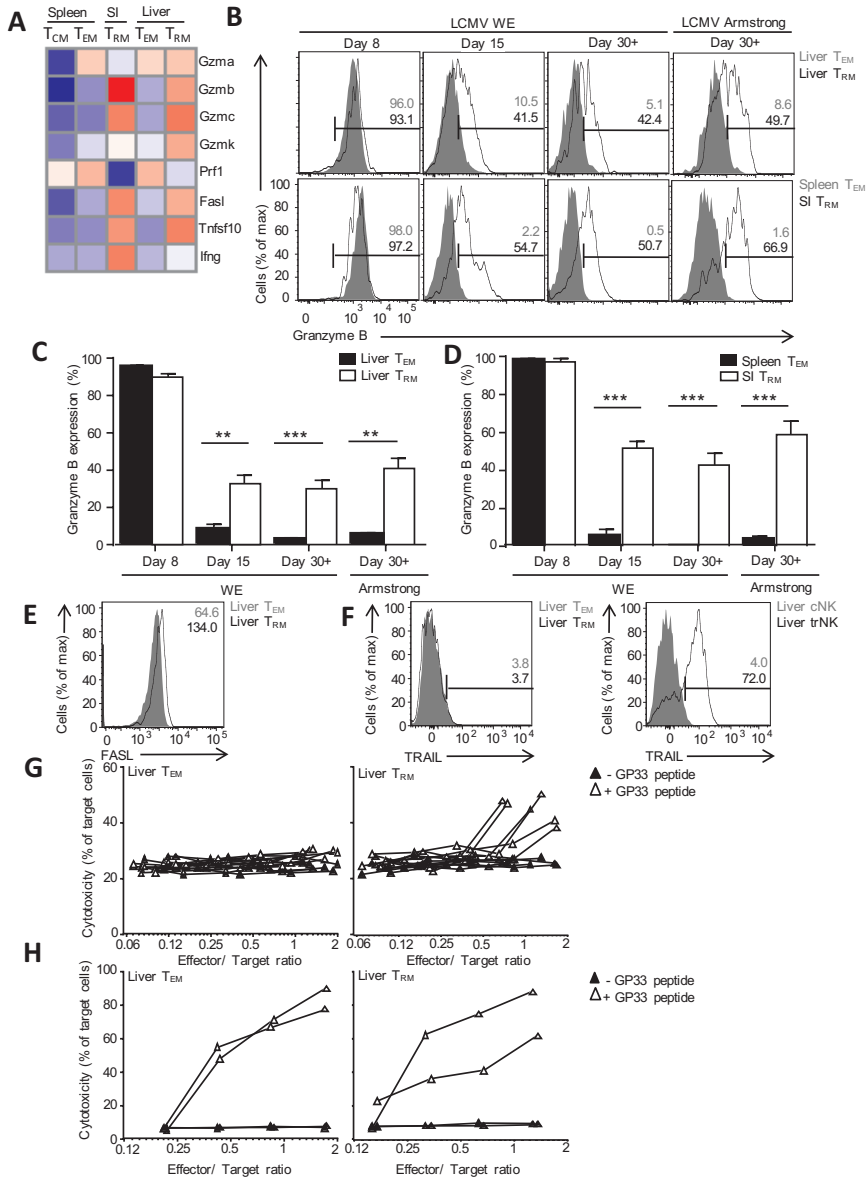


Figure 4: Trm specifically upregulate cytotoxic molecules to maintain immediate cytotoxic potential. (A) Heatmap displays the expression of the indicated cytotoxicity-associated genes in virus-specific circulating (T_{cm} and T_{em}) and resident memory CD8 T cells (T_{rm}) of WT mice after infection with LCMV, as determined using RNA sequencing. (B-D) The expression of granzyme B was analyzed in virus-specific CD69-CD62L- (T_{em}) and CD69+CD62L- CD8 T cells (T_{rm}) in spleen, liver and gut of WT mice at day 8, 15 and day 30+ after infection with LCMV-WE and LCMV-Armstrong, as indicated. (B) Histograms depict expression of granzyme B in the indicated populations of CD8 T cells. (C,D) The percentage of granzyme B+ CD8 T cells was quantified in (C) T_{em} and T_{rm} of liver and (D) in T_{em} of spleen and T_{rm} of small intestine (SI). (E,F) Histograms display expression of (E) FasL and (F) Trail in virus-specific T_{em} and T_{rm} within liver of WT mice at 30+ days after infection with LCMV. For control purposes, TRAIL expression was also analyzed in circulating (cNK) and tissue-resident NK cells (trNK) of the liver. (G,H) The killing of peptide-loaded EL4 target cells was analyzed at (G) 4 and (H) 24 hours of co-culture in the indicated effector/target ratios with virus-specific T_{em} (left panels) or T_{rm} (right panels) of LCMV-infected mice.

maintain cytotoxic activity. To determine the cytotoxic potential of the circulating and resident memory populations, we analyzed the ability of LCMV-specific CD8 T cells to mediate lysis of EL4 target cells loaded with cognate peptide. The virus-specific Trm population displayed cytotoxic activity within 4 hours after stimulation in contrast to the virus-specific Tem population (Fig. 4G). Both Tem and Trm killed target cells after 24 hours (Fig. 4H), suggesting that the main difference between both memory populations is in the kinetics of acquiring cytotoxic effector function. These findings indicate that Trm in contrast to circulating memory cells maintain expression of cytotoxic molecules at the protein level to enable the direct elimination of infected cells after secondary infection.

Blimp-1 drives granzyme B expression during effector phase and Hobit during the memory phase

In mice, Hobit expression in the CD8 T cell lineage is restricted to Trm, whereas Blimp-1 is broadly expressed in effector and memory CD8 T cells [21]. In line with previous findings [26;27], Blimp-1, but not Hobit, was required for granzyme B expression in effector CD8 T cells at day 8 after LCMV infection (Fig. 5, A and B). In contrast, the expression of granzyme B in Trm of liver and gut at day 30+ p.i. was largely dependent on Hobit (Fig. 5, C and D). The contribution of Blimp-1 to the regulation of granzyme B expression in the memory phase could not be addressed, as Blimp-1 deficient mice were unable to clear LCMV infection (unpublished observations). We observed that expression of granzyme B was compromised at the RNA level in Trm of Hobit KO mice, suggesting that Hobit was essential in the transcriptional regulation of granzyme B (Fig. 5E). The expression of other molecules involved in cytotoxicity including perforin was not dependent on Hobit (Fig. 5F). Granzyme B is stored together with perforin in secretory vesicles that contain the lysosomal protein LAMP-1/CD107a [15]. Peptide re-stimulation of virus-specific cells at day 30+ after LCMV infection induced normal degranulation of CD107a+ vesicles in liver-derived Trm in the absence of Hobit (Fig. 5, G and H), indicating that Hobit controls cytotoxicity specifically through the transcriptional regulation of granzyme B expression. These findings show that Blimp-1 and Hobit-driven regulation of granzyme B in CD8 T cells occurs at early and late time-points after infection, respectively. Thus, Hobit rather than Blimp-1 appears important for the long-term maintenance of granzyme B expression in memory CD8 T cells.

Total CD62L-CD69- CD8 T cells (Tem) and CD62L-CD69+ (Trm) fractions of CD8 T cells at day 30+ of infection were taken from liver of WT mice for use as effectors in the killing assays. Data in (B) displays representative examples from data in (C and D). Data in (C and D) displays the results from one representative experiment out of two with three or four mice per group. Data in (E and F) is representative of five to eight mice from two independent experiments. Data in (G) displays results of seven mice from two pooled experiments and data in (H) displays data of two mice from one representative experiment out of two. *** $p < 0.001$ (1-way ANOVA).

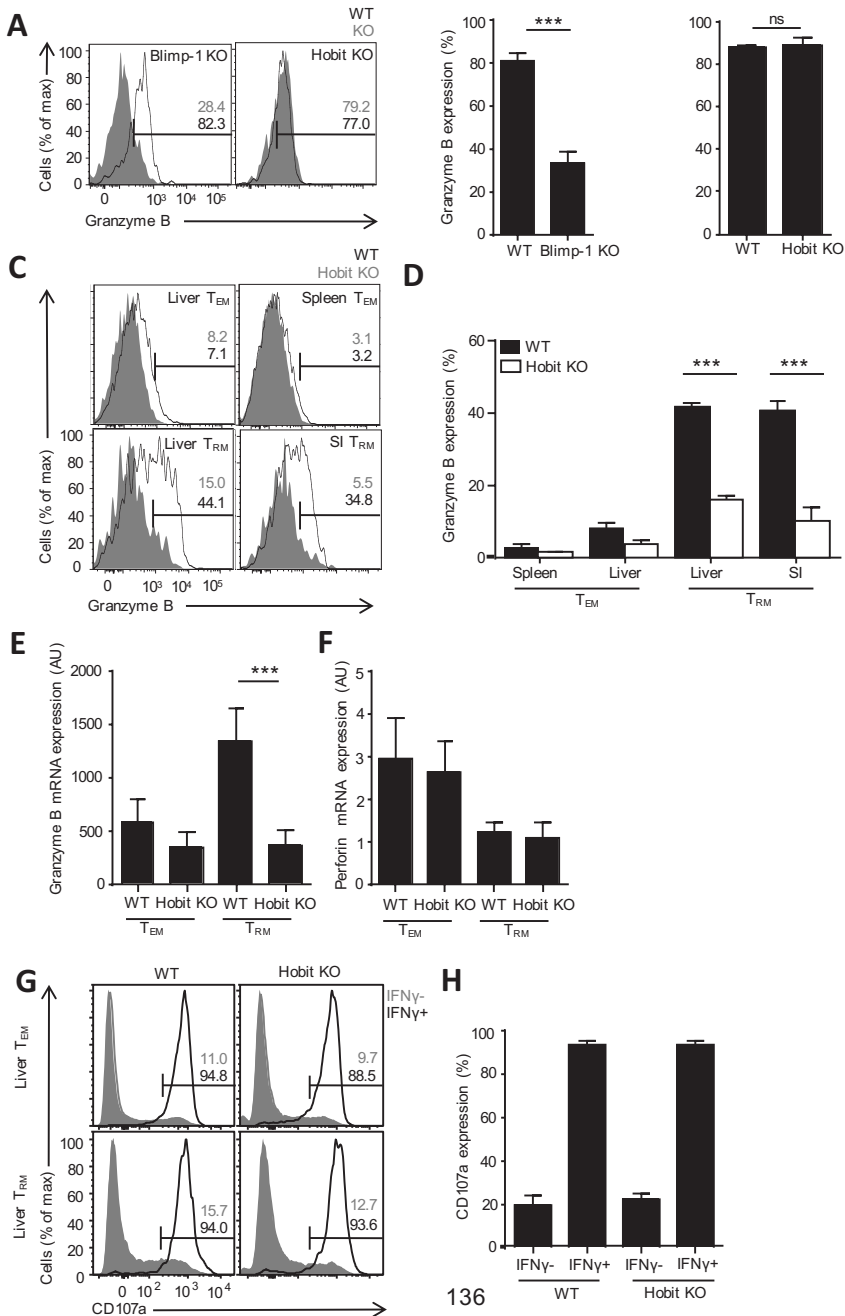


Figure 5: Blimp-1 induces granzyme B expression in effector CD8 T cells and Hobit in memory CD8 T cells after LCMV infection. (A) Histograms depict granzyme B expression in WT (filled grey) and mutant (solid line) virus-specific CD8 T cells of Blimp-1 KO (left panel) and Hobit KO mice (right panel) at day 8 after infection with LCMV. Numbers indicate percentage of granzyme B expressing CD8 T cells. (B) The percentage of effector CD8 T cells that express granzyme B was quantified in WT and Blimp-1 KO

mice (left panel) and in WT and Hobit KO mice (right panel). (C,D) Similarly, the expression of granzyme B was analyzed in virus-specific memory CD8 T cells of WT and Hobit KO mice at day 30+ after infection with LCMV. (C) Histograms depict granzyme B expression in the indicated populations of CD8 T cells. (D) The percentage granzyme B+ CD8 T cells was quantified in the indicated populations of CD8 T cells. (E,F) The expression of (E) granzyme B mRNA and (F) perforin was determined using qPCR in virus-specific CD62L-CD69- Tem and CD62L-CD69+ Trm of WT and Hobit KO mice at day 30+ after LCMV infection. (G,H) The degranulation of LCMV-specific CD8 T cells from liver of WT and Hobit KO mice was analyzed at day 30+ after infection. (G) Histograms and (H) bar graphs display CD107a labeling after brief stimulation with gp33 peptide in LCMV-specific CD8 T cells that were identified using intracellular labeling of IFN- γ . CD62L-CD69- (Tem) and CD62L-CD69+ fractions (Trm) of virus-specific CD8 T cells of WT and Hobit KO mice were separately analyzed. Data in (A, C and G) display representative results from at least four mice from two independent experiments. Data in (B) displays results from one independent experiment out of two with at least three mice per group. Data in (D) displays one representative experiment out of two with four or five mice per group. Data in (E and F) displays pooled results from two experiments with six to eleven mice per group. Data in (G) shows a representative example from data in (H). Data in (H) displays results from one representative experiment out of two with five mice per group. *** $p < 0.001$ (two-tailed t-test or 1-way ANOVA).

Discussion:

In this report, we describe that the expression regulation of Hobit and Blimp-1 occurs in opposite directions during CD8 T cell differentiation. In CD8 T cells, Blimp-1 is up-regulated by activation, whereas Hobit is downregulated by activation. Blimp-1 mRNA, but not Blimp-1 protein, is maintained in long-lived effector and memory populations of CD8 T cells, indicating that Blimp-1 is repressed by post-transcriptional mechanisms in CD8 T cells. These findings suggested that Blimp-1 did not contribute to the regulation of cytotoxicity in CD8 T cells at late time-points after infection. Indeed, we established that Hobit was an essential transcriptional regulator for the maintenance of granzyme B in CD8 T cells during the memory phase. Thus, the Hobit and Blimp-1-driven transcriptional regulation of cytotoxicity appears temporally separated in CD8 T cells with an early role for Blimp-1 in primary effector cells and a late role for Hobit in memory cells.

The Blimp-1 GFP reporter has been a highly valuable tool in the assessment of the expression pattern of Blimp-1 in B and T lymphocytes [26;32]. The reporter has been shown to truthfully reflect Blimp-1 expression at the mRNA level during B and T cell differentiation, but does not necessarily take into consideration the posttranscriptional regulation that may occur at the level of translation or at the level of proteasomal degradation. We have observed a discrepancy between the expression of Blimp-1 mRNA and protein during quiescence in memory CD8 T cells, suggesting that in these lymphocyte populations posttranscriptional regulation is relevant to acquire Blimp-1 protein. The mechanisms underlying posttranscriptional regulation of Blimp-1 are unclear. It is possible that sumoylation plays a role, as this process has previously been reported to target Blimp-1 for degradation by the proteasome [33]. The expression of Blimp-1 protein has not been directly examined in other Blimp-1+ populations such as regulatory T cells and plasma cells. Functional analyses using conditional deletion of Blimp-1 suggest that Blimp-1 protein activity remains during quiescence in plasma cells, although such analyses do not rule out that more subtle differences in protein expression occur [34]. As regulatory T cells and plasma cells in contrast to CD8 T cells are unable to up-regulate Hobit under homeostatic conditions, we speculate that persistence of Blimp-1 protein and acquisition of Hobit are alternative strategies of these separate lineages to maintain the Hobit/Blimp-1 transcriptional module during quiescence.

Hobit does not appear to share the posttranscriptional regulation with Blimp-1, as the expression of Hobit mRNA perfectly aligned with Hobit protein within human CD8 T cells and NK cells [22]. The functional analyses of Trm using granzyme B regulation as a readout for cytotoxic activity also indicate that murine Hobit remains expressed at the protein level, as it maintains the killing capacity of these cells during the memory phase. Currently, the full spectrum of the signaling pathways acting upstream of Hobit expression are unknown. In line with expression during the resting phase, we have found that the homeostatic cytokine IL-15 is involved in the induction of Hobit expression in Trm [21]. Consistent with an exclusive role during quiescence, we have shown that Hobit was downregulated within hours after T cell activation at both the mRNA and protein level. Indeed, Hobit is not found in short-lived effectors

during primary infection, but is present in Temra and Trm cells that display direct effector function and that persist during quiescence [21;22]. The rapid kinetics of the decrease in expression after triggering with PMA and ionomycin indicates direct involvement of TCR signaling pathways in Hobit downregulation. In contrast to Hobit, Blimp-1 appears to be induced in response to inflammatory signals. Blimp-1 expression markedly increases during effector differentiation of CD8 T cells in vivo [35-37], and the transcription factor is also upregulated after antigenic stimulation in combination with cytokines such as IL-2, IL-12 and IL-21 in vitro [38-41]. Similarly, human NK cells up-regulate Blimp-1 expression after stimulation in vitro with IL-12 and IL-18 [42]. The expression regulation suggests that despite the overlap in transcriptional targets, Hobit and Blimp-1 have non-redundant roles in immune regulation, as they are expressed under resting and inflammatory conditions, respectively.

Hobit and Blimp-1 are homologous transcription factors that display the highest degree of similarity in the Zinc Finger domains [20;22]. This region in both Hobit and Blimp-1 is essential for the binding to "GAAAG"-containing DNA sequences, providing rationale for their highly overlapping direct target genes in CD8 T cells [21;22]. Blimp-1 directly bound within the granzyme B locus, suggesting direct involvement in the transcriptional regulation of cytotoxicity [21]. In contrast, we were unable to find evidence for direct binding of Hobit at these sites. Technical reasons relating to sensitivity may underlie the difference, as the total number of target genes was about ten-fold lower for Hobit than for Blimp-1 [21]. Previously, we have shown in NKT cells that Hobit is involved in the regulation of granzyme B expression at the transcript level [20]. Here, we have established an essential role for Hobit in the transcriptional regulation of granzyme B in Trm of liver and gut. As Blimp-1 similar to Hobit positively regulates granzyme B expression and granzyme B-driven cytotoxicity in effector CD8 T cells during primary infection [26;27], it appears that both factors instruct the same transcriptional program to establish cytotoxicity. At odds with the induction of granzyme B expression, Blimp-1 has been described as a transcriptional repressor that silences the expression of target genes through the recruitment of co-repressors including the histone H3K9 methyltransferase G9a, Groucho family proteins and histone deacetylases [43-45]. Recently, it has become clear that during plasma cell differentiation Blimp-1 also associates with putative co-activators such as the chromatin-remodeling BAF complex to establish active histone marks in its target genes [46]. The epigenetic landscape of the granzyme B locus has been studied in human and mouse circulating memory cells and evidence for the presence of active hyperacetylation at H3K9 and the absence of repressive hypermethylation at H3K27 has been found [16;17]. At this stage it is unclear whether these epigenetic marks are preserved in Trm and Temra cells or whether these cells contain unique epigenetic marks. Thus, our findings suggest that Blimp-1 contributes to the transcriptional regulation of cytotoxicity during productive infection and Hobit after clearance of infection, but the potential role of these transcription factors in the establishment of these epigenetic marks remains unexplored.

In contrast to Trm that are formed in liver and gut after LCMV infection, Trm that develop in skin after HSV-1 infection and in lungs after infection with respiratory viruses do not express granzyme B protein [47;48]. As HSV-1-specific Trm within the skin maintain higher expression of granzyme B mRNA than circulating memory pop-

ulations [21], it appears that these Trm also display improved retention of cytotoxic capacity, although not at the level of granzyme B protein expression. The differences in the maintenance of granzyme B expression between Trm populations may relate to tissue-specific adaptations that arise between Trm located at different sites. In support of tissue-specific regulation of granzyme B expression, Trm within the dorsal root ganglia that co-arise with skin-resident Trm after infection with HSV-1 express granzyme B at the protein level [48]. As Hobit is expressed in Trm throughout tissues including the skin and lungs [21], Hobit expression does not appear to be sufficient for the induction of granzyme B protein in all of these Trm populations. We have previously observed that Hobit is essential for granzyme B protein expression in NKT cells located in the thymus, but is not sufficient to induce granzyme B protein in NKT cells residing in spleen and liver under steady state conditions [20]. However, after activation with type I IFN liver-resident NKT cells up-regulate granzyme B in a Hobit dependent manner [20]. Previously, it has been shown that stimulation with type I IFN up-regulates protein expression of granzyme B and granzyme B-driven cytotoxicity in antigen-specific memory CD8 T cells within the lungs [47;49]. Therefore, it is conceivable that Hobit is involved in the acquisition of granzyme B expression in Trm throughout tissues, but that the induction of granzyme B protein in skin and lungs requires stimulation with pro-inflammatory cytokines.

Long-lived CD8 T cells with direct cytotoxic potential are superior compared to other memory cells in that these cells are able to respond directly without the need of proliferation and differentiation, which enables them to mount immune responses at an accelerated pace. Here, we have identified that Hobit rather than Blimp-1 is an essential transcriptional regulator in the long-term maintenance of granzyme B-driven cytotoxicity of memory CD8 T cells. Other transcription factors such as T-bet, Eomes, Runx-3 and Notch, which have all been shown to establish cytotoxicity in effector CD8 T cells through the induction of granzyme B and or perforin [24;50;51], may contribute to the regulation of cytotoxicity in memory cells. In contrast to Hobit, these transcription factors are not exclusively expressed in memory cells with direct cytotoxic potential, suggesting that they do not have a specific role in the long-term maintenance of cytotoxicity. Moreover, T-bet and Eomes are downregulated in granzyme B+ Trm populations compared to granzyme B- circulating populations of memory cells [52]. Thus, our findings have established a Hobit-driven transcriptional network underlying the maintenance of cytotoxicity in CD8 T cells that may provide essential clues to the future use of memory cells with immediate killing capacity in adoptive therapies in patients.

Material and Methods:

Human material

Human PBMCs were obtained from fresh heparinized blood or buffy coats of healthy donors using Ficoll-Paque Plus (GE Healthcare) gradient centrifugation. Total, naive, effector and memory CD8⁺ T cells were isolated using magnetic sorting with CD8 microbeads (Miltenyi Biotec) and then flow-cytometric sorting for CD27 and CD45RA on a FACS Aria (BD Biosciences) to obtain CD27⁺CD45RA⁺ naive, CD27⁻CD45RA⁺ effector and CD27⁺CD45RA⁻ memory cells. We have used blood samples from a kidney transplant patient who was EBV and hCMV seronegative before transplant and who underwent a primary EBV and hCMV infection after receipt of a kidney from a EBV⁺ and hCMV⁺ donor. The patient received an immunosuppressive regimen that included prednisolone, cyclosporine A and mycophenolate mofetil. All donors gave written informed consent prior to inclusion in the study and the study was approved by the Amsterdam Medical Center institutional medical ethics committee.

Mice

WT, Zfp683^{-/-} (Hobit KO) [20] and Prdm1^{flox/flox} x Lck Cre (Blimp-1 KO) mice [26] were maintained on a C57Bl/6 background. Mice were bred under SPF conditions and animal experiments were performed according to national and institutional guidelines.

Antibodies

The following anti-mouse monoclonal antibodies for flow cytometry were purchased from eBioscience, BD Biosciences, Invitrogen or Biolegend: anti-CD3 (145-2C11), anti-TCR β (H57-597), anti-CD4 (RM4-5, GK1.5, and MT4), anti-CD8 (53-6.7), anti-CD44 (IM7), anti-CD62L (MEL-14), anti-CD69 (H1.2F3), anti-Ly5.1 (A20), anti-Ly5.2 (104), anti-IFN- γ (XMG1.2), anti-TRAIL (N2B2), anti-human Granzyme B (GB-11) and anti-FASL (MFL3). The following anti-human monoclonal antibodies for flow cytometry were purchased from Sanquin Reagents, eBioscience and BD Biosciences: anti-CD8 (RPA-T8), anti-CD27 (O323), anti-CD45RA (HI100) and anti-CD3 (SK7). Antibodies against human Hobit (Sanquin-Hobit/1) were made in house, as previously described [22]. The following antibodies were used for western blotting: anti-Blimp-1 (6D3; eBioscience), anti- β -actin (AC-15; Sigma-Aldrich) and conjugated goat anti-mouse secondary antibodies (DAKO).

Tetramers

To detect LCMV-specific CD8 T cells, MHC class I Db restricted tetramers for the viral epitopes GP33-41 and NP396-404 were produced as described [53].

LCMV infection

Mice were infected intraperitoneally with 30 plaque-forming units of the LCMV strain WE. At the indicated time points after infection mice were sacrificed and organs were collected for analysis of CD8 T cell responses.

Cell preparation

Spleen, liver, and small intestine were isolated and ground over 70 μ M nylon cell

strainers (BD Biosciences) to obtain single-cell suspensions in PBS containing 0.5% BSA. Small intestine and liver lymphocytes were separated from the other cell fractions via Percoll (GE Healthcare) gradient centrifugation. Liver-cell preparations were resuspended in 44% Percoll solution and pelleted lymphocyte-enriched fractions were collected after centrifugation. Erythrocytes in spleen and liver cell suspensions were lysed (155 mM NH₄Cl, 10 mM KHCO₃ and 1 mM EDTA) for removal of red blood cells. For the isolation of intraepithelial lymphocytes (IELs) the small intestine was cleared of fat tissue, Peyer's patches, and fecal content. Then, 1 cm² pieces of small intestine were incubated for 30 minutes at 37°C in Ca²⁺ and Mg²⁺ Free Hank's buffer (Gibco) containing 5mM EDTA and 1 mM DTT. IELs were separated from the other cell fractions via density gradient centrifugation using 44% and 66% Percoll that enable enrichment of IELs at the interface of these layers. Cells were counted with an automated cell counter (CaseyCounter (Innovatis)).

In vitro T cell stimulation

Human CD8 T cells were activated in 24 or 96-wells plates (Costar) coated with 3.5ug/ml goat anti-mouse IgG antibodies (Jackson Immunoresearch) and 5 µg/ml anti-CD3 (HIT3a; eBioscience) in the presence of 1 µg/ml anti-CD28 (CD28.2; eBioscience) and 50 U/ml IL-2 (Peprotech) for the indicated time. For short-term activation, CD8 T cells were cultured with PMA (2 ng/ml; Sigma-Aldrich) and ionomycin (1 µg/ml; Sigma-Aldrich) for 4 hours. For the degranulation assay LCMV-specific CD8 T cells were activated in 24 well plates in the presence of 5 µg/ml GP₃₃₋₄₁ and incubated for 4 hours in the presence of CD107a antibodies (eBio1D43; eBioscience). Brefeldin A (eBioscience) and Monensin (eBioscience) were added to enable intracellular capture of IFN-γ. For the cytotoxicity assay, EL-4 cells were labeled with Cell Trace Violet (Thermo Fisher Scientific) according to the manufacturer's protocol and loaded with 5 µg/ml GP₃₃₋₄₁ peptide. The percentage of killing was measured using the viability dye Near-IR (Thermo Fisher Scientific) as a readout.

PCR and quantitative PCR

RNA was isolated using Trizol Reagent (Invitrogen). cDNA synthesis was performed on a Verity 96 well Fast Thermo Cycler (Applied Biosystems) using the iScript RT PCR kit (Biorad). Quantitative PCR was performed on a StepOnePlus system (Applied Biosystems) using the FAST SybrGreen mix (Applied Biosystems). The following primersets were used: murine Hobit (forward: 5'-TCCTCCCACTCTCATCTCCAA-3', reverse: 5'-CAGACCCACTGGCTGTCAT-3'), murine Blimp-1 (forward: 5'-GACGGGGTACTTCTGTTCA-3', reverse: 5'-GGCATTCTTGGGAAGTGTGT-3') Granzyme-B (forward: 5'-AAACGTGCTTCCTTTTCGGG-3', reverse: 5'-GAAACTATGCCTGCAGCCACT-3'), HPRT (forward: 5'-TGAAGAGCTACTGTAATGATCAGTCAAC-3', reverse: 5'-AGCAAGCTTGCAACCTTAACCA-3'), Perforin (forward: 5'-GCAGCTGAGAAGACCTATCAGGAC-3', reverse: 5'-TCTGAGCGCCTTTTTGAAGTC-3'), human Hobit (forward: 5'-CATATGTGGCAAGAGCTTTGG-3', reverse: 5'-GGCAAGTTGAGTGAAGCTCT-3'), human Blimp-1 (forward: 5'-GTGTCAGAACGGGATGAACA-3', reverse: 5'-GCTCGGTTGCTTTAGACTGC-3'), 18S (forward: 5'-GGACAACAAGCTCCGTGAAGA-3', reverse: 5'-CAGAA GTGACGCAGCCCTCTA-3'). Values are represented relative to that of 18S or HPRT and calibrated relative to naive CD8 T cells unless indicated otherwise.

Flow cytometry

Cells were stained for 30 min at 4°C with fluorochrome-conjugated antibodies in PBS 0.5% BSA. Intracellular stainings were performed after fixation and permeabilization with the FoxP3 transcription factor staining set (eBioscience) or with the cytofix/cytoperm kit (BD Biosciences). Tetramer labeling was performed at room temperature. Samples were measured with an LSR Fortessa or a Canto II flow cytometer (BD Biosciences) and expression was analyzed using FlowJo software (Tree Star).

Western Blotting

Cells were lysed in buffer containing 2% SDS, 66 mM Tris pH 7, 16% β -mercaptoethanol and 1% protease inhibitor (Calbiochem). Proteins were separated on a NuPAGE 4-12% Bis-Tris gel (Novex, Life Technologies), after which proteins were transferred onto an iBlot Nitrocellulose Gel Transfer Stack (Novex, Life Technologies) using an iBlot or iBlot 2 (Life Technologies). Membranes were stained using the Pierce ECL Western Blot substrate kit (Life Technologies) and proteins were visualized on Fuji Medical X-ray Film using a Medical Film Processor (Konica Minolta Medical & Graphic, Inc, SRX-101A).

Statistics

Values are expressed as mean \pm SD or SEM as indicated. Differences between two groups were assessed by Student's t test. Differences between more than two groups were assessed using one-way ANOVA followed by a Bonferroni post-hoc test. A p-value of less than 0.05 was considered statistically significant (* = $p < 0.05$; ** = $p < 0.01$; *** = $p < 0.001$).

References:

1. Kagi, D., Vignaux, F., Ledermann, B., Burki, K., Depraetere, V., Nagata, S., Hengartner, H. and Golstein, P., Fas and perforin pathways as major mechanisms of T cell-mediated cytotoxicity. *Science* 1994. 265: 528-530.
2. Lowin, B., Hahne, M., Mattmann, C. and Tschopp, J., Cytolytic T-cell cytotoxicity is mediated through perforin and Fas lytic pathways. *Nature* 1994. 370: 650-652.
3. Voskoboinik, I., Whisstock, J.C. and Trapani, J.A., Perforin and granzymes: function, dysfunction and human pathology. *Nat.Rev.Immunol.* 2015. 15: 388-400.
4. Kaiserman, D., Bird, C.H., Sun, J., Matthews, A., Ung, K., Whisstock, J.C., Thompson, P.E., Trapani, J.A. and Bird, P.I., The major human and mouse granzymes are structurally and functionally divergent. *J.Cell Biol.* 2006. 175: 619-630.
5. Susanto, O., Stewart, S.E., Voskoboinik, I., Brasacchio, D., Hagn, M., Ellis, S., Asquith, S., Sedelies, K.A., Bird, P.I., Waterhouse, N.J. and Trapani, J.A., Mouse granzyme A induces a novel death with writhing morphology that is mechanistically distinct from granzyme B-induced apoptosis. *Cell Death. Differ.* 2013. 20: 1183-1193.
6. Kagi, D., Ledermann, B., Burki, K., Seiler, P., Odermatt, B., Olsen, K.J., Podack, E.R., Zinkernagel, R.M. and Hengartner, H., Cytotoxicity mediated by T cells and natural killer cells is greatly impaired in perforin-deficient mice. *Nature* 1994. 369: 31-37.
7. Smyth, M.J., Thia, K.Y., Street, S.E., Macgregor, D., Godfrey, D.I. and Trapani, J.A., Perforin-mediated cytotoxicity is critical for surveillance of spontaneous lymphoma. *J.Exp.Med.* 2000. 192: 755-760.
8. Chowdhury, D. and Lieberman, J., Death by a thousand cuts: granzyme pathways of programmed cell death. *Annu.Rev.Immunol.* 2008. 26: 389-420.
9. Hamann, D., Baars, P.A., Rep, M.H., Hooibrink, B., Kerkhof-Garde, S.R., Klein, M.R. and van Lier, R.A., Phenotypic and functional separation of memory and effector human CD8+ T cells. *J.Exp.Med.* 1997. 186: 1407-1418.
10. Sallusto, F., Lenig, D., Forster, R., Lipp, M. and Lanzavecchia, A., Two subsets of memory T lymphocytes with distinct homing potentials and effector functions. *Nature* 1999. 401: 708-712.
11. Sathaliyawala, T., Kubota, M., Yudanin, N., Turner, D., Camp, P., Thome, J.J., Bickham, K.L., Lerner, H., Goldstein, M., Sykes, M., Kato, T. and Farber, D.L., Distribution and compartmentalization of human circulating and tissue-resident memory T cell subsets. *Immunity.* 2013. 38: 187-197.
12. Casey, K.A., Fraser, K.A., Schenkel, J.M., Moran, A., Abt, M.C., Beura, L.K., Lucas, P.J., Artis, D., Wherry, E.J., Hogquist, K., Vezys, V. and Masopust, D., Antigen-independent differentiation and maintenance of effector-like resident memory T cells in tissues. *J.Immunol.* 2012. 188: 4866-4875.
13. Jiang, X., Clark, R.A., Liu, L., Wagers, A.J., Fuhlbrigge, R.C. and Kupper, T.S., Skin infection generates non-migratory memory CD8+ T(RM) cells providing global skin immunity. *Nature* 2012. 483: 227-231.
14. Mackay, L.K., Rahimpour, A., Ma, J.Z., Collins, N., Stock, A.T., Hafon, M.L., Vega-Ramos, J., Lauzurica, P., Mueller, S.N., Stefanovic, T., Tscharke, D.C., Heath, W.R., Inouye, M., Carbone, F.R. and Gebhardt, T., The developmental pathway for CD103(+)CD8+ tissue-resident memory T cells of skin. *Nat.Immunol.* 2013. 14: 1294-1301.
15. Wolint, P., Betts, M.R., Koup, R.A. and Oxenius, A., Immediate cytotoxicity but not degranulation distinguishes effector and memory subsets of CD8+ T cells. *J.Exp.Med.* 2004. 199: 925-936.
16. Zediak, V.P., Johnnidis, J.B., Wherry, E.J. and Berger, S.L., Cutting edge: persistently open chromatin at effector gene loci in resting memory CD8+ T cells independent of transcriptional status. *J.Immunol.* 2011. 186: 2705-2709.
17. Araki, Y., Fann, M., Wersto, R. and Weng, N.P., Histone acetylation facilitates rapid and robust memory CD8 T cell response through differential expression of effector molecules (eomesodermin and its targets: perforin and granzyme B). *J.Immunol.* 2008. 180: 8102-8108.
18. Masopust, D., Vezys, V., Wherry, E.J., Barber, D.L. and Ahmed, R., Cutting edge: gut microenvironment promotes differentiation of a unique memory CD8 T cell population. *J.Immunol.* 2006. 176: 2079-2083.
19. Steinbach, K., Vincenti, I., Kreutzfeldt, M., Page, N., Muschawekch, A., Wagner, I., Drexler, I., Pinschewer, D., Korn, T. and Merkler, D., Brain-resident memory T cells represent an autonomous cytotoxic barrier to viral infection. *J.Exp.Med.* 2016. 213: 1571-1587.
20. van Gisbergen, K.P., Kragten, N.A., Hertoghs, K.M., Wensveen, F.M., Jonjic, S., Ha-

- mann, J., Nolte, M.A. and van Lier, R.A., Mouse Hobit is a homolog of the transcriptional repressor Blimp-1 that regulates NKT cell effector differentiation. *Nat.Immunol.* 2012. 13: 864-871.
21. Mackay, L.K., Minnich, M., Kragten, N.A., Liao, Y., Nota, B., Seillet, C., Zaid, A., Man, K., Preston, S., Freestone, D., Braun, A., Wynne-Jones, E., Behr, F.M., Stark, R., Pellicci, D.G., Godfrey, D.I., Belz, G.T., Pellegrini, M., Gebhardt, T., Busslinger, M., Shi, W., Carbone, F.R., van Lier, R.A., Kallies, A. and van Gisbergen, K.P., Hobit and Blimp1 instruct a universal transcriptional program of tissue residency in lymphocytes. *Science* 2016. 352: 459-463.
 22. Vieira Braga, F.A., Hertoghs, K.M., Kragten, N.A., Doody, G.M., Barnes, N.A., Remmerswaal, E.B., Hsiao, C.C., Moerland, P.D., Wouters, D., Derks, I.A., van, S.A., Demkes, M., Hamann, J., Eldering, E., Nolte, M.A., Tooze, R.M., Ten Berge, I.J., van Gisbergen, K.P. and van Lier, R.A., Blimp-1 homolog Hobit identifies effector-type lymphocytes in humans. *Eur.J.Immunol.* 2015.
 23. Kallies, A. and Nutt, S.L., Terminal differentiation of lymphocytes depends on Blimp-1. *Curr.Opin.Immunol.* 2007. 19: 156-162.
 24. Backer, R.A., Helbig, C., Gentek, R., Kent, A., Laidlaw, B.J., Dominguez, C.X., de Souza, Y.S., van Trierum, S.E., van, B.R., Rimmelzwaan, G.F., ten, B.A., Willemsen, A.M., van Kampen, A.H., Kaech, S.M., Blander, J.M., van, G.K. and Amsen, D., A central role for Notch in effector CD8(+) T cell differentiation. *Nat.Immunol.* 2014. 15: 1143-1151.
 25. Joshi, N.S., Cui, W., Chande, A., Lee, H.K., Urso, D.R., Hagman, J., Gapin, L. and Kaech, S.M., Inflammation directs memory precursor and short-lived effector CD8(+) T cell fates via the graded expression of T-bet transcription factor. *Immunity.* 2007. 27: 281-295.
 26. Kallies, A., Xin, A., Belz, G.T. and Nutt, S.L., Blimp-1 transcription factor is required for the differentiation of effector CD8(+) T cells and memory responses. *Immunity.* 2009. 31: 283-295.
 27. Rutishauser, R.L., Martins, G.A., Kalachikov, S., Chande, A., Parish, I.A., Meffre, E., Jacob, J., Calame, K. and Kaech, S.M., Transcriptional repressor Blimp-1 promotes CD8(+) T cell terminal differentiation and represses the acquisition of central memory T cell properties. *Immunity.* 2009. 31: 296-308.
 28. Yang, C.Y., Best, J.A., Knell, J., Yang, E., Sheridan, A.D., Jesionek, A.K., Li, H.S., Rivera, R.R., Lind, K.C., D'Cruz, L.M., Watowich, S.S., Murre, C. and Goldrath, A.W., The transcriptional regulators Id2 and Id3 control the formation of distinct memory CD8+ T cell subsets. *Nat.Immunol.* 2011. 12: 1221-1229.
 29. Hertoghs, K.M., Moerland, P.D., van, S.A., Remmerswaal, E.B., Yong, S.L., van de Berg, P.J., van Ham, S.M., Baas, F., Ten Berge, I.J. and van Lier, R.A., Molecular profiling of cytomegalovirus-induced human CD8+ T cell differentiation. *J.Clin.Invest* 2010. 120: 4077-4090.
 30. Braga, F.A., Hertoghs, K.M., Kragten, N.A., Doody, G.M., Barnes, N.A., Remmerswaal, E.B., Hsiao, C.C., Moerland, P.D., Wouters, D., Derks, I.A., van, S.A., Demkes, M., Hamann, J., Eldering, E., Nolte, M.A., Tooze, R.M., Ten Berge, I.J., van Gisbergen, K.P. and van Lier, R.A., The Blimp-1 homologue Hobit identifies effector-type lymphocytes in humans. *Eur.J.Immunol.* 2015.
 31. Appay, V., Dunbar, P.R., Callan, M., Klenerman, P., Gillespie, G.M., Papagno, L., Ogg, G.S., King, A., Lechner, F., Spina, C.A., Little, S., Havlir, D.V., Richman, D.D., Gruener, N., Pape, G., Waters, A., Easterbrook, P., Salio, M., Cerundolo, V., McMichael, A.J. and Rowland-Jones, S.L., Memory CD8+ T cells vary in differentiation phenotype in different persistent virus infections. *Nat.Med.* 2002. 8: 379-385.
 32. Kallies, A., Hasbold, J., Tarlinton, D.M., Dietrich, W., Corcoran, L.M., Hodgkin, P.D. and Nutt, S.L., Plasma cell ontogeny defined by quantitative changes in blimp-1 expression. *J.Exp.Med.* 2004. 200: 967-977.
 33. Ying, H.Y., Su, S.T., Hsu, P.H., Chang, C.C., Lin, I.Y., Tseng, Y.H., Tsai, M.D., Shih, H.M. and Lin, K.I., SUMOylation of Blimp-1 is critical for plasma cell differentiation. *EMBO Rep.* 2012. 13: 631-637.
 34. Tellier, J., Shi, W., Minnich, M., Liao, Y., Crawford, S., Smyth, G.K., Kallies, A., Busslinger, M. and Nutt, S.L., Blimp-1 controls plasma cell function through the regulation of immunoglobulin secretion and the unfolded protein response. *Nat.Immunol.* 2016. 17: 323-330.
 35. Kallies, A., Xin, A., Belz, G.T. and Nutt, S.L., Blimp-1 transcription factor is required for the differentiation of effector CD8(+) T cells and memory responses. *Immunity.* 2009. 31: 283-295.
 36. Rutishauser, R.L., Martins, G.A., Kalachikov, S., Chande, A., Parish, I.A., Meffre, E., Jacob, J., Calame, K. and Kaech, S.M., Transcriptional repressor Blimp-1 promotes CD8(+) T cell terminal differentiation and represses the acquisition of central memory T cell properties. *Immunity.* 2009. 31: 296-308.
 37. Shin, H., Blackburn, S.D., Intlekofer, A.M., Kao, C., Angelosanto, J.M., Reiner, S.L. and Wherry, E.J., A role for the transcriptional repressor Blimp-1 in CD8(+) T cell exhaustion during chronic viral infection. *Immunity.* 2009. 31: 309-320.

38. Cimmino, L., Martins, G.A., Liao, J., Magnusdottir, E., Grunig, G., Perez, R.K. and Calame, K.L., Blimp-1 attenuates Th1 differentiation by repression of ifng, tbx21, and bcl6 gene expression. *J.Immunol.* 2008. 181: 2338-2347.
39. Martins, G.A., Cimmino, L., Liao, J., Magnusdottir, E. and Calame, K., Blimp-1 directly represses IL2 and the IL2 activator Fos, attenuating T cell proliferation and survival. *J.Exp.Med.* 2008. 205: 1959-1965.
40. Gong, D. and Malek, T.R., Cytokine-dependent Blimp-1 expression in activated T cells inhibits IL-2 production. *J.Immunol.* 2007. 178: 242-252.
41. Salehi, S., Bankoti, R., Benevides, L., Willen, J., Couse, M., Silva, J.S., Dhall, D., Mefre, E., Targan, S. and Martins, G.A., B lymphocyte-induced maturation protein-1 contributes to intestinal mucosa homeostasis by limiting the number of IL-17-producing CD4+ T cells. *J.Immunol.* 2012. 189: 5682-5693.
42. Smith, M.A., Maurin, M., Cho, H.I., Becknell, B., Freud, A.G., Yu, J., Wei, S., Djeu, J., Celis, E., Caligiuri, M.A. and Wright, K.L., PRDM1/Blimp-1 controls effector cytokine production in human NK cells. *J.Immunol.* 2010. 185: 6058-6067.
43. Gyory, I., Wu, J., Fejer, G., Seto, E. and Wright, K.L., PRDI-BF1 recruits the histone H3 methyltransferase G9a in transcriptional silencing. *Nat.Immunol.* 2004. 5: 299-308.
44. Ren, B., Chee, K.J., Kim, T.H. and Maniatis, T., PRDI-BF1/Blimp-1 repression is mediated by corepressors of the Groucho family of proteins. *Genes Dev.* 1999. 13: 125-137.
45. Yu, J., Angelin-Duclos, C., Greenwood, J., Liao, J. and Calame, K., Transcriptional repression by blimp-1 (PRDI-BF1) involves recruitment of histone deacetylase. *Mol.Cell Biol.* 2000. 20: 2592-2603.
46. Minnich, M., Tagoh, H., Bonelt, P., Axelsson, E., Fischer, M., Cebolla, B., Tarakhovsky, A., Nutt, S.L., Jaritz, M. and Busslinger, M., Multifunctional role of the transcription factor Blimp-1 in coordinating plasma cell differentiation. *Nat.Immunol.* 2016. 17: 331-343.
47. Kohlmeier, J.E., Cookenham, T., Roberts, A.D., Miller, S.C. and Woodland, D.L., Type I interferons regulate cytolytic activity of memory CD8(+) T cells in the lung airways during respiratory virus challenge. *Immunity.* 2010. 33: 96-105.
48. Mintern, J.D., Guillonneau, C., Carbone, F.R., Doherty, P.C. and Turner, S.J., Cutting edge: Tissue-resident memory CTL down-regulate cytolytic molecule expression following virus clearance. *J.Immunol.* 2007. 179: 7220-7224.
49. Piet, B., de Bree, G.J., Smids-Dierdorp, B.S., van der Loos, C.M., Remmerswaal, E.B., von der Thusen, J.H., van Haarst, J.M., Eerenberg, J.P., ten, B.A., van der Bij, W., Timens, W., van Lier, R.A. and Jonkers, R.E., CD8(+) T cells with an intraepithelial phenotype upregulate cytotoxic function upon influenza infection in human lung. *J.Clin.Invest* 2011. 121: 2254-2263.
50. Cruz-Guilloty, F., Pipkin, M.E., Djuretic, I.M., Levanon, D., Lotem, J., Lichtenheld, M.G., Groner, Y. and Rao, A., Runx3 and T-box proteins cooperate to establish the transcriptional program of effector CTLs. *J.Exp.Med.* 2009. 206: 51-59.
51. Pearce, E.L., Mullen, A.C., Martins, G.A., Krawczyk, C.M., Hutchins, A.S., Zediak, V.P., Banica, M., DiCioccio, C.B., Gross, D.A., Mao, C.A., Shen, H., Cereb, N., Yang, S.Y., Lindsten, T., Rossant, J., Hunter, C.A. and Reiner, S.L., Control of effector CD8+ T cell function by the transcription factor Eomesodermin. *Science* 2003. 302: 1041-1043.
52. Mackay, L.K., Wynne-Jones, E., Freestone, D., Pellicci, D.G., Mielke, L.A., Newman, D.M., Braun, A., Masson, F., Kallies, A., Belz, G.T. and Carbone, F.R., T-box Transcription Factors Combine with the Cytokines TGF-beta and IL-15 to Control Tissue-Resident Memory T Cell Fate. *Immunity.* 2015. 43: 1101-1111.
53. Altman, J.D., Moss, P.A., Goulder, P.J., Barouch, D.H., McHeyzer-Williams, M.G., Bell, J.I., McMichael, A.J. and Davis, M.M., Phenotypic analysis of antigen-specific T lymphocytes. *Science* 1996. 274: 94-96.

Hobit regulates human natural killer cell development and effector function

Felipe A Vieira Braga¹, Natasja A.M. Kragten¹ , Rene A.W. van Lier¹
, Bianca Blom² and Klaas P.J.M. van Gisbergen¹

¹Department of Hematopoiesis, Sanquin Research and Landsteiner Laboratory AMC/UvA, Plesmanlaan 125, 1066 CX, Amsterdam, The Netherlands ²Department of Cell Biology and Histology, Amsterdam Medical Centre, Amsterdam, The Netherlands

Abstract

Natural Killer (NK) cells are members of the innate lymphoid cell (ILC) family capable of direct killing infected cells. Our understanding of NK cell differentiation depends upon mouse studies, suggesting that differences between human and murine NK cells may impact current models of how human NK cells develop. We have found that *Hobit* is a transcription factor that is highly expressed in human NK cells, but not in murine NK cells. In this report, we describe that *Hobit* is not only expressed in NK cells found in peripheral blood, but also in NK cells in adult bone marrow and in foetal cord blood. Using an in vitro culture system to generate NK cells from cord blood derived progenitor cells, we find that *Hobit* is up-regulated in late stages of NK cell development. Genetic ablation of *Hobit* in progenitor cells enhanced expansion of NK cells upon IL-15 culture and impaired Eomes and granzyme K expression in NK cells. These findings suggest that *Hobit* contributes to the terminal differentiation and the acquisition of effector function of human NK cells.

Introduction

Innate lymphoid cells (ILCs) play an essential role in the establishment and maintenance of immunity, especially at mucosal sites [1]. Natural killer cells are important members of the ILC family that eliminate viruses through the production of IFN- γ and kill infected or transformed cells through the production of perforin and granzymes [2],[3]. NK cells are classified into CD56bright CD27+ CD16-/+ and CD56dim CD27-/+ CD16+ NK cell subsets [4],[5]. CD56dim NK cells express high levels of cytolytic molecules such as granzyme B and perforin [6], and can perform direct cell lysis [7]. CD56bright NK cells express high levels of granzyme K [8] and can produce large amounts of cytokines including IFN- γ , TNF- α , IL-10 and MIP-1 α [9] upon activation with IL-12, IL-15 and/or IL-18 [10]. In contrast to CD56dim NK cells, CD56bright NK cells are KIR negative, and express the hematopoietic marker c-kit (CD117) [11]. CD56bright NK cells vigorously proliferate in response to low doses of IL-2, while CD56dim NK cells require stronger IL-2 stimulation to achieve proliferative responses [12],[13]. These NK subsets also differ in their tissue distribution [14]. CD56dim NK cells form the major NK cell population in blood and bone marrow [14], while CD56bright NK cells dominate in lymph nodes, endometrium and liver [14], suggesting specialization in their functional roles.

Natural killer cell development is initiated from hematopoietic precursor cells in the bone marrow [15]–[17], but full maturation occurs in secondary lymphoid organs [18],[19]. IL-15 is essential for NK cell development and maintenance [20]–[22]. The lineage relationship between CD56dim and CD56bright NK cells is a topic of intense investigation. It has been suggested that CD56bright NK cells are an intermediate subset that terminally differentiates into CD56dim NK cells [23]. CD56bright NK cells appear prior to CD56dim NK cells during in vitro differentiation from CD34+ progenitor cells [19],[22] [23]. Furthermore, CD56bright NK cells have longer telomeres than CD56dim NK cells [24],[25]. However, specific mutations can lead to CD56bright NK cell deficiency without affecting CD56dim NK cells [26], suggesting that CD56dim NK cells can arise independently of CD56bright NK cells.

Several transcription factors are known to regulate murine NK cell development [1]. Id2 is a crucial transcription factor for the development of the ILC lineage and Id2 ablation leads to severe impairment of NK cell formation, due to impairment at an early NK cell precursor stage [27]. T-bet and Eomes are T-box family transcription factors that are also essential for murine NK cell development [28],[29]. Combined deficiency in both transcription factors results in severely impaired NK cell development [30]. Blimp-1 (PRDM1) is another transcription factor important for murine NK cell development [31]. Blimp-1 deficiency leads to a reduction in terminally differentiated NK cells in mice. Despite the extensive understanding of murine NK cell development, little is known about the transcriptional regulation of human NK cell development. The differentiation of NK cells into CD56dim and CD56bright NK cell subsets cannot be studied in mice, as expression of CD56 and the presence of these NK subsets is not conserved. Gata-2 is one of the few transcription factors known to be involved in the development of CD56bright NK cells, as patients with a Gata-2 mutation specifically lack this subset [26],[32]. We have recently shown that the transcriptional regulator Homologue of Blimp-1 in T cells (Hobit), also known as ZNF683, is highly expressed in CD56bright and CD56dim human NK cells [33], in

contrast to murine NK cells [34]. The expression pattern of Hobit suggests that this transcription factor contributes to differentiation pathways in human NK cells that are not shared with murine NK cells. In this report, we show that Hobit is upregulated late during human NK cell development. We also explore the role for Hobit in human NK cell development and in NK cell effector function.

Results & Discussion

Hobit is expressed in mature NK cells but not in NK precursor cells.

Early NK cell development occurs primarily in the bone marrow [15],[35],[36], in a multi-step process [37]. NK cell progenitors can be identified using the markers CD34 and CD117 (c-kit) [38]. We used multicolor flow cytometry to investigate Hobit expression in NK cell precursors present in human blood and bone marrow. CD34 is an adhesion molecule that identifies the earliest NK cell progenitors in both circulation and bone marrow [16]. In contrast to mature NK cells, we could not detect Hobit expression in CD34+ progenitor cells (Fig. 1a and b, left panels). As progenitor cells differentiate into NK cells, CD34+ cells up-regulate CD117 (c-kit) [38]. We could not detect any Hobit expression in CD117+ cells in the bone marrow (Fig. 1a and b, left panels), indicating that Hobit is completely absent from early NK progenitor cells. Nearly all mature NK cells in these tissues express high levels of Hobit (Fig. 1a and b, right panels). CD56bright NK cells consistently displayed lower Hobit expression compared to CD56dim cells, suggesting that Hobit expression increases during terminal differentiation of NK cells throughout tissues (Fig. 1a and b). Mature NK cell populations are heterogeneous cells and both CD56bright and CD56dim NK cells can be further divided into subpopulations based on surface expression of NK cell receptors [39],[40],[41]. The NKG2 co-receptor CD94 distinguishes functional mature NK cells in the CD56dim subset [42]. Hobit expression was found on CD94+ NK cells (Fig. 1a and b), suggesting that Hobit is expressed in functional mature NK cells. We further analyzed NK cell differentiation in cord blood to address whether Hobit expression was dependent on immunogenic challenge [43],[44]. Our analysis showed, that as in blood and bone marrow, Hobit expression was absent from progenitor cells (Fig. 1c, left panels), but that Hobit was highly expressed in mature NK cells derived from cord blood. A large population of cord blood NK cells lacks the expression of the classical NK cell marker CD56 [45], but does express CD16 and GnzB [45]. Hobit is present in the CD3- CD56- fraction of cord blood (Fig. 1c, right panels), suggesting that Hobit is expressed on CD16+CD56- NK cells. We have previously shown that Hobit induces IFN- γ production [33] and regulates the survival of effector lymphocytes (Chapter 4). The high expression of Hobit in mature NK cells in cord blood, bone marrow and the circulation suggests that Hobit may be involved in the transcriptional control of IFN- γ production maintenance of human NK cells throughout tissues.

Hobit expression increases during in vitro NK cell differentiation.

NK cell development is a highly regulated process in which IL-15 plays a fundamental role [4],[20]. Early studies have established that NK cells can be generated and expanded from progenitors in bone marrow (BM), lymph nodes and cord blood [15]–[17],[22]. We cultured NK cells from CD34+ cord blood progenitor cells during a period of three weeks using human serum, Flt3 ligand and IL-7. The addition of IL-15 to these cultures led to a progressive outgrowth of CD56+ NK cells over time (Fig. 2a). At week three, a fraction of CD56+ NK cells co-expressed CD16 (Fc γ R2A), recapitulating the phenotype of the CD56dim NK cell population (Fig. 2a). Compared

to circulating NK cells obtained ex vivo, in vitro generated NK cells expressed lower amounts of T-bet and Blimp-1, but displayed higher expression of Eomes (Fig. 2b). The findings on the expression levels of these transcription factors can be explained by the low percentage of CD16⁺ NK cells in the cultures compared to the high percentage of CD16⁺ NK cells in peripheral blood, as CD56^{dim}CD16⁺ NK cells are Blimp1-bright, T-bet-bright, Eomes-dim, while CD56^{bright}CD16⁻ NK cells are Blimp1-dim, T-bet-dim, Eomes-bright, [33],[46]. Hobit mRNA expression in in vitro cultured NK cells was similar to that in ex vivo obtained NK cells (Fig. 2b). Hobit expression was also detected at the protein level in the NK cell fraction of the cultures (Fig. 2c,d and e). Terminally differentiated CD16⁺ NK cells expressed higher levels of Hobit than CD16⁻ NK cells and Hobit expression progressively increased over time in the cultures (Fig. 2c and d and e), supporting a role for Hobit in the final stages of NK cell differentiation.

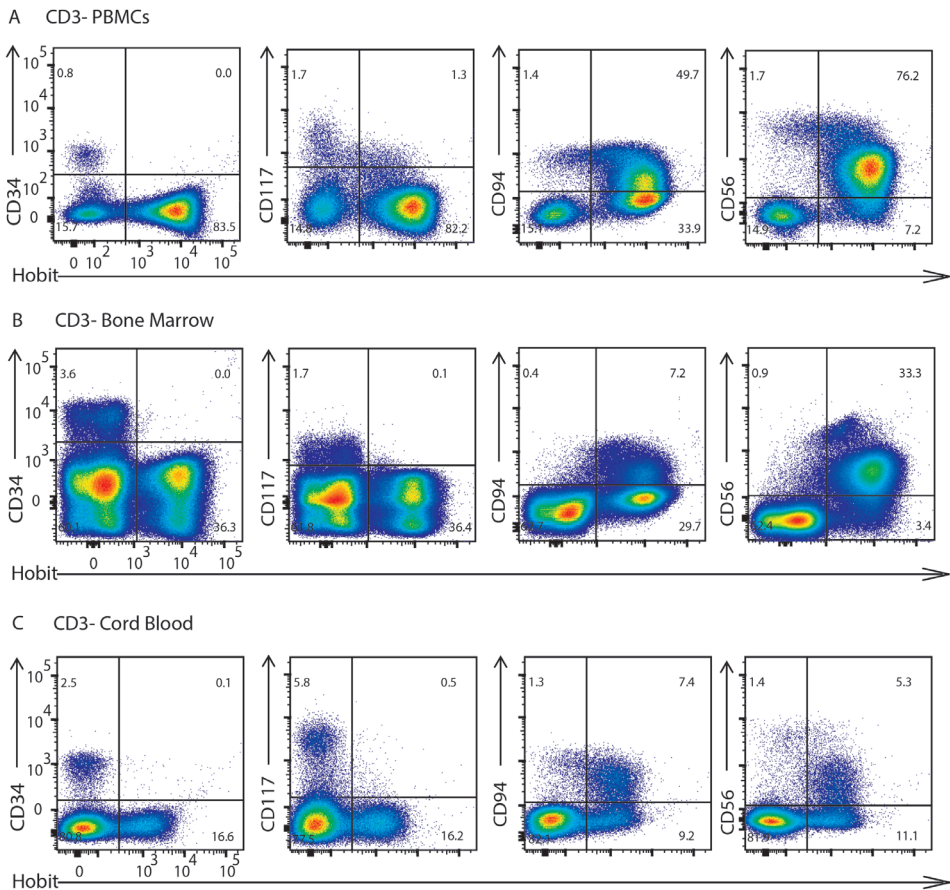


Figure 1. Hobit is expressed in mature NK cells but not in NK precursor cells. Hobit expression was analyzed in combination with NK cell progenitor markers in the indicated tissues. Flow cytometry plots display Hobit expression against CD34, CD117, CD94 and CD56 in CD3⁻ cells from (a) adult peripheral blood, (b) adult bone marrow or (c) cord blood. Representative data of at least three different donors (a,b) or two different donors (c) are shown.

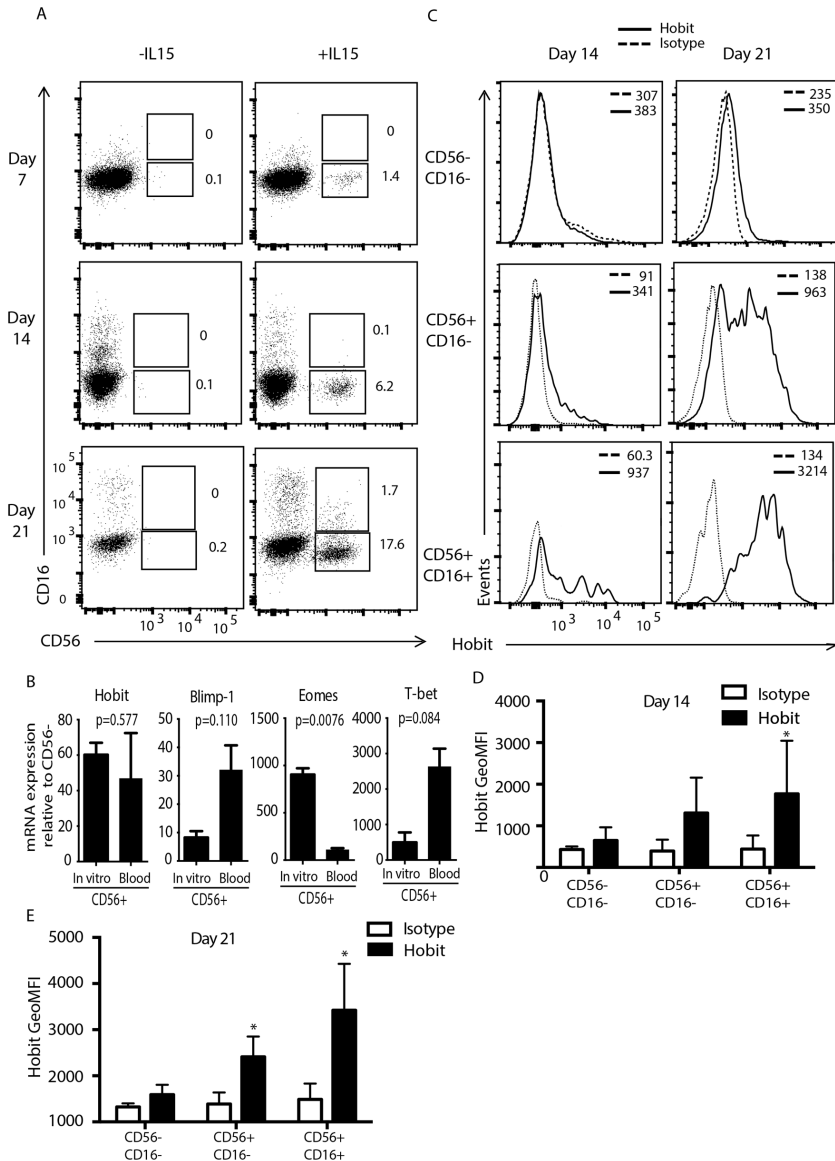


Figure 2. Hobit expression increases during in vitro NK cell differentiation. Hobit expression was followed over time in NK cells generated in vitro from hematopoietic stem cells using culture in IL-15. (a) Flow cytometry plots illustrate expression of CD16 and CD56 on lineage negative (CD3-CD19-CD14-) cells at the indicated days after initiation of the cultures. (b) Graphs show mRNA expression of the indicated transcription factors in the CD56+ fraction of the NK cell cultures and for comparison in NK cells isolated directly from peripheral blood. (c) Flow cytometry plots display Hobit expression in CD56- progenitors, CD56+CD16- NK cells and CD56+CD16+ NK cells at day 14 (left panels) and day 21 of culture (right panels). Solid line depicts expression of Hobit and dotted line depicts background of the isotype control. Values in the graph represent the geometric mean fluorescence intensity (GeoMFI). (d,e) Graphs display quantification of Hobit expression in the indicated subsets of the NK cell cultures at (d) day 14 and (e) day 21. Data in (a,c) displays one out of three representative donors. Data in (b,d and e) show quantification of three different donors from two different experiments. Graph displays mean + SD.

Hobit suppresses NK cell development.

In order to address the role of Hobit during NK cell development, we transduced CD34+ progenitor cells with an shRNA [33] that specifically knocks down Hobit expression (Fig. 3a). We achieved a partial knockdown of Hobit expression in the cultured NK cells. The partial Hobit knockdown resulted in an increase in the percentage of CD56+CD16- cells at day 21 of culture compared to mock transduced control cultures (Fig. 3b and c), suggesting that Hobit expression limits the development and / or expansion of NK cells. During NK cell development, IL-15 sustains the expansion of NK cells from precursors [22]. These results corroborate our previous findings in primary NK cell cultures, as we have recently shown that Hobit knockdown also increases the expansion of NK cell lines upon cytokine withdrawal (Chapter 4). The late expression of Hobit during NK cell differentiation suggests that Hobit acts in NK cells to induce terminal maturation.

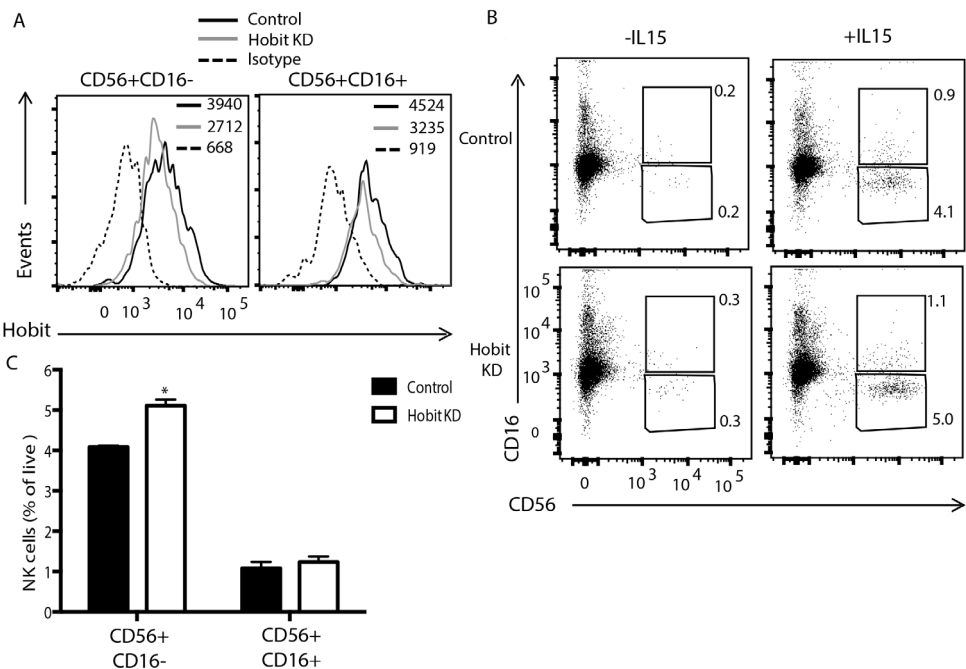


Figure 3. Hobit suppresses NK cell development. The role of Hobit in NK cell development was evaluated using Hobit knockdown in IL-15 cultures of hematopoietic progenitor cells. (a) Flow cytometry histograms show Hobit expression in CD16- and CD16+ NK cell populations at day 21 of culture. Solid line indicates control cells, grey line indicates Hobit KD cells and dotted line indicates the isotype control. (b) Flow cytometry dot plots display expression of CD16 and CD56 in NK cell cultures under control (top row) and Hobit KD conditions (bottom row). (c) Graph displays quantification of the percentage of cells that developed into the indicated subsets of NK cells. Data in (a,b) represents one donor. (c) Graph displays mean + SD of technical replicates from one donor.

Hobit contributes to the regulation of granzyme expression in NK cells.

Granzyme K is highly expressed by CD56^{bright} NK cells [8], while granzyme B is stored at high levels in the specific cytolytic granules of CD56^{dim} NK cells [6]. We have previously shown that Hobit regulates granzyme B expression in murine NKT cells [34] and tissue resident lymphocytes (Chapter 5). The majority of in vitro generated NK cells share several phenotypic characteristics with CD56^{bright} NK cells [19] such as the preferential expression of granzyme K (Fig. 4A). Hobit knockdown led to a reduction in granzyme K expression, in particularly in the CD56⁺CD16⁻ subset (Fig. 4a). Considering that we only achieved a partial knockdown in these cells, the full extent of granzyme K regulation by Hobit may be underestimated in our assay. Compared to circulating NK cells (data not shown), in vitro generated NK cells expressed low levels of granzyme B (Fig. 4B) and we could not detect an impact of Hobit in the regulation of granzyme B expression. Considering that Hobit regulates granzyme B in tissue resident lymphocytes (Chapter 5), and that we only achieved partial Hobit knockdown in our system, we cannot entirely rule out that Hobit also regulates granzyme B expression in human NK cells. Our data suggest that Hobit is involved in the regulation of NK cell differentiation and effector function, however, further studies are necessary to fully characterize Hobit regulation of granzymes and its effects in NK cell effector function.

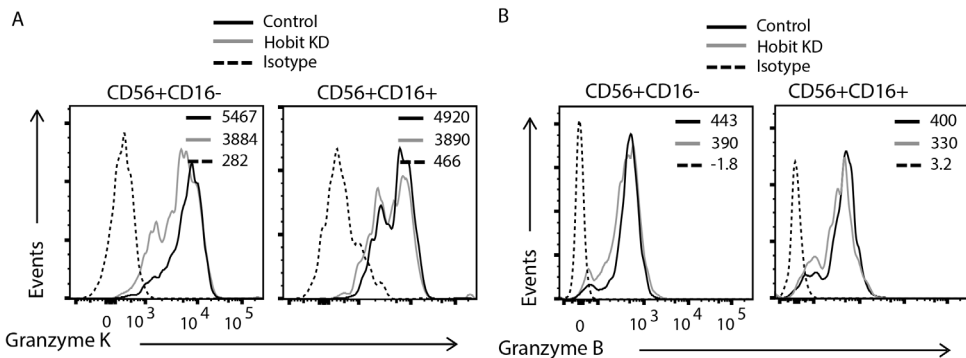


Figure 4. Hobit contributes to the regulation of granzyme expression in NK cells. Expression of Granzyme B and K was measured in in vitro generated NK cells under control and Hobit KD conditions. Flow cytometry histograms display (a) granzyme K and (b) Granzyme B expression in CD16⁻ and CD16⁺ NK cells. Solid line indicates control cells, grey line indicates Hobit KD cells and dotted line indicates the isotype control. Data in (a,b) display results from a single donor.

Hobit is involved in the regulation of Eomes, but not T-bet, expression in NK cells.

T-bet and Eomes play important roles in murine NK cell development [47] as deletion of both T-bet and Eomes causes a complete loss of NK cells in mice [30]. Eomes expression has been associated with granzyme K expression in both NK and T cells, while T-bet expression is associated with granzyme B [46],[48]. We analyzed the expression of T-bet and Eomes upon Hobit knockdown to determine whether Hobit

was upstream of these important transcription factors in NK cell differentiation. As Eomes but not T-bet expression is reduced upon Hobit knockdown (Fig. 5A), our preliminary data indicates that Hobit contributes to the transcriptional regulation

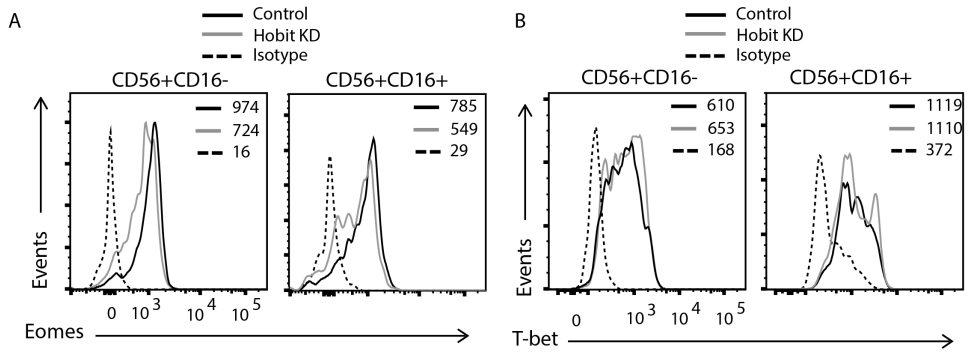


Figure 5. Hobit is involved in the regulation of Eomes, but not T-bet, expression in NK cells. The transcription factors Eomes and T-bet were measured in control and Hobit deficient NK cells that were generated after culture from hematopoietic stem cells. Flow cytometry histograms display (a) Eomes (a) and (b) T-bet expression in CD16⁻ and CD16⁺ NK cells. Solid line indicates control cells, grey line indicates Hobit KD cells and dotted line indicates the isotype control. Data in (a, b) display results from a single donor.

of Eomes, while the transcriptional regulation of T-bet expression appears to be Hobit independent (Fig. 5B). However, considering we only achieved a partial Hobit knockdown, further experiments are required to determine the exact extent of the transcriptional regulation driven by Hobit in primary NK cells.

Concluding remarks

Complex regulatory mechanisms are necessary to establish adequate effector function and survival of NK cells in vivo. Despite the invaluable contribution of murine models for our understanding of NK cell biology, human NK cells cannot be entirely understood by direct comparison to murine NK cells. In addition to crucial differences in their effector phenotype, such as steady state granzyme B protein expression, human NK cells express transcription factors such as Hobit, that are absent from murine NK cells. Therefore, our in vitro studies on human NK cells provide unique insights relevant for NK cell based immunotherapy in cancer, [49],[50].

Material and Methods

Antibodies.

The following antibodies were used: anti-CD117 (Life technologies), anti-CD94 (Life technologies), anti-CD3 (BD Biosciences), anti-CD19 (BD Biosciences), anti-CD16 (BD Biosciences), anti-CD56 (BD Biosciences), anti-CD34 (BD Biosciences), anti-Granzyme B (Life technologies), anti-Granzyme K (Life technologies), anti-Hobit (BD Biosciences, Sanquin-Hobit/1), anti-mouse IgM (BD, clone DS-1), anti-T-bet (BD Biosciences) and anti-Eomes (BD Biosciences).

Flow cytometry

Antibody labelling: cells were labeled with fluorochrome-conjugated or biotinylated antibodies in PBS 0.5% BSA for 30 min at RT. For intracellular and nuclear staining, cells were fixed and permeabilized using fixation and permeabilization buffers of BD Biosciences and eBioscience, respectively. Expression was analyzed on FACS-Canto II, BD LSRFortessa or BD LSR II flow cytometers (BD Biosciences).

Hobit staining: cells were fixed for 30 min at RT using the Foxp3 staining kit (eBioscience), washed, and then labeled with anti-Hobit antibodies for 30 min at 4°C. The primary antibodies were washed away, and Hobit expression was visualized using secondary antibodies conjugated with a fluorescent label after another incubation for 30 min at 4°C.

Plasmids.

Lentiviral pKLO.1 plasmids containing shRNA that target Hobit (TRCN0000162720; CAGAAGAGCTTCACTCAACTT) or that do not target Hobit as a control (MISSION Non-Target shRNA Control SHC002: CCGGCAACAAGATGAAGAGCACCAACTC) were obtained from Sigma (MISSION shRNA Lentiviral Transduction Particles).

Lentiviral transduction

Lentiviral particles were prepared by calcium transfection of 293T cells and concentrated by ultracentrifugation (3h, 20.000 RPM). Virus was incubated overnight with CD34+ cord blood progenitor cells cultured in Cellgro medium supplemented with 50 ng/ml TPO (n-Plate), 20 ng/ml IL-6, 100 ng/ml SCF and 100 ng/ml Flt3 ligand. After overnight incubation, viral supernatant was washed off and NK cell differentiation medium containing puromycin (1ug/ml) was added to both control and Hobit KD transduced cells. Puromycin was maintained in the medium until the end of the NK cell cultures.

Cell culture.

All human material was obtained with approval of the medical ethical committee of the Academical Medical Centre (AMC) and after informed consent. Human PB-MCs were obtained from fresh heparinized blood or buffy coats of healthy donors using Ficoll-Paque Plus (GE Healthcare) gradient centrifugation. Cord blood (CB) was collected according to the guidelines of Eurocord Nederland. Bone marrow mononuclear cells were isolated from the sternum of patients (age 40–70 years) undergoing cardiac surgery. Mononuclear cells were enriched by density gradient centrifugation over Ficoll-Paque PLUS (GE Healthcare Life Sciences). Mononuclear

cells were resuspended in MACS buffer, consisting of phosphate buffered saline (PBS), 0.5% bovine serum albumin (BSA; fraction V; Invitrogen), and 5 mM EDTA (Sigma-Aldrich). CD34-positive cells were isolated by magnetic cell sorting (MACS; Miltenyi Biotec), using the human CD34 Microbead Kit within 48 h after harvest. Purity was determined by flow cytometry and only samples with more than 95% purity were used for study.

Natural killer generation from CD34+ cells.

CD34+ cells from cord blood were cultured in 96 wells U bottom plates in IMDM + 4% Yssel's supplement [51] with 2% normal human serum, 100 ng/ml Flt3 ligand, 10 ng/ml IL-7 plus or minus 10 ng/ml IL-15. Medium was refreshed every seven days by removing half of the old medium and replenishing with fresh medium during the first two weeks. On week three, cells were resuspended then each well split into two different wells every two days. Fresh medium was added to each well after splitting the culture.

Statistics.

Values are expressed as mean \pm SD as indicated. Differences between two groups were calculated by student's t test. A p-value of less than 0.05 was considered significantly different.

References

1. Vosshenrich CAJ, Di Santo JP. Developmental programming of natural killer and innate lymphoid cells. *Curr. Opin. Immunol.* 2013; 25:130–138.
2. Huntington ND, Vosshenrich CAJ, Di Santo JP. Developmental pathways that generate natural-killer-cell diversity in mice and humans. *Nat. Rev. Immunol.* 2007; 7:703–714.
3. Kiessling R, Klein E, Wigzell H. „Natural” killer cells in the mouse. I. Cytotoxic cells with specificity for mouse Moloney leukemia cells. Specificity and distribution according to genotype. *Eur. J. Immunol.* 1975; 5:112–117.
4. Farag SS, Caligiuri MA. Human natural killer cell development and biology. *Blood Rev.* 2006; 20:123–137.
5. Vossen MTM, Matmati M, Hertoghs KML, Baars PA, Gent M-R, Leclercq G, Hamann J, et al. CD27 defines phenotypically and functionally different human NK cell subsets. *J. Immunol.* 2008; 180:3739–3745.
6. Leong JW, Fehniger TA. Human NK cells: SET to kill. *Blood.* 2011; 117:2297–2298.
7. Jacobs R, Hintzen G, Kemper A, Beul K, Kempf S, Behrens G, Sykora KW, et al. CD56bright cells differ in their KIR repertoire and cytotoxic features from CD56dim NK cells. *Eur. J. Immunol.* 2001; 31:3121–3127.
8. Jiang W, Chai NR, Maric D, Bielekova B. Unexpected role for granzyme K in CD56bright NK cell-mediated immunoregulation of multiple sclerosis. *J. Immunol.* 2011; 187:781–790.
9. Fehniger TA, Shah MH, Turner MJ, VanDeusen JB, Whitman SP, Cooper MA, Suzuki K, et al. Differential cytokine and chemokine gene expression by human NK cells following activation with IL-18 or IL-15 in combination with IL-12: implications for the innate immune response. *J. Immunol.* 1999; 162:4511–4520.
10. Fehniger TA, Cooper MA, Nuovo GJ, Cella M, Facchetti F, Colonna M, Caligiuri MA. CD56bright natural killer cells are present in human lymph nodes and are activated by T cell–derived IL-2: a potential new link between adaptive and innate immunity. *Blood.* 2003; 101:3052–3057.
11. Matos ME, Schnier GS, Beecher MS, Ashman LK, William DE, Caligiuri MA. Expression of a functional c-kit receptor on a subset of natural killer cells. *J. Exp. Med.* 1993; 178:1079–1084.
12. Caligiuri MA, Zmuidzinis A, Manley TJ, Levine H, Smith KA, Ritz J. Functional consequences of interleukin 2 receptor expression on resting human lymphocytes. Identification of a novel natural killer cell subset with high affinity receptors. *J. Exp. Med.* 1990; 171:1509–1526.
13. Nagler A, Lanier LL, Phillips JH. Constitutive expression of high affinity interleukin 2 receptors on human CD16-natural killer cells in vivo. *J. Exp. Med.* 1990; 171:1527–1533.
14. Melsen JE, Lugthart G, Lankester AC, Schilham MW. Human Circulating and Tissue-Resident CD56(bright) Natural Killer Cell Populations. *Front. Immunol.* 2016; 7:262.
15. Lotzová E, Savary CA, Champlin RE. Genesis of human oncolytic natural killer cells from primitive CD34+CD33- bone marrow progenitors. *J. Immunol.* 1993; 150:5263–5269.
16. Shibuya A, Nagayoshi K, Nakamura K, Nakauchi H. Lymphokine requirement for the generation of natural killer cells from CD34+ hematopoietic progenitor cells. *Blood.* 1995; 85:3538–3546.
17. Yu H, Fehniger TA, Fuchshuber P, Thiel KS, Vivier E, Carson WE, Caligiuri MA. Flt3 ligand promotes the generation of a distinct CD34(+) human natural killer cell progenitor that responds to interleukin-15. *Blood.* 1998; 92:3647–3657.
18. Freud AG, Yu J, Caligiuri MA. Human natural killer cell development in secondary lymphoid tissues. *Semin. Immunol.* 2014; 26:132–137.
19. Freud AG, Becknell B, Roychowdhury S, Mao HC. A human CD34 (+) subset resides in lymph nodes and differentiates into CD56 bright natural killer cells. *Immunity.* 2005. Available at: <http://www.sciencedirect.com/science/article/pii/S1074761305000427>.
20. Cooper MA, Bush JE, Fehniger TA, VanDeusen JB, Waite RE, Liu Y, Aguila HL, et al. In vivo evidence for a dependence on interleukin 15 for survival of natural killer cells. *Blood.* 2002; 100:3633–3638.
21. DiSanto JP, Müller W, Guy-Grand D, Fischer A, Rajewsky K. Lymphoid development in mice with a targeted deletion of the interleukin 2 receptor gamma chain. *Proc. Natl. Acad. Sci. U. S. A.* 1995; 92:377–381.
22. Mrózek E, Anderson P, Caligiuri MA. Role of interleukin-15 in the development of human CD56+ natural killer cells from CD34+ hematopoietic progenitor cells. *Blood.* 1996; 87:2632–2640.
23. Béziat V, Duffy D, Quoc SN, Le Garff-Tavernier M, Decocq J, Combadière B, Debré P, et al. CD56brightCD16+ NK cells: a functional intermediate stage of NK cell differentiation. *J. Immunol.* 2011; 186:6753–6761.
24. Romagnani C, Juelke K, Falco M, Morandi B, D’Agostino A, Costa R, Ratto G, et al. CD56brightCD16–Killer Ig-Like Receptor– NK Cells Display Longer Telomeres and Acquire Features of CD56dim NK Cells upon Activation. *The Journal of Immunology.* 2007; 178:4947–4955.
25. Ouyang Q, Baerlocher G, Vulto I, Lansdorp PM. Telomere length in human natural killer cell subsets.

Ann. N. Y. Acad. Sci. 2007; 1106:240–252.

26. Mace EM, Hsu AP, Monaco-Shawver L, Makedonas G. Mutations in GATA2 cause human NK cell deficiency with specific loss of the CD56bright subset. *Blood*. 2013. Available at: <http://www.bloodjournal.org/content/121/14/2669.short>.
27. Boos MD, Yokota Y, Eberl G, Kee BL. Mature natural killer cell and lymphoid tissue-inducing cell development requires Id2-mediated suppression of E protein activity. *J. Exp. Med.* 2007; 204:1119–1130.
28. Townsend MJ, Weinmann AS, Matsuda JL, Salomon R, Farnham PJ, Biron CA, Gapin L, et al. T-bet Regulates the Terminal Maturation and Homeostasis of NK and V α 14i NKT Cells. *Immunity*. 2004/4; 20:477–494.
29. Intlekofer AM, Takemoto N, Wherry EJ, Longworth SA, Northrup JT, Palanivel VR, Mullen AC, et al. Effector and memory CD8+ T cell fate coupled by T-bet and eomesodermin. *Nat. Immunol.* 2005; 6:1236–1244.
30. Gordon SM, Chaix J, Rupp LJ, Wu J, Madera S, Sun JC, Lindsten T, et al. The transcription factors T-bet and Eomes control key checkpoints of natural killer cell maturation. *Immunity*. 2012; 36:55–67.
31. Kallies A, Carotta S, Huntington ND, Bernard NJ, Tarlinton DM, Smyth MJ, Nutt SL. A role for Blimp1 in the transcriptional network controlling natural killer cell maturation. *Blood*. 2011; 117:1869–1879.
32. Maciejewski-Duval A, Meuris F, Bignon A, Aknin M-L, Balabanian K, Faivre L, Pasquet M, et al. Altered chemotactic response to CXCL12 in patients carrying GATA2 mutations. *J. Leukoc. Biol.* 2016; 99:1065–1076.
33. Vieira Braga FA, Hertoghs KML, Kragten NAM, Doody GM, Barnes NA, Remmerswaal E, Hsiao C-C, et al. Blimp-1 homolog Hobit identifies effector-type lymphocytes in humans. *Eur. J. Immunol.* 2015; 45:2945–2958.
34. van Gisbergen KPJM, Kragten NAM, Hertoghs KML, Wensveen FM, Jonjic S, Hamann J, Nolte MA, et al. Mouse Hobit is a homolog of the transcriptional repressor Blimp-1 that regulates NKT cell effector differentiation. *Nat. Immunol.* 2012; 13:864–871.
35. Carotta S, Pang SHM, Nutt SL, Belz GT. Identification of the earliest NK-cell precursor in the mouse BM. *Blood*. 2011; 117:5449–5452.
36. Miller JS, Alley KA, McGlave P. Differentiation of natural killer (NK) cells from human primitive marrow progenitors in a stroma-based long-term culture system: identification of a CD34+ 7+ NK *Blood*. 1994. Available at: <http://www.bloodjournal.org/content/83/9/2594.short>.
37. Yu J, Freud AG, Caligiuri MA. Location and cellular stages of natural killer cell development. *Trends Immunol.* 2013; 34:573–582.
38. Freud AG, Caligiuri MA. Human natural killer cell development. *Immunol. Rev.* 2006; 214:56–72.
39. Michel T, Poli A, Cuapio A, Briquemont B, Iserentant G, Ollert M, Zimmer J. Human CD56bright NK Cells: An Update. *J. Immunol.* 2016; 196:2923–2931.
40. Horowitz A, Strauss-Albee DM, Leopold M, Kubo J, Nemat-Gorgani N, Dogan OC, Dekker CL, et al. Genetic and environmental determinants of human NK cell diversity revealed by mass cytometry. *Sci. Transl. Med.* 2013; 5:208ra145.
41. Gunturi A, Berg RE, Forman J. The role of CD94/NKG2 in innate and adaptive immunity. *Immunol. Res.* 2004; 30:29–34.
42. Yu J, Mao HC, Wei M, Hughes T, Zhang J, Park I-K, Liu S, et al. CD94 surface density identifies a functional intermediary between the CD56bright and CD56dim human NK-cell subsets. *Blood*. 2010; 115:274–281.
43. Dalle J-H, Menezes J, Wagner E, Blagdon M, Champagne J, Champagne MA, Duval M. Characterization of cord blood natural killer cells: implications for transplantation and neonatal infections. *Pediatr. Res.* 2005; 57:649–655.
44. Chen Q, Ye W, Jian Tan W, Mei Yong KS, Liu M, Qi Tan S, Loh E, et al. Delineation of Natural Killer Cell Differentiation from Myeloid Progenitors in Human. *Sci. Rep.* 2015; 5:15118.
45. Jacobson A, Bell F, Lejarcegui N, Mitchell C, Frenkel L, Horton H. Healthy Neonates Possess a CD56-Negative NK Cell Population with Reduced Anti-Viral Activity. *PLoS One*. 2013; 8:e67700.
46. Knox JJ, Cosma GL, Betts MR, McLane LM. Characterization of T-bet and eomes in peripheral human immune cells. *Front. Immunol.* 2014; 5:217.
47. Simonetta F, Pradier A, Roosnek E. T-bet and Eomesodermin in NK Cell Development, Maturation, and Function. *Front. Immunol.* 2016; 7:241.
48. Smith C, Elhassen D, Gras S, Wynn KK, Dasari V, Tellam J, Tey S-K, et al. Endogenous antigen presentation impacts on T-box transcription factor expression and functional maturation of CD8+ T cells. *Blood*. 2012; 120:3237–3245.
49. Cheng M, Chen Y, Xiao W, Sun R, Tian Z. NK cell-based immunotherapy for malignant diseases. *Cell. Mol. Immunol.* 2013; 10:230–252.

50. Guillerey C, Huntington ND, Smyth MJ. Targeting natural killer cells in cancer immunotherapy. *Nat. Immunol.* 2016; 17:1025–1036.
51. Yssel H, De Vries JE, Koken M, Van Blitterswijk W, Spits H. Serum-free medium for generation and propagation of functional human cytotoxic and helper T cell clones. *J. Immunol. Methods.* 1984; 72:219–227.

The adhesion G protein-coupled receptor GPR56/ADGRG1 is an inhibitory receptor on human NK cells

Cell Reports 2016; 15:1757–1770.s

Gin-Wen Chang^{1*}, Cheng-Chih Hsiao^{2*}, Yen-Ming Peng¹, **Felipe A. Vieira Braga**⁴, Natasja A.M. Kragten⁴, Ester B. M. Remmerswaal^{2,3}, Martijn D. B. van de Garde², Rachel Straussberg⁵, Gabriele M. König⁶, Evi Kostenis⁶, Vera Knäuper⁷, Linde Meyaard⁸, René A.W. van Lier⁴, Klaas P.J.M. van Gisbergen⁴, Hsi-Hsien Lin^{1,9#}, and Jörg Hamann^{2#}

¹Department of Microbiology and Immunology, College of Medicine, Chang Gung University, Kwei-Shan, Tao-Yuan, Taiwan,

²Department of Experimental Immunology and ³Renal Transplant Unit, Academic Medical Center, University of Amsterdam, Amsterdam, The Netherlands,

⁴Department of Hematopoiesis, Sanquin Research and Landsteiner Laboratory, Academic Medical Center, University of Amsterdam, Amsterdam, The Netherlands,

⁵Department of Child Neurology, Neurogenetics Clinic, Schneider Children's Medical Center, Petach Tikva and Sackler Faculty of Medicine, Tel Aviv University, Tel Aviv, Israel,

⁶Institute for Pharmaceutical Biology and PharmaCenter, University of Bonn, Bonn, Germany,

⁷Dental School, Cardiff University, Cardiff, United Kingdom,

⁸Department of Immunology, University Medical Center Utrecht, Utrecht, The Netherlands,

⁹Chang Gung Immunology Consortium, Chang Gung Memorial Hospital and Chang Gung University, Tao-Yuan, Taiwan.

*Co-first authors, #Co-senior authors

Abstract

Natural killer (NK) cells possess potent cytotoxic mechanisms that need to be tightly controlled. We here explored the regulation and function of GPR56/ADGRG1, an adhesion G protein-coupled receptor implicated in developmental processes and expressed distinctively in mature NK cells. Expression of GPR56 was triggered by Hobit, a homolog of Blimp-1, and declined upon cell activation. Through studying NK cells from polymicrogyria patients with disease-causing mutations in the ADGRG1 gene, encoding GPR56, and NK-92 cells ectopically expressing the receptor, we found that GPR56 negatively regulates immediate effector functions, including production of inflammatory cytokines and cytolytic enzymes, degranulation, and target cell killing. GPR56 pursues this activity by associating with the tetraspanin CD81. We conclude that GPR56 inhibits natural cytotoxicity of human NK cells.

Introduction

Natural killer (NK) cells are innate lymphoid cells that develop, mainly in the bone marrow, through a series of distinct phenotypic stages before they enter the circulation to specifically eradicate virus-infected and transformed cells (Freud and Caligiuri, 2006). Upon target cell encounter, differentiated CD56dim NK cells produce large amounts of cytokines, chemokines, and cytolytic proteins, similar to effector-type CD8+ T cells (Fauriat et al., 2010; Nagler et al., 1989; Vivier et al., 2008). The activity of cytotoxic CD56dim NK and CD8+ T cells is regulated by a comprehensive repertoire of activating and inhibitory receptors, including immunoglobulin-like receptors and C-type lectins (Lanier, 2008; Pegram et al., 2011).

G protein-coupled receptors (GPCRs) guide numerous cellular processes, including development and differentiation (Pierce et al., 2002), yet, in the immune system, they have been linked primarily with chemotaxis (Walzer and Vivier, 2011). Others and we recently showed that human cytotoxic lymphocytes, including CD56dull NK cells and CD27–CD45RA+ T cells, express the adhesion family GPCR (aGPCR) GPR56/ADGRG1 (Chiesa et al., 2010; Peng et al., 2011). Expression of GPR56 correlated closely with production of the cytolytic proteins perforin, granzyme A, and granzyme B and was not found in non-cytotoxic lymphocytes or myeloid cells.

aGPCRs possess an N-terminal fragment (NTF) and a C-terminal fragment (CTF) that arise from autocatalytic cleavage at a GPCR-protolytic site (GPS), embedded in a juxtamembranous GPCR autoproteolysis-inducing (GAIN) domain (Araç et al., 2012; Lin et al., 2004). At the cell surface, the NTF remains non-covalently attached to the CTF, giving rise to a characteristic bipartite structure with the two fragments being engaged in distinct activities (Langenhan et al., 2013). The NTF of GPR56 binds transglutaminase and collagen III, while the CTF recruits Gα proteins leading to activation of RhoA (Ras homolog gene family member A) and mTOR (mechanistic target of rapamycin) pathways (Ackerman et al., 2015; Giera et al., 2015; Iguchi et al., 2008; Little et al., 2004; Luo et al., 2011; Paavola et al., 2011; White et al., 2014; Xu et al., 2006).

We here tested the relation of GPR56 with the differentiation, activation, and function of human NK cells. We provide evidence that GPR56 expression is triggered by the transcriptional repressor Hobit (homolog of Blimp-1 in T cells), is downregulated upon cellular activation, and inhibits immediate effector functions, including inflammatory cytokine and cytolytic protein production, degranulation, and target cell killing. We conclude that GPR56 is a differentiation marker and inhibitory receptor on human NK cells.

Results

Hobit, the human homolog of Blimp-1 in T cells, drives expression of GPR56 in non-dividing, fully differentiated human NK cells

GPR56 is expressed by all human cytotoxic lymphocytes, including CD56dim NK cells (Chiesa et al., 2010; Peng et al., 2011). Upon stimulation with common gamma chain cytokines, such as interleukin (IL)-2, proliferating NK cells lose expression of GPR56 (Chiesa et al., 2010) (Figure 1A). IL-2-dependent cytotoxic NK-92 cells weakly express GPR56. IL-2 withdrawal stopped NK-92 cell division, leading to cell cycle arrest in the G1 phase and surface expression of GPR56 (Figure 1B). Of note, IL-2 deprivation caused upregulation of surface markers commonly associated with terminal cell differentiation, such as KLRG1 (killer cell lectin-like receptor subfamily G member 1) and B3GAT1 (galactosylgalactosylxylosylprotein 3-beta-glucuronosyltransferase 1), the enzyme that generates the CD57 glycosylation epitope, and downregulation of the cell exhaustion marker PD1 (programmed cell death 1) (Figure 1C). These changes correlated with altered expression of transcription factors involved in effector lymphocyte development, such as Blimp-1 (B lymphocyte-induced maturation protein-1), Bcl-6 (B-cell lymphoma 6), T-bet (T-box expressed in T cells), Eomes (eomesodermin), and the recently identified Hobit (homolog of Blimp-1 in T cells) (van Gisbergen et al., 2012; Vieira Braga et al., 2015) (Figure 1C). In line with their in part contrary activities (Crotty et al., 2010; Daussy et al., 2014; Knox et al., 2014), downregulation of Blimp-1 and T-bet was accompanied by upregulation of Bcl-6 and Eomes, respectively. The most prominent change, with a ~25-fold induction, occurred with Hobit.

We next correlated GPR56 protein expression with the presence of various surface makers, cytolytic proteins, and transcription factors in primary NK cells. In line with its absence on immature CD56high NK cells, we detected almost no GPR56 on NK cells from tonsil (data not shown). In contrast, mature circulating NK cells commonly expressed GPR56. GPR56 was acquired prior to the late differentiation/senescence markers KLRG1 and CD57 (Björkström et al., 2010; Lopez-Vergès et al., 2010), as most clearly exemplified by cells from cord blood (Figure 1D). In line with the uniform presence of GPR56 on CD56dim NK cells, no association was found with the expression of activating or inhibitory natural cytotoxicity receptors (NKp30, NKp44, NKp46), NK-cell receptors (NKG2a, NKG2c, NKG2d), and killer immunoglobulin-like receptors (KIR2DL1/S1, KIR2DL2/L3, KIR3DL1) (Figure S1). Supporting previous findings (Peng et al., 2011), the presence of GPR56 correlated with production of the cytolytic mediators perforin and granzyme B (Figure S1). Cells expressing GPR56 were positive for the transcription factors T-bet, Eomes, and Hobit; in particular, expression of GPR56 and Hobit was strongly associated (Figure 1D). Thus, non-dividing, fully differentiated NK cells, found in the circulation and commonly indicated as CD56dim cells, express GPR56 in a distinctive manner.

Recent studies identified a subset of long-lived memory-like NK cells, associated with prior human cytomegalovirus infection, that can mount long-term effective recall responses (Lee et al., 2015; Schlums et al., 2015; Zhang et al., 2013). We found that these memory-like NK cells, which can be distinguished by low presence of the transcription factor PLZF (promyelocytic leukemia zinc finger) and lack of FcRγ

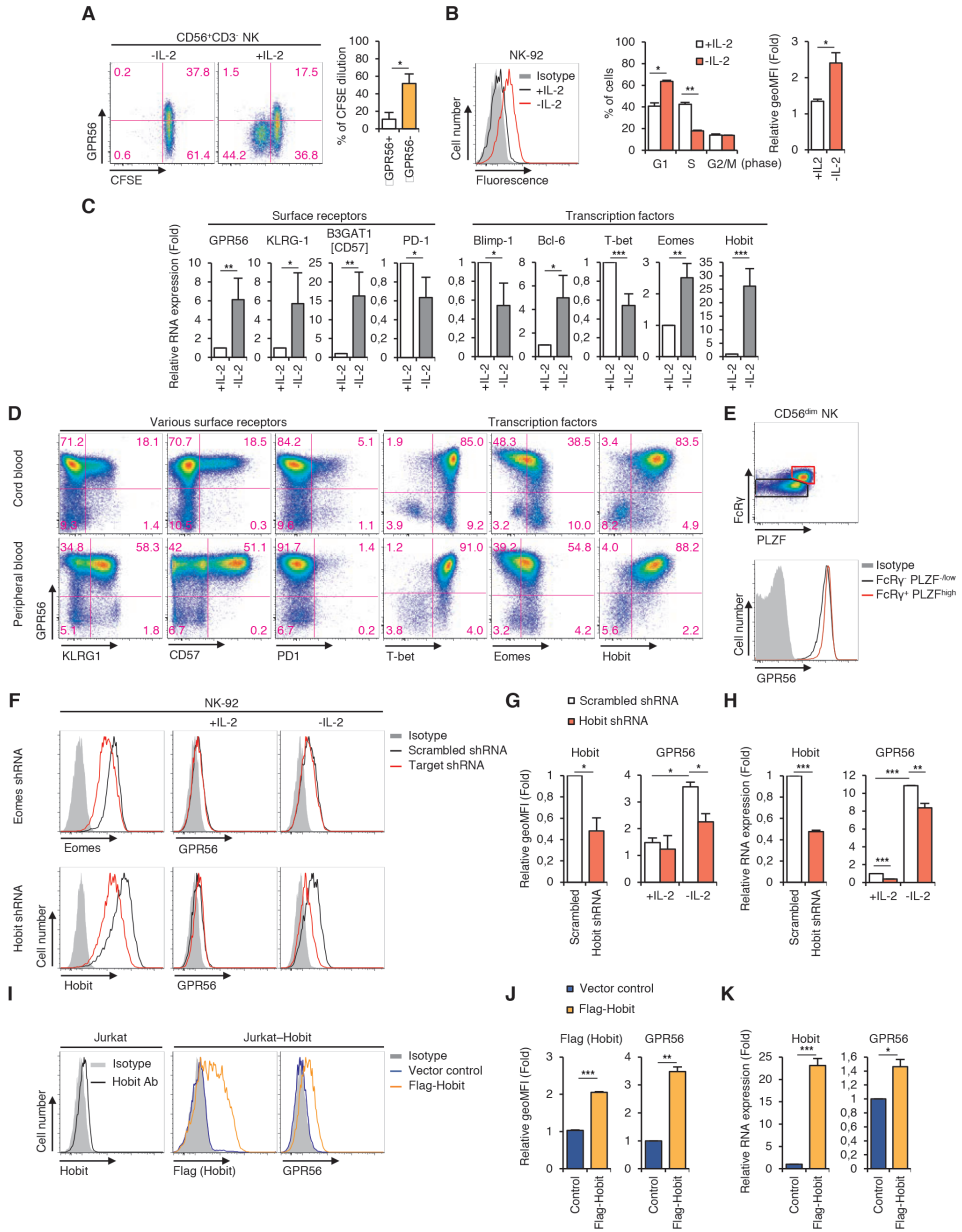


Figure 1. Hobit drives the expression of GPR56 in non-dividing, fully differentiated NK cells. (A) Expression of GPR56 and CD57 on proliferating CD56⁺CD3⁻ NK cells was measured using CFSE dilution after 6 days of stimulation with 50 U/ml IL-2. Flow cytometry plots of one representative experiment (left) and quantification of the mean percentage of proliferating cells (right). (B) NK-92 cells were incubated with or without 50 U/ml IL-2 for 18 h and analyzed for cell cycle and expression of GPR56 and CD57 by flow cytometry (left). Quantification of percentages of cells in G1, S, and G2/M phase, and relative geoMFI of GPR56 and CD57 expression, compared to isotype controls (right). (C) Quantification of mRNA expression of surface receptors and transcription factors by RT-PCR in NK-92 cells, incubated with or without 50 U/ml IL-2 for 18 h. (D) Protein expression of surface makers and transcription factors by CD56⁺CD3⁻ NK cells in cord blood and peripheral blood in relation to GPR56 expression, measured by flow cytometry. (E) Expression of GPR56 on long-lived memory-like NK cells, defined by absent/

low expression of FcR γ and PLZF, determined by flow cytometry. (F-H) NK-92 cells overexpressing scrambled shRNA, Eomes shRNA, or Hobit shRNA were incubated with or without 50 U/ml IL-2 for 18 h and analyzed by flow cytometry for expression of Eomes, Hobit, and GPR56. Representative flow cytometry plots (F), quantification of Hobit and GPR56 protein expression, compared to isotype controls, by flow cytometry (G), and quantification of mRNA expression of GPR56 by RT-PCR (H). (I-K) Parental Jurkat cells and Jurkat cells overexpressing Flag-tagged vector control or Hobit were incubated with 10 μ g/ml doxycycline for 48 h and analyzed by flow cytometry for expression of GPR56. Representative flow cytometry plots (I), quantification of Flag and GPR56 protein expression, compared to isotype controls, by flow cytometry (J), and quantification of mRNA expression of GPR56 by RT-PCR (K). All data are means \pm SEM of 3-5 independent experiments. * p <0.05, ** p <0.01, *** p <0.005

(high-affinity IgE receptor, γ subunit), express GPR56 (Figure 1E).

The T-box transcription factor Eomes (eomesodermin) is crucially involved in effector lymphocyte differentiation and, like GPR56, is expressed in differentiating neurons in the developing human brain (Elsen et al., 2013). Intriguingly, lack of Eomes causes a microcephaly syndrome (Baala et al., 2007) similar to the malformation seen in patients with null GPR56 expression (Piao et al., 2004). To test a causal relationship between Eomes and the expression of GPR56, we applied shRNA knockdown of EOMES in NK-92 cells. Reduced Eomes expression did not prevent GPR56 induction upon IL-2 withdrawal (Figure 1F). In contrast, knockdown of ZNF683, encoding Hobit, largely prevented GPR56 induction in NK-92 cells cultured without IL-2 (Figure 1F-H). Furthermore, ectopic expression of Hobit in Jurkat cells, which express neither GPR56 nor Hobit, induced expression of GPR56 (Figure 1I-K), indicating that Hobit drives the expression of GPR56 in human lymphocytes.

GPR56-deficient BFPP patients have normally developed but functionally elevated NK cells

Loss-of-function mutations in ADGRG1, encoding GPR56, cause a severe cortical malformation, known as bilateral frontoparietal polymicrogyria (BFPP) (Piao et al., 2004; 2005). To test whether defective expression of GPR56 would affect NK-cell differentiation and/or function, we studied two unrelated pairs of BFPP siblings bearing the mutations 1693C>T (R565W) and 1036T>A (C346S), respectively. Previous *in vitro*-analysis revealed that both mutations strongly reduce surface expression of GPR56 (Chiang et al., 2011; Jin et al., 2007). We found that the R565W mutation abolished GPR56 expression on NK (and T) cells completely, whereas the C346S mutation reduced surface levels of GPR56 by about 20-fold (Figure 2A, Figure S2, and data not shown). All patients had normal numbers of circulating NK cells (Figure 2A and data not shown). Moreover, their NK cells had a fairly normal phenotype, based on the expression of surface markers, including receptors with activating or inhibiting effector functions, cytolytic proteins, and transcription factors (Figure 2A, Figure S2, and data not shown). However, CD56dim NK cells in the R565W patients, which completely lacked GPR56, expressed lower levels of CD94 expression, indicating maturation. Moreover, the cells expressed less/no inhibitory KIR2DL1/S1, while steady-state expression of cytolytic enzymes was unchanged (granzyme B) or even marginally reduced (perforin).

The phenotypic changes found in CD56dim NK cells in the 1693C>T (R565W) siblings raised the possibility that the cytolytic capacity of NK cells in these patients was altered. Indeed, their NK cells killed K562 cells more efficiently than control

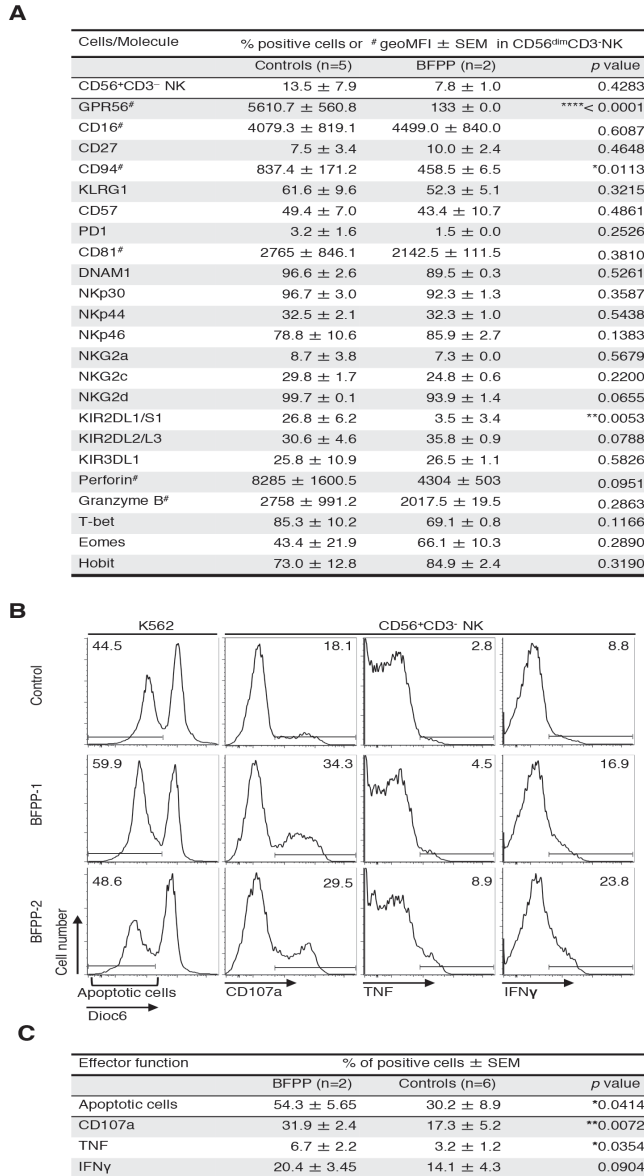


Figure 2. Normal development and functional competence of NK cells in BFPP patients. Analyzed were cells of four BFPP patients from pedigrees of Dutch and Palestinian descent, and age-matched healthy control donors. (A) Percentage of NK cells among circulating lymphocytes and expression of surface makers and cytolytic enzymes by CD56⁺CD3⁻ NK cells, measured by flow cytometry. (B) PBMCs were incubated with K562 target cells at an effector/target cell ratio of 1/1 for 5 h and analyzed by flow cytometry for K562 cell death, NK-cell degranulation (CD107a), and intracellular production of TNF and IFN γ . The control donor depicted here was analyzed in parallel with the Dutch patients. (C) Quantification of effector functions analyzed in (B), including additional control donors. All data are means \pm SEM. *p<0.05, **p<0.001

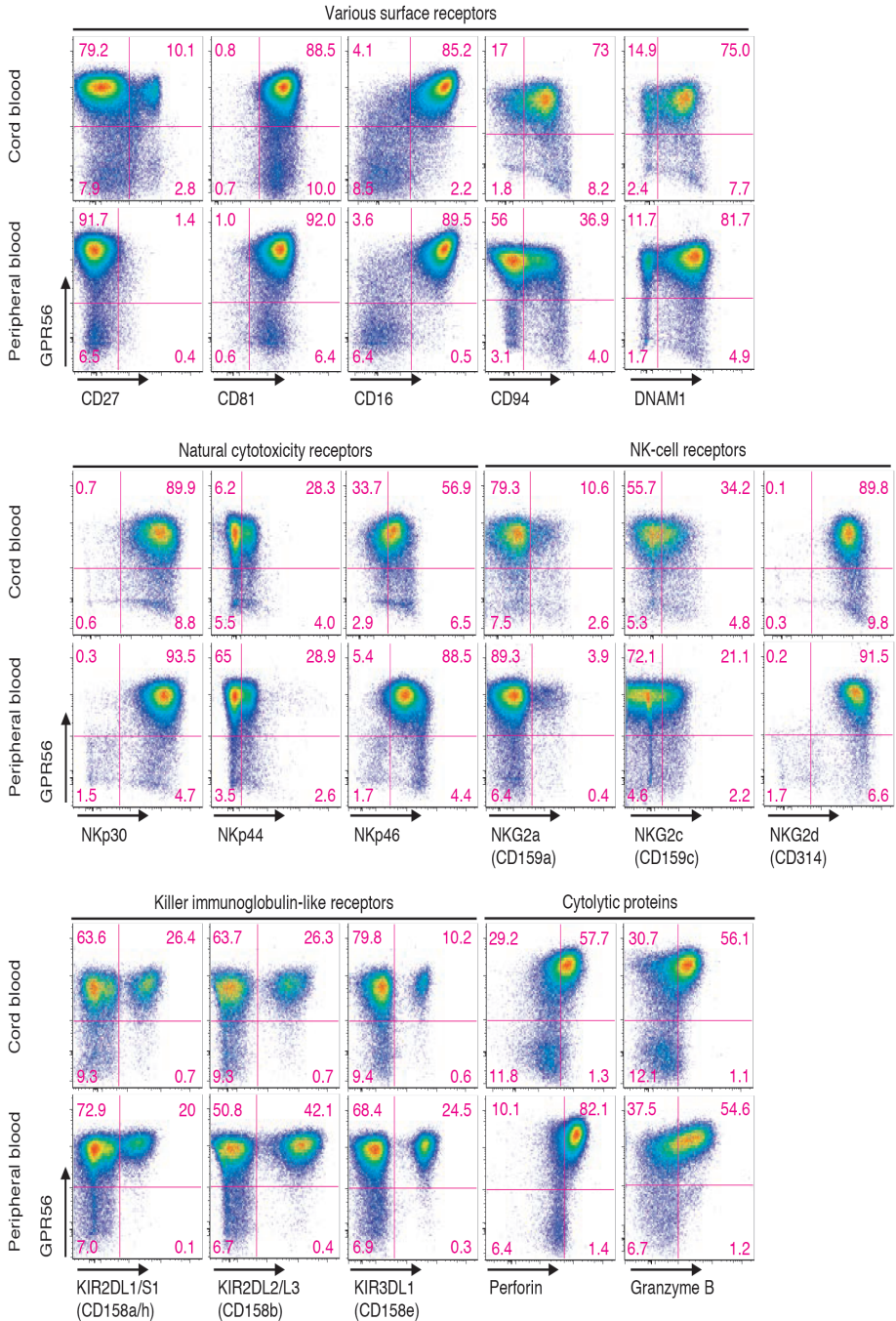


Figure S1. Expression profiling of NK cells from cord blood and peripheral blood in relation to GPR56 expression. Flow-cytometric analysis of CD56+CD3- NK cells for expression of various surface makers, natural cytotoxicity receptors, NK-cell receptors, and killer immunoglobulin-like receptors, and cytolytic proteins, measured by flow cytometry.

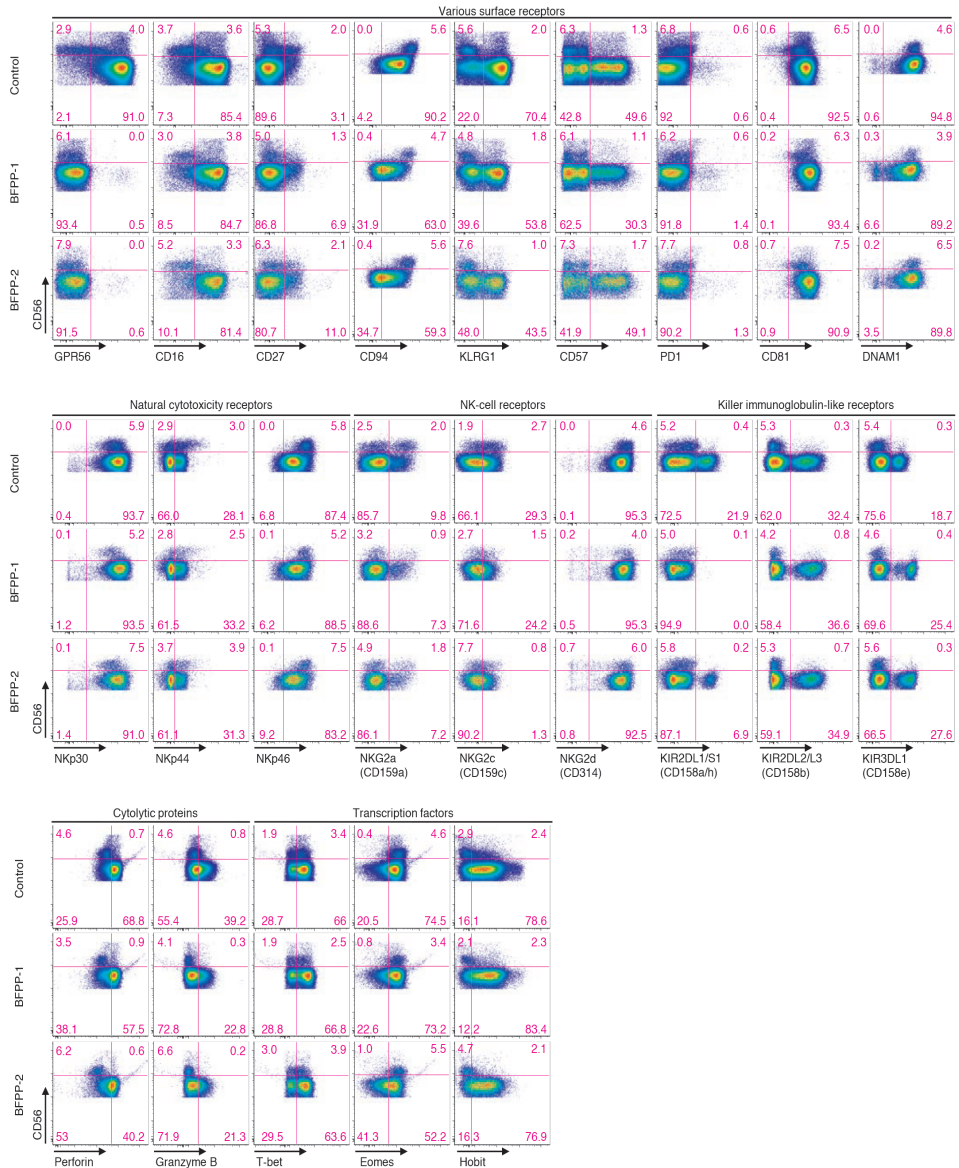


Figure S2. Expression of surface makers, enzymes, and transcription factors by CD56+CD3- NK cells in two related BFPP patients and a control donor. Shown are flow cytometry plots generated in parallel in the same experiment.

cells, as indicated by enhanced degranulation (CD107a expression) and induction of apoptosis in the target cells. In addition, target cell contacts resulted in enhanced production of tumor necrosis factor (TNF) and interferon (IFN) γ by GPR56-deficient NK cells (Figure 2B,C). Thus, lack of GPR56 did not hamper normal NK-cell development, but appeared to enhance their functional capacity.



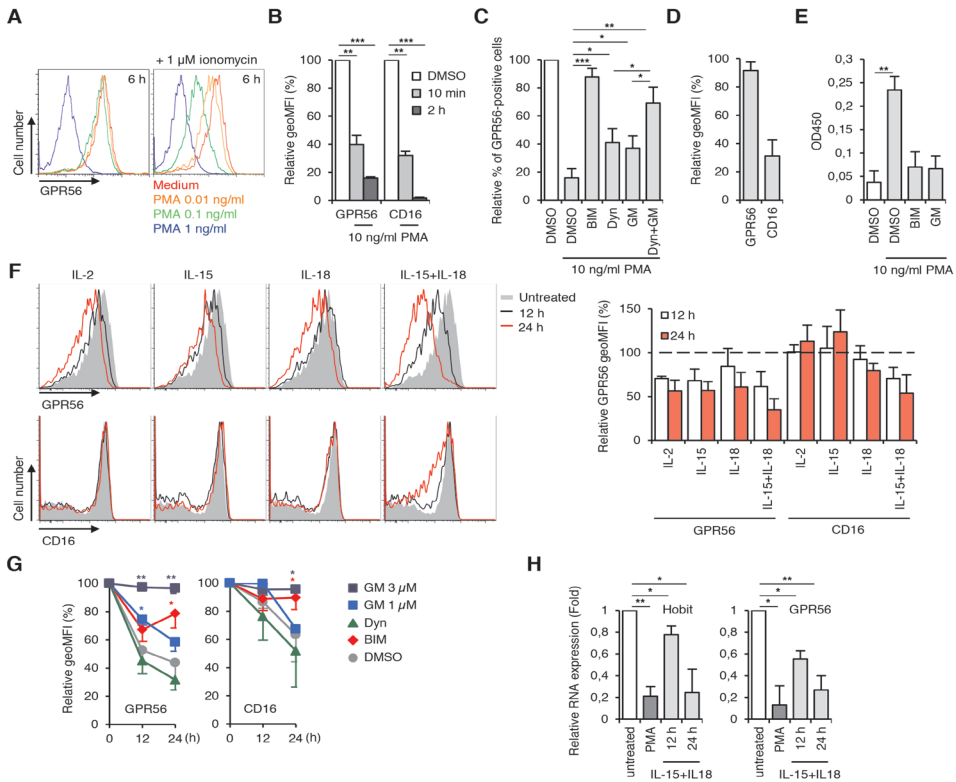


Figure 3. Inflammatory cytokines downregulate of GPR56 in primary NK cells. PBMCs were stimulated as indicated and analyzed by flow cytometry. (A) Expression of GPR56 on CD56+CD3⁻ NK cells, stimulated for 6 h with the indicated amounts of PMA, alone or in combination with ionomycin. (B) Expression of GPR56 and CD16 on CD56+CD3⁻ NK cells, stimulated for 10 min or 2 h with 10 ng/ml PMA. (C) Expression of GPR56 on CD56+CD3⁻ NK cells pre-incubated for 1 h with 1 μ M bisindolylmaleimide I (BIM), 100 μ M dynasore (Dyn), 10 μ M GM6001 (GM), or dynasore plus GM6001 before incubation with 10 ng/ml PMA for 2 h. (D) Expression of GPR56 and CD16 on CD56+CD3⁻ NK cells, pre-stained with anti-GPR56 or anti-CD16 mAb prior to incubation with 10 ng/ml PMA for 2 h. (E) Culture supernatants of PBMCs, pre-incubated for 1 h with inhibitors before incubation with 10 ng/ml PMA for 2 h, were analyzed by ELISA for soluble GPR56. (F) Expression of GPR56 and CD16 on CD56+CD3⁻ NK cells stimulated for 12 or 24 h with 500 U/ml IL-2, 10 ng/ml IL-15, 100 ng/ml IL-18, or IL-15 plus IL-18. Representative flow cytometry plots (left) and quantification of relative geoMFI (right). (G) Expression of GPR56 and CD16 on CD56+CD3⁻ NK cells pre-incubated with inhibitors and then stimulated for 12 or 24 h with IL-15 plus IL-18. (H) Quantification of mRNA expression of Hobit and GPR56 by RT-PCR in PBMCs, incubated with 10 ng/ml PMA for 2 h or with 10 ng/ml IL-15 plus 100 ng/ml IL-18 for 12 and 24 h. All data are means \pm SEM of 4 independent experiments. * p <0.05, ** p <0.01, *** p <0.005

NK cells downregulate GPR56 upon cytokine stimulation

Upon encounter of virus-infected or transformed cells, NK cells downregulate inhibitory receptors to acquire maximal killing capacity (Pegram et al., 2011). PMA (phorbol-12-myristate-13-acetate) stimulation downregulates ectopic GPR56 in monocytic U937 cells (Little et al., 2004). In primary NK cells, PMA treatment resulted in loss of GPR56 at concentrations as low as 0.01 ng/ml, which was enhanced by ionomycin (data not shown, Figure 3A, and Figure S3A). With a loss of >60% of cell surface GPR56 within 10 min and >80% after 2 h, kinetics resembled the downregulation

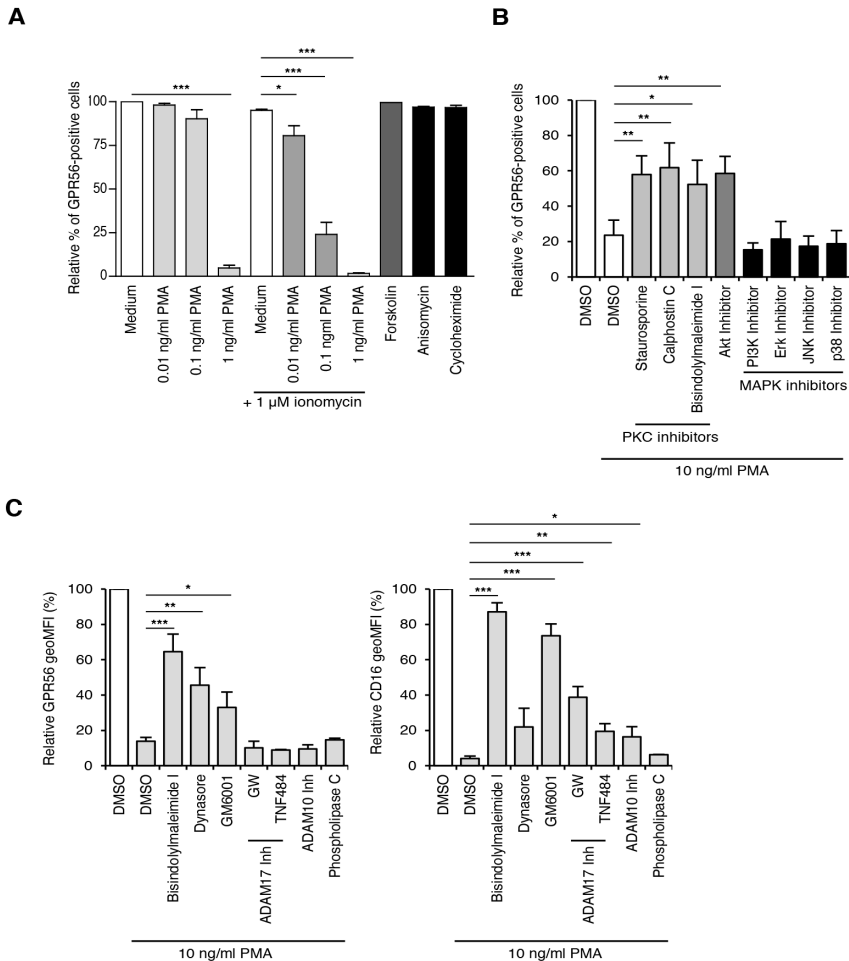


Figure S3. PKC activation induces downregulation of GPR56 in primary NK cells. PBMCs were stimulated as indicated and analyzed by flow cytometry. (A) Expression of GPR56 on CD56+CD3- NK cells incubated for 6 h with the indicated amounts of PMA, with or without 1 μ M ionomycin, or with 10 μ M forskolin, 10 μ M anisomycin, or 3.6 μ M cycloheximide. (B) Expression of GPR56 on CD56+CD3- NK cells pre-treated for 30 min with PKC inhibitors (1 μ M staurosporine, 1 μ M calphostin C, 1 μ M bisindolylmaleimide I) or with inhibitors of PKB/Akt (10 μ M), PI3K (10 μ M), and MAP kinases (Erk (10 μ M), JNK (20 μ M), and p38 (10 μ M)), after which cells were incubated with 10 ng/ml PMA for 2 h. (C) Expression of GPR56 and CD16 on CD56+CD3- NK cells pre-incubated for 1 h with inhibitors as in (A), inhibitors of ADAM17 (10 μ M GW and 100 nM TNF484) and 10 μ M ADAM10, or 1 μ g/ml phospholipase C in serum-free medium before incubation with PMA for 2 h. Provided are relative percentages of positive cells and geoMFIs. Data are means \pm SEM of 3–5 independent experiments. * p <0.05, ** p <0.01, *** p <0.005

of CD16 (Figure 3B). Studies with pharmacological inhibitors confirmed the involvement of protein kinase (PK)C, but not MAP kinases, in PMA-induced GPR56 downregulation (Figure S3B). Activation of PKA with forskolin did not affect GPR56 surface levels (Figure S3A).

aGPCRs are downregulated by internalization or shedding (Karpus et al., 2013; Langenhan et al., 2013). The dynamin inhibitor dynasore that prevents internalization

and GM6001, a broad-spectrum matrix metalloproteinase (MMP) inhibitor, synergistically blocked the downregulation of GPR56 upon PMA stimulation (Figure 3C). In contrast, downregulation of CD16 upon PMA stimulation was primarily blocked by GM6001 (Figure S3C). Cleavage of CD16 involves a disintegrin and metalloproteinase (ADAM)17, expressed in NK cells (Romee et al., 2013). Indeed, two ADAM17 inhibitors affected PMA-induced downregulation of CD16, but not GPR56 (Figure S3C). NK cells pre-incubated with fluorescently labeled anti-GPR56 or anti-CD16 monoclonal antibodies (mAbs) on ice and subsequently treated with PMA for 2 h had lost ~10% of the GPR56-bound mAb, but ~70% of the CD16-bound mAb, indicating that GPR56 was partially endocytosed from the cell surface (Figure 3D). Moreover, an increase in soluble GPR56 in the medium was detected after NK-cell stimulation with PMA, which was abrogated by inhibitors of PKC and MMPs (Figure 3E). Thus, PKC activation induces downregulation of GPR56 in primary NK cells via internalization and shedding.

Physiological activation of primary NK cells occurs through pro-inflammatory cytokines, crosslinking of activating receptors, or exposure to target cells. To test the effect of cytokines, we incubated peripheral blood mononuclear cells (PBMCs) for 12–24 h with IL-2, IL-15, or IL-18, alone or in combination. A combination of IL-15 and IL-18 reduced GPR56 surface levels by ~40% after 12 h and by ~70% after 24 h, which was more efficient as compared to the downregulation of CD16 by these cytokines (Figure 3F). Inhibition of PKC and MMPs blocked the downregulation of GPR56 and CD16, while blockade of endocytosis with dynasore had no effect (Figure 3G). In line with our former data, inhibition of ADAM17 blocked the downregulation of CD16, but not GPR56, leaving the identity of the sheddase that releases the NTF of GPR56 open (data not shown). Crosslinking CD16 or exposure to K562 had a small effect on GPR56 surface expression (data not shown). In sum, physiological NK-cell activation through cytokines causes downregulation of GPR56 by shedding of the NTF of the receptor.

Notably, activation of primary NK cells downregulates the expression of Hobit. In PBMCs stimulated for 2 h with PMA or for 12–24 h with cytokines, we found a clear decrease in Hobit and GPR56 transcript levels (Figure 3H), indicating that NK-cell activation causes downregulation of GPR56, immediately, by shedding of the NTF (see above), and permanently, by terminating gene expression.

GPR56 controls NK-cell effector functions

To further examine the role of GPR56 in NK-cell function, we applied ectopic GPR56 expression in NK-92 cells (Peng et al., 2011). Proper expression and auto-proteolytic modification of the receptor were confirmed by flow cytometry and Western blot analysis, respectively (Figure S4A). GPR56 overexpression did not affect cell growth (Figure S4B,C). Quantification of cytolytic proteins revealed a much-reduced expression of granzyme B, both at the transcript and protein level, in NK-92–GPR56 cells (Figure 4A,B). In contrast, mRNA and protein levels of perforin were comparable between NK-92–Neo and NK-92–GPR56 cells. Moreover, a lower level of TNF but not IFN γ transcript was detected in NK-92–GPR56 cells (Figure 4C). When activated by PMA, NK-92–GPR56 cells produced less TNF and IFN γ than NK-92–Neo cells (Figure 4D,E). These results suggested that forced GPR56 expression in NK-92 cells nega-

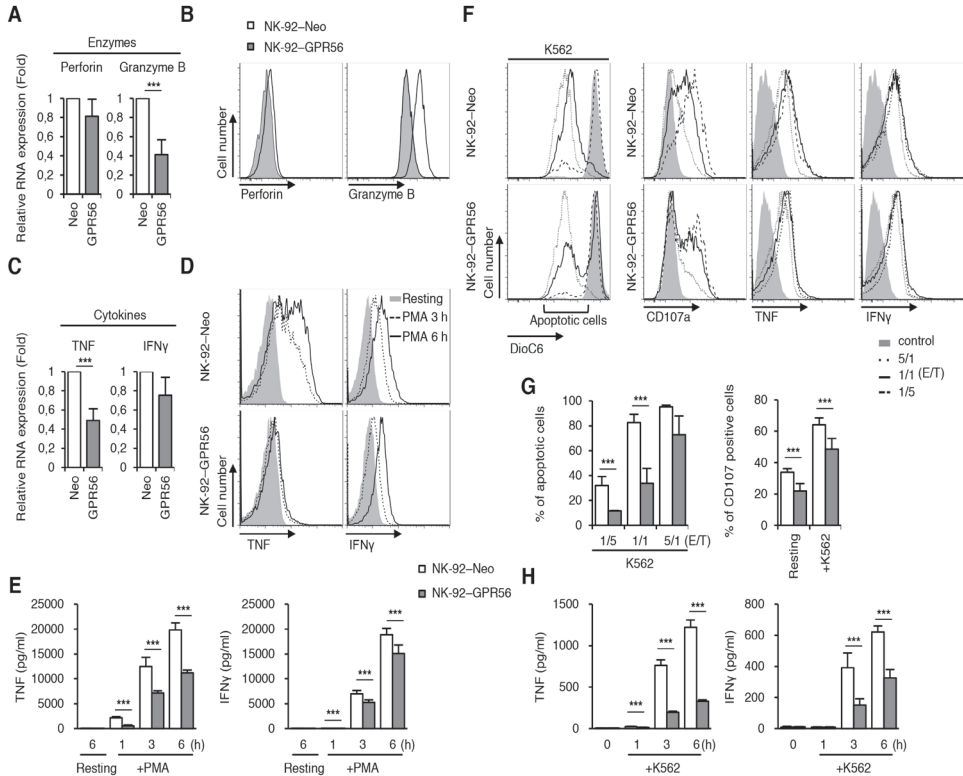


Figure 4. GPR56 expression in NK-92 cells reduces cytotoxic capacity. Vector-transduced (Neo) and GPR56-overexpressing NK-92 cells were studied. (A,B) Quantification of mRNA and protein expression of the cytolytic enzymes perforin and granzyme B by RT-PCR (A) and flow cytometry (B) in NK-92-Neo and NK-92-GPR56 cells. (C,D) Quantification of mRNA and protein expression of the cytokines TNF and IFN γ by RT-PCR (C) and flow cytometry (D) in NK-92-Neo and NK-92-GPR56 cells. Protein expression was determined after stimulating cells with 10 nM PMA for 3 and 6 h. (E) Secretion of TNF and IFN γ by NK-92-Neo and NK-92-GPR56 cells treated with PMA for 1, 3, and 6 h, measured by ELISA. (F,G) NK-92 cells were incubated with fluorescently labeled or unlabeled K562 target cell (E/T=effector/target cell ratio) for 5 h and analyzed by flow cytometry for K562 cell death, NK-cell degranulation (CD107a), and intracellular production of TNF and IFN γ . Shown are representative flow cytometry plots (F) and quantification (G). (H) Secretion of TNF and IFN γ by NK-92-Neo and NK-92-GPR56 cells cultured with K562 target cells for 1, 3, and 6 h, measured by ELISA. All data are means \pm SEM of 3 independent experiments. *** p <0.005

tively regulates the expression of effector molecules.

Hence, we examined various NK-cell effector activities, including target cell conjugation and killing, degranulation, and cytokine production (both intracellular and secreted). GPR56 significantly attenuated cytotoxicity against K562 cells, as indicated by reduced target cell apoptosis, NK-cell degranulation, and production of TNF and IFN γ , when compared with NK-92-Neo cells (Figure 4F-H). The compromising effects of GPR56 on NK-cell cytotoxicity were also observed when NK-92-GPR56 cells were incubated with target cells more resistant to cell conjugation and killing, such as THP-1 and HeLa cells (Figure S5). Taken together, we concluded that GPR56 expression in NK-92 cells attenuates cytotoxic capacity, in accordance with the findings derived from the primary NK cells of BFPP patients.

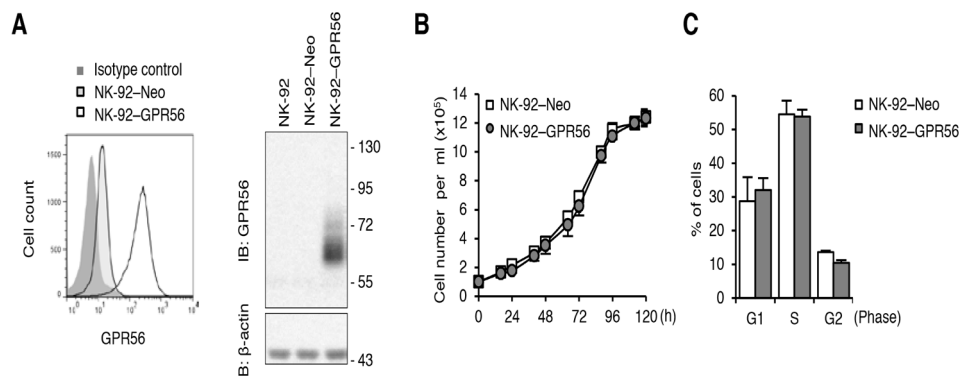


Figure S4. GPR56 overexpression does not affect proliferation of NK-92 cells. (A) Stable overexpression of GPR56 in NK-92 cells, confirmed by flow cytometry, using mAb CG4 (left), and by Western blot analysis of whole cell lysates, using mAb CG4 (right). β -actin was detected as loading control. (B) Growth curve of vector-transduced (Neo) and GPR56-overexpressing NK-92 cells. (C) Quantification of the percentage of vector-transduced and GPR56-overexpressing NK-92 cells in G1, S, and G2/M phase, analyzed by flow cytometry.

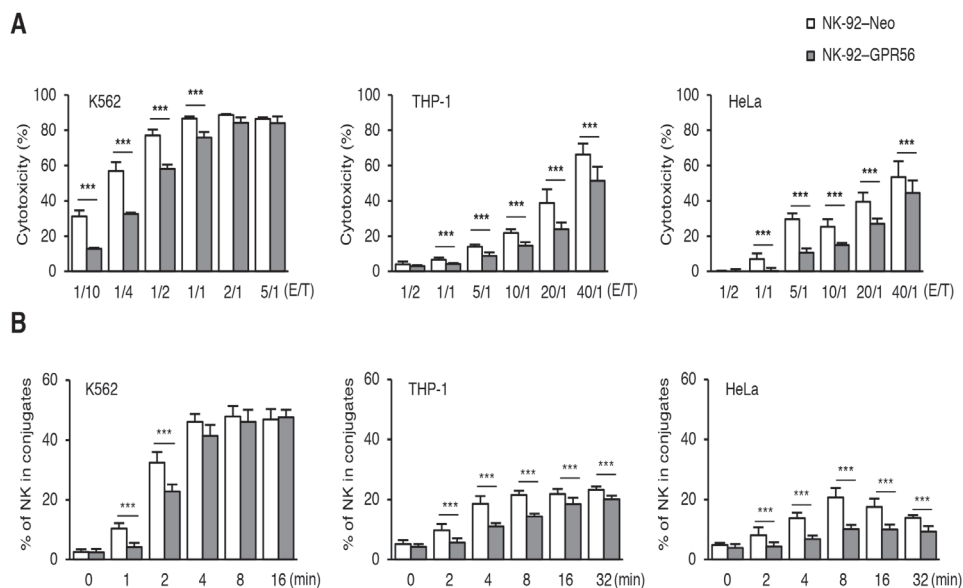


Figure S5. Forced GPR56 expression suppresses cytotoxicity and conjugation of NK-92 and target cells. (A) Quantification of cytotoxic killing of K562, THP-1, and HeLa target cells by NK-92-Neo and NK-92-GPR56 cells, assessed by flow cytometry. Various E/T ratios were tested as indicated. (B) Quantification of cell conjugates formed between NK-92 cells and K562, THP-1, or HeLa target cells incubated at an E/T ratio of 1/2 for the indicated time periods. Fixed cells were analyzed by flow cytometry. Data are means \pm SEM of 8 replicates from 4 independent experiments. *** $p < 0.005$

GPR56 complexes with CD81 to negatively regulate NK-cell effector functions

aGPCRs possess a characteristic bipartite structure (Hamann et al., 2015). Notably, target cell killing was also reduced in NK-92 cells expressing cleavage-deficient GPR56, indicating that autocatalytic processing at the GPS is not a prerequisite for the inhibitory activity of GPR56 in NK cells (Figure S6). Moreover, we could not confirm interaction with collagen III, the binding partner of GPR56 on neuronal cells (Luo et al., 2011) (Figure S7). These findings are in line with reports showing that the CTF of GPR56 can signal independently of the NTF (Paavola et al., 2011; L. Yang et al., 2011).

The CTF of GPR56 forms complexes with the tetraspanin proteins CD9 and CD81 at the cell surface (Little et al., 2004). CD81 has been previously reported to inhibit human NK-cell functions, when crosslinked by the major hepatitis C virus (HCV) envelope protein E2 or anti-CD81 mAbs (Crotta et al., 2002; Tseng and Klimpel, 2002). Flow-cytometric analysis showed significant amounts of CD81, but little CD9, in NK-92 cells. Interestingly, GPR56 overexpression strongly lowered CD81 protein levels, even though RNA transcript levels were reduced only slightly (Figure S8A), which might be explained by a relatively high turnover of GPR56 (and complexed CD81) in NK-92–GPR56 cells (data not shown). Western blotting indicated that NK-cell activation by PMA reduced GPR56 protein levels without affecting CD81, but interaction with K562 target cells diminished the levels of both GPR56 and CD81 (Figure S8B). On the other hand, no significant changes in CD81 protein levels were observed when NK-92–Neo cells were activated by PMA or by interaction with K562 cells (Figure S8B). This result suggested that NK-92–K562 cell interaction might cause dynamic changes of the GPR56–CD81 complex on the cell surface.

Indeed, confocal immunofluorescence microscopy revealed marked redistribution of GPR56 and CD81 in NK-92–GPR56 cells before and after target cell conjugation (Figure 5A). At steady state, GPR56 and CD81 were largely co-localized and distributed homogeneously on the cell surface. After conjugation with K562 cells, the levels of both GPR56 and CD81 were reduced, and the two receptors were clustered mostly to areas resembling immune synapses, where granzyme B also accumulated (Figure 5A). Such reduction and clustering of CD81 protein was not observed in NK-92–Neo cells, suggesting a critical role for GPR56 in this process.

We confirmed the formation and reduction of GPR56–CD81 complexes in NK-92–K562 co-cultures by (immunoprecipitation) IP and IP–re-IP experiments (Figure 5B). CD81 was readily detected in NK-92–GPR56 cell lysate immunoprecipitated with the anti-GPR56 CG2 mAb. Critically, the amount of precipitated CD81 was comparable in the lysate of resting and PMA-activated NK-92–GPR56 cells, but much reduced in the same cells co-cultured with K562 cells. This result was further verified by IP with the anti-CD81 mAb first, followed by re-IP with anti-GPR56 CG2 mAb (Figure 5B). These results indicated that GPR56 indeed associates with CD81 and that the GPR56–CD81 complexes are diminished upon NK-cell interaction with target cells.

To delineate how the GPR56–CD81 complex modulated NK-cell function, anti-GPR56 mAbs were employed. Cross-linking of GPR56 by mAb ligation with CG2 and CG5, but not CG3, caused a rapid dissociation of the GPR56–CD81 complex as shown by the IP experiments (Figure 5C and Figure S9). Importantly, the cytolytic function

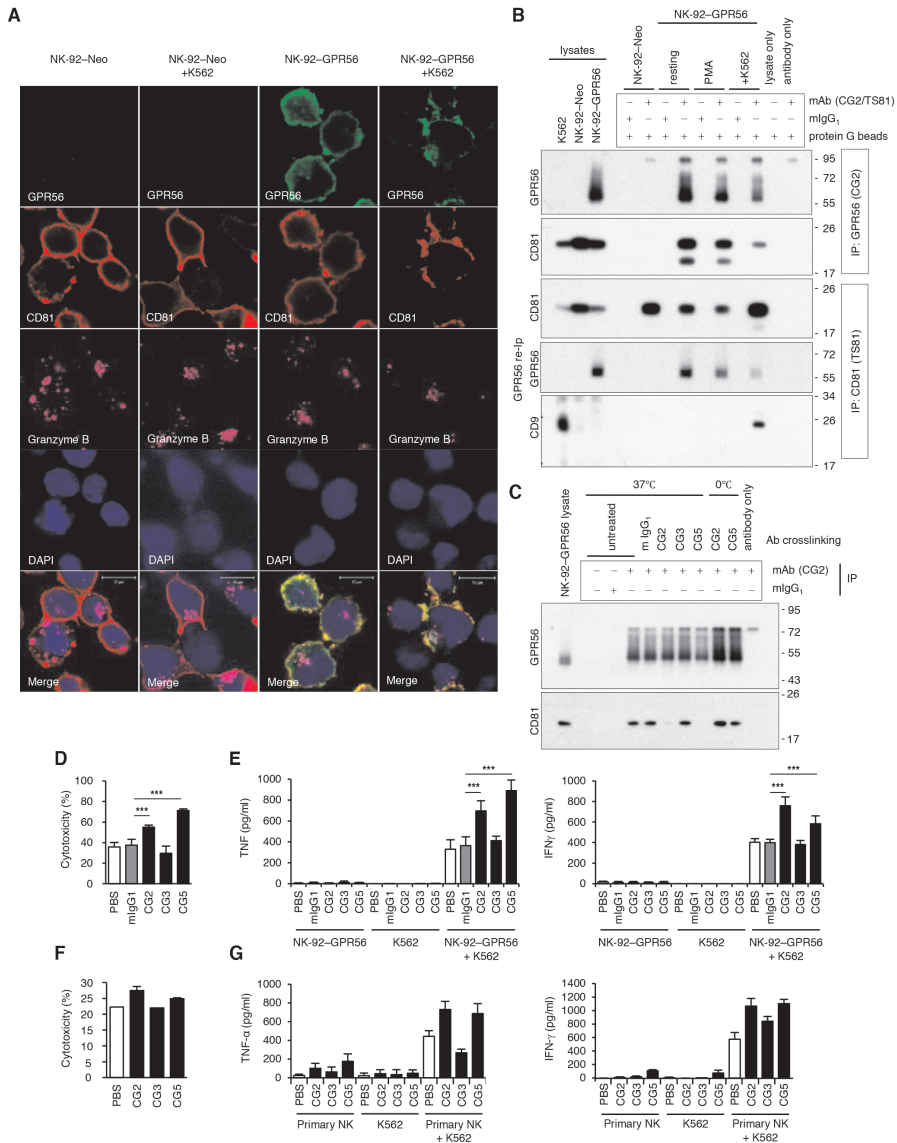


Figure 5. GPR56-CD81 complexes at the immune synapse repress cytotoxicity and cytokine production of NK cells. (A) Surface CD81 and GPR56, and intracellular granzyme B of NK-92-K562 cell conjugates were sequentially stained and detected using confocal microscopy. DAPI staining defined the morphology of nuclei. Scale bars, 10 μ m. (B) 1% CHAPS cell lysate was immunoprecipitated with either anti-GPR56 or anti-CD81 mAb, as indicated. The presence of GPR56, CD81, and CD9 was revealed by immunoblotting (IB) using specific mAbs. (C) NK-92-GPR56 cells were incubated in the absence (untreated) or presence of 10 μ g/ml of GPR56 mAbs at 37°C or 0°C for 15 min before lysate collection for IP using anti-GPR56 mAb. Mouse IgG1 was used as an isotype control. The presence of CD81 in each immunoprecipitate was revealed by immunoblotting. (D-F) NK-92-GPR56 (D,E) or human primary NK cells (F,G) were incubated in plates pre-coated with or without various anti-GPR56 mAbs (10 μ g/ml) as indicated for 2 h before adding K562 target cells. Percentage of dead target cells in each sample was quantified by flow cytometric analysis following 4 h of co-culture (D,F), and amount of TNF and IFN γ released into medium during 6 h incubation was measured by ELISA (E,G). Data are representative of 3 independent experiments; values indicate the mean \pm SEM. * p <0.005**

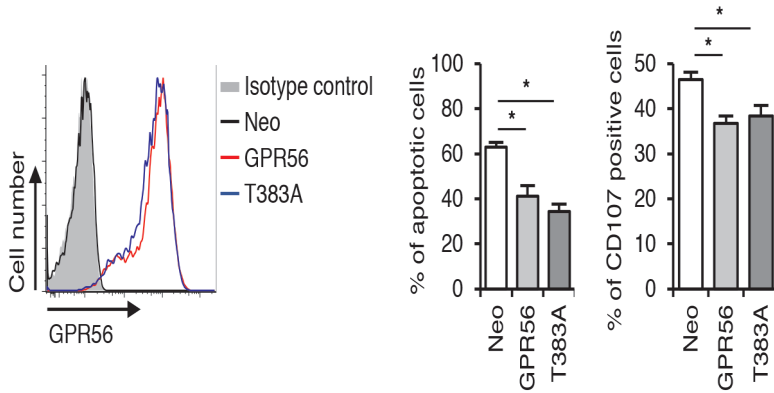


Figure S6. Suppression of cytotoxicity of NK-92 cells does not require autocatalytic processing of GPR56. (A) Overexpression of wild type and cleavage-deficient GPR56 in NK-92 cells, assessed by flow cytometry. (B) NK-92 cells were incubated with fluorescently labeled or unlabeled K562 target cell (E/T=effector/target cell ratio 1/1) for 5 h and analyzed by flow cytometry for K562 cell death and NK-cell degranulation (CD107a). Data are means \pm SEM of 3 independent experiments. * $p < 0.05$

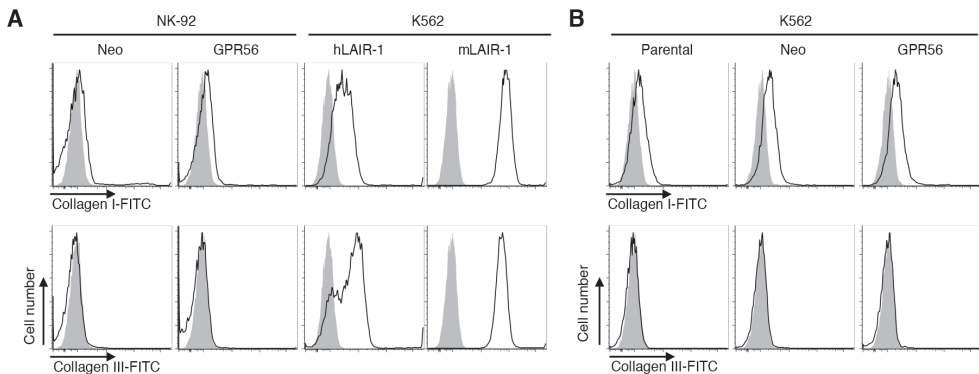


Figure S7. Collagen III does not bind GPR56 on NK-92-GPR56 cells. (A,B) NK-92 and K562 cells overexpressing GPR56 were incubated with 10 μ g/ml FITC-conjugated collagen I or III for 30 min and analyzed by flow cytometry for ligand binding. K562 cells overexpressing human (h) and mouse (m) LAIR were used to confirm collagen binding (Lebbink et al., 2006). FITC-conjugated collagen III also did not stain PBMCs (data not shown). Data are means \pm SEM of 3 independent experiments.

and cytokine (TNF and IFN γ) secretion of NK-92-GPR56 and human primary NK cells were greatly enhanced in the presence of CG2 or CG5 mAbs, whereas the isotype control Ab and CG3 mAb failed to show such an effect (Figure 5D-G). Similarly, shRNA knockdown of CD81 restored K562 target cell killing by NK-92-GPR56 cells (Figure S10). Finally, we tested whether G α q/11, which has been implicated in GPR56-CD81 complex signaling (Little et al., 2004), is required. Of note, a novel, highly selective G α q/11/14 inhibitor (FR900359) did not restore cytolytic activity in NK-92-GPR56 cells (data not shown). We concluded that association with CD81, but not G α q/11 signaling, is crucial for the ability of GPR56 to inhibit NK-cell functions.

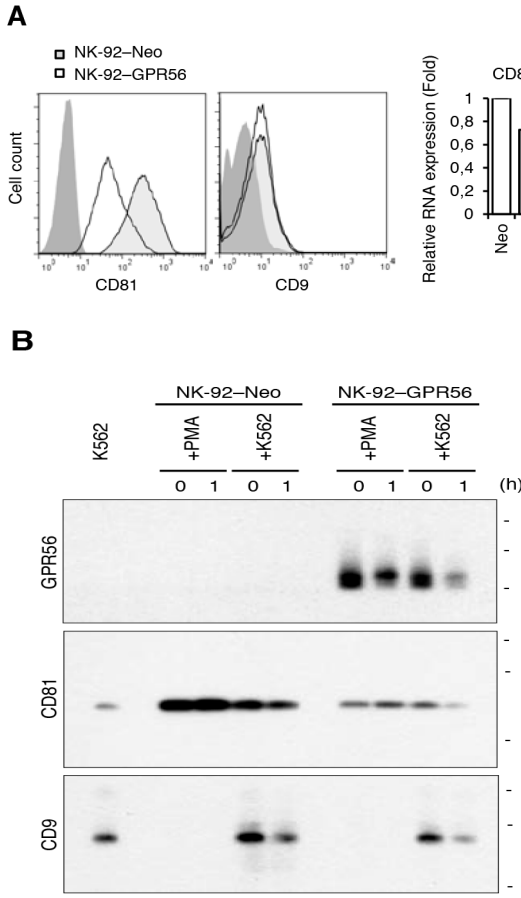


Figure S8. Cell activation and cross-linking of GPR56 with specific mAbs modulates GPR56-CD81 complexes in NK-92-GPR56 cells. (A) Expression of CD81 and CD9, analyzed by flow cytometry (left panel) and RT-PCR (right panel). (B) Western blot analysis of expression of GPR56, CD81, and CD9 in NK-92-Neo and NK-92-GPR56 cells. NK-92 cells were either stimulated with PMA or activated by target cells (effector/target cell ratio=1/2) for 1 h, as indicated. 1% CHAPS extract collected from 2×10^5 equivalents of K562 and 1×10^5 equivalents of NK-92 cells were loaded in each lane and analyzed by Western blotting using anti-GPR56, anti-CD81, and anti-CD9 mAbs. One of two comparable experiments is shown.

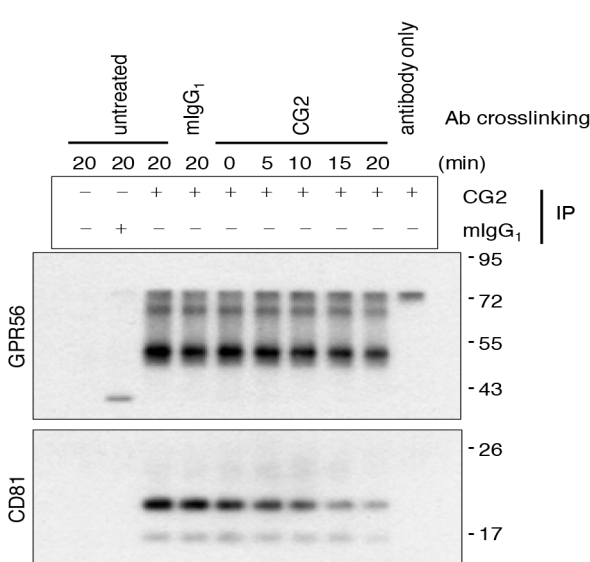


Figure S9. Cross-linking of GPR56 by mAb ligation rapidly dissociates the GPR56-CD81 complex. NK-92-GPR56 cells were pre-treated with 10 μ g/ml of CG2 for the indicated times from 0 to 20 min before lysate collection for IP using anti-GPR56 mAb CG2. Mouse IgG₁ was used as an isotype control. Mouse IgG₁ was used as an isotype control. The presence of CD81 in each immunoprecipitate was revealed by immunoblotting.

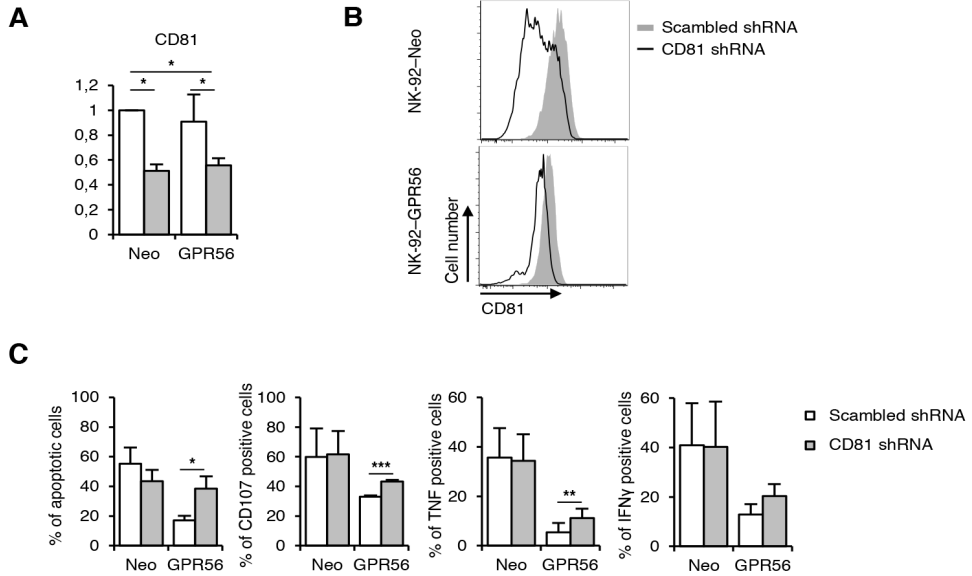


Figure S10. Knockdown of CD81 restores effector functions of GPR56. (A,B) NK-92-Neo and NK-92-GPR56 cells transduced with scrambled shRNA or CD81 shRNA were analyzed for expression of CD81. Quantification of mRNA expression by RT-PCR (A) and representative flow cytometry plots (B). (C) NK-92-Neo and NK-92-GPR56 cells transduced with scrambled shRNA or CD81 shRNA were incubated with fluorescently labeled or unlabeled K562 target cell (E/T=effector/target cell ratio 1/5) for 5 h and analyzed by flow cytometry for K562 cell death, NK-cell degranulation (CD107a), and intracellular production of TNF and IFN γ . All data are means \pm SEM of 3 independent experiments.

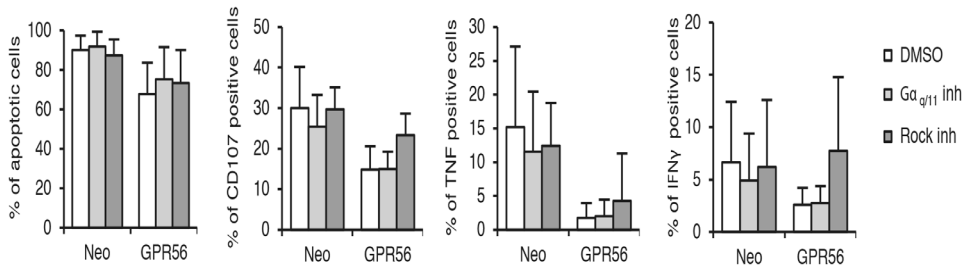


Figure S11. Inhibition of NK-cell cytotoxicity by GPR56 does not require G $\alpha_{q/11}$. NK-92-Neo and NK-92-GPR56 cells, pretreated with 1 μ M FR900359 (inhibits G $\alpha_{q/11/14}$) or 25 μ M Y27632 (inhibits Rock) for 5 h, were incubated with fluorescently labeled or unlabeled K562 target cell (E/T=effector/target cell ratio 5/1) for 5 h and analyzed by flow cytometry for K562 cell death, NK-cell degranulation (CD107a), and intracellular production of TNF and IFN γ . All data are means \pm SEM of 6 independent experiments.

Discussion

We here describe GPR56 as a novel inhibitory receptor expressed by human CD56dim NK cells. CD56dim NK and CD27–CD45RA+ T cells are highly reactive cytotoxic effector lymphocytes that protect the body against harmful viruses and neoplasms. The effective cytotoxicity, displayed by these cells, requires a tight interplay between activating and inhibiting control mechanisms (Caligiuri, 2008). We previously reported that cytotoxic human lymphocytes, in contrast to non-cytotoxic lymphoid or myeloid blood cells, express GPR56 (Peng et al., 2011). This study extends these findings by showing that GPR56 is induced in CD56dim NK cells prior to the upregulation of KLRG1 and CD57, which both appear at later stages of differentiation, associated with terminal differentiation (Björkström et al., 2010; Lopez-Vergès et al., 2010; Voehringer et al., 2002). Of note, long-lived memory-like NK cells, defined by absent/low expression of FcRγ and PLZF (Lee et al., 2015; Schlums et al., 2015; Zhang et al., 2013), also expressed GPR56. GPR56 seems to be the best currently available surrogate surface marker to indicate cytolytic capacity across all lymphocyte subsets. The restricted expression of GPR56 by only CD56dim NK (and CD27–CD45RA+ T) cells indicates tight control of its induction and regulation at the transcript and protein level. We obtained evidence that expression of GPR56 is induced by Hobit, a close relative of Blimp-1, recently discovered by us (van Gisbergen et al., 2012). In humans, Hobit is expressed in quiescent effector NK and T cells, very closely matching the expression of GPR56 (Vieira Braga et al., 2015). Implying a causal relationship, Hobit knockdown in NK-92 cells prevented induction of GPR56 upon IL-2 withdrawal, and ectopic Hobit enabled GPR56 expression in Jurkat T cells. In contrast, manipulating the expression of Eomes did not affect GPR56 expression, despite its prominent role in the differentiation and maturation of effector NK and T cells and, like GPR56, its expression in developing neurons and relationship with polymicrogyria (Baala et al., 2007). Thus, on current evidence, GPR56 is a transcriptional target of Hobit in human NK and T cells.

Of note, the GPR56 locus has 17 transcriptional start sites in humans, which are targets of different transcription factors, such as peroxisome proliferator-activated receptor gamma co-activator 1-alpha 4 (PGC-1α4) in muscle cells (White et al., 2014) and so-called heptad complex factors in hematopoietic stem cells (Solaimani Kartalaei et al., 2015), giving rise to a widespread cellular distribution (Hamann et al., 2015). Hobit comprises DNA-binding zinc finger domains, which closely resemble their homologous domains in Blimp-1 (van Gisbergen et al., 2012; Vieira Braga et al., 2015). In agreement with the presumed role of Hobit as transcription factor, multiple copies of the consensus binding sequence for Blimp-1/Hobit G(T/C)GAAAG(T/C) (G/T) (Doody et al., 2007) are identified in the 5'-region of GPR56 (data not shown). In mice, peripheral NK and T cells barely express GPR56 (www.immgen.org), which is in line with the absence of Hobit in these cells (van Gisbergen et al., 2012). Interestingly, resting murine NK cells are minimally cytotoxic; they contain little granzyme B or perforin protein, whereas the respective mRNAs are abundant (Fehniger et al., 2007). Cytokine- and virus-induced activation of murine NK cells results in potent cytotoxicity, associated with a strong increase in granzyme B and perforin protein. It is tempting to speculate that murine NK and T cells do not express GPR56 due to the different ways they acquire cytotoxic capacity.

By studying two pairs of BFPP siblings with the recurrent R565W and C346S mutations in the second extracellular loop and the GAIN domain, respectively (Piao et al., 2005; 2004), which both obstruct cell surface expression of the receptor (Chiang et al., 2011; Jin et al., 2007), we found that GPR56 is not required for the development of functionally competent NK cells. Entirely GPR56-deficient NK cells with the R565W mutation killed K562 cells even more efficiently, indicated by enhanced degranulation, enhanced cytokine secretion, and enhanced induction of apoptosis in target cells. This observation provided a first clue that GPR56 might regulate NK-cell cytotoxicity, a finding that we substantiated in NK-92 cells stably overexpressing GPR56. NK-92–GPR56 cells contained less granzyme B and TNF transcripts at resting state and produced less TNF and IFN γ protein upon PMA stimulation. Moreover, their ability to kill K562 was impaired, as indicated by reduced degranulation, reduced cytokine secretion, and reduced induction of apoptosis in target cells. Similar results were found in more killing-resistant THP1 and HeLa cells, altogether demonstrating that GPR56 inhibits NK-cell cytotoxicity.

Of note, no immune-related clinical phenotype has been reported for BFPP patients. This, however, is not surprising since effector functions of NK cells are balanced by activating and inhibitory signals that are simultaneously delivered to the cells following the engagement of several distinct families of transmembrane receptors (Caligiuri, 2008). GPR56 does not belong to a receptor family commonly associated with NK-cell regulation, such as immunoglobulin-like receptors and C-type lectins (Lanier, 2008; Pegram et al., 2011). GPR56 is a member of the aGPCR family. While the functional mechanism of aGPCRs is still poorly understood, evidence accumulates that they are true GPCRs that regulate wide cellular programs through the action of G proteins (Hamann et al., 2015; Monk et al., 2015). Indeed, the broad activity of GPR56 is indicated by its ability to control cytolytic enzymes and pro-inflammatory cytokines, which present the two major arms of NK-cell activity. Moreover, we previously showed that GPR56 inhibits spontaneous and SDF-1-stimulated NK-cell migration (Peng et al., 2011). Studies in other cell types have implicated roles of GPR56 in generation and maintenance of the hematopoietic stem cell pool, cortical development, male fertility, muscle hypertrophy, and melanoma tumor growth and progression (Ackerman et al., 2015; Bae et al., 2014; Chen et al., 2010; Giera et al., 2015; Piao et al., 2004; Saito et al., 2013; Solaimani Kartalaei et al., 2015; White et al., 2014; Xu et al., 2006).

Our data indicate that GPR56 executes its inhibitory activity in concert with the tetraspanin protein CD81. The GPR56–CD81 complex represented one of the first examples of a GPCR in the tetraspanin web, an important membrane protein scaffold for regulating signal transmission (Little et al., 2004). More recently, the *Drosophila* aGPCR Flamingo was shown to interact in cis with the tetraspanin Van Gogh in the acquisition of planar cell polarity (Lawrence et al., 2008). The tetraspanin web is well known to modulate immune signaling, and CD81 has been shown to inhibit NK-cell functions when cross-linked (Crotta et al., 2002; Tseng and Klimpel, 2002). Our findings that the GPR56–CD81 complex on the NK-cell surface was quickly reduced and relocated to the contact points with the target cells suggested a role in regulating NK-cell activities. Indeed, ligation of GPR56 receptor by mAbs was found to dissociate the GPR56–CD81 complex, leading to enhanced NK-cell cytotoxicity and increased cytokine secretion. Based on these results, we suggest that GPR56 acts

as a cell-autonomous NK-cell inhibitory receptor by laterally crosslinking with CD81. Removing GPR56 hence resulted in stronger NK-cell functions, as exemplified by the GPR56-deficient NK cells of BFPP patients as well as NK-92 and primary NK cells upon activation by PMA, cytokines, and contact with target cells.

At present, it is not known exactly how the GPR56–CD81 complex is recruited to the immune synapses upon NK–target cell conjugation. However, possible mechanisms can be envisioned based on earlier works. We have previously shown that while the majority of the GPR56 NTF–CTF heterodimeric receptor complex is located in the non-raft region, some of the GPR56 CTF is partitioned to the lipid raft microdomains (Chiang et al., 2011). Moreover, although lipid rafts and the tetraspanin-enriched microdomains (TEMs) are considered distinct membrane constitutions, co-clustering of lipid rafts and TEMs is possible upon cell activation or transformation (Krementsov et al., 2010; Ono, 2010).

Signaling molecules, including Gαq/11, Gα12/13, PKCa, RhoA, and mTOR, have been linked to GPR56 in different cell types (Ackerman et al., 2015; Giera et al., 2015; Iguchi et al., 2008; Little et al., 2004; Luo et al., 2011; Paavola et al., 2011; White et al., 2014). Of interest is the specific association with CD81 and Gαq/11, reported by Little et al., in which CD81 was critical in promoting/stabilizing the GPR56–Gαq/11 association (Little et al., 2004). The GPR56–CD81–Gαq/11 complex was dynamically regulated: anti-CD81 mAb led to the uncoupling of Gαq/11 from the GPR56–CD81 complex, while cell activation by PMA dissociated GPR56 from CD81 and Gαq/11, leading to GPR56 internalization. In the present report, we applied a novel, highly selective inhibitor of Gαq/11/14, called FR900359 (Schrage et al., 2015). Of note, FR900359 did not restore cytotoxicity in NK-92–GPR56 cells. Thus, signaling pathways downstream of the GPR56–CD81 complex remain to be elucidated.

The ability to downregulate inhibitory receptors enables effector NK and T cells to unfold their full functional capacity. We found that PMA rapidly and completely downregulates GPR56 through PKC-mediated shedding and internalization. Moreover, an inflammatory milieu, created by the potent NK-cell activating cytokines IL-15 and IL-18 (Fehniger et al., 1999), caused PKC-dependent shedding of GPR56. Receptor shedding is a hallmark of aGPCRs and likely relates to the extended extracellular domains (Hamann et al., 2015). Previous studies indicate that in absence of the NTF, the CTF of GPR56 and other aGPCRs can overtly provide activating signals (Liebscher et al., 2014; Paavola et al., 2011; Paavola and Hall, 2012; Paavola et al., 2014; Stephenson et al., 2013). GPR56 expression on cytotoxic lymphocytes will provide an interesting model to determine the fate and possible activities of an aGPCR upon activation-mediated release of its NTF and to explore therapeutic possibilities provided by the unique structure of this non-canonical GPCR.

Experimental Procedures

Donors and cell isolation

PBMCs were isolated using a Lymphoprep gradient (Axis-Shield, Oslo, Norway) from fresh blood of healthy donors and four BFPP patients, diagnosed with single mutations in GPR56. Studied were two newly identified Dutch siblings of 46 and 49 years (1693C>T, R565W) and 2 previously described Palestinian siblings (1036T>A, C346S) (Piao et al., 2004). Samples were obtained under informed consent and in accordance with ethical guidelines of the Academic Medical Center, Amsterdam, the Netherlands, the Radboudumc, Nijmegen, the Netherlands, and the Schneider Children's Medical Center, Petah Tiqva, Israel. CD56+CD3- NK cells with $\geq 99\%$ purity were isolated on a FACSAria™ III cell sorter (BD Biosciences, San Diego, CA, USA).

Cell culture and stable transduction

Cells were maintained in the following media supplemented with 10% heat-inactivated fetal bovine serum (FBS): PBMCs, purified CD56+CD3- NK cells, and monocytic THP-1 cells in Roswell Park Memorial Institute (RPMI) 1640 medium; erythroleukemic K562 cells and Jurkat T cells in Iscove's modified Dulbecco's medium (IMDM); HeLa cells in Dulbecco's Modified Eagle Medium (DMEM). Human NK-92 cells were cultured in nucleoside-free α -Minimum Essential Medium (α -MEM) containing 12.5% FBS, 12.5% horse serum, 0.2 mM inositol, 0.1 mM 2-mercaptoethanol, 0.02 mM folic acid, and 100 IU/ml IL-2. Cell culture media and supplements were obtained from Invitrogen (Carlsbad, CA, USA). All cell culture media were supplemented with 2 mM L-glutamine, 10 U/ml penicillin, and 100 μ g/ml streptomycin.

Generation of NK-92 cells stably overexpressing GPR56 has been described previously (Peng et al., 2011). The wild type and cleavage deficient mutant (T383A) of GPR56 were transduced using retroviruses in NK-92 cells. For gene knockdown, NK-92 cells were transduced using lentiviruses containing pKLO.1 plasmids with non-target scrambled short hairpin RNA (shRNA) (SHC002; sequence CCGGCAACAAGATGAAGAGCACCAACTC) from Sigma-Aldrich (St. Louis, MO, USA) or Eomes shRNA (TRCN0000013175; target sequence GCCCACTACAATGTGTTTCGTA) from Open Biosystems (GE Healthcare, Lafayette, CO, USA). Cells were transduced in retronectin (Takara Bio Inc., Shiga, Japan)-coated plates and selected on 2 ng/ml puromycin (Sigma-Aldrich). NK-92 cells expressing pKLO.1 with Hobit shRNA (TRCN0000162720; CAGAAGAGCTTCACTCAACTT) or Jurkat cells expressing LZRS pBM-IRES-EGFP with Hobit fragment were generated previously (Vieira Braga et al., in revision). Transduced Jurkat cells were sorted to $\geq 95\%$ purity on a FACSAria™ III cell sorter using green fluorescent protein (GFP) expression as selection marker.

Cytotoxicity assay

This assay employs 7-hydroxy-9H-(1,3-dichloro-9,9-dimethylacridin-2-one) (DDAO; Invitrogen) to label target cells and 3,3'-dihexyloxycarbocyanine iodide (DiOC6; Invitrogen) to label live cells. Washed target cells (5×10^6 cells/ml) were resuspended in 1 nM DDAO/phosphate-buffered saline (PBS), incubated at 37°C for 15 min in the dark, washed, and resuspended in NK-92 medium. PBMCs or NK-92 stable cells were incubated at various effector/target ratios (5/1 to 1/5) with target cells at 37°C for 5 h, followed by addition of 0.1 μ g/ml DiOC6 at 37°C for 15 min, and analysis by flow

cytometry.

Alternatively, target cells were labeled with carboxyfluorescein succinimidyl ester (CFSE; Invitrogen) and dead cells with 7-aminoactinomycin D (7-AAD; Invitrogen). Washed target cells (5×10^6 cells/ml) were resuspended in PBS containing CFSE (2 μ M for K562, 1 μ M for THP-1, and 2.5 μ M for HeLa) and incubated at 37°C for 10 min in the dark, followed by quenching the CFSE staining for 5 min on ice. Washed cells were resuspended in NK92 medium. NK-92 stable cells were incubated at various effector/target ratios (40/1 to 1/10) with target cells at 37°C for 4 h, followed by addition 0.5 ml of ice-cold Dulbecco's PBS (DPBS; Invitrogen), containing 1% bovine serum albumin (BSA) and 5 μ g/ml 7-AAD, for 15 min in the dark, and analysis by flow cytometry.

Cell stimulation

For activation, 1×10^6 cells/ml PBMCs were incubated for 2 h in medium plus 10 ng/ml PMA (Sigma-Aldrich). For cytokine stimulation, 1×10^6 cells/ml PBMCs were incubated for 12–24 h in medium containing 400 U/ml IL-2, 10 ng/ml IL-15, or 100 ng/ml IL-18 (all R&D Systems, Minneapolis, MN, USA), either alone or in the combination, as indicated. For CD16 Ab cross-linking stimulation, flat 96-well microplates (Corning, Corning, NY, USA) were pre-coated with 10 μ g/ml goat anti-mouse immunoglobulin (Ig)G in PBS at 37°C for 2 h. Plates were washed twice with PBS and coated with 10 μ g/ml purified anti-CD16 in PBS at 4°C for overnight. Then, plates were washed twice with PBS and blocked with RPMI 1640 medium/10% FBS at 37°C for 1 h. 2×10^6 cells/ml purified CD56+CD3– NK cells were added to the plates. For GPR56 Ab cross linking stimulation 48-well plates (Cellstar, Greiner bio-one) were coated with PBS containing mouse IgG, CG2, CG3, or CG5 at 37°C for 2 h followed by overnight coating at 4°C. After washing the plates with PBS, 2×10^6 /ml NK-92-GPR56 cells or primary human NK cells were incubated in coated wells in complete NK-92 medium. Following 2 h of crosslinking at 37°C, 8×10^6 /ml K562 cells were added to wells at E/T ratio=2. For NK cytotoxicity assay, K562 cells were labeled with DDAO before adding onto the plates as described above. For cytokine production assay, supernatants were collected following 6 h of stimulation with K562 cells.

Pharmacological inhibitors were added for 1 h at 37°C prior to stimulation. Specific inhibitors of PKC (staurosporine, calphostin, bisindolylmaleimide I), PKB/Akt (Akt1/2 kinase inhibitor), PI3K (LY294002), MAP kinases ((Erk (U0126), JNK (SP600125) and p38 (SB 203580)), MMPs (GM6001), and dynamin (dynasore) were all obtained from Sigma-Aldrich. Inhibitors of ADAM10 and ADAM17 (GW) were generated at the Chemistry Department of Cardiff University; a second ADAM17 inhibitor (TNF484) was kindly provided by Dr. U. Neumann (Novartis, Basel, Switzerland). Ga signaling was inhibited using Y27632 (Sigma-Aldrich), an inhibitor of ROCK downstream of Ga12/13, and FR900359, a selective inhibitor of Gaq/11/14 (Schrage et al., 2015)

Proliferation assay

PBMCs were washing three times in PBS, resuspended at 5×10^6 cells/ml in PBS, and labeled with 2.5 μ M CFSE by shaking at 37°C for 10 min. Cells were washed three times and subsequently cultured in RPMI 1640 medium with or without 50 U/ml IL-2

for 5 days.

Conjugation assay

Target cells were labeled with CFSE as described above. 1×10^6 of labeled target cells were mixed with 5×10^5 NK-92 cells at an effector/target ratio of 1/2. The cell mixture was centrifuged at 250g for 3 min at 4°C, then placed in a 37°C water bath for the desired lengths of time. After conjugation, cells were gently resuspended, fixed in 2% ice-cold paraformaldehyde/ PBS for 30 min, then subjected to Ab staining using either allophycocyanin (APC)-conjugated anti-CD56 mAb (if K562 and HeLa were used as targets) or APC-conjugated anti-CD2 mAb (if THP-1 was used as a target). Conjugation was analyzed by flow cytometry (FL-1 versus FL-4), and measured by percentage of NK cells that formed conjugates with target cells as calculated by the ratio of two-color events to total effector cell events.

Quantitative PCR

Total RNA was isolated with RNeasy mini kit (Qiagen, Hilden, Germany), and cDNA was synthesized using RevertAid First Strand cDNA Synthesis Kit (Thermo Fisher Scientific, Waltham, MA, USA). Relative gene expression levels were measured using Fast SYBR Green Master Mix (Applied Biosystems, Foster City, CA, USA) on a StepOnePlus™ System (Applied Biosystems) with the cycle threshold method. Expression of specific genes was normalized to human GAPDH (forward 5'-GAAGGTGAAG-GTCGGAGTC-3', reverse 5'-GAAGATGGT GATGGGATTTC-3') as endogenous control. The following primers were used: ADGRG1 (forward 5'-GATTGCTGGCCTGTTGTAG-3', reverse 5'-GAATGATGGCTCCCTGTCC-3'); B3GAT1 (forward 5'-GAAGCCAGGCCTACT-TCAAGCT-3', reverse 5'-GTTGAGGGTGACAAATTCTCGAA-3'); BCL6 (forward 5'-AACCTGAAAACCCACACTCG-3', reverse 5'-CTGGCTTTTGTGACGGAAAT-3'); CD81 (forward 5'-AGGGCTGCACCAAGTGC-3', reverse 5'-TGTCTCCCAGCTCCAGATA-3'); GZMB (forward 5'-TGGGGGACCCAGAGATTAATA-3', reverse 5'-TTTCGTCCATAGGAGACAATGC-3'); KLRG1 (forward 5'-AACGGACAATCAGGAAATGAG-3', reverse 5'-CCTTGAGAAGTT TAGAGGTGATCC-3'); PDCD1 (forward 5'-CTCAGGGTGACAGAGAGAAG-3', reverse 5'-GACACCAACCACAGGGTTT-3'); PRDM1 (forward 5'-GTGTCAGAACGGGATGAACA-3', reverse 5'-GCTCGGTTGCTTTAGACTGC-3'); PRF1 (forward 5'-CGCCTACCT-CAGGCTTATCTC-3', reverse 5'-CCTCGACAGTCAGGCAGTC-3'); TBR1 (forward 5'-ACT-GGTTCCCACTGGATGAG-3', reverse 5'-CCACGCCATCCTCTGTAAC-3'); TBX1 (forward 5'-GGGAACTAAAGCTCACAAAC-3', reverse 5'-CCCCAAGGAATTGACAGTTG-3'); TNF (forward 5'-CCCAGGGACCTCTCTAATCA-3', reverse 5'-AGCTGCCCTCAGCTTGAG-3'); ZNF683 (forward 5'-CATATGTGGCAAGAGCTTTGG-3', reverse 5'-GGCAA-GTTGAGTGAAGCTCT-3').

Antibodies and flow cytometry

Conjugated mAbs with the following specificity were used: anti-GPR56 (clone CG4; Biolegend, San Diego, CA, USA); anti-CD2 (clone RPA-2.10; BD Biosciences); anti-CD3 (clone SK7 and UCHT1; BD Biosciences); anti-CD9 (clone ML13; BD Biosciences); anti-CD16 (clone 3G8; BD Biosciences); anti-CD56 (clone NAM16.2; BD Biosciences); anti-CD57 (clone NK-1; BD Biosciences); anti-CD81 (clone 1D6-CD81; eBioscience, San Diego, CA, USA); anti-CD94 (clone HP-3D9; BD Biosciences); anti-CD107a (clone H4A3; eBioscience); anti-CD158a/h (KIR2DL1/S1; clone EB6B;

Beckman Coulter, Miami, FL, USA); anti-CD158b (KIR2DL2/L3; clone GL183; Beckman Coulter); anti-CD158e (KIR3DL1; clone DX9; BD Biosciences); anti-CD159a (NKG2a; clone #131411; R&D Systems); anti-CD159c (NKG2c; clone #134591; R&D Systems); anti-CD226 (DNAM-1; clone 11A8; Biolegend); anti-CD279 (PD-1; clone EH12.1; BD Biosciences); anti-CD314 (NKG2d; clone 1D11; Biolegend); anti-CD335 (NKp46; clone 9E2; AbD Serotec, Kidlington, UK); anti-CD336 (NKp44; clone P44-8; Biolegend); anti-CD337 (NKp30; clone P30-15; Biolegend); anti-KLRG1 (kindly provided by Prof. H.P. Pircher, Freiburg (Marcolino et al., 2004)); anti-Fc γ R (rabbit polyclonal antibody; Millipore, Bedford, MA, USA); anti-perforin (clone δ G9; BD Biosciences); anti-granzyme B (clone GB11; BD Biosciences); anti-TNF (clone MAb11; eBioscience); anti-IFN γ (clone 4s.B3; eBioscience); anti-T-bet (clone 4B10; Biolegend); anti-Eomes (clone WD1928; eBioscience); anti-PLZF (clone R17-809; BD Biosciences); anti-mouse IgM (clone II/41; eBioscience).

The following purified mAb were used: anti-GPR56 (clone CG2, CG4, CG3, and CG5; Biolegend and (Peng et al., 2011)); anti-CD9 (clone MM2/57; Millipore, Bedford, MA, USA); anti-CD16 (clone 3G8; Biolegend); anti-CD81 (clone TS81 and 5A6; Abcam, Cambridge, UK and Santa Cruz Biotechnology, Dallas, TX, USA); anti-Hobit (Vieira Braga et al., 2015); mouse IgG1 (clone MOPC-21, BD Biosciences).

Staining of extracellular antigens was performed according to standard procedures. For intracellular antigens, cells were first stained for surface markers, followed by fixation with Foxp3 Transcription Factor Staining Buffer Set (eBioscience) and incubation with antibodies directed against intracellular molecules. Flow cytometric analysis was performed on FACSCalibur, FACSCanto II, and LSRFortessa machines (BD Biosciences), and all data were analyzed with FlowJo software (Tree Star, Ashland, OR, USA).

To analyze cell cycle phase distribution, NK-92 cells were washed with cold PBS and fixed in 70% ethanol for 1 h. Fixed cells were stained with 20 μ g/ml propidium iodide/0.1% Triton-X (both from Sigma-Aldrich) in the presence of 200 μ g/ml RNaseA (Qiagen, Hilden, Germany) for 30 min at room temperature in the dark and analyzed by flow cytometry.

For intracellular cytokine and degranulation staining, PBMCs and stable NK-92 cells were mixed with K562 in the presence of anti-CD107a and incubated at 37°C for 1 h in the dark. A mixture of brefeldin A (1 μ g/ml; BD Biosciences) plus monensin (10 μ g/ml; BD Biosciences) was then added, and samples were incubated for a further 5 h. Cells were labeled with antibodies recognizing extracellular antigens, fixed/permeabilized, stained for TNF and IFN γ , and examined by flow cytometry.

Enzyme-linked immunosorbent assay

Soluble GPR56 was quantified as described (T.-Y. Yang et al., 2015). TNF and IFN γ levels in culture supernatants were assessed using DuoSet ELISA Development Systems from R&D. Spectrophotometric analysis was performed at 450 nm wavelength on a SpectraMax M2 spectrophotometer (Molecular Devices, Sunnyvale, CA, USA) using Softmax Pro 5.3 software (Molecular Devices).

Indirect immunofluorescence

NK-92 were conjugated to K562 at 2/1 ratio, centrifuged at 25g for 3 min at 4°C, and incubated for 30 min at 37°C. After conjugation, a total of 6×10^5 cells were

gently resuspended and allowed to adhere to each poly-D-lysine coated coverslip (BD Biocoat) at 37°C for 30 min, centrifuged again at 300g for 3 min, then washed by dipping in DPBS (Invitrogen) several times at room temperature. Subsequent fixation was carried out in 4% paraformaldehyde/PBS (Sigma-Aldrich) at room temperature for 20 min. Cells were blocked in PBS containing 2% normal goat serum and 0.5% BSA, and incubated first with mouse anti-CD81 mAb (TS81, Abcam) and Alexa Fluor 594 conjugated goat anti-mouse IgG (Invitrogen), then washed and blocked again before staining with Alexa Fluor 488 conjugated mouse anti-GPR56 mAb (CG2). Permeabilization was carried out using 0.5% saponin (Sigma-Aldrich) and cells were stained subsequently with Alexa Fluor 647-conjugated anti-granzyme B mAb (GB11, BD Biosciences). Coverslips were mounted using ProLong Gold (with DAPI) mounting medium (Invitrogen). Confocal images were captured on a Zeiss LSM 510 META confocal microscope using a $\times 64$ oil immersion objective. Single images were captured with an optical thickness of 1.5 μm . Analysis was performed using LSM510 META software (Zeiss).

Immunoprecipitation

Cells were lysed in a 1% 3-[(3-cholamidopropyl)dimethylammonio]-1-propanesulfonate (CHAPS) buffer containing 20 mM Tris-HCl, pH7.4, 150 mM NaCl, 5 mM MgCl₂, 5% glycerol, and protease inhibitors including 1 mM sodium orthovanadate, 10 $\mu\text{g}/\text{ml}$ aprotinin, 5 mM levanisole, 1 mM 4-(2-aminomethyl)benzenesulfonyl fluoride hydrochloride (AEBSF) and cOMplete protease inhibitor from Roche Diagnostics (Basel, Switzerland). Lysates were extracted on an end-over-end rotator at 4°C for 3 h and collected after removing insoluble fraction by centrifugation at 12,000 rpm for 25 min at 4°C. Supernatants were pre-cleared with Protein G Sepharose (Sigma-Aldrich) for at least 1 hour at 4°C on a rotator, or, for lysates collected from Ab-pre-treated cells, with mouse IgG conjugated to agarose (A0919; Sigma-Aldrich). Specific mAbs (4 μg) were then mixed with pre-cleared lysates (5×10^6 cell equivalents) and incubated on ice for 2 h before adding 20 μl of 1:1 diluted Protein G Sepharose beads. Immunoprecipitates were then collected overnight at 4°C on a rotator, washed five times with cold 1% CHAPS lysis buffer, eluted with 2% Laemmli buffer at 95°C for 8 min, and resolved on a 8% (for GPR56) or on a 12% (for CD81 and CD9) nonreduced SDS-PAGE. For re-IP, CD81 associated molecules were eluted with 1% Triton X-100 lysis buffer following anti-CD81 (clone TS81) IP. Eluates were then subjected for a second IP using anti-GPR56 (clone CG2) mAb. Immunoprecipitates were analyzed by immunoblotting using anti-GPR56 (clone CG4), anti-CD81 (clone 5A6), and anti-CD9 (clone MM2/57) mAbs.

Statistics

All results are expressed as means \pm standard error of the mean (SEM). A Student t test was used to determine P values. Significance was set at $P < 0.05$.

Acknowledgements

We thank the BFPP patients, their family, and the physicians Dr. D.J.J. Halley (Erasmus MC, Rotterdam), Dr. B. van Bon (Radboudumc, Nijmegen), and M. van Veldhoven (Cello, Rosmalen) for making the investigation possible. We thank Dr. X. Piao

for helpful suggestions and B. Hooibrink and T.M. van Capel for help with cell sorting. The study was supported by a scholarship from the Ministry of Education, Taiwan, and a fellowship from the European Federation of Immunological Societies (EFIS) to C.C.H. and by grants from the Ministry of Science and Technology, Taiwan (MOST101-2320-B-182-029-MY3 and MOST104-2320-B-182-035-MY3) and the Chang Gung Memorial Hospital (CMRPD1A0181-3, CMRPD1D0072-3, CMRPD1D0391-2) to H.H.L. as well as by the Thyssen Foundation (2015-00387) to K.P.J.M.v.G and J.H. J.H. is a Mercator Fellow of the German Research Foundation (Research Unit 2149).

Author contributions

G.W.C., C.C.H., Y.M.P., N.A.M.K., F.A.V.B., and M.D.B.v.d.G. performed experiments, E.B.M.R., R.S., G.M.K., E.K., V.K., L.M., K.P.J.M.v.G., and R.A.W.v.L. provided advice and critical samples of reagents, G.W.C., C.C.H., K.P.J.M.v.G., H.H.L., and J.H. designed experiments and wrote the manuscript.

Competing financial interests

The authors declare no competing financial interests.

References

- Ackerman, S.D., Garcia, C., Piao, X., Gutmann, D.H., Monk, K.R., 2015. The adhesion GPCR Gpr56 regulates oligodendrocyte development via interactions with Ga12/13 and RhoA. *Nat Commun* 6, 6122. doi:10.1038/ncomms7122
- Araç, D., Boucard, A.A., Bolliger, M.F., Nguyen, J., Soltis, S.M., Südhof, T.C., Brunger, A.T., 2012. A novel evolutionarily conserved domain of cell-adhesion GPCRs mediates autoproteolysis. *EMBO J.* 31, 1364–1378. doi:10.1038/emboj.2012.26
- Baala, L., Briault, S., Etchevers, H.C., Laumonier, F., Natiq, A., Amiel, J., Boddaert, N., Picard, C., Sbiti, A., Asermouh, A., Attié-Bitach, T., Encha-Razavi, F., Munnich, A., Sefiani, A., Lyonnet, S., 2007. Homozygous silencing of T-box transcription factor EOMES leads to microcephaly with polymicrogyria and corpus callosum agenesis. *Nat. Genet.* 39, 454–456. doi:10.1038/ng1993
- Bae, B.-I., Tietjen, I., Atabay, K.D., Evrony, G.D., Johnson, M.B., Asare, E., Wang, P.P., Murayama, A.Y., Im, K., Lisgo, S.N., Overman, L., Sestan, N., Chang, B.S., Barkovich, A.J., Grant, P.E., Topçu, M., Politsky, J., Okano, H., Piao, X., Walsh, C.A., 2014. Evolutionarily dynamic alternative splicing of GPR56 regulates regional cerebral cortical patterning. *Science* 343, 764–768. doi:10.1126/science.1244392
- Björkström, N.K., Riese, P., Heuts, F., Andersson, S., Fauriat, C., Ivarsson, M.A., Björklund, A.T., Flodström-Tullberg, M., Michaëlsson, J., Rottenberg, M.E., Guzmán, C.A., Ljunggren, H.-G., Malmberg, K.-J., 2010. Expression patterns of NKG2A, KIR, and CD57 define a process of CD56dim NK-cell differentiation uncoupled from NK-cell education. *Blood* 116, 3853–3864. doi:10.1182/blood-2010-04-281675
- Caligiuri, M.A., 2008. Human natural killer cells. *Blood* 112, 461–469. doi:10.1182/blood-2007-09-077438
- Chen, G., Yang, L., Begum, S., Xu, L., 2010. GPR56 is essential for testis development and male fertility in mice. *Dev. Dyn.* 239, 3358–3367. doi:10.1002/dvdy.22468
- Chiang, N.-Y., Hsiao, C.-C., Huang, Y.-S., Chen, H.-Y., Hsieh, I.-J., Chang, G.-W., Lin, H.-H., 2011. Disease-associated GPR56 mutations cause bilateral frontoparietal polymicrogyria via multiple mechanisms. *J. Biol. Chem.* 286, 14215–14225. doi:10.1074/jbc.M110.183830
- Chiesa, Della, M., Falco, M., Parolini, S., Bellora, F., Petretto, A., Romeo, E., Balsamo, M., Gambarotti, M., Scordamaglia, F., Tabellini, G., Facchetti, F., Vermi, W., Bottino, C., Moretta, A., Vitale, M., 2010. GPR56 as a novel marker identifying the CD56dull CD16+ NK cell subset both in blood stream and in inflamed peripheral tissues. *Int. Immunol.* 22, 91–100. doi:10.1093/intimm/dxp116
- Crotta, S., Stilla, A., Wack, A., D'Andrea, A., Nuti, S., D'Oro, U., Mosca, M., Filliponi, F., Brunetto, R.M., Bonino, F., Abrignani, S., Valiante, N.M., 2002. Inhibition of natural killer cells through engagement of CD81 by the major hepatitis C virus envelope protein. *J. Exp. Med.* 195, 35–41.
- Crotty, S., Johnston, R.J., Schoenberger, S.P., 2010. Effectors and memories: Bcl-6 and Blimp-1 in T and B lymphocyte differentiation. *Nat. Immunol.* 11, 114–120. doi:10.1038/ni.1837
- Dausy, C., Faure, F., Mayol, K., Viel, S., Gasteiger, G., Charrier, E., Bienvenu, J., Henry, T., Debien, E., Hasan, U.A., Marvel, J., Yoh, K., Takahashi, S., Prinz, I., de Bernard, S., Buffat, L., Walzer, T., 2014. T-bet and Eomes instruct the development of two distinct natural killer cell lineages in the liver and in the bone marrow. *J. Exp. Med.* 211, 563–577. doi:10.1084/jem.20131560
- Doody, G.M., Stephenson, S., McManamy, C., Tooze, R.M., 2007. PRDM1/BLIMP-1 modulates IFN-gamma-dependent control of the MHC class I antigen-processing and peptide-loading pathway. *J. Immunol.* 179, 7614–7623.
- Elsen, G.E., Hodge, R.D., Bedogni, F., Daza, R.A.M., Nelson, B.R., Shiba, N., Reiner, S.L., Hevner, R.F., 2013. The protomap is propagated to cortical plate neurons through an Eomes-dependent intermediate map. *Proc. Natl. Acad. Sci. U.S.A.* 110, 4081–4086. doi:10.1073/pnas.1209076110
- Fauriat, C., Long, E.O., Ljunggren, H.-G., Bryceson, Y.T., 2010. Regulation of human NK-cell cytokine and chemokine production by target cell recognition. *Blood* 115, 2167–2176. doi:10.1182/blood-2009-08-238469
- Fehniger, T.A., Cai, S.F., Cao, X., Bredemeyer, A.J., Presti, R.M., French, A.R., Ley, T.J., 2007. Acquisition of murine NK cell cytotoxicity requires the translation of a pre-existing pool of granzyme B and perforin mRNAs. *Immunity* 26, 798–811. doi:10.1016/j.immuni.2007.04.010
- Fehniger, T.A., Shah, M.H., Turner, M.J., VanDeusen, J.B., Whitman, S.P., Cooper, M.A., Suzuki, K., Wechsler, M., Goodsaid, F., Caligiuri, M.A., 1999. Differential cytokine and chemokine gene expression by human NK cells following activation with IL-18 or IL-15 in combination with IL-12: implications for the innate immune response. *J. Immunol.* 162, 4511–4520.
- Freud, A.G., Caligiuri, M.A., 2006. Human natural killer cell development. *Immunol. Rev.* 214, 56–72. doi:10.1111/j.1600-065X.2006.00451.x
- Giera, S., Deng, Y., Luo, R., Ackerman, S.D., Mogha, A., Monk, K.R., Ying, Y., Jeong, S.-J., Makinodan, M., Bialas, A.R., Chang, B.S., Stevens, B., Corfas, G., Piao, X., 2015. The adhesion G protein-coupled

- receptor GPR56 is a cell-autonomous regulator of oligodendrocyte development. *Nat Commun* 6, 6121. doi:10.1038/ncomms7121
- Hamann, J., Aust, G., Araç, D., Engel, F.B., Formstone, C., Fredriksson, R., Hall, R.A., Harty, B.L., Kirchoff, C., Knapp, B., Krishnan, A., Liebscher, I., Lin, H.-H., Martinelli, D.C., Monk, K.R., Peeters, M.C., Piao, X., Prömel, S., Schöneberg, T., Schwartz, T.W., Singer, K., Stacey, M., Ushkaryov, Y.A., Vallon, M., Wolfrum, U., Wright, M.W., Xu, L., Langenhan, T., Schiöth, H.B., 2015. International Union of Basic and Clinical Pharmacology. XCIV. Adhesion G Protein-Coupled Receptors. *Pharmacol. Rev.* 67, 338–367. doi:10.1124/pr.114.009647
- Iguchi, T., Sakata, K., Yoshizaki, K., Tago, K., Mizuno, N., Itoh, H., 2008. Orphan G protein-coupled receptor GPR56 regulates neural progenitor cell migration via a G alpha 12/13 and Rho pathway. *J. Biol. Chem.* 283, 14469–14478. doi:10.1074/jbc.M708919200
- Jin, Z., Tietjen, I., Bu, L., Liu-Yesucevitz, L., Gaur, S.K., Walsh, C.A., Piao, X., 2007. Disease-associated mutations affect GPR56 protein trafficking and cell surface expression. *Hum. Mol. Genet.* 16, 1972–1985. doi:10.1093/hmg/ddm144
- Karpus, O.N., Veninga, H., Hoek, R.M., Flierman, D., van Buul, J.D., Vandenakker, C.C., vanBavel, E., Medof, M.E., van Lier, R.A.W., Reedquist, K.A., Hamann, J., 2013. Shear stress-dependent downregulation of the adhesion-G protein-coupled receptor CD97 on circulating leukocytes upon contact with its ligand CD55. *J. Immunol.* 190, 3740–3748. doi:10.4049/jimmunol.1202192
- Knox, J.J., Cosma, G.L., Betts, M.R., McLane, L.M., 2014. Characterization of T-bet and eomes in peripheral human immune cells. *Front Immunol* 5, 217. doi:10.3389/fimmu.2014.00217
- Langenhan, T., Aust, G., Hamann, J., 2013. Sticky signaling--adhesion class G protein-coupled receptors take the stage. 6, re3. doi:10.1126/scisignal.2003825
- Lanier, L.L., 2008. Up on the tightrope: natural killer cell activation and inhibition. *Nat. Immunol.* 9, 495–502. doi:10.1038/ni1581
- Lawrence, P.A., Struhl, G., Casal, J., 2008. Planar cell polarity: A bridge too far? *Curr. Biol.* 18, R959–61. doi:10.1016/j.cub.2008.09.002
- Lebbink, R.J., de Ruiter, T., Adelmeyer, J., Brenkman, A.B., van Helvoort, J.M., Koch, M., Farndale, R.W., Lisman, T., Sonnenberg, A., Lenting, P.J., Meyaard, L., 2006. Collagens are functional, high affinity ligands for the inhibitory immune receptor LAIR-1. *J. Exp. Med.* 203, 1419–1425. doi:10.1084/jem.20052554
- Lee, J., Zhang, T., Hwang, I., Kim, A., Nitschke, L., Kim, M., Scott, J.M., Kamimura, Y., Lanier, L.L., Kim, S., 2015. Epigenetic modification and antibody-dependent expansion of memory-like NK cells in human cytomegalovirus-infected individuals. *Immunity* 42, 431–442. doi:10.1016/j.immuni.2015.02.013
- Liebscher, I., Schön, J., Petersen, S.C., Fischer, L., Auerbach, N., Demberg, L.M., Mogha, A., Cöster, M., Simon, K.-U., Rothemund, S., Monk, K.R., Schöneberg, T., 2014. A tethered agonist within the ectodomain activates the adhesion G protein-coupled receptors GPR126 and GPR133. *Cell Rep* 9, 2018–2026. doi:10.1016/j.celrep.2014.11.036
- Lin, H.-H., Chang, G.-W., Davies, J.Q., Stacey, M., Harris, J., Gordon, S., 2004. Autocatalytic cleavage of the EMR2 receptor occurs at a conserved G protein-coupled receptor proteolytic site motif. *J. Biol. Chem.* 279, 31823–31832. doi:10.1074/jbc.M402974200
- Little, K.D., Hemler, M.E., Stipp, C.S., 2004. Dynamic regulation of a GPCR-tetraspanin-G protein complex on intact cells: central role of CD81 in facilitating GPR56-Galpa q/11 association. *Mol. Biol. Cell* 15, 2375–2387. doi:10.1091/mbc.E03-12-0886
- Lopez-Vergès, S., Milush, J.M., Pandey, S., York, V.A., Arakawa-Hoyt, J., Pircher, H., Norris, P.J., Nixon, D.F., Lanier, L.L., 2010. CD57 defines a functionally distinct population of mature NK cells in the human CD56dimCD16+ NK-cell subset. *Blood* 116, 3865–3874. doi:10.1182/blood-2010-04-282301
- Luo, R., Jeong, S.-J., Jin, Z., Strokes, N., Li, S., Piao, X., 2011. G protein-coupled receptor 56 and collagen III, a receptor-ligand pair, regulates cortical development and lamination. *Proc. Natl. Acad. Sci. U.S.A.* 108, 12925–12930. doi:10.1073/pnas.1104821108
- Marcolino, I., Przybylski, G.K., Koschella, M., Schmidt, C.A., Voehringer, D., Schlesier, M., Pircher, H., 2004. Frequent expression of the natural killer cell receptor KLRG1 in human cord blood T cells: correlation with replicative history. *Eur. J. Immunol.* 34, 2672–2680. doi:10.1002/eji.200425282
- Monk, K.R., Hamann, J., Langenhan, T., Nijmeijer, S., Schöneberg, T., Liebscher, I., 2015. Adhesion G Protein-Coupled Receptors: From In Vitro Pharmacology to In Vivo Mechanisms. *Mol. Pharmacol.* 88, 617–623. doi:10.1124/mol.115.098749
- Nagler, A., Lanier, L.L., Cwirla, S., Phillips, J.H., 1989. Comparative studies of human FcRIII-positive and negative natural killer cells. *J. Immunol.* 143, 3183–3191.
- Paavola, K.J., Hall, R.A., 2012. Adhesion G protein-coupled receptors: signaling, pharmacology, and mechanisms of activation. *Mol. Pharmacol.* 82, 777–783. doi:10.1124/mol.112.080309
- Paavola, K.J., Sidik, H., Zuchero, J.B., Eckart, M., Talbot, W.S., 2014. Type IV collagen is an activating

- ligand for the adhesion G protein-coupled receptor GPR126. *J Biol Chem* 286, 28914–28921. doi:10.1074/jbc.M111.247973
- Paavola, K.J., Stephenson, J.R., Ritter, S.L., Alter, S.P., Hall, R.A., 2011. The N terminus of the adhesion G protein-coupled receptor GPR56 controls receptor signaling activity. *J Biol Chem* 286, 28914–28921. doi:10.1074/jbc.M111.247973
- Pegram, H.J., Andrews, D.M., Smyth, M.J., Darcy, P.K., Kershaw, M.H., 2011. Activating and inhibitory receptors of natural killer cells. *Immunol Cell Biol* 89, 216–224. doi:10.1038/icb.2010.78
- Peng, Y.-M., van de Garde, M.D.B., Cheng, K.-F., Baars, P.A., Remmerswaal, E.B.M., van Lier, R.A.W., Mackay, C.R., Lin, H.-H., Hamann, J., 2011. Specific expression of GPR56 by human cytotoxic lymphocytes. *J Leukoc Biol* 90, 735–740. doi:10.1189/jlb.0211092
- Piao, X., Chang, B.S., Bodell, A., Woods, K., Benzeev, B., Topçu, M., Guerrini, R., Goldberg-Stern, H., Sztrihai, L., Dobyns, W.B., Barkovich, A.J., Walsh, C.A., 2005. Genotype-phenotype analysis of human frontoparietal polymicrogyria syndromes. *Ann Neurol* 58, 680–687. doi:10.1002/ana.20616
- Piao, X., Hill, R.S., Bodell, A., Chang, B.S., Basel-Vanagaite, L., Straussberg, R., Dobyns, W.B., Qasrawi, B., Winter, R.M., Innes, A.M., Voit, T., Ross, M.E., Michaud, J.L., Descarie, J.-C., Barkovich, A.J., Walsh, C.A., 2004. G protein-coupled receptor-dependent development of human frontal cortex. *Science* 303, 2033–2036. doi:10.1126/science.1092780
- Pierce, K.L., Premont, R.T., Lefkowitz, R.J., 2002. Seven-transmembrane receptors. *Nat Rev Mol Cell Biol* 3, 639–650. doi:10.1038/nrm908
- Romee, R., Foley, B., Lenvik, T., Wang, Y., Zhang, B., Ankarlo, D., Luo, X., Cooley, S., Verneris, M., Walcheck, B., Miller, J., 2013. NK cell CD16 surface expression and function is regulated by a disintegrin and metalloprotease-17 (ADAM17). *Blood* 121, 3599–3608. doi:10.1182/blood-2012-04-425397
- Saito, Y., Kaneda, K., Suekane, A., Ichihara, E., Nakahata, S., Yamakawa, N., Nagai, K., Mizuno, N., Kogawa, K., Miura, I., Itoh, H., Morishita, K., 2013. Maintenance of the hematopoietic stem cell pool in bone marrow niches by EVI1-regulated GPR56. *Leukemia* 27, 1637–1649. doi:10.1038/leu.2013.75
- Schlums, H., Cichocki, F., Tesi, B., Theorell, J., Beziat, V., Holmes, T.D., Han, H., Chiang, S.C.C., Foley, B., Mattsson, K., Larsson, S., Schaffer, M., Malmberg, K.-J., Ljunggren, H.-G., Miller, J.S., Bryceson, Y.T., 2015. Cytomegalovirus infection drives adaptive epigenetic diversification of NK cells with altered signaling and effector function. *Immunity* 42, 443–456. doi:10.1016/j.immuni.2015.02.008
- Schrage, R., Schmitz, A.-L., Gaffal, E., Annala, S., Kehraus, S., Wenzel, D., Bülesbach, K.M., Bald, T., Inoue, A., Shinjo, Y., Galandrin, S., Shridhar, N., Hesse, M., Grundmann, M., Merten, N., Charpentier, T.H., Martz, M., Butcher, A.J., Slodczyk, T., Armando, S., Effern, M., Namkung, Y., Jenkins, L., Horn, V., Stöbel, A., Dargatz, H., Tietze, D., Imhof, D., Galés, C., Drewke, C., Müller, C.E., Hölzel, M., Milligan, G., Tobin, A.B., Gomez, J., Dohlman, H.G., Sondek, J., Harden, T.K., Bouvier, M., Laporte, S.A., Aoki, J., Fleischmann, B.K., Mohr, K., König, G.M., Tüting, T., Kostenis, E., 2015. The experimental power of FR900359 to study Gq-regulated biological processes. *Nat Commun* 6, 10156. doi:10.1038/ncomms10156
- Solaimani Kartalaei, P., Yamada-Inagawa, T., Vink, C.S., de Pater, E., van der Linden, R., Marks-Bluth, J., van der Sloot, A., van den Hout, M., Yokomizo, T., van Schaick-Solernó, M.L., Delwel, R., Pimanda, J.E., van IJcken, W.F.J., Dzierzak, E., 2015. Whole-transcriptome analysis of endothelial to hematopoietic stem cell transition reveals a requirement for Gpr56 in HSC generation. *J Exp Med* 212, 93–106. doi:10.1084/jem.20140767
- Stephenson, J.R., Paavola, K.J., Schaefer, S.A., Kaur, B., Van Meir, E.G., Hall, R.A., 2013. Brain-specific angiogenesis inhibitor-1 signaling, regulation, and enrichment in the postsynaptic density. *J Biol Chem* 288, 22248–22256. doi:10.1074/jbc.M113.489757
- Tseng, C.-T.K., Klimpel, G.R., 2002. Binding of the hepatitis C virus envelope protein E2 to CD81 inhibits natural killer cell functions. *J Exp Med* 195, 43–49.
- van Gisbergen, K.P.J.M., Kragten, N.A.M., Hertoghs, K.M.L., Wensveen, F.M., Jonjic, S., Hamann, J., Nolte, M.A., van Lier, R.A.W., 2012. Mouse Hobit is a homolog of the transcriptional repressor Blimp-1 that regulates NKT cell effector differentiation. *Nat Immunol* 13, 864–871. doi:10.1038/ni.2393
- Vieira Braga, F.A., Hertoghs, K.M.L., Kragten, N.A.M., Doody, G.M., Barnes, N.A., Remmerswaal, E.B.M., Hsiao, C.-C., Moerland, P.D., Wouters, D., Derks, I.A.M., van Stijn, A., Demkes, M., Hamann, J., Eldering, E., Nolte, M.A., Tooze, R.M., Berge, Ten, I.J.M., van Gisbergen, K.P.J.M., van Lier, R.A.W., 2015. Blimp-1 homolog Hobit identifies effector-type lymphocytes in humans. *Eur J Immunol* doi:10.1002/eji.201545650
- Vivier, E., Tomasello, E., Baratin, M., Walzer, T., Ugolini, S., 2008. Functions of natural killer cells. *Nat Immunol* 9, 503–510. doi:10.1038/ni1582
- Voehringer, D., Koschella, M., Pircher, H., 2002. Lack of proliferative capacity of human effector and memory T cells expressing killer cell lectinlike receptor G1 (KLRG1). *Blood* 100, 3698–3702. doi:10.1182/blood-2002-02-0657
- Walzer, T., Vivier, E., 2011. G-protein-coupled receptors in control of natural killer cell migration. *Trends Immunol* 32, 486–492. doi:10.1016/j.it.2011.05.002

- White, J.P., Wrann, C.D., Rao, R.R., Nair, S.K., Jedrychowski, M.P., You, J.-S., Martínez-Redondo, V., Gygi, S.P., Ruas, J.L., Hornberger, T.A., Wu, Z., Glass, D.J., Piao, X., Spiegelman, B.M., 2014. G protein-coupled receptor 56 regulates mechanical overload-induced muscle hypertrophy. *Proc. Natl. Acad. Sci. U.S.A.* 111, 15756–15761. doi:10.1073/pnas.1417898111
- Worzfeld, T., Wettschureck, N., Offermanns, S., 2008. G(12)/G(13)-mediated signalling in mammalian physiology and disease. *Trends Pharmacol. Sci.* 29, 582–589. doi:10.1016/j.tips.2008.08.002
- Xu, L., Begum, S., Hearn, J.D., Hynes, R.O., 2006. GPR56, an atypical G protein-coupled receptor, binds tissue transglutaminase, TG2, and inhibits melanoma tumor growth and metastasis. *Proc. Natl. Acad. Sci. U.S.A.* 103, 9023–9028. doi:10.1073/pnas.0602681103
- Yang, L., Chen, G., Mohanty, S., Scott, G., Fazal, F., Rahman, A., Begum, S., Hynes, R.O., Xu, L., 2011. GPR56 Regulates VEGF production and angiogenesis during melanoma progression. *Cancer Res.* 71, 5558–5568. doi:10.1158/0008-5472.CAN-10-4543
- Yang, T.-Y., Chiang, N.-Y., Tseng, W.-Y., Pan, H.-L., Peng, Y.-M., Shen, J.-J., Wu, K.-A., Kuo, M.-L., Chang, G.-W., Lin, H.-H., 2015. Expression and immunoaffinity purification of recombinant soluble human GPR56 protein for the analysis of GPR56 receptor shedding by ELISA. *Protein Expr. Purif.* 109, 85–92. doi:10.1016/j.pep.2014.11.013
- Zhang, T., Scott, J.M., Hwang, I., Kim, S., 2013. Cutting edge: antibody-dependent memory-like NK cells distinguished by FcR γ deficiency. *J. Immunol.* 190, 1402–1406. doi:10.4049/jimmunol.1203034

CHAPTER 8

General Discussion

Discussion

Human CMV infection generate a lifelong specific T cell response with strong cytotoxic potential [1]. However, not much is known on how these cells are maintained in a quiescent and nonproliferative state, whilst maintaining a large reserve of cytotoxic granules that enable immediate effector function. Transcriptome analysis of CMV [2] specific CD8 T cells has identified Hobit as one of the most differentially expressed genes in these effector cells compared to naive and other non-cytolytic immune populations. Indeed, we have demonstrated that Hobit is a transcription factor, of which expression in the human immune system is restricted to long lived effector CD8 T cells, cytotoxic CD4 T cells and NK cells. Hobit regulates effector functions such as IFN- γ and granzyme B production. Hobit mediates maintenance of effector lymphocytes as a metabolic suppressor and regulator of survival under cellular stress. In addition, Hobit plays a role in NK cell development and controls the expression of the surface receptor GPR56, which suppresses NK cell effector functions. Here, I would like to discuss the impact of these findings on the effector functions and maintenance of Hobit+ CD4 T cells, CD8 T cells and NK cells.

Hobit suppresses glycolysis and induces effector functions

Hobit induces the production of effector molecules such as IFN- γ (**Chapter 2**) and granzyme B (Chapter 5). IFN- γ exerts both antiviral and immunostimulatory effects [3]–[5], while granzymes can directly destroy infected cells [6]–[8] or virus related proteins [9]. It is interesting that both IFN- γ and granzyme B are induced by Hobit, as the regulatory mechanisms of these molecules vary largely. IFN- γ mRNA but not protein can be detected in resting cells [10], while granzyme B is expressed in large amounts at both the mRNA and protein level in resting effector lymphocytes (**Chapter 5**) [1],[2],[11]. We have shown that Hobit regulates IFN- γ expression at both the mRNA level and the protein level (**Chapter 2**) in line with a role of Hobit as a transcriptional regulator of IFN- γ expression. The regulation of IFN- γ expression is a multistep process that involves both transcriptional [12] and post-transcriptional [13],[14] regulatory mechanisms. Glycolysis contributes to the regulation of IFN- γ production by inducing IFN- γ protein production from pre-formed mRNA molecules [15],[16],[15],[16]. We have shown that Hobit has the potential to suppress glycolysis (**Chapter 4**)[15],[16]. We hypothesize that the interaction between Hobit, glycolysis and IFN- γ is a complex process that effectively maintains these highly effective killer cells in check in the absence of an inflammatory milieu. The low glycolytic status of resting CD45RA+ effector (EMRA) cells (**Chapter 4**) might operate as a safety mechanism, guaranteeing that IFN- γ is not produced until these cells encounter antigen; despite the high levels of Hobit that upregulate IFN- γ expression. The mechanism of interaction between metabolic pathways and the regulation of cytotoxicity in EMRA cells is unknown. EMRA cells store pre-formed granzyme B protein inside cytolytic granules [17]–[19]. Murine memory cells that express high granzyme B mRNA transcripts but no granzyme B protein [20],[21]. However, EMRA cells lack spare respiratory capacity (SRC), while murine memory cells have SRC (Chapter 4), suggesting that EMRA cells are less capable of providing energy for protein synthesis [22]. As proteomic analysis of activated cytotoxic lymphocytes revealed

that the majority of proteins in these cells are granzymes, and protein synthesis is a high energy demanding process [23]–[25] (**Chapter 4**), an important question is how EMRA cells maintain high levels of pre-formed granzyme B protein. It is unlikely that EMRA cells can maintain continuous granzyme B production. An alternative for maintaining high levels of protein stocks without high energy expenditure is through the development of efficient storage mechanisms. Similar to pickles, granzyme molecules are stored in an acidic environment [26], suggesting that these granules have been developed to provide stable and energy-efficient long term protein storage. Thus, we hypothesize that EMRA cells have evolved mechanisms to maintain a high cytotoxic potential at minimal metabolic cost.

Hobit and the extended lifespan of EMRA cells

A hallmark of HCMV infection is memory inflation [27]–[29]. The impact of HCMV infection and memory inflation to the immune system is not entirely understood [30]–[38]. One of the main unanswered questions in the field relates to the molecular mechanisms behind memory inflation. EMRA CD8 T cells have a suppressed metabolic state with low glycolysis and low oxygen consumption (**Chapter 4**). It is interesting to note that dietary restriction which reduces metabolism extends the lifespan of organisms [39]–[42]. Metabolic suppression resulting in long-term survival might be the key to population expansion, despite the low basal replication rate of these cells [27]–[29],[43]. Considering that Hobit is expressed in EMRA cells during the expansion and maintenance phase (**Chapters 2, 5 and 6**), an important question is whether Hobit plays a role in memory inflation. During persistent infection with HCMV, Hobit may be involved in maintaining cytotoxic EMRA cells at a low metabolic state, thereby extending their lifespan and reducing the high energetic demand of constant proliferation. Alternatively, Hobit may be primarily expressed to induce a cytotoxic phenotype and metabolic suppression leading to life extension might arise as a byproduct. This is a difficult question to address in the human immune system, but murine Hobit might give us insight into how Hobit regulates the long term maintenance of CD8 T cells.

Hobit: A tale of mice and men

Murine and human Hobit may regulate similar molecules, but the expression pattern of Hobit in both species is quite dissimilar, as circulating murine, in contrast to human CD8 T cells and NK cells, do not express Hobit [44],[45]. Murine Hobit expression is restricted to NKT cells [45], Tissue Resident Memory (TRM) T cells and Tissue Resident NK cells [46]. In these lymphocyte populations, murine Hobit regulates effector functions such as granzyme B production (**Chapter 5**) [45],[46] as well as development and/or maintenance in non lymphoid tissues [45],[46]. TRM cells have high effector potential [47] and are known to reside within non lymphoid tissues for extended periods of time in a quiescent state [48]–[50]. These characteristics are remarkably similar to human EMRA cells. Hobit expression is essential for the formation of TRM populations in mice [46], suggesting that murine and human Hobit both regulate lymphocyte maintenance and effector function in a similar fashion (**Chapters 2 and 5**) [44],[46].

Compared to Blimp-1 [51], the gene sequences of Hobit orthologues are not well conserved among vertebrates [52]. Despite the low overall homology, murine and human Hobit have a high degree of similarity within their zinc finger region [53], which encodes its transcriptional activity (**Chapter 2**) [44]. The shared transcriptional activity of murine and human Hobit [44]–[46] suggests that evolutionary pressures selectively retain the Zinc Finger region. In contrast, environmental forces between mice and humans may have driven genetic differences underlying the distinct expression pattern of murine and human Hobit. The most simple explanation for the divergence in Hobit cell type expression between mice and men is co-evolution between host and virus [54]. Murine CMV and human CMV might have shaped the immune system of their hosts in different ways, inducing differences including the expression pattern of Hobit. Another possibility relates directly to different experimental conditions. The laboratory environment in which mice are maintained does not recapitulate the diversity of microorganisms and pathogenic challenges that humans face on a day to day basis. A recent paper has shown that changes in the environment, in which mice are maintained can lead to a closer recapitulation of the human T cell compartment [55]. Feral mice and conventional lab mice co-housed with feral mice contain a Klrp1+GranzymeB+CD27- CD8 T cell population that resembles the phenotype of human EMRA cells. It would be interesting to check whether the murine “EMRA” population expresses Hobit. Thus, despite the differential pattern of Hobit expression between mice and humans, Hobit regulates similar pathways in both species, suggesting experiments in both systems are complementary and can provide better understanding on the functions and mechanisms of Hobit-driven transcriptional regulation.

On the maintenance of natural killer cells.

The transcriptional machinery behind human NK cell development is not entirely understood. The high expression of Hobit within the NK cell lineage suggests that Hobit might also play a role in NK cell development and/or maintenance. Our preliminary results suggests that Hobit is involved in the final stages of NK cell development from CD34+ progenitor cells (Chapter 6). In order to understand this data, analogies with its paralogue Blimp-1 (PRDM1) are informative. In human NK cells, Blimp-1 acts as tumor suppressor that inhibits proliferation [56]–[58]. Dysregulation of Blimp-1 expression can lead to very aggressive NK cell lymphomas. Considering the extent of shared functions and transcriptional targets between Hobit and Blimp-1 (Chapter 2 and 5) [46], it is reasonable to assume that Hobit is also capable of suppressing proliferation in NK cells. Thus, our data indicate that Hobit regulates terminal NK cell differentiation that may include instruction of a cytotoxic program (**Chapters 2,4, 6 and 7**).

IL-15 can induce Hobit mRNA expression in activated murine CD8 T cells, in a T-bet dependent manner [46]. Interestingly, we have shown that IL-15 in the presence of IL-7 and Flt-3 also induces Hobit expression during human NK cell development from CD34+ progenitor cells (Chapter 6). IL-15 is absolutely essential for NK cell development [59],[60] and this might be one of the mechanisms underlying high Hobit expression in the human NK cell lineage. Circulating murine NK cells differ largely from CD56dim human NK cells. Despite the absolute necessity of IL-15 to their de-

velopment [59], murine NK cells do not express Hobit and do not express pre formed granzyme B cytotoxic granules [61]. Thus, it appears that the expression regulation of Hobit is a complex process yet to be fully elucidated, as IL-15 is necessary, but not sufficient to induce Hobit expression.

One ring to rule them all: Concluding remarks

In 2013 cancer immunotherapy was selected by the magazine Science as the breakthrough of the year [62] and the therapeutic use of T cells [63]–[67] and NK cells [68]–[70] experience continuous and steady growth. Achievement of the ultimate balance between effector function and expansion potential is essential for successful cell therapy [71]. Our current understanding of Hobit suggests that it acts as a master regulator of terminally differentiated lymphocytes across multiple lineages. These findings suggest that a better understanding of the mechanisms and roles of Hobit in the immune system might offer opportunities to improve current strategies of cell therapy.

References

1. Vieira Braga FA, Hertoghs KML, van Lier RAW, van Gisbergen KPJM. Molecular characterization of HC-MV-specific immune responses: Parallels between CD8(+) T cells, CD4(+) T cells, and NK cells. *Eur. J. Immunol.* 2015; 45:2433–2445.
2. Hertoghs KML, Moerland PD, van Stijn A, Remmerswaal EBM, Yong SL, van de Berg PJEJ, van Ham SM, et al. Molecular profiling of cytomegalovirus-induced human CD8+ T cell differentiation. *J. Clin. Invest.* 2010; 120:4077–4090.
3. Dalton D. IFN- γ and IFN- γ Receptor Knockout Mice. In: Fantuzzi G, ed. *Cytokine Knockouts*. Contemporary Immunology. Humana Press; 2003:347–359.
4. Paul WE. Pleiotropy and redundancy: T cell-derived lymphokines in the immune response. *Cell.* 1989; 57:521–524.
5. McNab F, Mayer-Barber K, Sher A, Wack A, O'Garra A. Type I interferons in infectious disease. *Nat. Rev. Immunol.* 2015; 15:87–103.
6. Anthony DA, Andrews DM, Watt SV, Trapani JA, Smyth MJ. Functional dissection of the granzyme family: cell death and inflammation. *Immunol. Rev.* 2010; 235:73–92.
7. Chowdhury D, Lieberman J. Death by a thousand cuts: granzyme pathways of programmed cell death. *Annu. Rev. Immunol.* 2008; 26:389–420.
8. Peters PJ, Borst J, Oorschot V, Fukuda M, Krähenbühl O, Tschopp J, Slot JW, et al. Cytotoxic T lymphocyte granules are secretory lysosomes, containing both perforin and granzymes. *J. Exp. Med.* 1991; 173:1099–1109.
9. Domselaar R, Bovenschen N. Cell death-independent functions of granzymes: hit viruses where it hurts. *Rev. Med. Virol.* 2011; 21:301–314.
10. Young HA, Hodge D. Posttranscriptional Regulation of IFN-gamma gene Expression. *The FASEB Journal.* 2007; 21:A281–A281.
11. Takata H, Naruto T, Takiguchi M. Functional heterogeneity of human effector CD8+ T cells. *Blood.* 2012; 119:1390–1398.
12. Glimcher LH, Townsend MJ, Sullivan BM, Lord GM. Recent developments in the transcriptional regulation of cytolytic effector cells. *Nat. Rev. Immunol.* 2004; 4:900–911.
13. Savan R. Post-transcriptional regulation of interferons and their signaling pathways. *J. Interferon Cytokine Res.* 2014; 34:318–329.
14. Salerno F, Wolkers MC. T-cells require post-transcriptional regulation for accurate immune responses. *Biochem. Soc. Trans.* 2015; 43:1201–1207.
15. Chang C-H, Curtis JD, Maggi LB Jr, Faubert B, Villarino AV, O'Sullivan D, Huang SC-C, et al. Posttranscriptional control of T cell effector function by aerobic glycolysis. *Cell.* 2013; 153:1239–1251.
16. Gubser PM, Bantug GR, Razik L, Fischer M, Dimeloe S, Hoenger G, Durovic B, et al. Rapid effector function of memory CD8+ T cells requires an immediate-early glycolytic switch. *Nat. Immunol.* 2013; 14:1064–1072.
17. Hamann D, Baars PA, Rep MH, Hooibrink B, Kerkhof-Garde SR, Klein MR, van Lier RA. Phenotypic and functional separation of memory and effector human CD8+ T cells. *J. Exp. Med.* 1997; 186:1407–1418.
18. Hamann D, Baars PA, Rep MHG, Hooibrink B, van Lier RAW. Phenotypic and functional separation of memory and effector human CD8pos T cells. *Immunol. Lett.* 1997; 56:198.
19. van Aalderen MC, Remmerswaal EBM, Verstegen NJM, Hombrink P, ten Brinke A, Pircher H, Kootstra NA, et al. Infection history determines the differentiation state of human CD8+ T cells. *J. Virol.* 2015; 89:5110–5123.
20. Baars PA, Sierro S, Arens R, Tesselaar K, Hooibrink B, Klenerman P, van Lier RAW. Properties of murine CD8+ CD27-T cells. *Eur. J. Immunol.* 2005; 35:3131–3141.
21. Mouchacca P, Chasson L, Frick M, Foray C, Schmitt-Verhulst A-M, Boyer C. Visualization of granzyme B-expressing CD8 T cells during primary and secondary immune responses to *Listeria monocytogenes*. *Immunology.* 2015; 145:24–33.
22. Henson SM, Lanna A, Riddell NE, Franzese O, Macaulay R, Griffiths SJ, Puleston DJ, et al. p38 signaling inhibits mTORC1-independent autophagy in senescent human CD8+ T cells. 2014. Available at: <http://www.jci.org/articles/view/75051>. DOI: 10.1172/JCI75051.
23. Pannevis MC, Houlihan DF. The energetic cost of protein synthesis in isolated hepatocytes of rainbow trout (*Oncorhynchus mykiss*). *J. Comp. Physiol. B.* 1992; 162:393–400.
24. Li G-W, Burkhardt D, Gross C, Weissman JS. Quantifying absolute protein synthesis rates reveals principles underlying allocation of cellular resources. *Cell.* 2014; 157:624–635.
25. Hukelmann JL, Anderson KE, Sinclair LV, Grzes KM, Murillo AB, Hawkins PT, Stephens LR, et al. The cytotoxic T cell proteome and its shaping by the kinase mTOR. *Nat. Immunol.* 2016; 17:104–112.

26. Kataoka T, Takaku K, Magae J, Shinohara N, Takayama H, Kondo S, Nagai K. Acidification is essential for maintaining the structure and function of lytic granules of CTL. Effect of concanamycin A, an inhibitor of vacuolar type H(+)-ATPase, on CTL-mediated cytotoxicity. *J. Immunol.* 1994; 153:3938–3947.
27. Wallace DL, Masters JE, de Lara CM, Henson SM, Worth A, Zhang Y, Kumar SR, et al. Human cytomegalovirus-specific CD8+ T-cell expansions contain long-lived cells that retain functional capacity in both young and elderly subjects. *Immunology.* 2011; 132:27–38.
28. Weekes MP, Carmichael AJ, Wills MR, Mynard K, Sissons JG. Human CD28-CD8+ T cells contain greatly expanded functional virus-specific memory CTL clones. *J. Immunol.* 1999; 162:7569–7577.
29. van de Berg PJEJ, van Stijn A, Ten Berge IJM, van Lier RAW. A fingerprint left by cytomegalovirus infection in the human T cell compartment. *J. Clin. Virol.* 2008; 41:213–217.
30. Kim J, Kim A-R, Shin E-C. Cytomegalovirus Infection and Memory T Cell Inflation. *Immune Netw.* 2015; 15:186–190.
31. O'Hara GA, Welten SPM, Klenerman P, Arens R. Memory T cell inflation: understanding cause and effect. *Trends Immunol.* 2012; 33:84–90.
32. Mekker A, Tchang VS, Haerberli L, Oxenius A, Trkola A, Karrer U. Immune senescence: relative contributions of age and cytomegalovirus infection. *PLoS Pathog.* 2012; 8:e1002850.
33. Klenerman P, Oxenius A. T cell responses to cytomegalovirus. *Nat. Rev. Immunol.* 2016; 16:367–377.
34. Sauce D, Larsen M, Fastenackels S, Duperrier A, Keller M, Grubeck-Loebenstien B, Ferrand C, et al. Evidence of premature immune aging in patients thymectomized during early childhood. *J. Clin. Invest.* 2009; 119:3070–3078.
35. Hadrup SR, Strindhall J, Kølgaard T, Seremet T, Johansson B, Pawelec G, thor Straten P, et al. Longitudinal studies of clonally expanded CD8 T cells reveal a repertoire shrinkage predicting mortality and an increased number of dysfunctional cytomegalovirus-specific T cells in the very elderly. *J. Immunol.* 2006; 176:2645–2653.
36. Strandberg TE, Pitkala KH, Tilvis RS. Cytomegalovirus antibody level and mortality among community-dwelling older adults with stable cardiovascular disease. *JAMA.* 2009; 301:380–382.
37. Roberts ET, Haan MN, Dowd JB, Aiello AE. Cytomegalovirus antibody levels, inflammation, and mortality among elderly Latinos over 9 years of follow-up. *Am. J. Epidemiol.* 2010; 172:363–371.
38. Furman D, Jojic V, Sharma S, Shen-Orr SS, Angel CJL, Onengut-Gumuscu S, Kidd BA, et al. Cytomegalovirus infection enhances the immune response to influenza. *Sci. Transl. Med.* 2015; 7:281ra43.
39. Chiba T, Tamashiro Y, Park D, Kusudo T, Fujie R, Komatsu T, Kim SE, et al. A key role for neuropeptide Y in lifespan extension and cancer suppression via dietary restriction. *Sci. Rep.* 2014; 4:4517.
40. Lamming DW. Diminished mTOR signaling: a common mode of action for endocrine longevity factors. *Springerplus.* 2014; 3:735.
41. Zhao G, Guo S, Somel M, Khaitovich P. Evolution of human longevity uncoupled from caloric restriction mechanisms. *PLoS One.* 2014; 9:e84117.
42. Taormina G, Mirisola MG. Calorie restriction in mammals and simple model organisms. *Biomed Res. Int.* 2014; 2014:308690.
43. Faint JM, Annels NE, Curnow SJ, Shields P, Pilling D, Hislop AD, Wu L, et al. Memory T cells constitute a subset of the human CD8+CD45RA+ pool with distinct phenotypic and migratory characteristics. *J. Immunol.* 2001; 167:212–220.
44. Vieira Braga FA, Hertoghs KML, Kragten NAM, Doody GM, Barnes NA, Remmerswaal EBM, Hsiao C-C, et al. Blimp-1 homolog Hobit identifies effector-type lymphocytes in humans. *Eur. J. Immunol.* 2015; 45:2945–2958.
45. van Gisbergen KPJM, Kragten NAM, Hertoghs KML, Wensveen FM, Jonjic S, Hamann J, Nolte MA, et al. Mouse Hobit is a homolog of the transcriptional repressor Blimp-1 that regulates NKT cell effector differentiation. *Nat. Immunol.* 2012; 13:864–871.
46. Mackay LK, Minnich M, Kragten NAM, Liao Y, Nota B, Seillet C, Zaid A, et al. Hobit and Blimp1 instruct a universal transcriptional program of tissue residency in lymphocytes. *Science.* 2016; 352:459–463.
47. Hombrink P, Helbig C, Backer RA, Piet B, Oja AE, Stark R, Brassler G, et al. Programs for the persistence, vigilance and control of human CD8(+) lung-resident memory T cells. *Nat. Immunol.* 2016; 17:1467–1478.
48. Zaid A, Mackay LK, Rahimpour A, Braun A, Veldhoen M, Carbone FR, Manton JH, et al. Persistence of skin-resident memory T cells within an epidermal niche. *Proc. Natl. Acad. Sci. U. S. A.* 2014; 111:5307–5312.
49. Wakim LM, Woodward-Davis A, Bevan MJ. Memory T cells persisting within the brain after local infection show functional adaptations to their tissue of residence. *Proc. Natl. Acad. Sci. U. S. A.* 2010; 107:17872–17879.
50. Shane HL, Klonowski KD. Every breath you take: the impact of environment on resident memory CD8T

- cells in the lung. *Diverse functions of mucosal resident memory T cells*. 2015;7.
51. Anon. Gene: PRDM1 (ENSG0000057657) - Orthologues - Homo sapiens - Ensembl genome browser 86. Available at: http://www.ensembl.org/Homo_sapiens/Gene/Compar Ortholog?db=core;g=ENSG0000057657;r=6:106086320-106109939 [Accessed October 12, 2016].
52. Anon. Gene: ZNF683 (ENSG00000176083) - Orthologues - Homo sapiens - Ensembl genome browser 86. Available at: http://www.ensembl.org/Homo_sapiens/Gene/Compar Ortholog?collapse=31481371%2C31481319%2C31481476%2C31481465;db=core;g=ENSG00000176083;gtr=species;r=1:26361634-26374522 [Accessed October 12, 2016].
53. EMBL-EBI. EMBOSS Needle - Alignment. Available at: http://www.ebi.ac.uk/Tools/services/web/tool-result.ebi?jobId=emboss_needle-I20161117-233743-0849-19469479-pg [Accessed November 17, 2016].
54. Sharp PM, Simmonds P. Evaluating the evidence for virus/host co-evolution. *Curr. Opin. Virol.* 2011; 1:436–441.
55. Beura LK, Hamilton SE, Bi K, Schenkel JM, Odumade OA, Casey KA, Thompson EA, et al. Normalizing the environment recapitulates adult human immune traits in laboratory mice. *Nature*. 2016; 532:512–516.
56. Küçük C, Iqbal J, Hu X, Gaulard P, De Leval L, Srivastava G, Au WY, et al. PRDM1 is a tumor suppressor gene in natural killer cell malignancies. *Proc. Natl. Acad. Sci. U. S. A.* 2011; 108:20119–20124.
57. Zhang T, Ma J, Nie K, Yan J, Liu Y, Bacchi CE, Queiroga EM, et al. Hypermethylation of the tumor suppressor gene PRDM1/Blimp-1 supports a pathogenetic role in EBV-positive Burkitt lymphoma. *Blood Cancer J.* 2014; 4:e261.
58. Zhang Z, Liang L, Li D, Nong L, Liu J, Qu L, Zheng Y, et al. Hypermethylation of PRDM1/Blimp-1 promoter in extranodal NK/T-cell lymphoma, nasal type: an evidence of predominant role in its downregulation. *Hematol. Oncol.* 2016. Available at: <http://dx.doi.org/10.1002/hon.2362>. DOI: 10.1002/hon.2362.
59. Lodolce JP, Boone DL, Chai S, Swain RE, Dassopoulos T, Trettin S, Ma A. IL-15 receptor maintains lymphoid homeostasis by supporting lymphocyte homing and proliferation. *Immunity*. 1998; 9:669–676.
60. Liu CC, Perussia B, Young JD. The emerging role of IL-15 in NK-cell development. *Immunol. Today*. 2000; 21:113–116.
61. Fehniger TA, Cai SF, Cao X, Bredemeyer AJ, Presti RM, French AR, Ley TJ. Acquisition of murine NK cell cytotoxicity requires the translation of a pre-existing pool of granzyme B and perforin mRNAs. *Immunity*. 2007; 26:798–811.
62. Couzin-Frankel J. *Cancer Immunotherapy*. *Science*. 2013; 342:1432–1433.
63. Holzinger A, Barden M, Abken H. The growing world of CAR T cell trials: a systematic review. *Cancer Immunol. Immunother.* 2016; 65:1433–1450.
64. June CH, Riddell SR, Schumacher TN. Adoptive cellular therapy: a race to the finish line. *Sci. Transl. Med.* 2015; 7:280ps7.
65. Linnemann C, Schumacher TNM, Bendle GM. T-cell receptor gene therapy: critical parameters for clinical success. *J. Invest. Dermatol.* 2011; 131:1806–1816.
66. Yang F, Jin H, Wang J, Sun Q, Yan C, Wei F, Ren X. Adoptive Cellular Therapy (ACT) for Cancer Treatment. *Adv. Exp. Med. Biol.* 2016; 909:169–239.
67. Maus MV, Levine BL. Chimeric Antigen Receptor T-Cell Therapy for the Community Oncologist. *Oncologist*. 2016; 21:608–617.
68. Li Y, Yin J, Li T, Huang S, Yan H, Leavenworth J, Wang X. NK cell-based cancer immunotherapy: from basic biology to clinical application. *Sci. China Life Sci.* 2015; 58:1233–1245.
69. Schmeel FC, Schmeel LC, Gast S-M, Schmidt-Wolf IGH. Adoptive immunotherapy strategies with cytokine-induced killer (CIK) cells in the treatment of hematological malignancies. *Int. J. Mol. Sci.* 2014; 15:14632–14648.
70. Giraud L, Gammaitoni L, Cangemi M, Rotolo R, Aglietta M, Sangiolo D. Cytokine-induced killer cells as immunotherapy for solid tumors: current evidence and perspectives. *Immunotherapy*. 2015; 7:999–1010.
71. Crompton JG, Sukumar M, Restifo NP. Uncoupling T-cell expansion from effector differentiation in cell-based immunotherapy. *Immunol. Rev.* 2014; 257:264–276.

APPENDICES

English Summary
Nederlandse Samenvatting
List of Co-authors
PhD Portfolio
Curriculum Vitae
Acknowledgement

English summary

CD8 T cells and Natural Killer (NK) cells are capable of destroying cells that have been infected by viruses. Destruction of virally infected cells is an essential point to eradicate and/or limit viral infections. CD8 T cell immune responses to viral infections come in different flavours. Influenza virus responses are dominated by central memory (CM) CD8 T cells. Epstein bar virus predominantly generates an effector memory (EM) response, while human cytomegalovirus (HCMV) mainly induces long term memory cells with an effector phenotype (EMRA cells). Previous transcriptome analysis of virus-specific CD8 T cells during primary HCMV infection identified ZNF683 (Hobit) as one of the most differentially expressed genes in these cells. Hobit is a Zinc finger factor containing protein that is homologous to Blimp-1, an important transcriptional regulator of terminal B and T cell differentiation. In vivo studies in mice showed that Hobit regulated the development and/or maintenance of tissue resident memory CD8 T cells (TRM) and NKT cells. However, the role of Hobit in human immune cells remained unclear. The work developed in this thesis aimed to unveil the biological role of Hobit in the human immune system.

In **chapter 1** we present a broad introduction to key points on how the human immune system responds to infections with the focus on the HCMV response. CD4 and CD8 T cells and NK cells are programmed in a similar way upon HCMV infection. These three subsets share many surface receptors and display similar maintenance requirements. They are also characterized by strong effector function, with accumulation of pre-formed cytolytic granules and strong IFN- γ production upon activation. We hypothesized a universal Hobit-driven program of transcriptional regulation to underlie the common phenotype of the HCMV-specific T cells and HCMV-activated NK cells.

In **chapters 2 and 3** we present a comprehensive analysis of the expression of Hobit in the human immune system. To fully characterize Hobit expression in the human immune system, we generated a specific monoclonal antibody against human Hobit. Hobit was highly expressed in peripheral blood NK cells, CD8 T cells with a cytotoxic phenotype, a subpopulation of NKT cells (**Chapter 2**), cytotoxic CD4 T cells and effector $\gamma\delta$ T cells (**Chapter 3**), but Hobit was not expressed on other leukocytes including monocytes, dendritic cells, neutrophils and regulatory CD4 T cells. Hobit expression was also not found on NK cells and CD8 T cells in tonsils. Hobit expression analysis in transplant patients undergoing primary HCMV infection or using HCMV-specific tetramers showed that Hobit was upregulated in CD4 (**Chapter 3**) and CD8 T cells (**chapter 2**) after HCMV infection. The high degree of homology in the zinc finger region between Hobit and Blimp-1 suggested Hobit might possess transcriptional activity similar to Blimp-1. We used electrophoretic mobility shift assay and luciferase reporter assays of Blimp-1 target sequences to show that Hobit can directly bind DNA target sequences of Blimp-1 and represses transcription at these sites. These findings suggest that Hobit can be classified as a transcription factor with similar specificity as Blimp-1. One of the common features of Hobit+ NK and T cells is their capacity to produce high levels of INF- γ . Our data shows that Hobit regulates IFN- γ production, suggesting that Hobit mediates early cytokines responses of effector lymphocytes.

In recent years, energy metabolism has been firmly established as a key process

driving effector and memory T cell differentiation and memory recall responses. Despite extensive analysis of effector, CM and EM CD8 T cells, the metabolic requirements of EMRA CD8 T cells have not been fully addressed before. In **Chapter 4**, we have performed metabolic phenotyping of EMRA CD8 T cells compared to CM and EM CD8 T cells. Peripheral blood EMRA cells possess several characteristics indicative of a quiescent state. In line with its quiescent phenotype, EMRA cells had lower basal glycolytic activity and basal respiratory activity than CM and EM CD8 T cells. Glycolysis is an important regulator of immediate effector function of both effector and memory cells. Despite the low basal glycolysis levels, EMRA cells possessed spare glycolytic capacity similar to CM and EM cells. Metabolomic analysis showed that EMRA cells accumulated glycolytic intermediates, suggesting that these cells can boost their glycolysis output upon re-challenge to fuel the production of pro-inflammatory cytokines. Memory CD8 T cells have the capacity to increase oxygen consumption upon activation by increasing their respiratory capacity. The increase in energy production is essential during T cell proliferation. In line with their poor proliferative capacity upon restimulation, EMRA cells have low spare respiratory capacity, hence being incapable of increasing their respiratory activity to the same extent of CM and EM cells. We observed that the mitochondrial activity in EMRA cells was low compared to other memory cells. Blimp-1 has been shown to suppress mitochondrial activity in murine B cells. In line with Blimp-1 expression in B cells, Hobit expression negatively correlated with mitochondrial activity. We observed that Hobit instructed suppression of both glycolysis and oxygen consumption in lymphocytes. Our findings indicate that, Hobit contributes to metabolic pathways that are important in the maintenance of EMRA CD8 T cells.

Hobit and Blimp-1 have been shown to co-regulate TRM maintenance in mice, but the contribution of each transcription factor has remained unclear. In **chapter 5**, we describe how Hobit and Blimp-1 expression are regulated in human lymphocytes, which sheds new light on the collaboration between these transcription factors. We found that Blimp-1 protein expression was not maintained in memory and EMRA cells, despite persisting high levels of Blimp-1 mRNA during steady state. In contrast, Hobit protein was maintained at high levels during steady state conditions. We observed in infection models that certain populations of TRM cells constitutively expressed high levels of cytotoxic molecules during homeostasis. In line with the expression data, we demonstrate that Hobit regulated granzyme B expression during the memory phase. These findings suggest that Hobit and Blimp-1 regulate cytotoxic effector molecules during different stages of the immune response.

Chapters 6 is focused on the role of Hobit in the NK cell lineage. To address the kinetics of Hobit expression during NK cell differentiation, the sequential stages of NK cells were analysed. Hobit was not present in any of the NK cell precursors present in cord blood or in bone marrow, despite being present in mature NK cells. Both CD56 dim NK and CD56 bright NK cells expressed high levels of Hobit. As CD56 bright NK cells are believed to form a developmental stage just prior of end stage CD56 dim NK cells, these findings suggest that Hobit expression in the NK cell lineage marks terminal differentiation. In **Chapter 7**, we show that Hobit induces the expression of the G protein coupled receptor GPR56 in human NK cells. Similar to Hobit, GPR56 expression has been shown to be restricted to NK cells and cytotoxic CD8, CD4, and $\gamma\delta$ T cells. We analysed NK cells from patients with loss of function

mutations in the gene encoding GPR56. GPR56 null NK cells had increased effector functions including cytotoxicity and the production of pro-inflammatory cytokines, while ectopic expression of GPR56 induced the reverse effects. Thus, the Hobit target gene GPR56 mediates an inhibitory role in NK cells.

Finally, in **chapter 8**, we have integrated our findings from the previous chapters into a general discussion. We have shown that Hobit plays diverse roles in cytotoxic lymphocytes that include the instruction of immediate effector functions, cellular metabolism and immunomodulation through the regulation of inhibitory surface molecules. Hence, the findings presented in this thesis might offer new insights and possibilities into the use of long-lived lymphocytes with immediate effector potential in cellular therapy.

Nederlandse Samenvatting

CD8 T cellen en Natural Killer (NK) cellen kunnen cellen vernietigen die geïnfecteerd zijn door virussen. Vernietiging van viraal geïnfecteerde cellen is van essentieel belang voor de uitroeiing en/of beperking van virale infecties. CD8 T-cel immuunresponsen tegen virale infecties zijn er in allerlei soorten en maten. Influenzavirus reacties worden gedomineerd door central memory (CM) CD8 T-cellen. Epstein bar virus veroorzaakt voornamelijk een effector-memory (EM) respons, terwijl het humane cytomegalovirus (HCMV), voornamelijk long term memory cellen met een effector fenotype (EMRA cellen) induceert. Een eerdere transcriptoom analyse van virus-specifieke CD8+ T-cellen in primaire HCMV infectie heeft ZNF683 (Hobit) geïdentificeerd als een van de differentieel tot expressie gebrachte genen in deze cellen. Hobit eiwit bevat een Zinc Finger factor dat homoloog is aan Blimp-1, een belangrijke transcriptionele regulator van terminale B- en T-celdifferentiatie. In vivo studies bij muizen hebben laten zien dat Hobit de ontwikkeling en/of het onderhoud regelt van tissue resident memory CD8 T-cellen (TRM) en NKT cellen. De rol van Hobit in menselijke immune cellen blijft onduidelijk. De in dit proefschrift verrichte werkzaamheden hebben tot doel de biologische rol van Hobit in het menselijk immuunsysteem te ontrafelen.

Hoofdstuk 1 bespreekt aan de hand van kernpunten hoe het menselijke immuunsysteem reageert op infecties, waarbij een specifieke nadruk is gelegd op HCMV geïnduceerde responsen. CD4 en CD8 T-cellen en NK-cellen worden op een soortgelijke wijze geprogrammeerd tijdens HCMV infectie. Naast dat deze drie subsets veel gemeenschappelijke oppervlakte receptoren hebben, vertonen ze ook vergelijkbare behoeftes wat betreft onderhoud. Kenmerkend is ook dat ze alle drie een sterke effectorfunctie hebben, met accumulatie van voorgevormde cytolytische korrels en sterke IFN- γ productie na activering. Onze hypothese is dan ook dat er een universele, door Hobit aangedreven, transcriptionele regulatie plaatsvindt dat de grondslag vormt voor het gemeenschappelijk fenotype van de HCMV-specifieke T-cellen en HCMV-geactiveerde NK-cellen.

In de **hoofdstukken 2 en 3** presenteren we een uitgebreide analyse van de expressie van Hobit in het menselijk immuunsysteem. Om Hobit expressie volledig te karakteriseren in het menselijk immuunsysteem, hebben wij een specifiek monokonaal antilichaam gecreëerd tegen humaan Hobit. Hobit werd sterk tot expressie gebracht in perifere bloed NK-cellen, CD8 T-cellen met een cytotoxisch fenotype, een subpopulatie van NKT cellen (hoofdstuk 2), cytotoxische CD4 T-cellen en effector $\gamma\delta$ T-cellen (hoofdstuk 3), maar Hobit werd niet tot expressie gebracht op andere leukocyten waaronder monocytten, dendritische cellen, neutrofielen en regulatoire CD4 T-cellen. Hobit expressie werd ook niet gevonden op NK-cellen en CD8 T-cellen uit keelamandelen.

In transplantatiepatiënten die een primaire HCMV infectie ondergingen is gebleken dat Hobit expressie in zowel CD4 (hoofdstuk 3) als CD8 T-cellen (hoofdstuk 2) toenam. Middels tetrameren kon worden vastgesteld dat Hobit tot expressie kwam in de HCMV-specifieke CD4 en CD8 T-cellen. De hoge mate van homologie in het Zinc Finger gebied tussen Hobit en Blimp-1 suggereerde dat Hobit wellicht een aan Blimp-1 vergelijkbare transcriptie-activiteit kon bezitten. Een "electrophoretic mobility shift" assay en luciferase reporter assays met Blimp-1 doelsequenties toonden aan dat Hobit direct kan binden aan diezelfde DNA doelsequenties en dat

Hobit daar ook de transcriptie van deze sites kan onderdrukken. Deze bevindingen suggereren dat Hobit ingedeeld zou kunnen worden als een transcriptiefactor met dezelfde specificiteit als Blimp-1. Een van de gemeenschappelijke kenmerken van Hobit+ NK en T-cellen is hun vermogen om hoge levels van IFN- γ te produceren. Onze data toont aan dat Hobit IFN- γ productie reguleert, wat erop kan wijzen dat Hobit betrokken is bij de regulatie van de vroege respons van cytokines die effector lymfocyten kunnen aanmaken.

In de afgelopen jaren is vast komen te staan dat energiemetabolisme een belangrijke rol speelt bij aan het aansturen van effector en memory T-cel differentiatie en bij de memory recall respons. Ondanks uitgebreide analyse van effector, CM en EM CD8 T-cellen, zijn de metabolische vereisten van EMRA CD8 T cellen nog niet eerder volledig onderzocht.

In **hoofdstuk 4** hebben we de metabole fenotypering van EMRA CD8 T-cellen vergeleken met die van CM en EM CD8 T-cellen. Perifeer bloed EMRA cellen bezitten een aantal kenmerken die erop kunnen wijzen dat de cellen zich in rusttoestand bevinden. In lijn met dit rusttoestand fenotype, hadden EMRA cellen een lagere basale glycolytische activiteit en een lagere basale respiratoire activiteit vergeleken met CM en EM CD8 T-cellen.

Glycolyse is een belangrijke regulator van onmiddellijke effectorfunctie van zowel effector en memory cellen. Ondanks de lage basale glycolyse levels, bezaten EMRA cellen een reserve glycolytische capaciteit vergelijkbaar aan CM en EM-cellen. Metabolische analyse toonde aan dat EMRA cellen glycolytische tussenproducten accumuleerden, wat suggereert dat deze cellen hun glycolyse output kunnen stimuleren om de productie van pro-inflammatoire cytokines te boosten na activatie. Memory CD8 T-cellen hebben het vermogen om het energie metabolisme te verhogen na activatie door hun reserve respiratoire capaciteit aan te spreken.

Deze toegenomen energie productie is van essentieel belang tijdens T-cel proliferatie. In lijn met hun slechte proliferatieve capaciteit na re-stimulatie hebben EMRA cellen een lage reserve respiratoire capaciteit, waardoor ze niet in staat zijn om een energie boost te leveren in een mate vergelijkbaar met die van CM en EM cellen. We zagen verder dat de mitochondriale activiteit van EMRA cellen laag was vergeleken met andere memory cellen. Er is aangetoond dat Blimp-1 de mitochondriale activiteit kan onderdrukken in muizen B-cellen.

In lijn met de onderdrukkende rol van Blimp-1 in B-cellen bleek dat Hobit expressie negatief gecorreleerd was met de mitochondriale activiteit. We zagen dat Hobit suppressie van zowel de glycolyse als de oxidatieve fosforylatie in lymfocyten induceerde. Onze bevindingen tonen aan dat Hobit bijdraagt aan metabole pathways die belangrijk zijn bij het handhaven van EMRA CD8 T-cellen

Er is aangetoond dat Hobit en Blimp-1 TRM onderhoud bij muizen co-reguleren, maar de precieze bijdrage van elke transcriptiefactor is onduidelijk gebleven. In **hoofdstuk 5** beschrijven we hoe Hobit en Blimp-1 expressie zijn geregeld in menselijke lymfocyten, waarbij een nieuw licht wordt geworpen op de samenwerking tussen deze transcriptiefactoren.

We hebben ontdekt dat Blimp-1 eiwitexpressie niet in memory en EMRA cellen werd gehandhaafd, ondanks de hoge levels van Blimp-1 mRNA in deze cellen tijdens steady state. Daarentegen bleven Hobit eiwit levels hoog tijdens homeostase. We observeerden in infectiemodellen dat sommige populaties van TRM cellen permanent

hoge levels van cytotoxische moleculen tot expressie brachten in de rustende fase. In lijn met de expressie data hebben we aangetoond dat Hobit de granzyme B expressie reguleert tijdens de memory fase terwijl al eerder was aangetoond dat Blimp-1 granzyme B tijdens de effector fase reguleert. Deze bevindingen suggereren dat Hobit en Blimp-1 cytotoxische effectormoleculen reguleren tijdens verschillende fasen van de immuunrespons.

Hoofdstuk 6 is gericht op de rol van Hobit in de NK-cel lineage. Om de kinetiek van Hobit expressie tijdens NK cel differentiatie in kaart te brengen werden de opeenvolgende stadia van NK-cellen geanalyseerd. Hobit was aanwezig in geen van de NK-cel precursors die aanwezig zijn in navelstrengbloed of beenmerg. Daarentegen was Hobit wel aanwezig in rijpe NK-cellen. Zowel CD56 dim NK als CD56 bright NK-cellen hadden hoge Hobit expressie levels.

Aangezien er van CD56 bright NK-cellen wordt geloofd dat zij zich in een ontwikkelingsfase bevinden vlak voor de eindontwikkelingsfase waarin de CD56 dim NK cellen zich bevinden suggereren deze bevindingen dat Hobit expressie in de NK-cel lijn een marker is voor terminale differentiatie. In **hoofdstuk 7** laten we zien dat Hobit de expressie induceert van het G-eiwit gekoppelde receptor GPR56 in humane NK cellen. Vergelijkbaar aan Hobit is er van GPR56 expressie aangetoond dat het zich beperkt tot NK-cellen en cytotoxische CD8, CD4 en $\gamma\delta$ T-cellen. We analyseerden de NK-cellen van patiënten met mutaties die functieverlies tot gevolg hebben in het gen dat codeert voor GPR56. De GPR56 null NK-cellen hadden verhoogde effectorfuncties waaronder cytotoxiciteit en een toegenomen productie van pro-inflammatoire cytokines. Daarentegen had de geïnduceerde ectopische expressie van GPR56 het omgekeerde effect. Daaruit kunnen we concluderen dat het Hobit doelwit gen GPR56 een remmende rol heeft in NK-cellen.

Tenslotte worden in **hoofdstuk 8** onze bevindingen uit de voorgaande hoofdstukken geïntegreerd in een algemene discussie. We hebben aangetoond dat Hobit diverse rollen speelt in cytotoxische lymfocyten waaronder het instrueren van directe effectorfuncties, cellulair metabolisme en immunomodulatie door de regulatie van remmende oppervlakte moleculen. De bevindingen beschreven in dit proefschrift bieden wellicht nieuwe inzichten en mogelijkheden voor het gebruik van langlevende lymfocyten met onmiddellijke effector potentieel in cellulaire therapie.

List of co-authors

Name of author	Designed experiments	Performed experiments	Analysed data	Wrote manuscript	Approved manuscript
Amber van Stijn	X	X	X		X
Anna E. Oja	X	X	X	X	X
Anna T. Hoekstra	X	X	X		X
Bianca Blom			X		X
Celia R. Berkers	X		X		X
Cheng-Chih Hsiao	X	X	X	X	X
Diana Wouters	X		X		X
Eric Eldering			X		X
Ester B.M. Remmerswaal	X	X	X		X
Evi Kosteni			X		X
Felipe A. Vieira Braga	X	X	X	X	X
Felix M. Behr	X	X	X		X
Gabriele M. König			X		X
Gin-Wen Chang	X	X	X		X
Gina M. Doody	X		X		X
Hsi-Hsien Lin	X		X		X
Ineke J.M. ten Berge	X		X		X
Ingrid A.M. Derks	X	X	X		X
Jianmin Zuo		X	X		X
Jörg Hamann	X		X	X	X
Kirstenn M.L. Hertoghs	X	X	X	X	X
Klaas P.J.M. van Gisbergen	X		X	X	X
Linde Meyaard	X		X		X
Marc Demkes	X	X	X		X
Martijn A. Nolte			X		X
Martijn D. B. van de Garde		X	X		X
Natasja A.M. Kragten	X	X	X	X	X
Nicholas A. Barnes	X	X	X		X
Nicole N van der Wel	X	X	X		X
Paul Moss		X			X
Perry D. Moerland	X		X		X
Pleun Hombrink	X	X	X	X	X
Rachel Straussberg			X		X
Regina Stark	X	X	X		X
Rene A.W. van Lier	X		X		X
Reuben M. Tooze	X		X		X
Vera Knäuper			X		X
Wikky Tigchelaar		X	X		X
Yen-Ming Peng	X		X		X

PhD Portfolio

Name PhD student:	Felipe Augusto Vieira Braga	
PhD period:	09/2011-08/2015	
Name PhD supervisor:	prof. dr. R.A.W. van Lier	
Name PhD c0-supervisor:	dr. K.P.J.M. van Gisbergen	
1. PhD training		
	Year	Workload (Hours/ECTS)
General courses		
– Advanced Immunology	2012	2.5
Specific courses		
– Analysis of microarray gene expression data using R/BioC and web tools	2012	2.5
– Laboratory Animal Science	2011	2.5
Seminars, workshops and master classes		
– Weekly department meetings	2011-2015	4.5
– Journal Club	2011-2015	3.0
– Landsteiner Lectures and Guest speakers	2011-2015	2.0
– Landsteiner Master Class	2011-2015	0.5
Presentations		
– Work presentations within Sanquin	2011-2015	2.0
– Journal Club	2011-2015	0.5
(Inter)national conferences		
– Keystone meeting - T Cells: Regulation and Effector Function (Poster), USA	2015	1.0
– European Federation of Immunological Societies Meeting (Poster), AUS	2015	1.0
– Dutch Society of Immunology (Oral), NED	2014	0.5
– Cambridge Immunology network (attendance), UK	2014	0.25
– Dutch Society of Immunology (Oral), NED	2013	0.5
– European Federation of Immunological Societies - Summer School (oral), ITA	2013	1.0
– Dutch Society of Immunology (Poster), NED	2012	0.5
– Dutch Society of Immunology (attendance), NED	2011	0.25
–		

2. Teaching

	Year	Workload (Hours/ECTS)
Supervising		
- C. Kweekel, Master thesis	2015	2

Total:

27 ECTS

List of Publications:

Oja AE, Vieira Braga FA, Remmerswaal EBM, Kragten NAM, Hertoghs KML, Zuo J, Moss PA, et al. The Transcription Factor Hobit Identifies Human Cytotoxic CD4+ T Cells. *Frontiers in Immunology*. 2017;

Vieira Braga FA, Teichmann SA, Stubbington MJT. Are cells from a snowman realistic? Cryopreserved tissues as a source for single-cell RNA-sequencing experiments. *Genome Biol*. 2017; 18:54.

Vieira Braga FA, Teichmann SA, Chen X. Genetics and immunity in the era of single-cell genomics. *Human Molecular Genetics*. 2016.

Santegoets KCM, Wenink MH, Vieira Braga FA, Cossu M, Lamers-Karnebeek FBG, van Riel PLCM, Sturm PDJ, et al. Impaired Porphyromonas gingivalis-Induced Tumor Necrosis Factor Production by Dendritic Cells Typifies Patients With Rheumatoid Arthritis. *Arthritis & Rheumatology*. 2016; 68:795–804.

Chang G-W, Hsiao C-C, Peng Y-M, Vieira Braga FA, Kragten NAM, Remmerswaal EBM, van de Garde MDB, et al. The Adhesion G Protein-Coupled Receptor GPR56/ADGRG1 Is an Inhibitory Receptor on Human NK Cells. *Cell Reports*. 2016; 15:1757–1770.

Vieira Braga FA, Hertoghs KML, Kragten NAM, Doody GM, Barnes NA, Remmerswaal EBM, Hsiao C-C, et al. Blimp-1 homolog Hobit identifies effector-type lymphocytes in humans. *European Journal of Immunology* 2015; 45:2945–2958.

Vieira Braga FA, Hertoghs KML, van Lier RAW, van Gisbergen KPJM. Molecular characterization of HCMV-specific immune responses: Parallels between CD8(+) T cells, CD4(+) T cells, and NK cells. *European Journal of Immunology*. 2015; 45:2433–2445.

Amaral MPM, Vieira Braga FA, Passos FFB, Almeida FRC, Oliveira RCM, Carvalho AA, Chaves MH, et al. Additional evidence for the anti-inflammatory properties of the essential oil of Protium heptaphyllum resin in mice and rats. *Latin American Journal of Pharmacy*. 2009; 28:775–782.

Curriculum Vitae

Felipe Augusto Vieira Braga was born in Teresina, Piaui, Brazil on the 8th of September 1985. He attended primary school at Instituto Magister and middle and High School in the catholic school Diocesano. After high school Felipe started two universities at the same time, Law at the State University of Piaui and Pharmacy at the Federal University of Piaui. Midway through law school Felipe decided to quit and focus solely on his scientific career. In his second year as undergraduate Felipe joined the lab of Professor Francisco de Assis Oliveira, where he stayed as an undergrad student for 2 years, studying the anti-inflammatory properties of the plant *Protium heptaphyllum*, work published in the Latin American Journal of Pharmacy. After leaving professor Oliveira's lab, Felipe worked two years as a bank clerk at Bank of Brazil, while finishing his undergraduate studies. Soon after his graduation, Felipe was awarded a master scholarship at Radboud University Nijmegen, in the Netherlands. During his master Felipe did research internships in Professor Timothy Radstake lab (Nijmegen, NL) and Professor Fiona Watt lab (Cambridge, UK), working first on rheumatoid arthritis then on skin biology. After his short stay in Cambridge, Felipe decided to move back to the land of bicycles and tulips, where he spent four exciting years in the lab of Klaas van Gisbergen and Rene van Lier at Sanquin Blood Supply Foundation in Amsterdam. During his PhD, Felipe worked on the role of Hobit in the human immune system. Currently Felipe moved back to Cambridge UK, where he works as a post-doctoral fellow in the lab of Sarah Teichmann, where he uses single cell transcriptomics technologies to decipher human immunity.

Acknowledgements

Minha Mãe, Tia e Pai

Para minha Mãe Iris, minha Tia Claudia e meu Pai Humberto. Um obrigado de coração. Eu cheguei aqui devido ao investimento e apoio que todos vocês deram para minha educação desde pequeno. Por isso serei eternamente grato. Amo vocês.

Klaas van Gisbergen

Thanks for all the support and teaching during the past years. I learned a lot, but not everything I could. I wish we could have had closer contact during your stay in Australia. We did the best we could, with all skype meetings and e-mail exchanges, but only in the last 1.5 years in Sanquin I could actually realise how much I lost by not having you around during my whole PhD. I am proud of what I achieved, and I hope you are as well.

Rene van Lier

Despite all your compromises, I am grateful for the time you took from your busy agenda to guide me. I learned a lot about science. Of notice, I must mention three things I learned: "Shit happens"; "There is no magic in science" and "Science is like a tennis match". These things really helped me to get here.

Esther Niessen

My love, thank you for all the support during the writing of this thesis. It was not always easy, but you always helped me as much as you could. I am happy to be with you. With you by my side, I know I can do always more. Love you.

Sara Niessen

Sarinha meu amor. Desde que você chegou, minha vida mudou para melhor. Apesar das noites mal dormidas, você me ajudou a desenvolver um foco em terminar minha tese como nunca antes. Te amo, minha princesa.

Natasja Kragten

Hello Tas. When people ask me what is the greatest thing I learned during my PhD, I say it is how I learned to listen better and to understand my colleagues by their values and views, and how by doing that, I got someone that didn't really like me at first to be one of my dearest friends. I am happy that despite my move from the Netherlands, we are still constantly in touch. I am happy to be your friend. Count with me for whatever you need, always.

Tamara Stegmann

My dear Tamara. The one thing I have to say to you is: the thing I miss most about my Sanquin years is the coffee/coca cola breaks we used to have always we could. I enjoyed every moment of our science and non-science conversations. I miss you dearly.

Jesse Ernstman

Yo Dude, I am glad for having you as my friend. All the dinners, picnics, beers, pizza and terror movies made my past years a blast. I also learned a lot from you about blood groups, haemoglobins and other non-immune stuff. Thanks for all.

Fiamma Salerno

Dear Fiamma. Despite our rocky start, I managed to survive all the occasions in which my life was at risk ;) I even got you to try some Hawaii pizza. This means we are great pals, right? I miss our T cell conversations and all the other moments we shared. Best of luck with whatever path you follow.

Anna Elisabeth

Hello my friend. Despite the relatively brief time we shared in the lab, quality counts more than quantity right? Our scientific paths are still very close, as I moved on to lungs and you started working on Hobit. This makes me happy, as it makes easier to keep you around. There are so many other memorable things I could say about you, but to be appropriate, I will keep this short ;) .

Nahuel Paolini

My BBQ brother. The only other person around Sanquin that knows how to eat a proper piece of meat. I am glad for all the fun we had. Your taste for movies is quite unique and I congratulate you on that. Football apart, you're my brother.

Pleun Hombrink

Thanks for all the fun and interesting moments in the past year. Despite "you knowing nothing", I learned much from you, both in and out of the lab. Especially, that good scientists tend to be stubborn.

Sulima Geerman

My dear Sulima. I still look forward for another trip together. It is great we have a similar style on enjoying life: lots of food, lots of rest, not much nature, not much activity. I admire you a lot, you are a very brave person, both in science and in your personal life.

Eric Mull

Dear Eric, I had so much fun in our sorting afternoons. I enjoyed every moment of our discussion about flow cytometry, microscopy, image stream, etc. I learned a lot from you and I admire you. You are an example of how you can do a good job and still have fun.

Ester Remmerswaal

Dear Ester. Despite the limited number of times we met, I learned a lot about flow cytometry with you. Thanks for everything.

Hematopoiesis Group Leaders

Dear Derk Amsen, Martijn Nolte and Monika Wolkers. It was a pleasure to share so many group meetings and informal conversations with you all. I learned a lot on how

to take as many controls as possible in order to convince everybody on how solid (or not) is my data. Derk, I specially thank you for sharing your experiences on how you decided what to do after your PhD, it was of great help.

Chris Kweekel

You were my favourite student during my PhD ;) I had fun during your time around and I learned a lot from that time. I hope life is treating you well

All other colleagues at Sanquin

There are many other people to whom I am thankful for to have met. Carlijn Kuijk, despite you being "pure evil", you will always have a special place in my heart. Esther Heideveld, since you first joined us, I have always admired you, by the way you do your science as well as how you live your life. Felix Behr, I wish we could have had a longer overlap in the lab. I wish you success. Rick Kapur and Sabrina Zeddies, just one thing I have to say: I miss our legendary Tuesdays.

The Playerz

Eugenio "miguxo" Verçosa, Sebastiao "tome julgamento" Bezerra, Felix "não pegue sniper" Silva, Daniel "anão" Bona, Romulo "Jesus" Verçosa, Alexandre "herói" Barbosa e Dyego "ursão" Costa. Sou grato pela amizade de vocês em todos esses anos. Especialmente pelas conversas durante a fase Nelson Rodrigues da minha vida. E apesar do peso imenso que vocês são na lane, (quase) sempre me divirto. Mesmo quando levamos taca, ainda é legal ficar no Skype falando merda. GGEZ

Valve

Last, but not least, I thank Valve and Ice Frog for creating and maintaining Dota 2. Dota 2 has been my heaven and my hell during my PhD. It kept me awake at night, and probably I would have finished my PhD a bit quicker without it. But without Dota 2 I might have not finished at all, as it gave me a way to keep my sanity and deal with the frustration inherent to science.

